

INFORMATION TO USERS

This manuscript has been reproduced from the microfilm master. UMI films the text directly from the original or copy submitted. Thus, some thesis and dissertation copies are in typewriter face, while others may be from any type of computer printer.

The quality of this reproduction is dependent upon the quality of the copy submitted. Broken or indistinct print, colored or poor quality illustrations and photographs, print bleedthrough, substandard margins, and improper alignment can adversely affect reproduction.

In the unlikely event that the author did not send UMI a complete manuscript and there are missing pages, these will be noted. Also, if unauthorized copyright material had to be removed, a note will indicate the deletion.

Oversize materials (e.g., maps, drawings, charts) are reproduced by sectioning the original, beginning at the upper left-hand corner and continuing from left to right in equal sections with small overlaps.

Photographs included in the original manuscript have been reproduced xerographically in this copy. Higher quality 6" x 9" black and white photographic prints are available for any photographs or illustrations appearing in this copy for an additional charge. Contact UMI directly to order.

ProQuest Information and Learning
300 North Zeeb Road, Ann Arbor, MI 48106-1346 USA
800-521-0600

UMI[®]

**SOLUTION PROPERTIES OF CATIONIC HYDROPHOBICALLY-MODIFIED
HYDROXYETHYL CELLULOSE ETHERS**

By

SUDARSHI TANUJA ANGELIQUE REGISMOND, B.Sc.

A Thesis

Submitted to the School of Graduate Studies

in Partial Fulfilment of the Requirements

for the Degree

Doctor of Philosophy

McMaster University

©Copyright by Sudarshi Tanuja Angelique Regismond, January, 2000

SOLUTION PROPERTIES OF CATIONIC HM-HEC ETHERS

I would like to dedicate this thesis to the best chemist I know...

Hettiarachchige Don Anthony Regismond

October 29, 1935 to November 14, 1997

I love you Daddy. I am sorry it took so long.

DOCTOR OF PHILOSOPHY (2000)
(Chemistry)

McMaster University
Hamilton, Ontario

TITLE: **Solution Properties of Cationic Hydrophobically-Modified Hydroxyethyl Cellulose Ethers**

AUTHOR: **Sudarshi Tanuja Angelique Regismond, B.Sc.**
(McMaster University)

SUPERVISOR: **Professor Françoise M. Winnik**

NUMBER OF PAGES: **xvi, 149**

ABSTRACT:

This doctoral thesis has investigated various aspects of the solution properties of water-soluble amphiphilic polymers. The ultimate goal was to achieve a better understanding of the macroscopic phenomena demonstrated by these systems by elucidating the molecular interactions causing them. Two commercial cationic cellulose ethers were studied, the cationic derivative of hydroxyethyl cellulose, HEC-N+CH₃ and its hydrophobically-modified analogue, HEC-N+C₁₂. Their interpolymeric associations and their interactions with surfactants were studied using photophysical techniques, such as UV-vis and fluorescence spectroscopy.

Initial fluorescence probe experiments were directed at investigating the interactions between these cationic polymers and a series of cationic surfactants. No interaction was predicted to occur in systems where the polymer and surfactant were of the same charge due to electrostatic repulsions. However, the results obtained clearly indicated that polymer/surfactant complexes formed if the polymer contained hydrophobic groups. A more detailed picture of the interactions was then obtained by using polymers to which the dye was covalently attached via an ether linkage. Various pyrene labelled and naphthalene labelled analogues of the two cellulose ethers were synthesised and characterised by standard methods. The interpolymeric associations of cationic polymer solutions was studied using mixed solutions of naphthalene and pyrene labelled polymers using non-radiative energy transfer experiments. Fluorescence studies of these labelled polymers in the presence of cationic surfactants confirmed the results of the probe studies.

Other fluorescence studies investigated the interactions of the pyrene labelled HEC-N+C₁₂ with a series of anionic surfactants. A stronger interaction was observed due to the electrostatic attraction of the two species. Additionally, an unexpected feature of the fluorescence spectra led to the speculation of the presence of two possible labelling sites on HEC-N+C₁₂. Fluorescence quenching experiments confirmed this hypothesis.

To study the microenvironment around each site, specifically pyrene labelled cationic hydrophobically-modified hydroxyethyl cellulose ethers were prepared and characterised. An analogous series of naphthalene labelled polymers were prepared for investigations of the interpolymeric associations of polymers of like charge using mixed naphthalene and pyrene labelled polymer solutions. Other investigations of these polymers include studying how the site of hydrophobic modification affects the solution properties of the polymer and the interactions of mixed polymer/surfactant systems.

The interactions that occur simultaneously at the air/water interface have been studied briefly for example in the investigations of the relationship between the interfacial composition and the interfacial viscoelastic behaviour and the foaming properties of polymer/surfactant systems. It was found that in a critical surfactant concentration region, interaction occurs between polymers and surfactants of opposite charge at the air/water interface. This surface flow behaviour was more prevalent in systems where the polymer was also hydrophobically-modified. Dynamic surface tension experiments were conducted to investigate the surface behaviour of dilute aqueous solutions of these cellulosic polyelectrolytes.

ACKNOWLEDGEMENTS:

There are many people whom I wish to acknowledge for their contribution to this thesis. First and foremost, I would like to thank Professor Françoise Winnik for her guidance and support throughout this thesis. Over the course of my graduate work, she has become more than a supervisor to me, and I wish to thank her for her friendship during the dark times. I am very grateful to my committee members Professor Robert Pelton and Professor Michael Brook for their assistance towards this thesis. A very special thank you to Dr. E. Desmond Goddard, for his guidance, encouragement and endless wisdom.

I am very grateful for having had the opportunity to work with Torsten Mäurer and Michael Berg from the Department of Chemical Engineering, Universität Karlsruhe(TH), Germany. A huge thank you to both of them for much help in my research and for their friendship. Vielen Dank! I have had the opportunity to work with a large number of wonderful people over the years. Many thanks to Alex Adronov, Dan Anghel, Markus Brune, Kim Gracie, Neela Khaloo, Martin Köhler, Neil Kopek, Masanobu Mizusaki (for the interesting late night coffee conversations!), André Morneau, Shalini Nigam, Peter Opdam, Alla Polozova, Ilya Reviakine, Jean-François Stumbé, Leona Tomicic and Jing Zhang for all the great moments! To Elizabeth Kroll and Akiko Yamazaki, friends, sisters, Charlie's Angels, thank you so much for all the good times and for your endless love and support through the years. To the present members of Winnik's research group: Ester Goh, Ming Li, Roger Liu, Gangadhara, and Jayanthi Saraswathymmal, it has been a great honour to work with all of you.

I would like to thank Don Hughes (NMR) and Yew-Meng Heng (Electron Microscopy) for their technical assistance. Special thanks to Tracy Morkin for her assistance with the fluorescence lifetime measurements. Zdenka Policova and Professor Wilhelm Neumann of the Department of Mechanical Engineering, University of Toronto, for assistance with the dynamic surface tension experiments. Jim Garrett (BIMR) for his fascinating coffee talk and great hugs! ! A special thanks to the entire faculty and staff in the department of chemistry at McMaster for their continued support.

I'd like to thank the good friends I've had the privilege to study with over the years: Adrienne Boden, Rabah Boukherroub, Jeffery Downey, Randy Frank, Michael Gerken, Nicolas LeBlond, Denny Lin, Phillipa Lock, Helen Manolopoulos, Mustafa Mohamed, John Pezacki, Bernard Pointner, and Daryl Vanbesien. Thanks for making graduate school such a blast! A very grateful thank you to Frank LaRonde for his countless help in synthesis and NMR over the years. Special thanks to Craig Bridges and Ayumi Goto for all their love and support. Big hug to Christophe Lux for his encouragement during the hardest part of this thesis. To Luca Maretti, thank you for your love and support through the home stretch... I will never forget you, my darlingo.

To my sister Aruni, and brother Pravin, words can not express what you both mean to me. Thanks for all your love and continued support. Finally, I would like to thank the person who means the world to me... my mom. Your courage, strength and love of life have been a constant role model for me. Thank you for teaching me to always strive for the best and to settle for nothing less.

TABLE OF CONTENTS

TITLE PAGE	i
DEDICATION	ii
DESCRIPTIVE NOTE	iii
ABSTRACT	iv
ACKNOWLEDGEMENTS	vi
TABLE OF CONTENTS	viii
OTHER PUBLICATIONS NOT INCLUDED IN THESIS	xi
LIST OF FIGURES	xii
LIST OF TABLES	xv
LIST OF ABBREVIATIONS	xvi
CHAPTER 1: INTRODUCTION AND BACKGROUND	1
1.1 Introduction	1
1.2 Background	3
1.2.1 Types of Interactions	3
1.2.2 Amphiphilic Molecules and their Behaviour in Aqueous Solution	6
1.2.2.1 Surfactants	6
1.2.2.2 Solution Behaviour of Surfactants	6
1.2.2.3 Polymers	11
1.2.2.4 Amphiphilic Polymers	12
1.2.2.5 Solution Behaviour of Polymers and Amphiphilic Polymers	12
1.2.2.6 Amphiphilic Polymer/Surfactant Mixtures	16
1.3 Techniques Used to Study Solution Properties	19
1.3.1 Probe Studies	24
1.3.2 Label Studies	26

1.3.3	Fluorescence Quenching Studies	30
1.3.4	Fluorescence Non-Radiative Energy Transfer Studies	32
1.4	Techniques Used to Study the Solution Properties at the Air/Water Interface	33
1.4.1	Surface Viscoelasticity Studies [Appendices 3 and 4]	36
1.4.2	Foam/Film Stability Studies [Appendix 4]	36
1.5	Cellulose Ethers	37
1.6	Literature Review	42
1.6.1	Aqueous Solution Properties of Non-Ionic Cellulose Ethers	42
1.6.2	Aqueous Solution Properties of Cationic Hydrophobically-Modified Cellulose Ethers	43
1.7	Scope of Thesis	47
CHAPTER 2: RESULTS AND DISCUSSION		49
2.1	Randomly Labelled Cationic Hydrophobically-Modified Hydroxyethyl Cellulose	49
2.1.1	Synthesis and Characterisation	49
2.1.2	Solution Properties and Interpolymeric Associations	65
2.1.3	Interactions of Labelled Polymers with Surfactants in Aqueous Solution	68
2.1.4	Section Summary	80
2.2	Towards Site-Specifically Labelled Cationic Hydrophobically-Modified Hydroxyethyl Cellulose	82
2.2.1	Synthesis and Characterisation	83
2.2.1.1	Synthesis of the Pyrene Labelled Polymers	83
2.2.1.2	Characterisation of the Pyrene Labelled Polymers	87
2.2.1.3	Synthesis and Characterisation of the Naphthalene Labelled Polymers	102
2.2.2	Interpolymeric Association Studies by Non-Radiative Energy Transfer	107
2.2.3	Interaction with Surfactants in Aqueous Solution	108
2.2.4	Section Summary	113
2.3	Interfacial Behaviour of Cationic Hydroxyethyl Cellulose Ethers	115
2.3.1	Dynamic Surface Tension using Axisymmetric Drop Shape Analysis-Profile [Appendix 5] ⁷¹	115
2.3.1.1	Dynamic Surface Tension of Mixed HEC-N+CH ₃ /SDS	116
2.3.2	Surface Viscoelasticity [Appendices 3 and 4]	116

2.3.2.1 Effect of Hydrophobic Modification [Appendix 3]	117
2.3.2.2 Mixed Cationic Polymer/Anionic Surfactant Complexation [Appendices 3 and 4]	117
2.3.3 Section Summary	118
CHAPTER 3: CONCLUSIONS AND RECOMMENDATIONS FOR FUTURE WORK	119
3.1 Conclusions	119
3.2 Recommendations for Future Work	121
CHAPTER 4: EXPERIMENTAL	124
4.1 Materials	124
4.2 Instrumentation and Methods	126
4.3 Labelled Polymer Characterisation Methods	128
4.4 Synthetic Preparations	131
4.4.1 Preparation of Randomly Labelled Cationic Hydrophobically- Modified Cellulose Ethers	131
4.4.2 Preparation of Site-Specifically Labelled Cationic Hydrophobically-Modified Cellulose Ethers	135
4.5 Solution Preparation	140
CHAPTER 5: REFERENCES	142
APPENDICES:	
1. Brief Note: Interactions of cationic surfactants with a hydrophobically-modified cationic cellulose polymer: a study by fluorescence spectroscopy, F.M. Winnik, S.T.A. Regismond and E.D. Goddard, Colloids and Surfaces A: Physicochemical and Engineering Aspects, 1996, 106, 243-247.	
2. Interactions of an anionic surfactant with a fluorescent-dye-labelled hydrophobically-modified cationic cellulose ether, F.M. Winnik, S.T.A. Regismond and E.D. Goddard, Langmuir, 1997, 13, 111-114.	
3. Surface viscoelasticity in mixed polycation anionic surfactant systems studied by a simple test, S.T.A. Regismond, F.M. Winnik and E.D. Goddard, Colloids and Surfaces A: Physicochemical and Engineering Aspects, 1996, 119, 221-228.	

4. Stabilization of aqueous foams by polymer/surfactant systems: effect of surfactant chain length, S.T.A. Regismond, F.M. Winnik and E.D. Goddard, *Colloids and Surfaces A: Physicochemical and Engineering Aspects*, 1998, 141, 165-171.
5. Static and dynamic surface tension of dilute polyelectrolyte solutions, S.T.A. Regismond, Z. Policova, A.W. Neumann, E.D. Goddard and F.M. Winnik, *Colloids and Surfaces A: Physicochemical and Engineering Aspects*, 1999, 156, 157-162.

OTHER PUBLICATIONS NOT INCLUDED IN THESIS:

1. Fluorescence microscopy study of the sorption of cationic polymers on hair, S.T.A. Regismond, Y.-M. Heng, E.D. Goddard and F.M. Winnik, in *Polysaccharide Applications: Cosmetics and Pharmaceuticals*, ed. M.A. El-Nokaly and H.A. Soini, ACS Symposium Series 737, American Chemical Society, Washington, DC, 1999.
2. Fluorescence microscopy observation of the adsorption onto hair of a fluorescently-labelled cationic cellulose ether, S.T.A. Regismond, Y.-M. Heng, E.D. Goddard and F.M. Winnik, *Langmuir*, 1999, 15, 3007.
3. Fluorescence methods in the study of polymer-surfactant systems, F.M. Winnik and S.T.A. Regismond, in *Polymer-Surfactant Systems*, ed. J.C.T. Kwak, Surfactant Science Series/77, Marcel Dekker Inc., New York, 1998.
4. Polymer/surfactant complexes at the air/water interface detected by a simple measure of surface viscoelasticity, S.T.A. Regismond, K. Gracie, F.M. Winnik and E.D. Goddard, *Langmuir*, 1997, 13, 5558.
5. Fluorescence methods in the study of the interactions of surfactants with polymers, F.M. Winnik and S.T.A. Regismond, *Colloids and Surfaces A: Physicochemical and Engineering Aspects*, 1996, 118, 1.

LIST OF FIGURES

CHAPTER 1:

- 1.2.1: Variety of association structures of surfactants and lipids in aqueous solution ¹.
- 1.2.2: Surfactant packing parameter is dependent on head-group area a_0 , chain volume v , and chain length l_c ¹.
- 1.2.3: Dynamic packing properties of lipids and the structures they form ¹.
- 1.2.4: Association of N surfactants into a micelle ¹.
- 1.2.5: Structure of a generic amphiphilic polymer.
- 1.2.6: Apparent viscosity of solutions illustrated by plotting the shear stress versus strain rate ².
- 1.2.7: Characteristic behaviour of polymer solution viscosity as a function of shear rate ³.
- 1.2.8: Schematic diagram illustrating the aqueous solution behaviour of amphiphilic a) polymers and b) polyelectrolytes.
- 1.2.9: a) Plot of surface tension versus the logarithm of surfactant concentration with a schematic representation of the complexes formed as surfactant concentration is increased ⁴.
- 1.2.10: Schematic representation of polymer/surfactant complexes occurring in solution with increasing surfactant concentration ⁵.
- 1.3.1: Jablonski diagram illustrating the radiative and non-radiative processes possible after electronic excitation ⁶.
- 1.3.2: Potential energy curves showing individual vibrational energy levels and their involvement in a) adsorption and b) emission; c) illustrates the resulting structured absorption and emission spectra ⁷.
- 1.3.3: a) Structure of pyrene b) solvent dependence of vibronic band intensities in pyrene monomer fluorescence at room temperature (pyrene conc. 2×10^{-6} mol/L, $\lambda_{exc} = 310$ nm) ⁶.
- 1.3.4: Change in the intensity of I_1 and I_3 of pyrene emission spectra with increasing surfactant concentration.
- 1.3.5: Emission spectrum of pyrene labelled onto polymers: broad excimer emission centred at 485nm ($\lambda_{exc} = 344$ nm).
- 1.3.6: Intermolecular potential energy curves for monomer and excimer ⁷.
- 1.3.7: Excitation spectra monitored at the monomer (377nm) and excimer (485nm) emission wavelengths indicating the presence of static excimers ⁸.
- 1.5.1: a) Structure of cellulose, b) synthetic routes to cellulose ethers.
- 1.5.2: Heterogeneous reaction of fibrous cellulose and stages of solvation as a function of the extent of reaction ⁹.
- 1.5.3: Structures of a) HEC, b) HEC-N+CH₃ and c) HEC-N+C₁₂.

CHAPTER 2:

- 2.1.1: Synthetic scheme for pyrene labelling of the polymers by an ether reaction in DMF.
- 2.1.2: Synthetic scheme for naphthalene labelling of polymers using a modified ether reaction.
- 2.1.3: Structures of HEC-N+CH₃, HEC-N+CH₃-Py/212, HEC-N+C₁₂ and HEC-N+C₁₂-Py/240.
- 2.1.4: Steady-state fluorescence emission spectra of HEC-N+CH₃/212 (top) and HEC-N+C₁₂/240 (bottom) in water (1.0g/L, $\lambda_{exc} = 344\text{nm}$, 25 °C).
- 2.1.5: Excitation spectra of HEC-N+C₁₂-Py/240 at monomer (solid) and excimer (dashed) wavelengths (377nm and 485nm, respectively, 25 °C).
- 2.1.6: Fluorescence decay curves of HEC-N+C₁₂-Py/240 monomer and inset excimer in a) 80% DMSO, excitation wavelength 346nm and b) water, excitation wavelength 344nm (logarithmic representation, monomer monitored at 377nm, excimer at 485nm).
- 2.1.7: Steady-state fluorescence spectra of non-radiative energy transfer from HEC-N+C₁₂-Np/184 to HEC-N+C₁₂-Py/240 ($\lambda_{exc} = 290\text{nm}$, ratio of naphthalene to pyrene: 5:1, polymer concentration 0.5 g/L, 25 °C).
- 2.1.8: Plot of I_E/I_M as a function of DTAB concentration (logarithmic scale, 0.1 g/L polymer concentration) for HEC-N+CH₃-Py/212 (open circles) and HEC-N+C₁₂-Py/240 (closed circles).
- 2.1.9: Plot of a) I_E/I_M and b) I_M and I_E as a function of DTAC concentration (logarithmic scale) for 1.0 g/L HEC-N+C₁₂-Py/240.
- 2.1.10: Plot of I_E/I_M as a function of HTAC concentration (logarithmic scale) for 0.1 g/L HEC-N+C₁₂-Py/240.
- 2.1.11: Plot of I_E/I_M as a function of surfactant concentration (logarithmic scale) for 0.1 g/L HEC-N+C₁₂-Py/240: DTAC (open circles), HTAC (closed circles).
- 2.1.12: Stern-Volmer plot of monomer emission quenching by CPC in a) HEC-N+C₁₂-Py/240 and b) HEC-N+CH₃-Py/212 solutions ($\lambda_{exc} = 344\text{nm}$, 25 °C).
- 2.1.13: Fluorescence emission quenching by EPB in a) HEC-N+CH₃-Py/212 and b) HEC-N+C₁₂-Py/240 solutions ($\lambda_{exc} = 344\text{nm}$, 25 °C).
- 2.1.14: Plot of I_E/I_M as a function of anionic surfactant concentration (logarithmic scale) for 0.1 g/L HEC-N+C₁₂-Py/240: SDS (circles), SDeS (squares), and SOS (triangles).
- 2.1.15: Schematic diagram of the interactions occurring between HEC-N+C₁₂-Py/240 and anionic surfactants.
- 2.1.16: a) Fluorescence spectra of HEC-N+CH₃-Py/212 and SOS mixed solutions b) plot of I_M and I_E as a function of SOS concentration (logarithmic scale).
- 2.2.1: Idealised structures of the labelled hydroxyethyl cellulose ethers prepared.
- 2.2.2: Synthetic scheme for labelling method 1.
- 2.2.3: Synthetic scheme for labelling method 2.

- 2.2.4: 500MHz ^1H NMR spectra of a) HEC (LMW) and b) HEC-Py/145-N+C₁₂ (LMW) in D₂O.
- 2.2.5: Fluorescence spectra of 1.0 g/L HEC-Py/370-N+C₁₂ (HMW) in aqueous solution (solid line) and in aqueous DMSO (80% v/v, dashed line).
- 2.2.6: Fluorescence spectra of 1.0 g/L HEC-Py/97-N+C₁₂ (HMW) in aqueous solution (solid line) and in aqueous DMSO (80% v/v, dashed line).
- 2.2.7: Fluorescence monomer decay curve and inset excimer decay curve of HEC-Py/370-N+C₁₂ (HMW) in a) water and b) aqueous DMSO (80% v/v).
- 2.2.8: Structures of the naphthalene labelled polymers prepared.
- 2.2.9: 500 MHz ^1H NMR spectrum of HEC-Np/205-N+C₁₂ (LMW).
- 2.2.10: Fluorescence spectra of 1.0 g/L aqueous solutions of HEC-Np/205 (dashed line) and HEC-Np/205-N+C₁₂ (solid line) ($\lambda_{\text{exc}} = 282 \text{ nm}$, 25 °C).
- 2.2.11: Fluorescence spectra of HEC-Np/333-N+C₁₂ (HMW, 0.5 g/L, dotted line), and HEC-Py/97-N+C₁₂ (HMW, 0.027 g/L, dashed line) and non-radiative energy transfer from HEC-Np/333-N+C₁₂ (HMW, 0.5 g/L) to HEC-Py/97-N+C₁₂ (HMW, 0.027 g/L), (5 mol Np : 1 mol Py; $\lambda_{\text{exc}} = 290 \text{ nm}$, solid line).
- 2.2.12: a) Plot of I_E/I_M versus the logarithm of DTAB concentration (mol/L) for HEC-Py/145-N+C₁₂, HEC-Py/145 (LMW) and HEC-Py/370-N+C₁₂ (HMW) and b) plot of fluorescence intensity of the monomer and excimer emission versus the logarithm of DTAB concentration, for 0.1g/L aqueous solutions of HEC-Py/145-N+C₁₂ (LMW).
- 2.2.13: a) Plot of I_E/I_M versus the logarithm of SDS concentration (mol/L) and b) plot of fluorescence intensity of the monomer and excimer emission versus the logarithm of SDS concentration, for 0.1g/L aqueous solutions of HEC-Py/145-N+C₁₂ LMW.

CHAPTER 3:

- 3.2.1: Idealised chemical structures of cationic pyrene and naphthalene labelled polymers.

LIST OF TABLES

CHAPTER 1:

1.5.1: Characteristic properties of the cellulose ethers studied.

CHAPTER 2:

- 2.1.1: Characterisation of labelled polymers in 80% dimethylsulfoxide.
- 2.1.2: Absorption spectra peak-to-valley ratios for pyrene labelled polymers.
- 2.1.3: Fluorescence excitation peak-to-valley ratios and values of I_E/I_M for the pyrene labelled polymers.
- 2.1.4: Quantum yield determination of the labelled polymers.
- 2.1.5: Fluorescence decay measurements of pyrene labelled polymers.
- 2.1.6: Stern-Volmer (K_{SV}) and rate constants of quenching of monomer ($k_{q,mon}$) and excimer ($k_{q,exc}$) emission of pyrene labelled polymers with various pyridinium halide derivatives.
- 2.2.1: Characterisation of pyrene labelled polymers.
- 2.2.2: Cationic hydrophobe content on modified pyrene labelled polymers.
- 2.2.3: UV-vis absorption spectra peak-to-valley ratios for pyrene labelled polymers (1.0 g/L).
- 2.2.4: Fluorescence decay measurements of the pyrene labelled polymers in aqueous solution and aqueous DMSO (80% v/v).
- 2.2.5: Fluorescence decay measurements of the pyrene labelled cationic hydrophobically-modified polymers in deionised water and aqueous DMSO (80% v/v).
- 2.2.6: Excitation peak-to-valley ratios and values of I_E/I_M for the pyrene labelled polymers.
- 2.2.7: Characterisation of the naphthalene labelled hydroxyethyl cellulose ethers.
- 2.2.8: Fluorescence decay measurements of 1.0 g/L naphthalene labelled polymers in aqueous and 80% DMSO solutions.
- 2.3.1: Dynamic surface tension values of mixed HEC-N+CH₃/SDS solutions at 23 °C, mJ/m².

CHAPTER 4:

- 4.4.1: Synthetic preparation of pyrene labelled cationic hydrophobically-modified hydroxyethyl cellulose ethers.
- 4.4.2: Synthetic preparation of naphthalene labelled cationic hydrophobically-modified hydroxyethyl cellulose ethers.

LIST OF ABBREVIATIONS

C ₁₂ E ₈	Octa-ethyleneglycol-mono-n-dodecyl ether
CAC	Critical aggregation concentration
CMC	Critical micelle concentration
CPC	Cetylpyridinium chloride
DMF	Dimethylformamide
DMSO	Dimethyl sulfoxide
DPC	Dodecylpyridinium chloride
DTAB	Dodecyltrimethylammonium bromide
DTAC	Dodecyltrimethylammonium chloride
EHEC	Ethylhydroxyethyl cellulose
EPB	Ethylpyridinium bromide
HEC	Hydroxyethyl cellulose
HEC-N+CH ₃	Polymer JR400
HEC-N+C ₁₂	Quatrisoft LM200
HEC-N+CH ₃ -Np	Naphthalene labelled analogue of JR400
HEC-N+C ₁₂ -Np	Naphthalene labelled analogue of LM200
HEC-N+CH ₃ -Py	Pyrene labelled analogue of JR400
HEC-N+C ₁₂ -Py	Pyrene labelled analogue of LM200
HM-EHEC	Hydrophobically-modified ethylhydroxyethyl cellulose
HM-HEC	Hydrophobically-modified hydroxyethyl cellulose
HPC	Hydroxypropyl cellulose
HTAC	Hexadecyltrimethylammonium chloride
JR400	Polymer JR400
LM200	Quatrisoft LM200
Np	Naphthalene
OTG	Octyl-β-D-thioglucopyranoside
Py	Pyrene
SDS	Sodium dodecylsulfate
SDeS	Sodium decylsulfate
SOS	Sodium octylsulfate
TTAB	Tetradecyltrimethylammonium bromide

CHAPTER 1

CHAPTER 1: INTRODUCTION AND BACKGROUND

1.1 Introduction

The field of polymer science has attracted considerable interest both academically and industrially in the pursuit of new materials with better performance, higher tensile strength, improved optical properties and increased heat resistance. These polymers have typically involved volatile organic compounds for their preparation, purification and/or application. With the enhanced environmental conscience of consumers and manufacturers, there is a demand for products that are safe for the environment and yet have a high degree of performance. This driving force has led to the growing interest in water-soluble and especially amphiphilic macromolecules able to deliver the same macroscopic physical properties that their organic soluble analogues have attained.

The term 'amphiphilic' refers to ionic or polar derivatives of hydrocarbons containing one segment that is water-soluble and another that is water-insoluble. The most common amphiphiles are surfactants and lipids. Water-soluble polymers consisting of a hydrophilic backbone to which hydrophobic segments are attached may also be considered amphiphilic or 'hydrophobically-modified'. Due to this dual nature, this class of polymer is known to exhibit interesting aqueous solution properties, leading to a variety of applications. The diversity of these applications originates from their ability to function as viscosity enhancers, thickeners, adsorbants and/or flow control agents. As an example,

improved viscosity can be achieved by polymers that contain both hydrophilic and hydrophobic segments.

The obvious attractiveness of water-soluble polymers has renewed interest, both academically and industrially, in materials found in nature, particularly polysaccharides. These biomass polymers or their derivatives have been found to possess thickening and gelation properties in water. Some examples of commercially successful biopolymers include sodium alginate obtained from seaweed kelp, hyaluronic acid or hyaluronan extracted from cocks combs, vitreous fluids or produced by bacteria, and a variety of derivatives of wood or cotton cellulose. These materials have found applications in the pharmaceutical, cosmetic, food, detergency and paint industries.

Due to the importance in industrial applications of these polymers, it is imperative to gain an understanding of the relationship between the chemical structure and the physical properties they exhibit in solution. Of particular interest, is the study of the synergistic interactions that exist between the polymers and co-solutes such as surfactants, alcohols and/or salts. At present, studies are directed towards determining aspects of the polymer/surfactant aggregates such as structure, composition and the mechanism of the association phenomena. It is evident by the enormous magnitude of articles published in scientific journals and presented at international conferences each year that these polymers are of incredible industrial value on a global scale.

Traditionally, the macroscopic interactions between polymers and polymer/surfactant mixed systems in solution have been investigated by methods such as viscosity and precipitation phase diagrams. As a means of elucidating the macroscopic

phenomena observed, studies were designed to investigate the molecular interactions producing these effects by such methods as dynamic light scattering, small angle x-ray scattering, small angle neutron scattering and nuclear magnetic resonance. A sensitive method that has come to be used as an informative means of studying the molecular associations between these species is fluorescence spectroscopy. A chromophore is used to detect changes in the microenvironment in which it exists. This is enhanced when the chromophore is chemically bound to the polymer. A further understanding of the aqueous solution behaviour of these systems can be investigated by studying the simultaneous surface interactions occurring at the air/water interface.

1.2 Background

Before proceeding, a brief background into the types of interactions, the nature of the polymers investigated and the techniques used to elucidate these molecular interactions will be presented.

1.2.1 Types of Interactions

The interactions that play a major role between molecules in aqueous solution can be classified as follows: electrostatic, hydrogen bonding and/or hydrophobic interactions.

Electrostatic Interactions

These interactions arise from forces of attraction or repulsion between charged particles of opposite (positive-negative) or like (positive-positive or negative-negative)

charge, respectively. Factors affecting the strength of the interaction include the size and charge of the counter-ion, steric effects and the ionic strength of the solution ¹⁰.

Hydrogen Bonding

Hydrogen bonding is a special type of Debye interaction. It is a weak chemical bond having the following distinguishing features : a) directional bond where the H...O combination is linear, b) two hydrogen bonded electronegative atoms can approach each other more closely than the sum of their crystal radii, c) the bond between the hydrogen atom involved in the bridge and the remainder of the molecule to which it belongs can be weakened due to a hydrogen bridge formation with another electronegative atom and d) bond enthalpy is in the range of 10-40 kJ/mol, which is lower than a chemical bond but higher than the three types of van der Waals forces ^{11,12}.

Hydrophobic Interaction

This type of interaction contributes greatly to the effects observed between species in aqueous solution and will therefore be discussed in more detail. Hydrophobic interaction is an unusually strong attraction between hydrophobic molecules or hydrophobic segments of molecules when dissolved in water. This interaction arises as a result of the unusual properties of water as a solvent and the known incompatibility of "oil and water" ¹¹.

When a non-polar molecule is introduced in an aqueous solution, the hydrogen bonds between water molecules must be rearranged from a tetrahedral orientation into

networks creating a cage-like cavity. A considerable amount of energy is required since many hydrogen bonds between water molecules have to be broken. The van der Waals energy gained by inserting the non-polar molecule into the cavity is not enough to compensate for the loss in energy incurred in the formation of the cavity ¹¹. If nothing else happens, the total Gibbs energy of dissolution would be high, positive and very unfavourable. Thus, other processes have to occur in order to compensate for this loss in energy. Water tetrahedrons in contact with the non-polar molecule will tend to reorient themselves so as to reform hydrogen bridges with as many neighbouring water molecules as possible ¹¹. There is a loss in entropy however, due to the reduction of the degrees of freedom of the adjacent water molecules. The formation of a cage of ordered water with a stronger structure than in liquid water is called the hydrophobic effect ¹². This ordered water is sometimes referred to as 'iceberg' water because it behaves as if it were frozen, even though it has no ice structure or any permanency ¹¹. The structure strongly depends on such properties of the solute as its size, shape, charge distribution, and ability to adjust its structure upon dissolution ¹¹.

Hydrophobic bonding is the direct consequence of the hydrophobic effect. Association of two non-polar molecules (or non-polar segments in molecules) in aqueous solution takes place because the hydrophobic bonding of the aggregate has a more negative Gibbs energy than the sum of the hydrophobic effects of the individual molecules

1.2.2 Amphiphilic Molecules and their Behaviour in Aqueous Solution

Amphiphilic molecules such as fatty acids, phospholipids and surfactants contain two segments that have drastically different solubility in water. A brief discussion of the behaviour of surfactants in aqueous solution will be followed by an extension to amphiphilic polymers and finally the interactions that exist between the two species will be considered.

1.2.2.1 Surfactants

Like other amphiphilic molecules, surfactants are a class of compounds comprised of two molecular blocks having a different affinity towards water. The non-polar or hydrophobic part is usually a linear or slightly branched hydrocarbon chain. The polar or hydrophilic part can be either ionic, for instance sulfate (OSO_3^-) and trialkylammonium (R_3N^+) moieties, or non-ionic such as oligo(ethylene oxide), saccharide, and glyceride groups⁵. The hydrophilic part is usually water-soluble showing a strong demixing with hydrocarbons. The hydrophobic part shows the opposite behaviour^{13, 1, 12}.

1.2.2.2 Solution Behaviour of Surfactants

Comprised of both a hydrophilic headgroup and a hydrophobic alkyl tail, surfactants tend to gather at the interface of two media of differing polarity. This decreases the interfacial energy and lowers the surface tension of the solution^{14, 15}. When all surfaces in contact with the solution are saturated with surfactants, other ways to hide the hydrophobic tails from the aqueous environment must be found. Macroscopic phase

separation is unlikely, since the hydrophilic headgroups prefer water contact. A microscopic phase separation takes place through the formation of aggregates where the surfactant headgroups are directed towards the aqueous environment, while the tails are hidden in an 'oil-like' interior^{14, 16, 17, 18}. Figure 1.2.1 illustrates the possible structures amphiphiles such as surfactants and lipids form in aqueous solution¹.

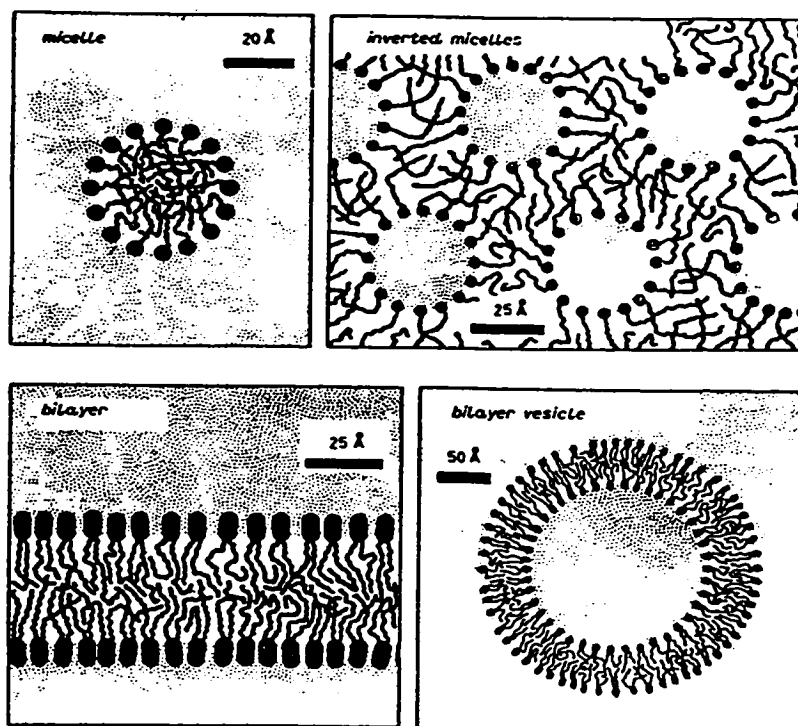


Figure 1.2.1: Variety of association structures of surfactants and lipids in aqueous solution¹.

Geometrical considerations have been used to rationalise the shape of these structures. The surfactant packing parameter:

$$N_s = v/l_c a_0 \quad (1.2.1)$$

describes the shape of a cone defining the volume that each surfactant has in the aggregate, where a_0 is the effective surfactant headgroup area, l_c is the effective length of the hydrocarbon tail, and v is the volume of the hydrocarbon chain (see figure 1.2.2) ^{19, 20, 21}.

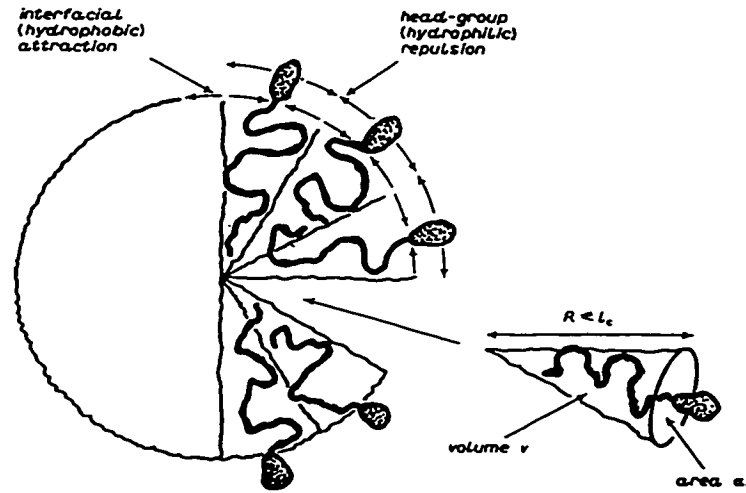


Figure 1.2.2: Surfactant packing parameter is dependent on head-group area a_0 , chain volume v , and chain length l_c ¹.

Figure 1.2.3 illustrates the dynamic packing properties of lipids and the variety of structures they may form. When the headgroup area is large, spherical aggregates form since the value of N_s is low, and there is a strong curvature towards the hydrocarbon tails ^{1, 16}. A smaller surfactant headgroup leads to a larger value of N_s , resulting in a decreased curvature towards oil and growth of the aggregate in one or two dimensions ¹⁶. Values of N_s over unity favour inverted structures having a curvature towards water. The hydrophilic headgroups generally struggle to achieve the biggest possible area, which increases the curvature of the aggregates formed. This is opposed by an increased unfavourable exposure of the surfactant hydrocarbon tails to water ¹⁶. These two opposing forces,

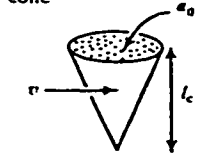

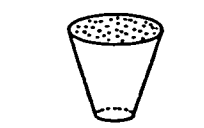
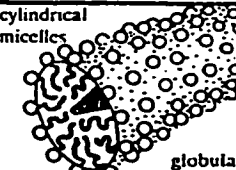
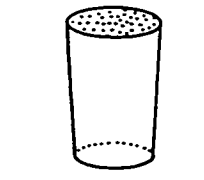
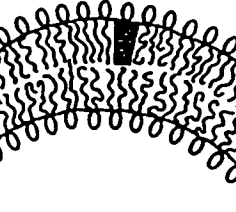
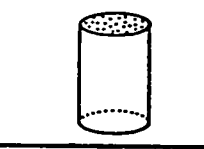
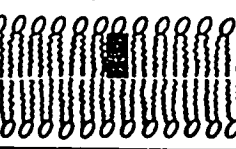
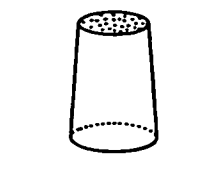
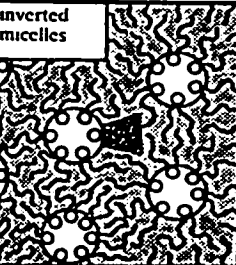
Lipid	Critical packing parameter v/a_0l_c	Critical packing shape	Structures formed
Single-chained lipids with large head-group areas: NaDS in low salt some lysophospholipids	< 1	cone 	spherical micelles 
Single-chained lipids with small head-group areas: NaDS in high salt C ₁₆ TAB in high salt, lysolecithin nonionic surfactants	$\frac{1}{2} - 1$	truncated cone or wedge 	cylindrical micelles  globular micelles
Double-chained lipids with large head-group areas, fluid chains: (C ₁₂) ₂ DAB, lecithin, sphingomyelin, phosphatidylserine, phosphatidylglycerol phosphatidylinositol, phosphatidic acid disugardiglycerides	$\frac{1}{2} - 1$	truncated cone 	vesicles, flexible bilayers 
Double-chained lipids with small head-group areas: anionic lipids in high salt saturated frozen chains, e.g. phosphatidylethanolamine phosphatidylserine + Ca ²⁺	~ 1	cylinder 	planar bilayers 
Double-chained lipids with small head-group areas, nonionic lipids, poly (cis) unsaturated chains, high T: unsaturated phosphatidylethanolamine Cardiolipin + Ca ²⁺ phosphatidic acid + Ca ²⁺ monosugardiglycerides, cholesterol (rigid)	> 1	inverted truncated cone 	inverted micelles 

Figure 1.2.3: Dynamic packing properties of lipids and the structures they form ¹.

together with the length of the hydrocarbon tail, determine the shape of the aggregate. At low surfactant concentrations, the first aggregation step is the formation of spherical aggregates or micelles. The surfactant concentration at which micelles first form, is referred to as the critical micelle concentration, or CMC^{22, 23}.

The tendency of surfactants to adhere to surfaces and later to form micelles is entropically driven by hydrophobic attraction. The thermodynamics of micelle formation may be rationalised by following figure 1.2.4. The rate of association is given by:

$$k_1 X_1^N \quad (1.2.2)$$

where k_1 is the rate constant of association, $N=1$ and X_1 correspond to isolated molecules or monomers in solution. Similarly, the rate of dissociation can be expressed by:

$$k_2 (X_N/N) \quad (1.2.3)$$

where k_2 is the rate constant of micelle dissociation, N is the aggregation number and X_N is the density of molecules incorporated in aggregates of number N . The ratio of the two 'reaction rates' may be expressed as:

$$k_1/k_2 = \exp[-N(\mu_N^0 - \mu_1^0)/kT] \quad (1.2.4)$$

where μ_N^0 is the mean free energy of interaction per molecule in aggregates of aggregation number N and μ_1^0 is the free energy of interaction corresponding to isolated monomers in solution. Thermodynamics requires that the chemical potential of all identical molecules be the same in a system of molecules that form aggregated structures in solution. The combination of these equations leads to¹:

$$\mu_N = \mu_1^0 + (kT/N) \ln(X_N/N) = \text{constant} \quad (1.2.5)$$

The higher CMC values for ionic compared to non-ionic surfactants results from the additional unfavourable contribution of the counter-ion entropy to micelle formation since the counter-ions have to be in the vicinity of the micelles ¹⁶. This can also be seen as an electrostatic repulsion between surfactant headgroups at the micellar surface.

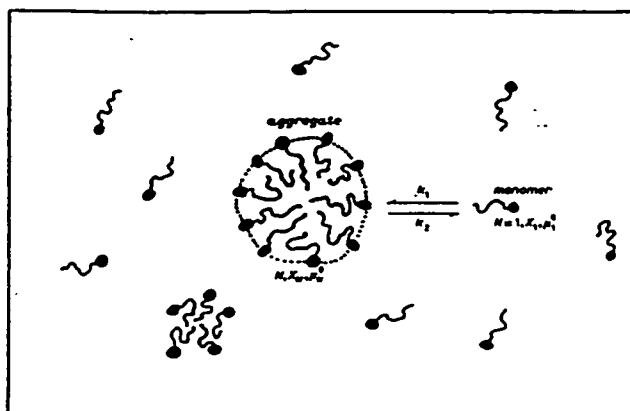


Figure 1.2.4: Association of N surfactants into a micelle ¹.

1.2.2.3 Polymers

A polymer can be described in simplest terms as a molecule of very high molecular weight comprised of many repeating monomer units. A homopolymer is a polymer that is made up of the same monomer unit. When the polymer consists of more than one monomer, the distribution of monomers along the chain may be: random, alternating in an ABAB fashion, or comprised of blocks of two or more monomers (ie. AAAABBBB....). If the monomer unit carries a charge, the polymer is referred to as a polyelectrolyte ²⁴.

1.2.2.4 Amphiphilic Polymers

A special class of polymers containing both hydrophilic and hydrophobic segments, are amphiphilic polymers (figure 1.2.5). Usually, the polymer backbone is hydrophilic and to it is chemically grafted a small amount of hydrophobic chains which give the resultant polymer properties that the precursor did not have. It is important to note that most amphiphilic polymers retain the water-solubility of their precursors. The hydrophilic portions are exposed to the aqueous solution, and the hydrophobic segments form 'oil-like' microdomains^{25, 26, 27}.

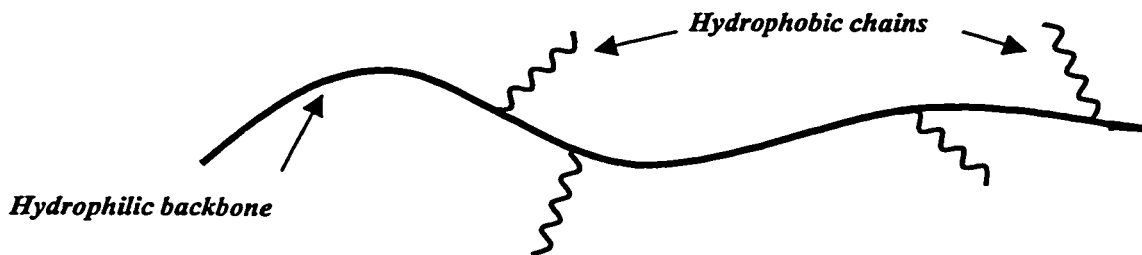


Figure 1.2.5: Structure of a generic amphiphilic polymer.

1.2.2.5 Solution Behaviour of Polymers and Amphiphilic Polymers

There are two types of fluid flow: Newtonian and non-Newtonian. Newtonian fluids obey Newton's law for viscous flow:

$$\tau = \eta\gamma \quad (1.2.6)$$

where τ represents the shear stress of a fluid given in Pascal, η is the viscosity of the solution and γ is the shear rate, in s^{-1} . Non-Newtonian fluids such as polymer melts, colloids and suspensions do not obey this law.

Non-Newtonian fluids display two types of flow behaviour: viscoelastic and viscoelastic. Polymer solutions are known to exhibit viscoelastic flow behaviour characterised by both viscous (permanent) and elastic (temporary) responses to applied stress. For polymer solutions, the viscous responses to stress are more important than the elastic responses and can be treated separately.

The viscous character of non-Newtonian fluids depends on the flow conditions specified by the rate of strain described by:

$$\tau = \eta_a(\dot{\gamma})\dot{\gamma} \quad (1.2.7)$$

In this equation, $\eta_a(\dot{\gamma})$ is the apparent viscosity where η_a depends on the value of the local strain rate $\dot{\gamma}$. Apparent viscosity is illustrated in figure 1.2.6 plotting the shear stress τ vs. the strain rate $\dot{\gamma}$. For Newtonian fluids, the plot is linear, where the slope is the viscosity of the solution. However, for non-Newtonian fluids there are two deviations from linearity: shear thinning and shear thickening. In shear thinning, the apparent viscosity decreases as the strain rate increases, whereas in shear thickening, there is an increase in the apparent viscosity with increasing strain rate. Shear thinning behaviour is important for polymer solutions and melts. This can be illustrated by figure 1.2.7. When the shear rate is low as in region A, there is a nearly constant viscosity value. As the shear is increased, there is a decrease in the viscosity of the solution. This second region is characterised by a power-law dependence of shear stress and viscosity on shear rate:

$$\tau = K\dot{\gamma} \quad (1.2.8)$$

where K is the fluid consistency. Finally at very high shear rates, the viscosity of a polymer solution will again approach a constant value.

On a molecular scale, when a dilute polymer solution is at rest, the polymers are oriented in an aggregate of entangled chains. When a stress is applied and flow occurs, the chains must slide past one another causing disentangling of the polymer chains to occur. When the stress rate is low, there is a low level of disentangling. As the stress rate is increased, the amount of disentangling will also increase. Since the resistance to flow or viscosity is dependent on the degree of entanglement of the polymer chains, viscosity will decrease as the strain rate is increased.

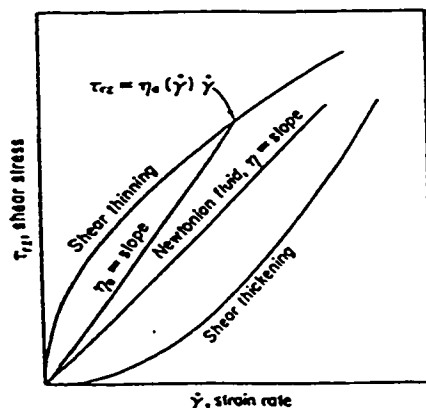


Figure 1.2.6: Apparent viscosity of solutions illustrated by plotting the shear stress versus strain rate ².

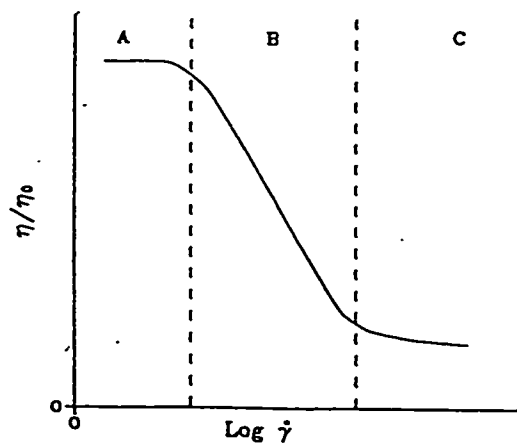


Figure 1.2.7: Characteristic behaviour of polymer solution viscosity as a function of shear rate ³.

As in the case of small amphiphilic molecules, water molecules around hydrophobic segments in amphiphilic polymers are known to adopt an ‘ice-like’ structure. Solvent structuring occurs because the water molecules surrounding the hydrophobic residues tend to form the largest possible number of hydrogen bonds among themselves¹⁶. When the hydrophobic residues interact with one another in solution, they will tend to aggregate by releasing the structured water into free water in the bulk phase (figure 1.2.8a). Again, the driving force for this hydrophobic aggregation is a large increase in entropy which is sufficient to overcome a positive enthalpy change due to the break-up of the hydrogen bonds²⁸. The aggregation creates a three dimensional network structure in solution resulting in a significant macroscopic effect on solution properties such as viscosity¹⁶.

In the case of amphiphilic polyelectrolytes, the hydrophobic attractive force is balanced to some extent by the electrostatic repulsive forces. The degree of ionisation plays a critical role in determining if hydrophobic aggregation will occur²⁸.

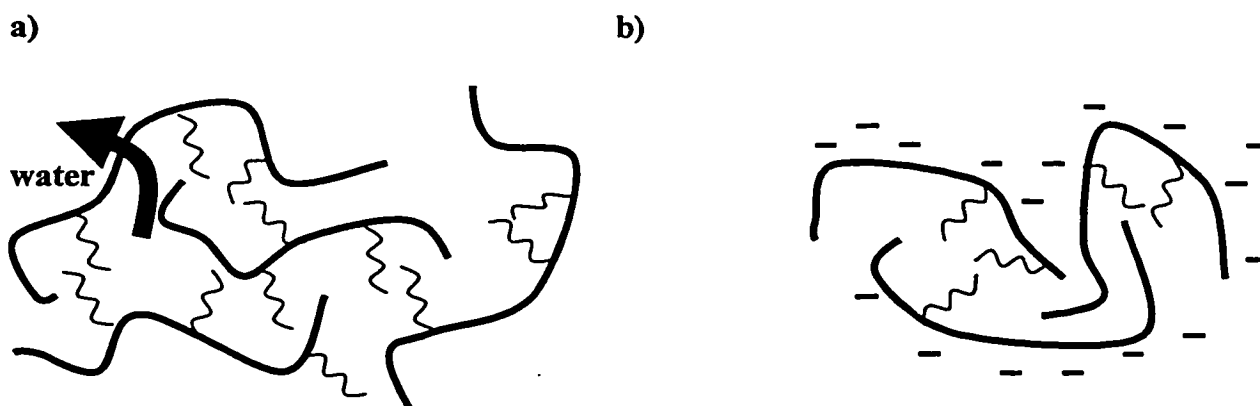


Figure 1.2.8: Schematic diagram illustrating the aqueous solution behaviour of amphiphilic a) polymers and b) polyelectrolytes.

1.2.2.6 Amphiphilic Polymer/Surfactant Mixtures

Air/Water Interface

Investigations of the interactions between polymers and surfactants at the air/water interface have been studied by a variety of experimental techniques such as specular reflection of neutrons^{29, 30}, surface tension^{25, 26, 27, 31}, and radiotracer measurements³². They have demonstrated that solutions of polymer/surfactant mixtures differ substantially from solutions of pure polymer or pure surfactant.

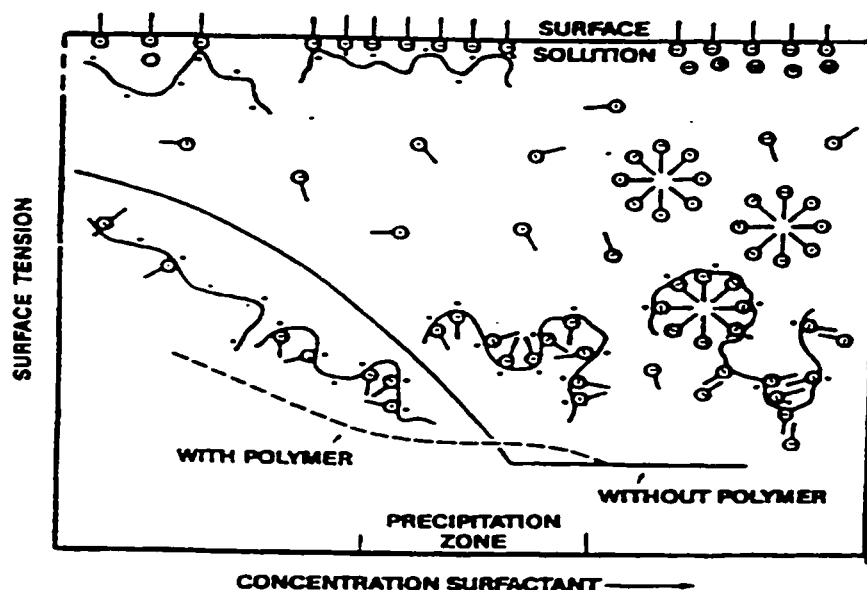


Figure 1.2.9: a) Plot of surface tension versus the logarithm of surfactant concentration with a schematic representation of the complexes formed as surfactant concentration is increased⁴.

A plot of surface tension vs. the logarithm of surfactant concentration given in figure 1.2.9 illustrates that three distinct regions can be observed. At low surfactant

concentrations, single surfactant molecules may be binding to the polymer. Increasing the surfactant concentration leads to a first transition point, which represents the onset of formation of polymer/surfactant complexes, consisting of surfactant molecules clustered in sub-units adsorbed onto the polymer, resembling a string of beads. Further addition of surfactant to the solution leads to the formation of more of these polymer bound micelles until the polymer is saturated. After this point, regular surfactant micelles start to form and the behaviour at the interface is that of pure surfactant solutions²⁹.

Solution

In the presence of polymers, surfactant molecules will generally bind forming clusters that resemble the micelles formed in the absence of polymer^{33, 34, 35}. This gives rise to polymer/surfactant systems that are able to control the rheology of the solution over wide concentration ranges³⁶. The binding interaction is greatly enhanced if the polymer is less polar or contains hydrophobic segments⁵. Here, the contact between a surfactant cluster and two polymer segments is favourable. The two segments can be in the same polymer chain, a behaviour typical in dilute solutions. Surfactant clusters may also entrap segments of polymers if the solution is concentrated enough to allow extensive chain overlap⁵. This will result in the creation of a three dimensional network structure (figure 1.2.10) having dramatic rheological effects on the solution.

Amphiphilic or hydrophobically-modified polymers show a weak tendency to self-associate even in the absence of surfactant. This may be strongly enhanced by the formation of surfactant aggregates around hydrophobic segments from two or more

polymer molecules. At very high surfactant concentration, the three-dimensional network will be broken due to the saturation of the polymer by the surfactant and the solution will lose its enhanced rheological effects^{33, 16}.

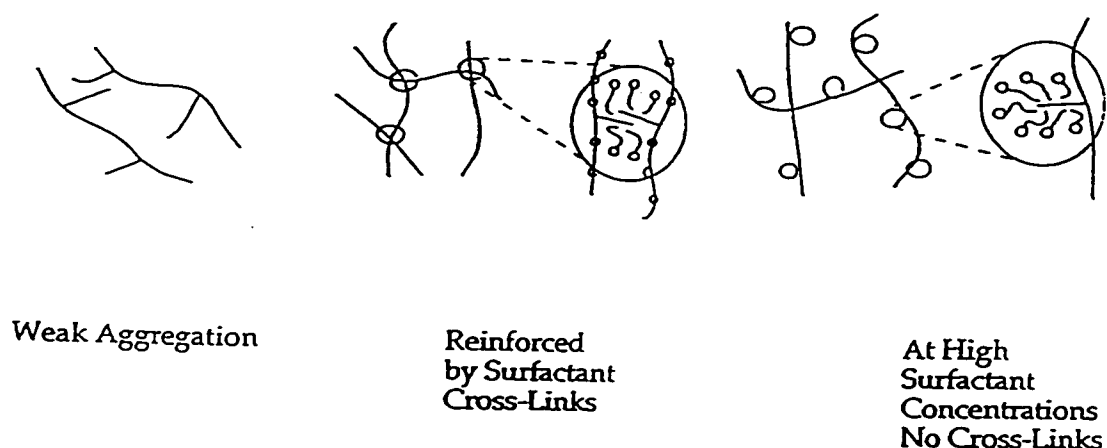


Figure 1.2.10: Schematic representation of polymer/surfactant complexes occurring in solution with increasing surfactant concentration⁵.

Two models have been proposed to interpret polymer/surfactant interactions³⁷. One model looks at the surfactant binding to the polymer chain. Binding isotherms indicate a strong cooperativity in binding and the onset of binding is defined by a critical aggregation concentration or CAC^{25, 38, 5}. The CAC varies depending on the system and will decrease strongly with increasing surfactant chain length. The other model analyses the effect of the polymer on the micellisation of the surfactant. The polymer affects the stability of a micelle by short or long range interaction^{35, 5, 39}. The main driving force for surfactant self-assembly in polymer/surfactant systems is also the hydrophobic interaction between alkyl chains. Usually surfactants carrying a charge will interact more significantly

with charged polymers. This is attributed to the unfavourable contribution of electrostatic effects and their partial elimination due to charge neutralisation or lowering of the charge density on the energetics of aggregate formation³⁹. Ionic surfactants are also known to interact with neutral polymers, however the association is not as strong as in the case of polyelectrolytes. In the case of non-ionic surfactants, there is little to gain in forming aggregates in the presence of a polymer and they generally do not interact strongly with polymers. If the polymer is hydrophobically-modified, a hydrophobic group/surfactant interaction will be significant. This higher specificity in the interaction leads to a lower CAC, a lower cooperativity and a lower aggregation number⁵.

1.3 Techniques Used to Study Solution Properties

Traditional methods used to study the macroscopic interactions occurring between polymers and surfactants in bulk solution include viscosity^{40, 41} and precipitation experiments. As a means of understanding these macroscopic phenomena, studies were directed at interpreting the molecular interactions causing them. A method that has come to be used as an informative means of studying the molecular interactions between these species is fluorescence spectroscopy^{42, 28, 43, 44, 45}.

The absorption of electromagnetic radiation by a molecule results in the excitation of an electron from a lower ground state to a higher excited molecular quantum state. This energetically unstable excited molecule may rearrange, chemically fragment or undergo physical pathways to lose its excitation and return to the ground state. These rapid de-excitation pathways may be classified as being radiative, non-radiative or quenching

processes. A Jablonski diagram as shown in figure 1.3.1 may be used to illustrate the radiative and non-radiative processes that occur after the absorption of radiation. Radiative transitions are indicated by straight arrows and non-radiative processes are indicated by wavy arrows. Absorption is shown to occur from the vibrationless level of S_0 ($v'' = 0$) to some vibrationally excited level of S_1 ($v' = 0,1,2,3\dots$). Fast vibrational relaxation ($< 10^{-12}$ s) due to collisions with solvent molecules collapses the vibrational population down to the vibrationless level of S_1 ($v' = 0$). From this level, the excited electron may undergo radiative fluorescence or non-radiative internal conversion (IC) back down to the singlet ground state (S_0). Fluorescence, a spin-allowed transition has no change in the spin multiplicity of the electron and typically occurs on a time scale between 10^{-9} and 10^{-7} seconds. Another non-radiative process which may occur is intersystem

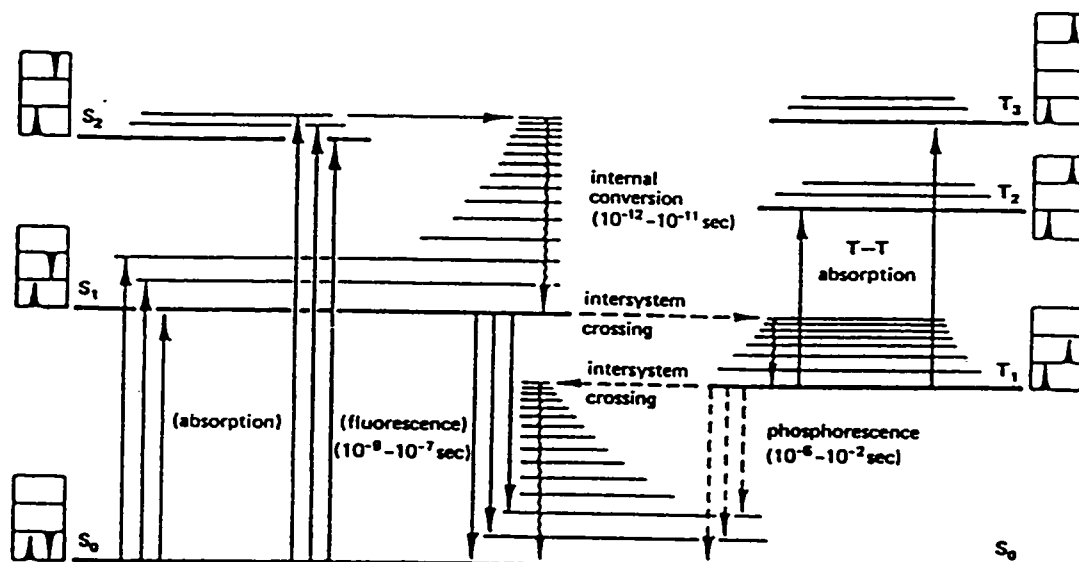


Figure 1.3.1: Jablonski diagram illustrating the radiative and non-radiative processes possible after electronic excitation ⁶.

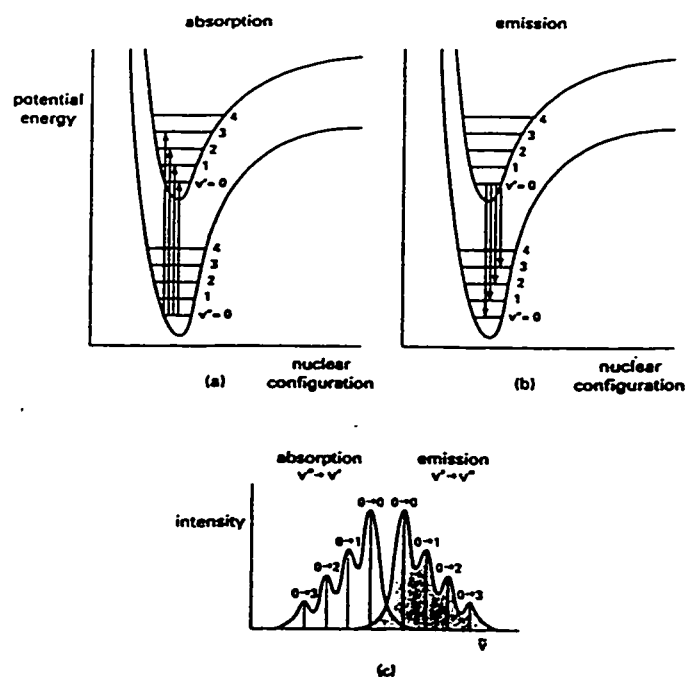


Figure 1.3.2: Potential energy curves showing individual vibrational energy levels and their involvement in a) adsorption and b) emission; c) illustrates the resulting structured absorption and emission spectra ⁷.

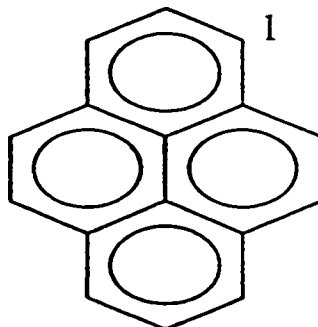
crossing (ISC) to an excited triplet state (T_1). This process results in the inversion of the spin multiplicity of the excited electron. From T_1 , the excited electron may relax down to S_0 by the emission of phosphorescence or it may undergo a reverse ISC leading to delayed fluorescence ^{7, 46, 47}.

The mirror symmetry observed for the absorption and emission spectra of an organic compound in a non-polar solvent may be explained by following figure 1.3.2. The broad absorption spectrum (figure 1.3.2c left) has features that are assigned to different Franck-Condon vibronic transitions, the most intense being due to the Franck-Condon vibrational overlap integral. By the Franck-Condon principle, the 0-0 transition will be the most intense if there is not a great difference in the nuclear configuration of the molecule

in its excited and ground states (figure 1.3.2a). Vibrational excitation to higher excited states will be rapidly lost by collisions with solvent molecules and the excited electron will relax down to $v' = 0$ level of the first excited electronic state. Applying the Franck-Condon principle for the emission process will mean that the 0-0 transition is the most intense (figure 1.3.2b). Emission from $v' = 0$ down to $v'' = 1,2,3$ etc. is also possible and is accompanied by the emission of radiation to lower energy (longer wavelengths) than that of the 0-0 transition. If the vibrational level spacings are similar in both the ground and excited states, the emission spectrum will appear as a mirror image of the absorption spectrum (figure 1.3.2c). The small difference in the wavelengths of the 0-0 absorption and emission transitions is related to the properties of the solvent molecules and their slightly different interactions with the two electronic states.

Molecules that are able to absorb energy and emit radiation in the form of light are usually aromatic compounds containing delocalised electrons. Pyrene (structure shown in figure 1.3.3a) has been used extensively as a fluorescent dye since it has a characteristic emission that is sensitive to changes in its environment. The absorption and fluorescence spectra of aromatic molecules such as pyrene having a minimum D_{2h} symmetry are known to exhibit mixed polarisation due to the vibronic coupling between the first (S_1) and second (S_2) singlet excited states ⁶. The weak first singlet absorption ($S_0 \rightarrow S_1$) band is symmetry forbidden. Solvent interactions have been shown to perturb the relative intensities of the weak electronic transitions of the forbidden vibrational fine structures of the fluorescence spectra. This is known as the Ham effect. Figure 1.3.3b shows the room temperature fluorescence spectra of pyrene in various solvents. The principal vibronic

a)



b)

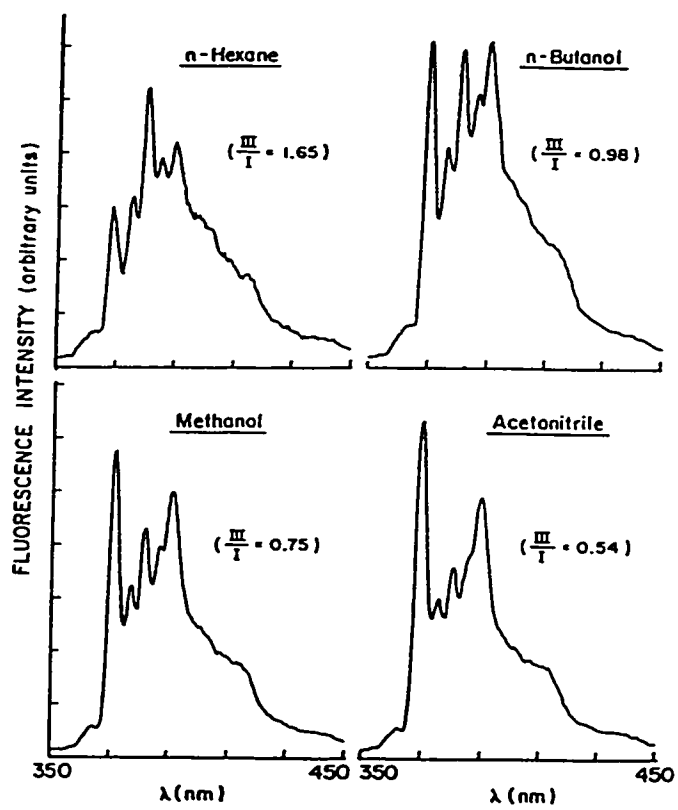


Figure 1.3.3: a) Structure of pyrene b) solvent dependence of vibronic band intensities in pyrene monomer fluorescence at room temperature (pyrene conc. 2×10^{-6} mol/L, $\lambda_{exc} = 310$ nm) ⁶.

bands are numbered I-V, where band III ($0-737\text{ cm}^{-1}$) is at 398 nm and band I (0-0) is at 372 nm⁶. It can be seen that the variation of the allowed band III is minimal, whereas band I shows significant changes in intensity in polar environments. The peak intensity ratio I/III (or I_1/I_3) of the fluorescence spectrum can therefore serve as a measure of the polarity of the pyrene environment. The solubility of pyrene in water is very low ($\sim 5 \times 10^{-7}$ mol/L). In a solution of amphiphilic compounds pyrene will prefer to reside in non-polar micro-domains. This preferred solubilisation will be reflected by a change in the emission spectrum. Thus, the I_1/I_3 ratio is used to determine the critical micelle concentration of surfactant micelles and the critical aggregation concentration of mixed polymer/surfactant systems.

There are several photophysical techniques available to help elucidate the molecular behaviour of aqueous polymer solutions. These include fluorescence probe, label, lifetime, quenching and non-radiative energy transfer experiments.

1.3.1 Probe Studies

A probe study is one in which the chromophore is dissolved in solution. Probes such as pyrene are able to give an indication of the presence of hydrophobic microdomains in aqueous solution. As described above, the tool is the ratio of the first vibronic band to the third vibronic band (I_1/I_3) in the emission spectrum of pyrene^{46, 47, 48}.

Figure 1.3.4 illustrates the changes that occur in the fluorescence spectrum of pyrene with increasing surfactant concentration. In the absence of polymer or in very

dilute polymer or surfactant solutions this ratio is usually about 1.8⁴⁸. As the probe enters hydrophobic microdomains created either by the aggregation of hydrophobic groups on the polymer or by mixed polymer/surfactant aggregates, this ratio decreases to about 1.3. The CMC of surfactant or the CAC of mixed polymer/surfactant systems was taken as the midpoint in the drop of the ratio of I_1/I_3 plotted against the logarithm of the surfactant concentration.

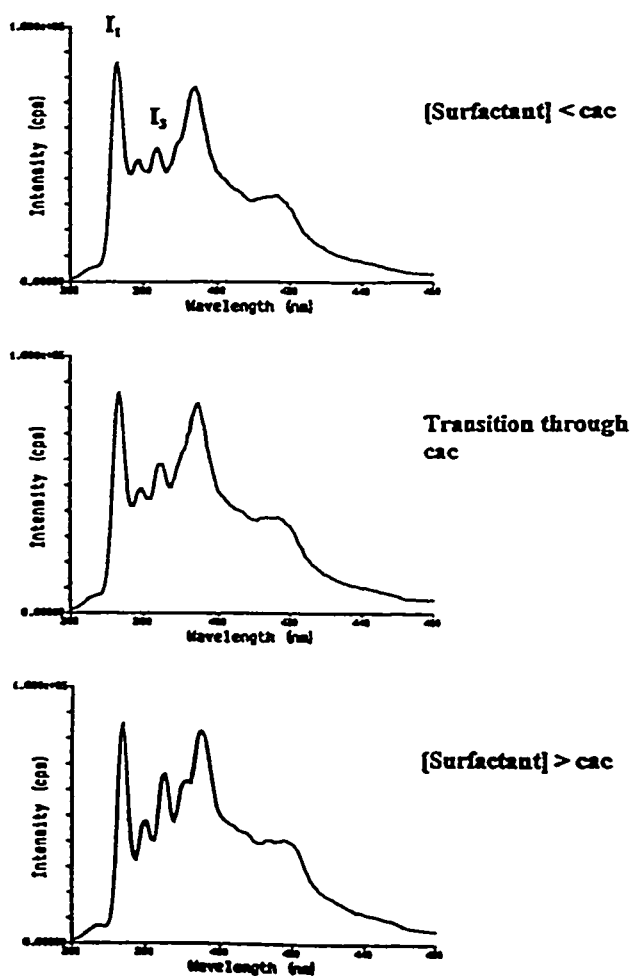


Figure 1.3.4: Change in the intensity of I_1 and I_3 of pyrene emission spectra with increasing surfactant concentration.

1.3.2 Label Studies

Chromophores can be attached to polymer chains by three methods: copolymerisation of a dye-substituted monomer, polymer post-modification, or labelling of a reactive polymer. By polymer post-modification, commercial or natural polymers can be labelled without any significant change in molecular weight or distribution. Ether, ester and amide linkages are normally used. In all cases, it is important that the chromophore attached to the polymer does not drastically change the properties of the polymer from that of the unmodified polymer. The degree of labelling is therefore usually kept low.

A distinct difference in comparing the emission spectra of dilute pyrene concentrations with that of higher pyrene concentrations as is the case in label studies, is the presence of a rather broad structureless low energy band centred at 485 nm referred to as an excimer (figure 1.3.5)^{49, 46, 47, 8}. Birks⁵⁰ explained this phenomenon in terms of the formation of a complex containing two pyrene molecules, one in its first electronically excited state and the other in the ground state.

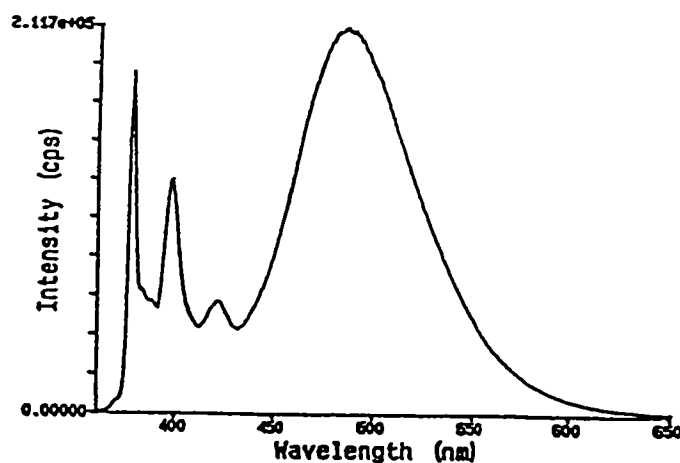
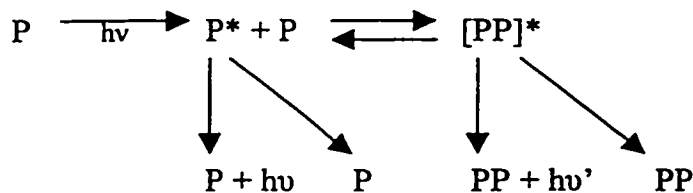


Figure 1.3.5: Emission spectrum of pyrene labelled onto polymers: broad excimer emission centred at 485nm ($\lambda_{exc} = 344\text{nm}$).

The complex was given the name “excimer” since it is a *dimer* stable only in the electronically *excited* state ⁷. The formation of a pyrene excimer requires the encounter of an electronically excited pyrene with a second pyrene in its ground electronic state ^{47, 50, 8}. Förster and Kasper proposed the following scheme for excimer formation ⁶:



The classical mechanism, referred to as a dynamic excimer formation, assumes that the two pyrenes are sufficiently far apart when a photon is absorbed, so that the excitation is localised on one of them. In this case, both the monomer and excimer emission originates from the same excited species. Excimer-like emissions, referred to as static excimers, where the monomer and excimer emissions arise from two different excited species can also be observed under special conditions ⁸.

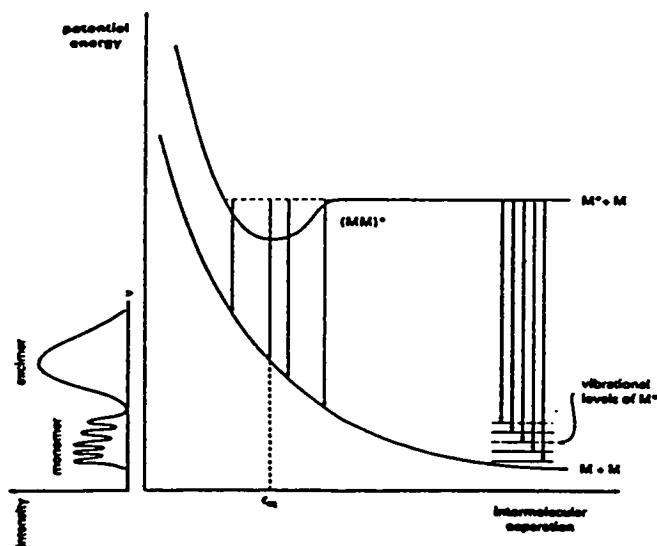


Figure 1.3.6: Intermolecular potential energy curves for monomer and excimer ⁷.

Figure 1.3.6 illustrates the potential energy versus the separation distance between the two components of the excimer. At small intermolecular separation, two ground state molecules undergo mutual repulsion resulting in the lower potential energy curve. If one of the molecules has electronic excitation, considerable attraction between the excited state and ground state species occurs. At a distance r_{eq} , a bound complex or excimer is formed. The electronically excited excimer will undergo all the photophysical processes available to an excited species. Due to the absence of a bound ground state, the emission leads to dissociation of the complex. As observed in figure 1.3.6, the vibrationless level of the bound excimer has a lower energy than that of the separated components $M^* + M$. Emission of light from the lowest level of the excimer involves a transition to the lower repulsive potential energy surface with a considerably smaller energy difference compared to the emission from the excited monomer. A release of photons at lower frequency or longer wavelengths compared to the monomer emission explains the red-shift of the excimer emission band compared to the monomer. The excimer emission is structureless since the Franck-Condon envelope now includes a multitude of overlapping levels associated with the low-frequency vibrations making it impossible to distinguish any vibronic structure in the emission spectrum^{46, 7, 6}.

The photophysical parameters that can be utilised in label studies are obtained from several sources. From the absorption spectrum, one is able to obtain an indication of pyrene pre-association by the broadening of the absorption bands compared to systems where the pyrene is molecularly dissolved. This information is given by the peak-to-valley ratio of the absorption spectrum (P_A), which is usually > 3.0 in the absence of pre-

association, and decreases with the extent of pre-association ⁸. Accompanying this broadening is a small red shift in the maximum position and a decrease in the extinction coefficients (hypochromicity).

From excitation spectra, one can determine if the pyrene excimer emission originates from a dynamic or static mechanism. In the dynamic case, spectra monitored at the monomer and excimer emission wavelengths are superimposable, indicating that they originate from the same excited species. In the static case, the spectra will not be superimposable. The spectrum monitored at the excimer emission wavelength will be red shifted by 1 to 4 nm and broadened relative to that of the monomer emission wavelength (figure 1.3.7), indicating that this pyrene excimer originates from two different absorbing species: pre-associated pyrenes and spatially isolated excited pyrene forming an excited state complex with a pyrene in its ground state.

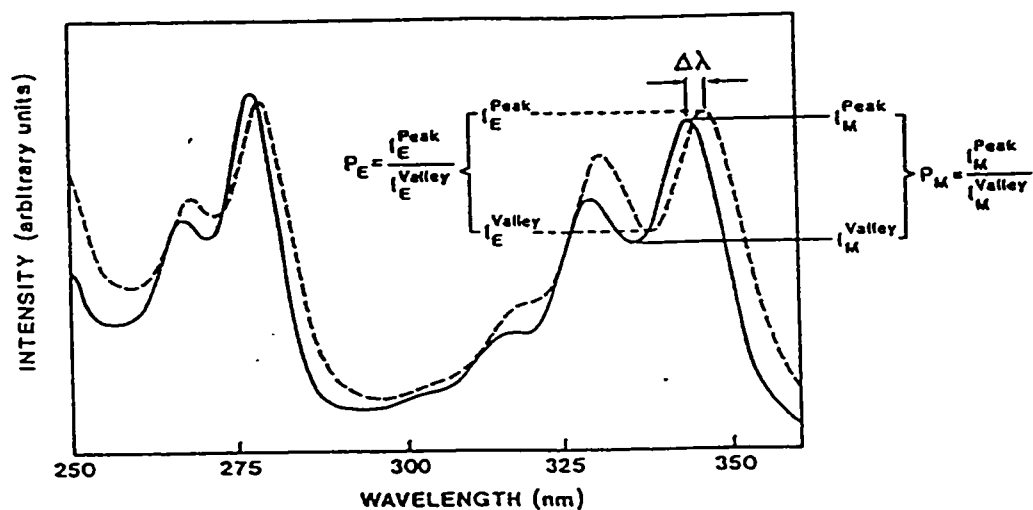


Figure 1.3.7: Excitation spectra monitored at the monomer (377 nm) and excimer (485 nm) emission wavelengths indicating the presence of static excimers ⁸.

Fluorescence spectra can be obtained from steady state or time dependent experiments. From the steady state fluorescence spectrum, one obtains two useful parameters. The ratio of the intensity of the excimer emission to the intensity of the monomer emission (I_E/I_M) and λ_E , the wavelength corresponding to the maximum of excimer emission.

The lifetime of the pyrene emission from the singlet excited state (S_1) to the singlet ground state (S_0) was determined by time-correlated single photon counting experiments^{47, 7, 51}. The emission intensity of an excited species is monitored as a function of time after the generation of an excitation pulse. Decay profiles are fit to the sum of exponentials. The complexity of the analysis may give an indication of the chromophore distribution in the labelled polymers.

1.3.3 Fluorescence Quenching Studies

The quenching of molecular emission involves the transfer of excitation energy from an excited donor chromophore (M^*) to a non-radiative acceptor molecule (Q) in a bimolecular process:



In the presence of quencher, the rate of decay of the excited state is increased due to this additional deactivation pathway^{7, 6}.

Quenching in homogeneous solutions is a diffusion controlled reaction. The rate of this bimolecular reaction is equal to:

$$k_q[M^*][Q] \quad (1.3.2)$$

where k_q is the rate constant of the quenching process. If the rate of the absorption process ($M + h\nu \rightarrow M^*$) is given by:

$$k_{\text{abs}}[M][h\nu] \quad (1.3.3)$$

where k_{abs} is the rate constant for excitation. The fluorescence ($M^* \rightarrow M + h\nu'$) rate is given by:

$$k_f^0[M^*] \quad (1.3.4)$$

where k_f^0 is the rate constant for fluorescence; and the rate of all other decay pathways ($M^* \rightarrow M$) is given by:

$$\Sigma'k_i[M^*] \quad (1.3.5)$$

where $\Sigma'k_i$ is the sum of the rate constants for all other intramolecular decay pathways, then by assuming steady state conditions, M^* may be expressed as:

$$[M^*] = \frac{k_{\text{abs}}[M][h\nu]}{\Sigma k_i + k_q[Q]} \quad (1.3.6)$$

The corresponding quantum yield for fluorescence is given by:

$$\Phi_f = \frac{k_f^0}{k_f + k_q[Q]} \quad (1.3.7)$$

where $k_f = \Sigma k_i$ is the observed rate constant for fluorescence decay in the absence of quencher. The fluorescence yield is reduced by the presence of quencher by an amount that is proportional to the concentration of quencher. The quantum yield in the absence of quencher is given by:

$$\Phi_f^0 = k_f^0/k_f = \tau_f/\tau_f^0 \quad (1.3.8)$$

where τ_f and τ_f^0 are the fluorescence lifetimes in the presence and absence of quencher.

The ratio of these quantum yields, called the Stern-Volmer relation:

$$\Phi_f^0/\Phi_f = 1 + \frac{k_q [Q]}{k_f} \quad (1.3.9)$$

is linearly dependent on $[Q]$, with an intercept at $[Q] = 0$ of unity.

This describes the classical dynamic quenching case. Static quenching may occur as the solute concentrations are increased if the added solute forms a nonfluorescent complex with the ground-state probe. In this case, the process is viscosity independent since no molecular collisions are involved ^{7, 6}.

Fluorescence quenching experiments using surfactant quenchers will lead to further evidence of polymer/surfactant complexation since interaction should result in an overall decrease in the fluorescence emission intensity of the labelled polymer. Using the lifetime of the chromophore in the absence of quencher, one is able to apply the Stern-Volmer model to determine the rate constant (k_q) of bimolecular quenching in mixed polymer/surfactant systems ⁷.

1.3.4 Fluorescence Non-Radiative Energy Transfer Studies

A photophysical technique used to investigate the mechanism of association between polymer chains is the non-radiative transfer of energy from an excited state donor chromophore (M^*) to an acceptor chromophore in its ground state (N) whose absorption spectra overlaps the fluorescence of the excited molecule ^{7, 47, 52, 6}:



The probability of energy transfer is dependent on the extent of the overlap. In addition to the trivial reabsorption of the emitted fluorescence of the donor by the acceptor, there is

transfer of excitation energy by coulombic and/or electronic exchange interactions. The rate of dipole-dipole coulombic energy transfer may be expressed as:

$$k = (1/\tau_D)(R_0/r)^6 \quad (1.3.11)$$

where τ_D is the mean lifetime of the donor excited state, r is the interchromophore distance and R_0 is the critical distance at which the energy transfer and donor excited state deactivation by fluorescence or internal quenching are of equal probability. Coulombic energy transfer occurs over long distances, typically 20-60 Å⁶.

The naphthalene (donor, M*) labelled polymer and pyrene (acceptor, N) labelled polymer pair are extensively used in such studies. They are known to interact by transfer of energy at a critical distance, $R_0 = 30 \text{ Å}$ ⁵³. The probability of this interaction is dependent on the separation distance of the chromophore as well as their relative orientation. By exciting the naphthalene donor at a wavelength of 290 nm, it is possible to detect both a direct emission from excited naphthalene as well as the emission of pyrene excited by the transfer of energy from excited naphthalene moieties. The ratio of the intensity of pyrene emission originating from energy transfer to the intensity of the naphthalene emission, I_{Py}/I_{Np} , gives an indication of the extent of energy transfer in the system and thus illustrates the extent of association of the polymer chains.

1.4 Techniques Used to Study the Solution Properties at the Air/Water Interface

Fluorescence spectroscopy is a useful method for studying the interactions occurring between polymers and co-solutes in bulk solution. The determination of the simultaneous interactions occurring at the surface of the solution is also of interest⁵⁴.

Traditional methods to assess the interaction of polymers and surfactants at the air/water interface have included surface tension and interfacial tension measurements ⁵⁵.

The interest in the microscopic interactions occurring at the air/water interface of polymer and mixed polymer/surfactant systems has prompted many investigations recently to elucidate both the experimental and theoretical aspects involved in these interactions. Prigogine and co-workers introduced a monolayer theory to explain the surface tension of polymers where the amount of polymer adsorbed remains constant over a wide range of polymer solution compositions ⁵⁶. This theory was confirmed by Gaines ⁵⁷ and Siow and Patterson ⁵⁸, if the polymer segments were preferentially adsorbed at the interface, and the molecular weight of the polymer was sufficiently high. In this case, the interface concentration of polymer remained high and constant for a wide range of bulk concentrations ⁵⁹.

Surface tension experimental results of water-soluble polymers have not been as easily explained, as is the case in organic solvents. It is expected that most water-soluble organic polymers should be preferentially adsorbed at the solution surface due to the high surface tension of water ⁶⁰. Studies have been reported on the surface tension of aqueous solutions of poly(ethylene oxide) ⁶¹, poly(vinyl alcohol), poly(vinyl acetate) and poly(vinyl pyrrolidone) ^{62, 63} however, none displayed a relatively constant steady-state surface tension over more than one order of magnitude in concentration.

It was reported by Chang and Gray ⁵⁹, that in the case of aqueous solutions of hydroxypropyl cellulose (HPC), the steady-state surface tension is independent of large changes in concentration and molecular weight. It was also reported that the rate of change

of surface tension with time, depends on the concentration and diffusion constant of the solute for low solute concentrations and high molecular weights.

Evidence of surface activity as observed by the surface tension reduction of water by polymer and mixed polymer/surfactant solutions can be determined by dynamic surface tension studies ^{64, 65, 66, 67, 68, 31, 69}.

Experimentally, there are several techniques available for measuring the surface tension of polymeric solutions. These include the Wilhelmy plate, Du Nuoy ring, and capillary rise techniques. An alternative approach is based on the shape of a sessile or pendant drop. There are several advantages of pendant and sessile drop methods. These include the small amount of liquid required. The methods are easily facilitated to study either liquid-vapour or liquid-liquid interfacial tensions, and they can be applied to materials ranging from organic liquids to molten metals and from pure solvents to concentrated solutions. The magnitude of the measured surface or interfacial tension is without limitation. Additionally, the measurements can be made over a range of temperatures and pressures. Finally, since the drop profile can be recorded by photographs or digital images ⁷⁰, dynamic systems where the surface properties are time dependent may also be studied ⁷¹.

To quantify the observations made by the simple talc method (described below), investigations into the interactions occurring at the air/water interface of Polymer JR400 and mixed polymer/surfactant solutions were studied by dynamic surface tension. Experiments were conducted using the Axisymmetric Drop Shape Analysis-Profile method described by Neumann ⁷². In such experiments, a pendant drop is continuously

expanded and compressed in order to reach equilibrium at a faster rate. The digitised profile of the pendant drop is then fit to a Laplacian equation to obtain the surface tension

71.

1.4.1 Surface Viscoelasticity Studies [Appendices 3 and 4]

A simple technique referred to as the talc method was devised to determine if interfacial association structures are present in mixed polymer/surfactant systems ^{73, 74}. It relies on the effect of the interfacial composition on the surface rheology of mixed solutions. The presence of high molecular weight polymers at the interface is expected to affect the two dimensional flow properties. The flow property of the polymer/surfactant system is expected to show surface viscoelasticity at concentrations of the polymer below the saturation point of the mixed system. As the surfactant concentration is increased above this point, mixed polymer/surfactant aggregates will fall away from the interface and the surface will then consist of only surfactant molecules showing no viscoelasticity.

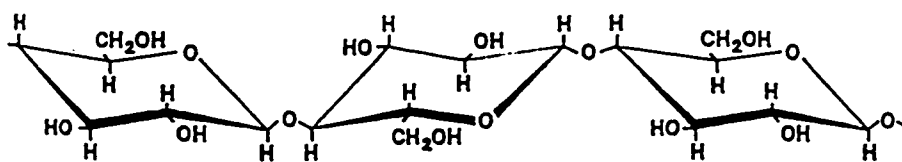
1.4.2 Foam/Film Stability Studies [Appendix 4]

Association of mixed polymer/surfactant complexes can also be studied by observing the stability of foams and lamellar films. A rigid interfacial interaction results due to complexation of polymers and surfactants of opposite charge. This leads to increased stability of either the aqueous foam or film in comparison to the surfactant or polymer solution alone ⁷⁵.

1.5 Cellulose Ethers

Ether derivatives of natural cellulose and their hydrophobically-modified analogues can function as thickeners, flow-control agents, suspending aids, protective colloids, water binders, liquid crystals, film formers or thermoplastics. These diverse functions have led to applications in such industries as food, paint, oil recovery, paper, cosmetics, pharmaceuticals, adhesives, printing, agriculture, ceramics, textiles, and building materials ^{76, 77}. Cellulose ethers can be either soluble in organic or aqueous media, but for the context of this thesis, only water soluble cellulose ethers will be discussed.

a)



b)

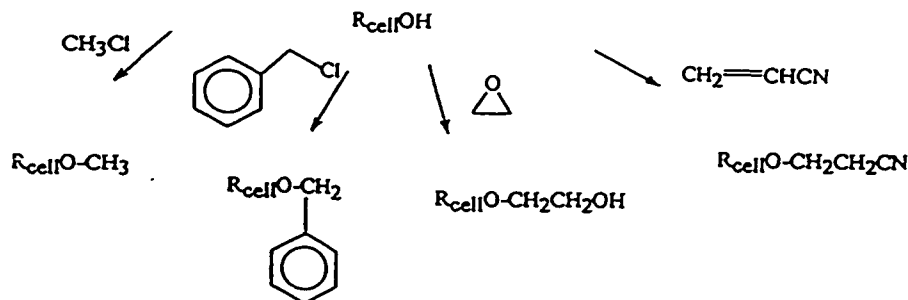


Figure 1.5.1: a) Structure of cellulose, b) synthetic routes to cellulose ethers.

The starting material, cellulose, is a polydisperse linear homopolymer made up of anhydroglucose rings bound through acetal β -1,4 linkages, where each ring contains three hydroxyl groups, one primary and two secondary (structure shown in figure 1.5.1a). Cellulose ethers are produced by the nucleophilic reaction of cellulose under alkaline conditions with an alkyl halide, aryl-alkyl halide, epoxide, or an activated ethylenic compound (figure 1.5.1b).

Commercial cellulose ethers are manufactured by heterogeneous processes, where the cellulose and cellulose ether remain in a particulate state throughout the reaction^{9, 78, 79}. The difficulties encountered with the chemical modification of cellulose are related to the crystalline-amorphous nature, which establishes a gradient of reactivity under heterogeneous conditions. The inaccessibility of crystalline regions in the cellulose matrix to alkylating reagents confines reactions to the amorphous regions and to the surface of the crystalline regions. This problem is alleviated if one uses an activated cellulose substrate formed *in situ*, prior to the addition of the alkylating reagent⁷⁸. This activated cellulose substrate generated by reagents such as water, alkali metal hydroxide solutions or liquid ammonia can disrupt the crystalline regions without dissolution. Usually aqueous solutions of sodium hydroxide (>18%) are used above 20 °C, acting to promote decrystallisation and catalyse the etherification reaction⁹.

Commercial cellulose ethers are graded according to solution viscosity, the chemical nature of the substituent, the degree of substitution (DS) or molar substitution (MS), purity, and solubility. The degree of substitution is defined as the average number of hydroxyl groups substituted per anhydroglucose unit, up to a maximum of three. Water-

soluble cellulose ethers usually have DS values between 0.4 and 2.0. Etherification reactions resulting in new reactive sites are capable of chain branching and are described by the extent of reaction or molecular substitution (MS). MS is defined as the moles (molecules) of reagent combined per mole of anhydroglucose. The ratio of MS to DS is a measure of the average length of the hydroxyalkyl chain.

The degree of substitution determines the ability of the cellulose ether to function as a thickener or flow control agent. The chemical nature of the substituent determines properties such as salt compatibility, thermal stability, colloidal stabilisation, surface activity and cross-linking. The degree of substitution and substituent distribution along the chain also determine the solution properties and rheological characteristics of cellulose ether solutions⁹. Following figure 1.5.2, it can be seen that at low DS of about 0.2, most of the reaction has occurred at the amorphous regions or on the surface of residual crystalline domains, where the polymers are insoluble swollen fibers. With continued reaction, there is an increasing disruption and reaction of the crystalline regions. At a DS of about 0.5, the material exhibits partial solubility, where aggregates of poorly substituted regions appear as highly swollen opaque or transparent macrogel particles. At a degree of substitution of about 0.7, there is sufficient substitution to yield only residual chain associations, so that the application of high shear will break any weak chain associations producing useful solution rheological properties. At this stage, the solution shows classical thixotropic solution rheology, which is defined as a time-dependent change in viscosity resulting from reversible, weak chain associations at unsubstituted anhydroglucose sites on the cellulose backbone. Reaction to a DS of about 1.0 produces

substituted chains with very low levels of unsubstituted anhydroglucose sites having little tendency for chain association. At this stage, it exhibits pseudoplastic rheology showing little or no hysteresis loop, but exhibiting shear thinning behaviour.

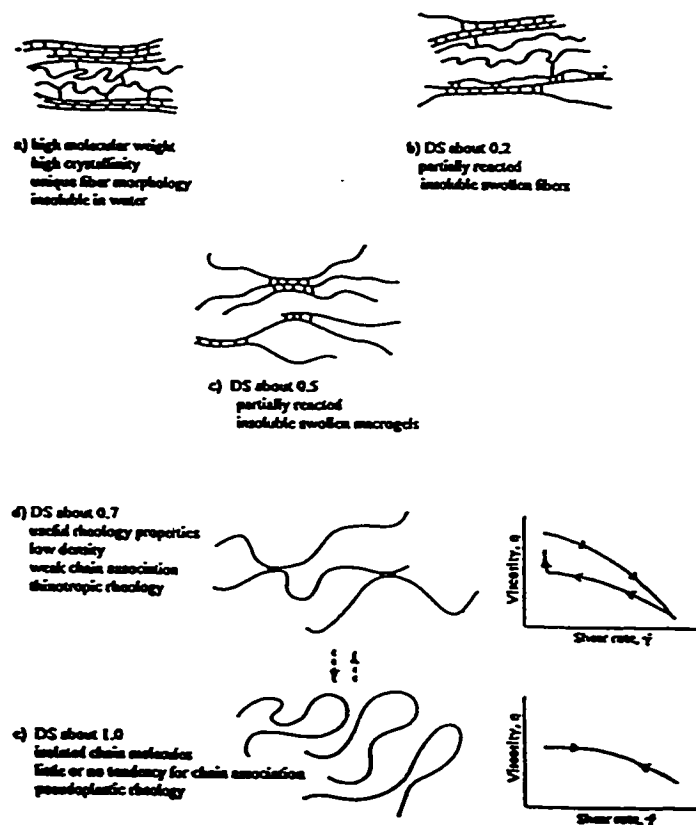


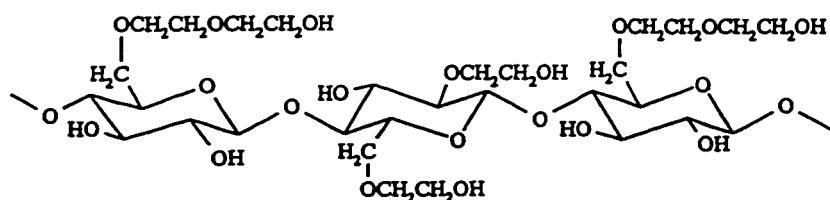
Figure 1.5.2: Heterogeneous reaction of fibrous cellulose and stages of solvation as a function of the extent of reaction ⁹.

These polymers are made amphiphilic by chemically grafting a small amount of hydrophobic alkyl chains. The backbone is rigid due to the nature of cellulose and the

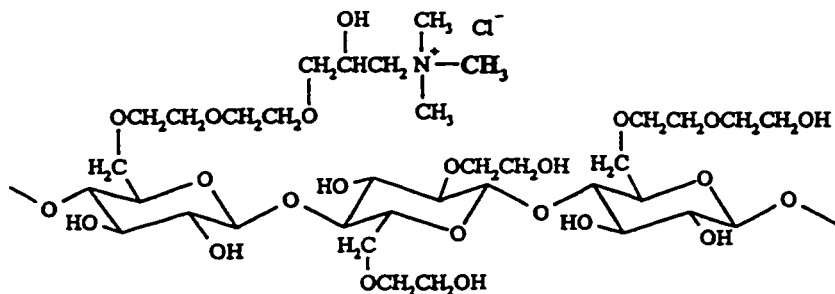
hydrophobic segments are usually flexible leading to predominantly intermolecular aggregation in solution.

The cellulose ethers studied in this thesis are hydroxyethylcellulose (HEC) and its cationic derivatives containing the chloride salt of trimethylammonium and dimethyldodecylammonium groups attached randomly along the cellulose backbone. The structures and some physical properties of these polymers are given below.

a)



b)



c)

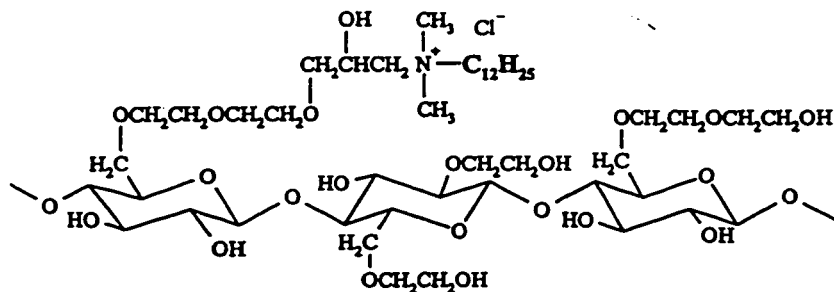


Figure 1.5.3: Structures of a) HEC, b) HEC-N+CH₃, and c) HEC-N+C₁₂.

Table 1.5.1: Characteristic properties of the cellulose ethers studied.

Description	Abbreviation	Nature	Molecular Weight (Dalton)	DS and/or MS	Degree of Modification
Hydroxyethylcellulose LMW	HEC LMW	Non-ionic	100,000 ^a	DS = 3	
Hydroxyethylcellulose HMW	HEC HMW	Non-ionic	400,000 ^a	DS = 3	
Chloride salt of the N,N,N-trimethyl-ammonium derivative of hydroxyethylcellulose	HEC-N+CH ₃	Cationic	400,000 ^b	MS = 2.5	
Chloride salt of the N,N-dimethyl-N-dodecyl-ammonium derivative of hydroxyethylcellulose	HEC-N+C ₁₂	Hydrophobically-modified, Cationic	100,000 ^c	MS = 2.5	5.4 mol%

a determined by gel permeation chromatography using SHODEX standard P-82

b ⁸⁰

c ⁸¹

1.6 Literature Review

The body of published research in the area of polymer and mixed polymer-surfactant systems behaviour in aqueous solution is too large to review in any detail in this section. This following literature review has focussed on the solution properties of non-ionic and cationic cellulose ethers with emphasis on the effect of hydrophobic modification and surfactant interactions in aqueous solution.

1.6.1 Aqueous Solution Properties of Non-Ionic Cellulose Ethers

A considerable amount of research has been conducted in the area of non-ionic cellulose ethers, with much of the focus on ethylhydroxyethyl cellulose (EHEC). The aqueous solution properties of this polymer have been studied extensively ^{82, 83, 84, 85, 86, 87, 88, 68, 89, 90, 91}. Attention has been directed to the effect of surfactants, alcohols, salts,

temperature and pH on the phase behaviour and gelation properties of these polymers. Studies have also been directed towards the effect of hydrophobic modification on the aqueous solution behaviour. Hydrophobic modification was found to substantially increase the solution viscosity compared to the unmodified EHEC. In mixed hydrophobically-modified EHEC/anionic surfactant (SDS) solutions, the solution viscosity reached a maximum at a surfactant concentration of 0.004 mol/L and then decreased to a solution viscosity below the initial viscosity⁹². Additionally, the addition of salt was found to either increase or decrease the solution viscosity depending on the nature of the anion. The viscosity of EHEC solutions showed negligible changes on addition of various co-solutes.

Other non-ionic cellulose ethers that have attracted research interest are the hydroxyethyl cellulose (HEC) and its hydrophobically-modified analogue (HM-HEC)^{93, 94, 41, 95, 96}. The solution properties of hydroxypropyl cellulose (HPC) ethers have been studied extensively by fluorescence techniques^{97, 98, 99, 100}.

1.6.2 Aqueous Solution Properties of Cationic Hydrophobically-Modified Cellulose Ethers

Polycationic cellulose ethers such as HEC-N+CH₃ containing a small mole percentage of quaternary trimethylammonium groups chemically grafted onto the cellulose backbone have found extensive use in the personal care industries as additives in cosmetics and shampoo formulations. The addition of a small amount of hydrophobic modification as in HEC-N+C₁₂, can dramatically improve the viscosity of solutions

compared to the nonhydrophobically-modified analogue HEC-N+CH₃. Research on these polycationic cellulose ethers has focused on the interaction of surfactants on the solution properties of these polymers as a means of understanding the conformation of mixed system complexes.

Interaction of ionic surfactants with oppositely charged polymers is known to cause precipitation of the polymer-surfactant complexes in a certain surfactant concentration range. An early study by Ananthapadmanabhan on the interaction of SDS with these cationic cellulose ethers used fluorescence probe, dye-solubilisation and solubility measurements. The results pointed to a hemi-micelle/inverse cylindrical micelle-type aggregate in the pre-precipitation zone and a conventional micelle-type structure beyond the point of maximum precipitation ¹⁰¹.

The solution and macroscopic properties of HEC and cationic HEC (HEC-N+CH₃) were reported by Kästner and co-workers using rheological, electric birefringence and scanning electron microscopy ¹⁰². The chemical modification of HEC was found to have a profound effect on the solution viscosity compared to the native polymer. The addition of surfactant substantially increased the viscosity. These solutions were found to exhibit viscoelastic behaviour and a yield stress value. The increased viscosity was attributed to an interaction of the side chains of the polymer with the surfactant molecules forming a three-dimensional network structure. The visualisation of this three-dimensional network was made possible by freeze-fracture scanning electron microscopy. Further investigations with the cat-HMHEC (HEC-N+C₁₂) samples also found improved viscosity in the presence of anionic surfactants ³¹.

Studies using surface tension measurements indicated an interaction between the HEC-N+C₁₂ with surfactants of the same charge where interaction can be interpreted in terms of association between the oppositely charged and/or the hydrophobic parts of both components. Kästner and co-workers have also studied the macroscopic behaviour of several samples of modified cationic HEC¹⁰³. Differences between the hydrophobic and cationic derivatives were found, depending on whether the charges and the hydrophobic parts are separately attached to the polymer backbone or belonged to one substituent. They reported that on the addition of anionic surfactants, the former exhibited a strong gel behaviour in the pre-precipitation area and a dilute sol behaviour in the post-precipitation area. The latter formed highly viscoelastic gels in both areas. A viscosity enhancement with increasing cationic surfactant concentration was only observed for samples of the first type of polymer.

The effect of added salt on aqueous mixtures of SDS with HEC-N+C₁₂ was investigated by various techniques by Guillemet and Piculell¹⁰⁴. Evidence of hydrophobic microdomains at polymer solution concentrations as low as 1% was shown by steady state fluorescence measurements. Liquid-liquid phase separation occurred near charge neutralisation of the system, on addition of SDS for HEC-N+C₁₂ solutions in the range 0.02-1% for the salt free mixture and earlier in the presence of added salt. In all cases, resolubilisation occurred upon further SDS addition. By viscosity measurements, association of SDS to HEC-N+C₁₂ occurred at concentrations as low as 10⁻⁵ mol/L SDS and binding continued even after redissolution. A binding isotherm was determined to interpret the results. The first stages involved the binding of individual surfactant

molecules to the mixed micelles. In the last stage, a strong, co-operative binding related to the self-association of the surfactant occurs when the free surfactant concentration approaches the CMC.

The phase behaviour and rheology of polymer mixtures of aqueous solutions of oppositely charged polyelectrolytes: HEC-N+C₁₂ and polyacrylates, was investigated by Thuresson and co-workers¹⁰⁵. The effect of hydrophobic modification and addition of salt was emphasised. The associative phase separation observed when mixing oppositely charged polyelectrolytes was prevented over a large miscibility region for the hydrophobically-modified polymers. The viscosity of mixed polyelectrolyte systems was found to be 3-4 orders of magnitude higher compared to either polymer alone. Addition of electrolytes decreased the viscosity strongly and higher electrolyte contents were found to induce phase separation.

The adsorption behaviour of cationic hydrophobically-modified cellulose ether HEC-N+C₁₂ onto mica surfaces by ESCA analysis, was compared to a non-ionic analogue using surface force apparatus¹⁰⁶. The difference in adsorption behaviour between HEC-N+C₁₂ and HM-HEC indicated that electrostatic attraction between the cationic sites of HEC-N+C₁₂ and the anionic sites on the mica surface dominates the interaction. The polymer adsorbed strongly onto mica from aqueous solutions, where the addition of non-ionic surfactants led to a marked increase in the long-range forces. This gave an indication of an expanded polymer-surfactant complex. Shubin et al¹⁰⁷ have recently reported the influence of anionic, cationic and non-ionic surfactants on the structure and composition of adsorbed layers of HEC-N+C₁₂ on hydrophilic surfaces such as mica and silica using

surface force apparatus and *in situ* null ellipsometry. In contrast to SDS and $C_{12}E_4$ exhibiting aggregation on the polymer hydrophobes, no evidence of interaction was observed between HEC-N+ C_{12} and TTAB. In this case, a competitive adsorption on the surface resulted in a partial displacement of the polymer and looser attachment to the surface.

1.7 Scope of Thesis

This doctoral thesis presents the results of experiments aimed to elucidate various aspects of the molecular associations exhibited by hydrophobically-modified cationic cellulose ethers, as a means of interpreting their behaviour on a macroscopic level. The polymers chosen for investigation were the cationic derivative of hydroxyethyl cellulose, HEC-N+ CH_3 and its hydrophobically-modified analogue, HEC-N+ C_{12} . Past research has focussed on the macroscopic rheology and phase behaviour of these polymers with emphasis on the effect of hydrophobic modification and surfactant interaction.

The molecular association interactions in dilute aqueous solutions of these polyelectrolyte cellulose ethers were investigated by using fluorescent dye labelled derivatives. The first section in chapter 2 presents the preparation, characterisation and solution properties of randomly labelled HEC-N+ CH_3 and HEC-N+ C_{12} . Fluorescence studies were directed towards determining the solution properties, interpolymeric associations and interactions with cationic, anionic and non-ionic surfactants. The results obtained from these studies suggested the possibility of two sites of pyrene attachment to the cellulosic polymers. To examine the solution behaviour of cationic cellulose ethers

labelled exclusively along the cellulose chain, site-specifically labelled polymers were designed. The preparation, characterisation and solution properties of these polymers are presented in the second section of chapter 2. The interactions occurring at the air/water interface were detected by methods to determine surface viscoelasticity and dynamic surface tension with emphasis on the effect of hydrophobic modification and mixed polymer/surfactant complexation on interfacial stabilisation. Chapter 3 presents the general conclusions and suggestions for further investigations. The appendices consist of five published works, which are touched upon in chapter 2 sections 1 and 3 and have been made available for further reading.

CHAPTER 2

CHAPTER 2: RESULTS AND DISCUSSION

2.1 Randomly Labelled Cationic Hydrophobically-Modified Hydroxyethyl Cellulose

The growing interest in amphiphilic water-soluble polymers is driven by their use in numerous industrial applications. Polysaccharides and in particular cellulosic derivatives are being extensively investigated for their commercial value. Of specific interest, is the study of the synergistic interactions existing between polymers and co-solutes such as surfactants, alcohols and/or salts.

This section presents the results of experiments conducted to elucidate the molecular association behaviour of perhaps the most commercially successful cationic hydroxyethylcellulose ethers: HEC-N+CH₃ and HEC-N+C₁₂ (structures shown in figure 2.1.3). Pyrene and naphthalene labelled analogues of these polymers were prepared by the attachment of small amounts of fluorescent dye through ether linkages. The preparation and characterisation of these labelled polymers is presented. Various fluorescence techniques were used to study the aqueous solution properties, interpolymeric associations and mixed system interactions with cationic, anionic and non-ionic surfactants.

2.1.1 Synthesis and Characterisation

The post-modification of polymers containing reactive functional groups is one method currently used to incorporate fluorescent dyes. The polymers investigated in this

thesis contain primary hydroxyl groups on the substituted side chains in addition to the secondary hydroxyl groups on the glucose rings. These functional groups were used to attach the pyrene derivatives via ether linkages. In a classical Williamson ether synthesis, the formation of C-O-C bonds is carried out by the addition of base to the alcohol affording alkoxide groups which may then react with another alcohol forming the ether linkage. The synthetic procedure used to attach pyrene onto the cationically modified hydroxyethyl cellulose (HEC) ethers: HEC-N+CH₃ and HEC-N+C₁₂, was as described by Winnik and coworkers⁹⁷ for the preparation of pyrene labelled hydroxypropyl cellulose (HPC-Py). The synthetic scheme is shown in figure 2.1.1.

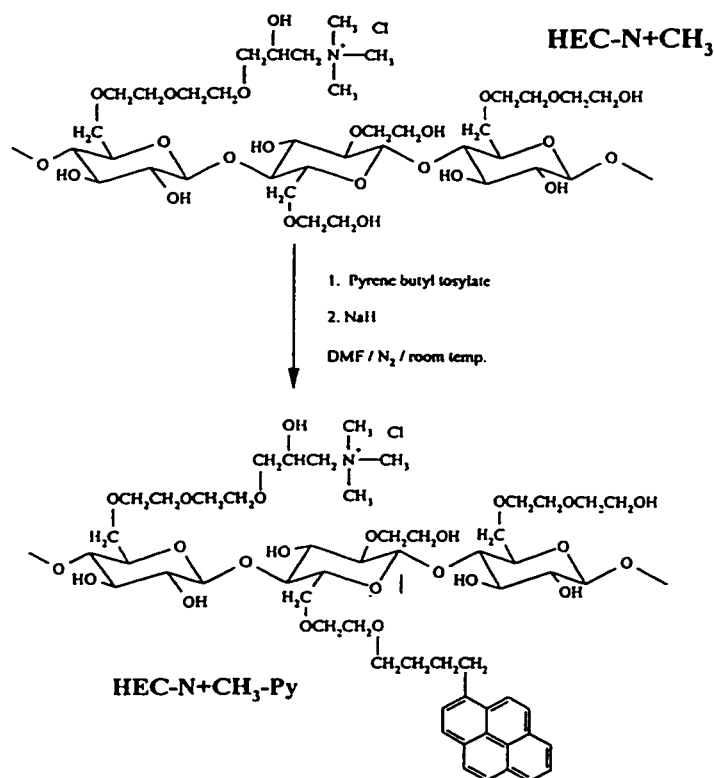


Figure 2.1.1: Synthetic scheme for pyrene labelling of the polymers by an ether reaction in DMF.

As in the case of HPC-Py, the covalent attachment of pyrene chromophores to these polycations proceeded by reaction of the sodium alkoxide derivatives of HEC with 4-(1-pyrenyl)butyl tosylate. Polymer solutions of HEC-N+CH₃ and HEC-N+C₁₂ in the solvent dimethylformamide (DMF) were very viscous. The addition of the tosylate to the reaction mixture prior to the addition of the base ensured that the dye was uniformly distributed in the solvent medium.

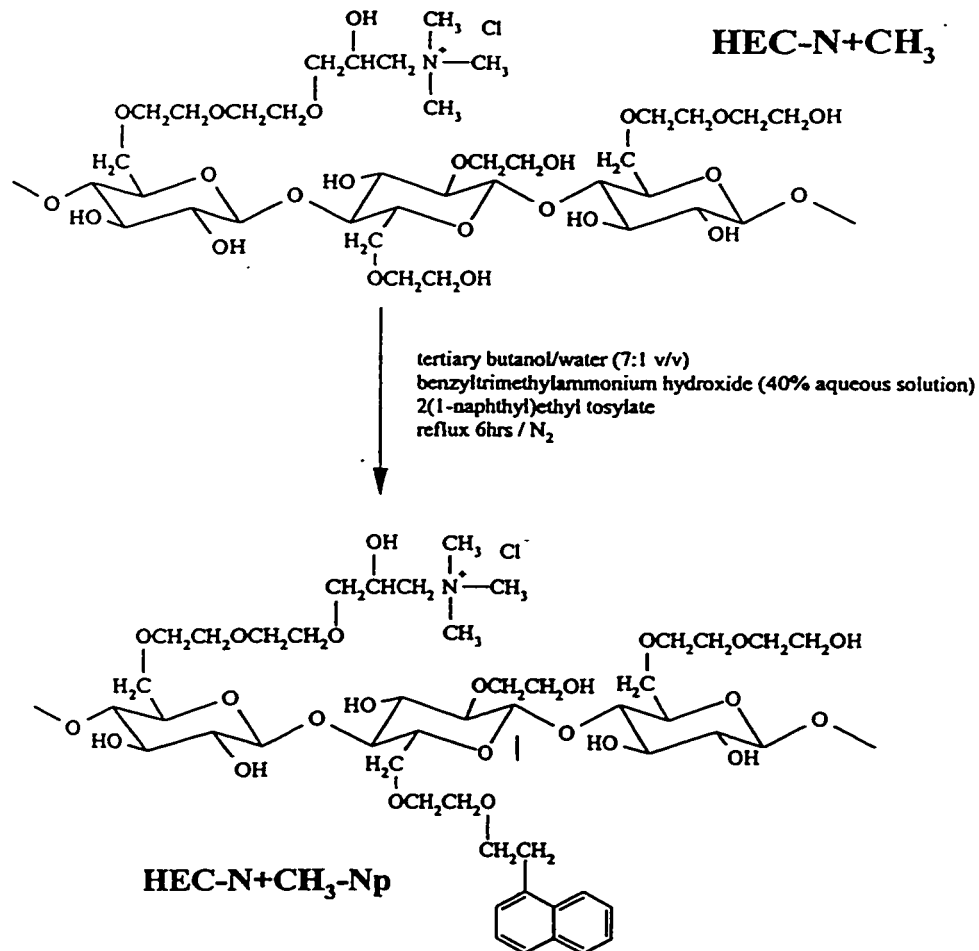


Figure 2.1.2: Synthetic scheme for naphthalene labelling of polymers using a modified ether reaction.

A modified procedure was used to prepare the naphthalene labelled polymers. In this method, adapted from Glass and co-workers ⁷⁸, the ether reaction occurred in a heterogeneous slurry of the polymer in 7:1 (v/v) tertiary butanol/water solvent system (reaction scheme is shown in figure 2.1.2). The bulky base benzyltrimethylammonium hydroxide (40% aqueous solution) was added first to the reaction mixture to afford hydroxide ions of the swollen cellulose ether particles. After the addition of the tosylate derivative of 2-(1-naphthyl)ethanol, the reaction mixture was heated to reflux. This etherification reaction was stopped after 8 hours. Comparison of polymer samples prepared by the two procedures indicated that this method led to higher yields of recovered polymer, less degradation of the polymer and higher levels of attachment of dye.

The absence of low molecular weight contaminants of the labelled polymers was confirmed by gel permeation chromatography. Chromatograms obtained from UV absorbance and refractive index detectors used in tandem confirmed that the fluorescent chromophores were chemically bound to the polymers and that negligible amounts (< 1%) of free dye was present in solution. Comparison of the chromatograms of the labelled and precursor polymers also confirmed that the labelling reaction did not substantially affect the molecular weight or molecular weight distribution.

The amount of fluorescent dye incorporated onto the polymers was determined from the UV-vis spectra of polymer solutions in a 80% (v/v) dimethyl sulfoxide (DMSO:water) solution. This was a good solvent system for the pyrene labelled polymers, as evidenced by the sharp absorbance peaks, with a peak-to-valley ratio of 2.0 or greater,

indicating minimal pyrene aggregation (see table 2.1.2) ^{108, 8}. The pyrene content of 0.1 g/L polymer solutions was determined by comparison with 4-(1-pyrenyl)butanol as standard ($\epsilon = 45000 \pm 400$ L/mol·cm at 346 nm, 0.001 g/L in 80% (v/v) DMSO) and is presented in table 2.1.1. Using the reported molecular weight of HEC-N+CH₃ (400,000 Dalton), the pyrene content on HEC-N+CH₃-Py/212 was estimated to be 10.5 pyrene moieties per polymer chain. This corresponds to roughly 212 glucose units per pyrene assuming an average of 2200 glucose units per polymer chain. In the case of HEC-N+C₁₂-Py/240, the reported mass of HEC-N+C₁₂ (100,000 Dalton) was used to determine the pyrene content. It corresponded to approximately 2.3 chromophores per chain or 1 pyrene per 240 glucose units (assuming an average of 550 glucose units per chain).

Table 2.1.1: Characterisation of labelled polymers in 80% dimethyl sulfoxide.

Polymer	mols Py per gram polymer ^a	Py per chain	Py per glucose unit ^c	Ratio of Py to Glucose
HEC-N+CH ₃ -Py/212	$2.6 \times 10^{-3} \pm 5.2 \times 10^{-7}$	10.5	$4.7 \times 10^{-3} \pm 9.4 \times 10^{-5}$	1 : 212
HEC-N+C ₁₂ -Py/240	$2.9 \times 10^{-3} \pm 4.9 \times 10^{-7}$	2.3	$4.2 \times 10^{-3} \pm 8.9 \times 10^{-5}$	1 : 240
	mols Np per gram polymer ^b	Np per chain	Np per glucose unit ^c	Ratio of Np to Glucose
HEC-N+CH ₃ -Np/549	$1.0 \times 10^{-3} \pm 2.6 \times 10^{-7}$	4.1	$1.8 \times 10^{-3} \pm 4.7 \times 10^{-5}$	1 : 549
HEC-N+C ₁₂ -Np/184	$3.1 \times 10^{-3} \pm 4.4 \times 10^{-7}$	3.1	$5.5 \times 10^{-3} \pm 8.0 \times 10^{-5}$	1 : 184

^a determined using 4-(1-pyrenyl)butanol as a standard compound ($\epsilon = 45435$ L/mol·cm at 346nm), polymer concentration 0.1g/L.

^b determined using 2-(1-naphthyl)ethanol as a standard compound ($\epsilon = 6638$ L/mol·cm at 286nm), polymer concentration 1.0g/L.

^c calculated assuming an average number of glucose units in HEC-N+CH₃ to be 2200 and 550 in HEC-N+C₁₂.

Table 2.1.1 also presents the values obtained for 1.0 g/L solutions of the naphthalene labelled polymers. By using 2-(1-naphthyl)ethanol as standard ($\epsilon = 6600 \pm 60$ L/mol·cm at 286nm, 0.01 g/L in 80% (v/v) DMSO), the naphthalene content of HEC-N+CH₃-Np/549 corresponded to 4.1 naphthalene moieties per polymer chain of molecular

weight 400,000 Dalton. In the case of HEC-N+C₁₂-Np/184, the naphthalene content was calculated to be 3.1 moieties per polymer chain of molecular weight 100,000 Dalton.

Having ascertained that the dye was linked to the polymer, attempts were made to identify the actual site of attachment of the dye to the polymer. It should be recalled that the commercial preparation of the precursor cellulose ether is performed using a heterogeneous ethoxylation process. The hydroxyethyl substitution was reported to be statistically distributed between the three hydroxyl groups of the glucose ring^{78, 79}. Pyrene labelling is expected to occur randomly along the cellulose backbone either at the primary hydroxyethyl groups or, to a lesser extent, at the secondary hydroxyl groups of the cellulose ring. Primary hydroxyl groups were thought to be the predominant sites of pyrene incorporation, but no direct evidence could be obtained.

In the case of the hydrophobically-modified cationic cellulose ether HEC-N+C₁₂, there is a second possible site: the secondary hydroxyl group in close vicinity to the cationic hydrophobic moieties (see figure 2.1.3)¹⁰⁹ [see Appendix 2]. Fluorescence studies using pyrene, a probe sensitive to changes in its local micropolarity, were conducted under the conditions of the labelling reactions for HEC-N+C₁₂ and HEC-N+CH₃ solutions in DMF (40 g/L). In pure DMF, the ratio of I₁/I₃ is 1.81⁴⁸. The ratio of I₁/I₃ of pyrene in a solution of HEC-N+CH₃ in DMF was determined to be 1.73. In a solution of HEC-N+C₁₂ in DMF, this ratio decreased to 1.58, suggesting the possible existence of hydrophobic microdomains. Due to the order of addition of reagents, the 4-(1-pyrenyl)butyl tosylate may have accumulated in these hydrophobic regions and reacted with secondary hydroxyl groups in close proximity once the sodium hydride was added

leading to a preferential substitution of pyrene on sites next to the dodecyl substituent.

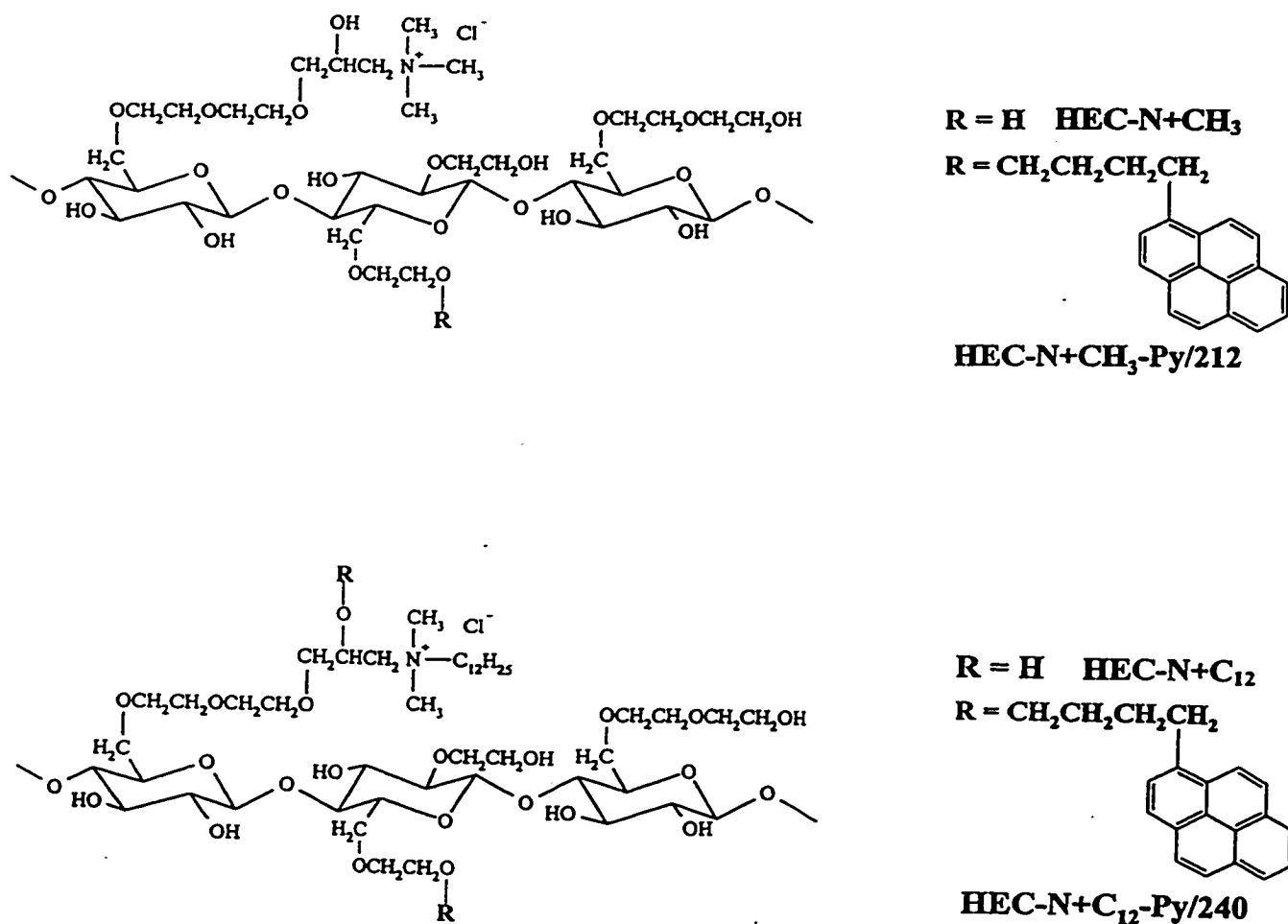


Figure 2.1.3: Structures of HEC-N+CH₃, HEC-N+CH₃-Py/212, HEC-N+C₁₂ and HEC-N+C₁₂-Py/240.

Further characterisation of the labelled polymers was attempted by 500 MHz nuclear magnetic resonance spectroscopy. However, due to the rather uncharacteristic

spectra of the polymers obtained from both the ^1H and ^{13}C NMR, determination of the labelled cellulose ether structure by this technique was not pursued further.

Spectroscopic Characterisation of the Polymers

1. UV-vis Absorbance Spectra – Solvent Effects

UV spectra were obtained for pyrene labelled polymers in aqueous solutions of methanol (50% v/v), DMSO (80% v/v) and in deionised water. HEC-N+CH₃-Py/212 has an absorbance maximum at 344 nm in both water and 50% methanol. In the case of HEC-N+C₁₂-Py/240, the wavelengths of maximum absorbance were 346 nm and 344 nm, respectively. In addition to the shift in the observed maximum absorption wavelength, there was also a decrease in the apparent extinction coefficient of pyrene in solutions of this labelled polymer in water compared to that in 50% methanol. This suggested that aqueous solutions of HEC-N+C₁₂-Py/240 exhibited a hypochromic effect^{46, 47, 97, 8}. For polymer solutions in 50% aqueous methanol, the extinction coefficient of pyrene was calculated to be 38,600 L/mol·cm. The extinction coefficient of aqueous pyrene labelled polymer solutions was determined to be 24,800 L/mol·cm. There was also some peak broadening in the absorbance spectrum of HEC-N+C₁₂-Py/240 in 50% methanol solution as exhibited by the decrease in the ratio of peak-to-valley intensities in comparison with 4-(1-pyrenyl)butanol (see table 2.1.2). This suggested the possible presence of pre-associated pyrene aggregates in solution. In 80% DMSO, the maximum absorbance wavelength for both polymers was 346 nm and the peak-to-valley ratios of the absorbance spectra are given in the table below.

Table 2.1.2: Absorption spectra peak-to-valley ratios for pyrene labelled polymers.

Sample	Conc. (g/L)	Solvent	Abs. (344)/ Abs. (332)
Py(CH ₂) ₄ OH	0.001	50% MeOH	2.74
HEC-N+CH ₃ -Py/212	0.1	50% MeOH	1.97
HEC-N+C ₁₂ -Py/240	0.1	50% MeOH	1.77
Py(CH ₂) ₄ OH	0.001	80% DMSO	2.60
HEC-N+CH ₃ -Py/212	0.1	80% DMSO	3.95
HEC-N+C ₁₂ -Py/240	0.1	80% DMSO	2.39
HEC-N+CH ₃ -Py/212	0.01	H ₂ O	1.60
HEC-N+CH ₃ -Py/212	0.1	H ₂ O	1.74
HEC-N+C ₁₂ -Py/240	0.01	H ₂ O	1.54
HEC-N+C ₁₂ -Py/240	0.1	H ₂ O	1.49

2. *Emission and Excitation Spectra*

Emission and excitation spectra of the pyrene labelled polymers were measured from solutions of the polymer in water, aqueous methanol (50% v/v) and aqueous DMSO (80% v/v). In these solvent systems, spectra were characterised by an emission due to locally excited pyrene moieties (monomer intensity, I_M), with the (0,0) vibronic band located at 377 nm. A broad band centred at 485 nm arising from pyrene excimer emission (excimer intensity, I_E) was also present. Figure 2.1.4 depicts the fluorescence emission spectra of both labelled polymers in aqueous solution (polymer concentration: 1.0 g/L). The ratio of the relative intensities of the two emissions, I_E/I_M , was taken as the ratio of the excimer intensity (485 nm), to the monomer intensity calculated as the half sum of the emission intensities at 377 nm and 398 nm.

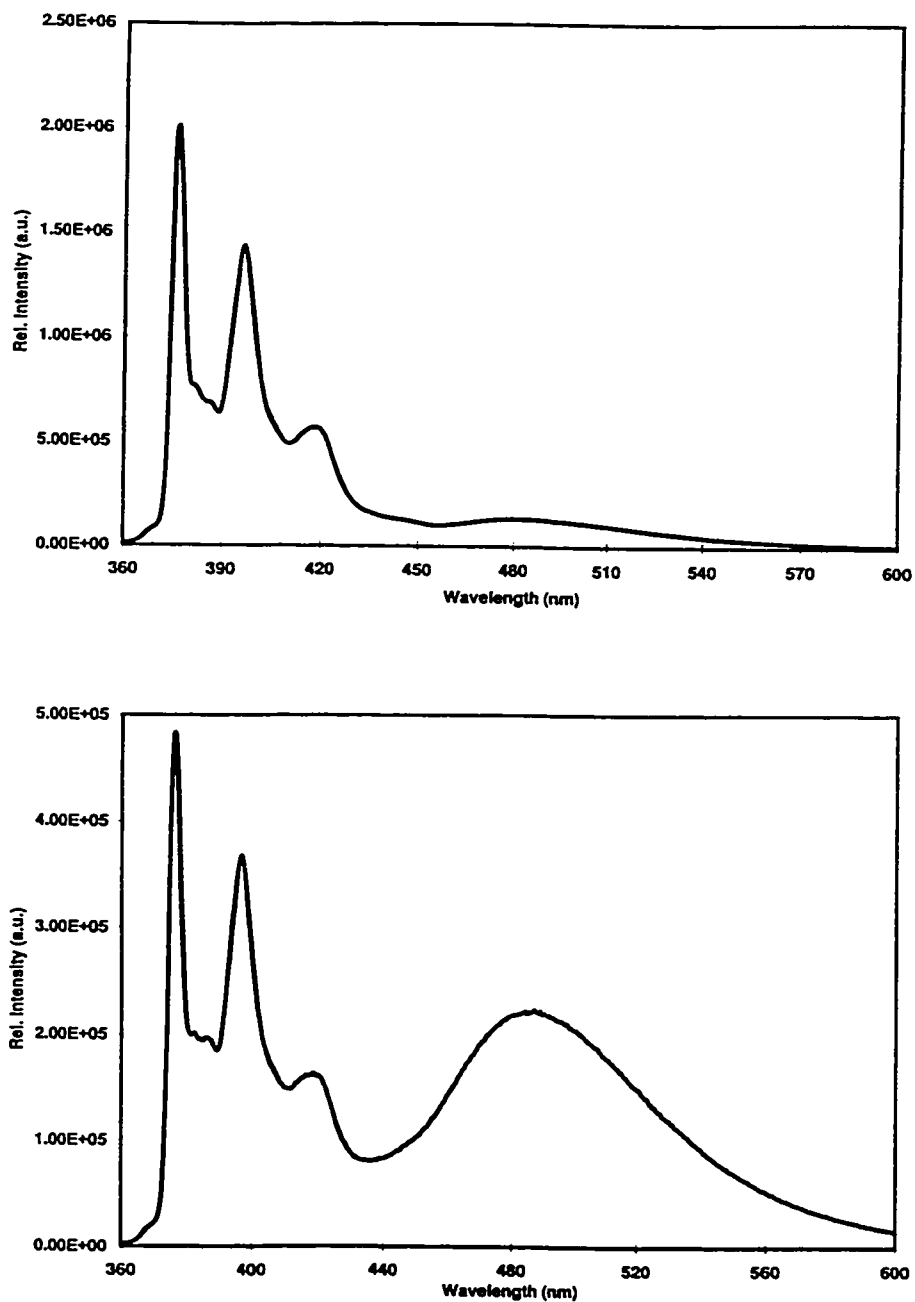


Figure 2.1.4: Steady-state fluorescence emission spectra of HEC-N+CH₃/212 (top) and HEC-N+C₁₂/240 (bottom) in water (1.0g/L, λ_{exc} = 344nm, 25 °C).

HEC-N+C₁₂-Py/240

The values of I_E/I_M recorded from spectra of 0.1 g/L solutions of HEC-N+C₁₂-Py/240 in 50% methanol and in deionised water were determined to be 0.51 and 0.86, respectively (see table 2.1.3). The larger value of I_E/I_M for aqueous solutions of the labelled polymer suggested that the polymer exhibited a conformation where pyrene moieties are in close contact. The lower value of I_E/I_M for solutions of HEC-N+C₁₂-Py/240 in 50% methanol suggests that the pyrenes were less aggregated in this solvent system. It is interesting to note that the method of dissolution of the labelled polymers in water had an effect on the fluorescence spectrum obtained. Polymer solutions (1.0 g/L) dissolved in hot water (60 °C) and allowed to cool down slowly to room temperature showed a substantial reduction in the excimer band (I_E/I_M value of 0.52), compared to the emission spectrum of polymer solutions dissolved in water at room temperature. This seems to indicate that there is less pyrene aggregation in this solution, possibly due to the increased solvation of the polymer chains.

Fluorescence excitation spectra were monitored at 377 nm (monomer emission) and 485 nm (excimer emission). Spectra were obtained for solutions of HEC-N+C₁₂-Py/240 in both deionised water and 50% aqueous methanol. Excitation spectra monitored at these two wavelengths are presented in figure 2.1.5. Comparison of the mathematically normalised spectra showed that they were non-superimposable. The general features of the spectra were the same, however the excitation spectrum monitored at 377 nm was blue shifted by 3 nm for polymer solutions in both water and 50% methanol. The excitation spectrum monitored at 485 nm corresponded to the UV absorption spectrum. Peak-to-

valley ratios of the excitation spectra monitored at both wavelengths are given in table 2.1.3. These observations confirm that the excimer is generated from preformed ground state pyrene dimers or higher aggregates. It is uncertain however, if the intense excimer emission of aqueous HEC-N+C₁₂-Py/240 solutions originates from an intrapolymeric or interpolymeric pyrene association. The excitation spectra of solutions of this polymer in 80% DMSO monitored at the monomer and excimer wavelengths were superimposable. This indicated that excimer formation in this solvent system occurred by a diffusion controlled dynamic mechanism.

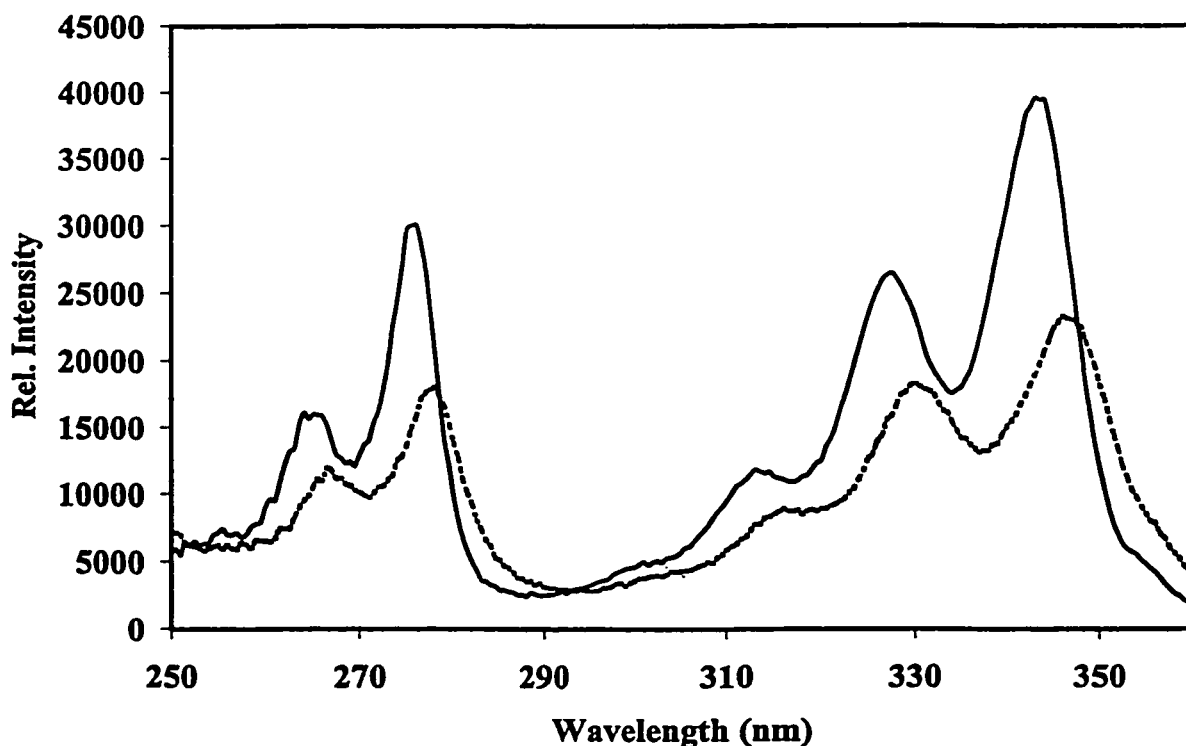


Figure 2.1.5: Excitation spectra of HEC-N+C₁₂-Py/240 at monomer (solid) and excimer (dashed) wavelengths (377nm and 485nm, respectively, 25 °C).

HEC-N+CH₃-Py/212

In contrast, the emission spectra of HEC-N+CH₃-Py/212 were very similar in both deionised water and 50% aqueous methanol solutions. The weak excimer emission centred at 485 nm suggests that very little aggregation occurs between these polymer chains in the concentration range studied. The fluorescence spectrum of polymer solutions in 80% DMSO was characterised by a strong monomer emission arising from isolated pyrene moieties without excimer emission.

Interestingly, the excitation spectra monitored at 377 nm and 485 nm for aqueous HEC-N+CH₃-Py/212 solutions show that the small excimer emission arises from pre-associated pyrene aggregates. However, excitation spectra monitored at these wavelengths in 50% methanol solutions of the polymer were the same and corresponded to the UV absorption spectrum. This suggested a dynamic mechanism for the excimer emission observed in this solvent system.

Table 2.1.3: Fluorescence excitation peak-to-valley ratios and values of I_E/I_M for the pyrene labelled polymers.

Sample	Conc. (g/L)	Solvent	$I(344)/I(332)$ monomer	$I(344)/I(332)$ excimer	I_E/I_M
HEC-N+CH ₃ -Py/212	0.1	50% MeOH	2.62	2.08	0.08
HEC-N+C ₁₂ -Py/240	0.1	50% MeOH	2.70	1.73	0.51
HEC-N+CH ₃ -Py/212	0.1	80% DMSO	1.94	2.18	0.04
HEC-N+C ₁₂ -Py/240	0.1	80% DMSO	2.13	2.03	0.23
HEC-N+CH ₃ -Py/212	0.01	H ₂ O	2.36	2.15	0.06
HEC-N+CH ₃ -Py/212	0.1	H ₂ O	2.39	1.83	0.07
HEC-N+C ₁₂ -Py/240	0.01	H ₂ O	2.45	2.02	0.77
HEC-N+C ₁₂ -Py/240	0.1	H ₂ O	2.37	1.76	0.86

3. *Fluorescence Quantum Yields*

The quantum yield of pyrene attached to the polymers was determined for aqueous

solutions of HEC-N+CH₃-Py/212 and HEC-N+C₁₂-Py/240 at a concentration of 0.1 g/L. It was determined to be 0.75, 0.0 (monomer, excimer) for HEC-N+CH₃-Py/212 and 0.10, 0.26 (monomer, excimer) for HEC-N+C₁₂-Py/240. The low value of the monomer quantum yield in the latter may be attributed to the formation of the excimer emission and/or from the contribution of other decay pathways of the excited state such as self-quenching. The quantum yield for solutions of HEC-N+CH₃-Py/212 in 50% aqueous methanol was similar to that in deionised water. For solutions of HEC-N+C₁₂-Py/240 in 50% aqueous methanol, an increase in the quantum yield of the monomer emission was observed and a decrease in excimer yield in comparison to that obtained in deionised water (table 2.1.4). Evidence from steady-state spectra indicates that there is less pyrene aggregation of HEC-N+C₁₂-Py/240 in 50% methanol than in aqueous solutions.

Table 2.1.4: Quantum yield determination of the labelled polymers.

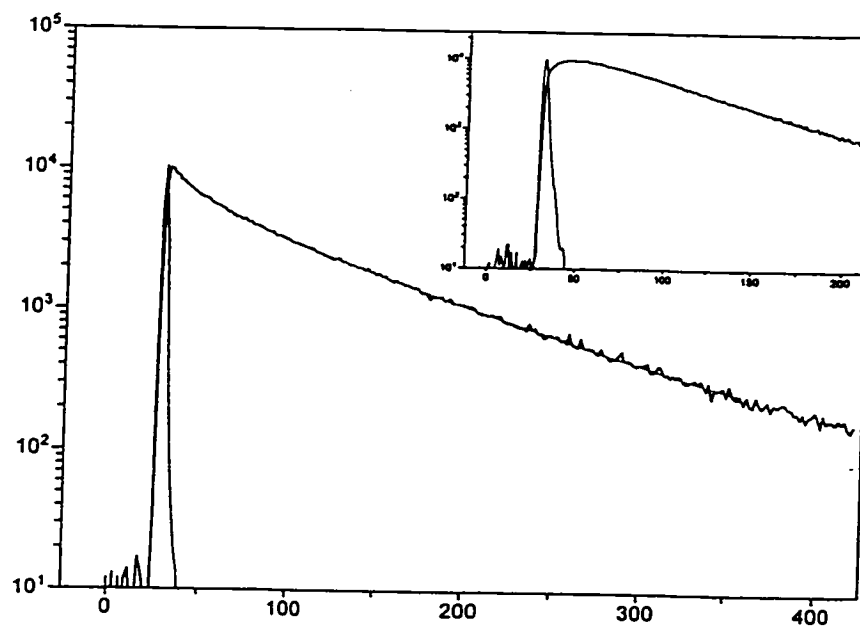
Sample	Solvent	Quantum Yield ^a , monomer	Quantum Yield ^a , excimer
HEC-N+CH ₃ -Py/212	H ₂ O	0.75	-
HEC-N+C ₁₂ -Py/240	H ₂ O	0.10	0.26
HEC-N+CH ₃ -Py/212	50% MeOH	0.77	-
HEC-N+C ₁₂ -Py/240	50% MeOH	0.16	0.18

^a calculated using quinine bisulfate in 0.1N H₂SO₄ as standard

4. *Fluorescence Lifetimes*

Fluorescence decay measurements were performed on solutions of the labelled polymers in water and in 80% DMSO. The values obtained are given in table 2.1.5. Decay curves were fit to a sum of exponentials⁵¹. When necessary, fits consisting of up to three terms were used to ensure that the Chi squared (χ^2) value was as close to unity as

a)



b)

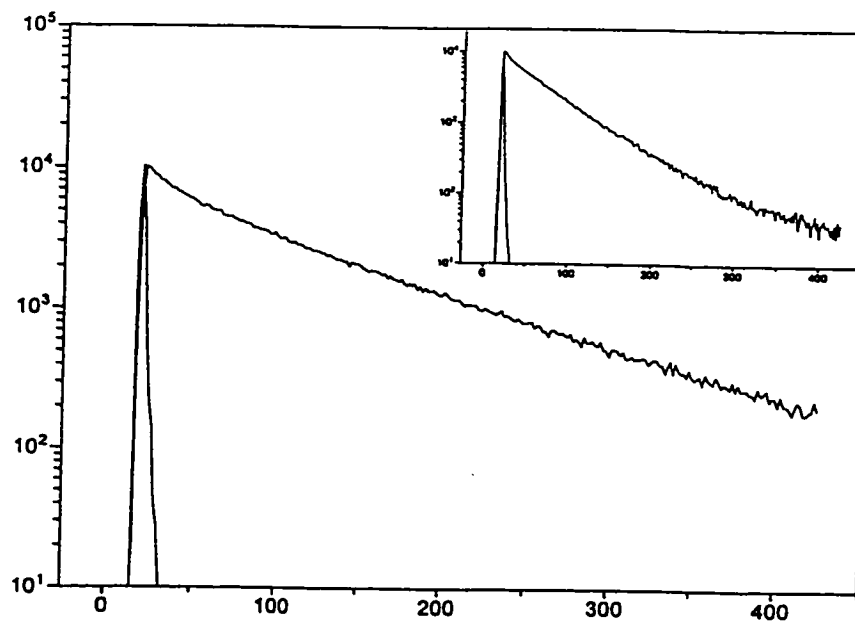


Figure 2.1.6: Fluorescence decay curves of HEC-N+C₁₂-Py/240 monomer and inset excimer in a) 80% DMSO, excitation wavelength 346nm and b) water, excitation wavelength 344nm (logarithmic representation, monomer monitored at 377nm, excimer at 485nm).

possible. In such cases, an average lifetime is reported in brackets.

The pyrene fluorescence monomer decay recorded from a solution of HEC-N+CH₃-Py/212 (0.3 g/L) in 80% DMSO can be fitted to a two component exponential decay with decay times of 103.2 and 31.3 ns ($\chi^2 = 1.05$ average lifetime of 95 ns). In the case of HEC-N+C₁₂-Py/240, the decay curve also consisted of two components (98 and 20 ns, $\chi^2 = 1.13$) with a greater contribution of the short-lived species (an average lifetime of 67 ns). These results imply a complex distribution of the pyrene moieties on this polymer⁹⁷. The time profile of the excimer emission from solutions of both polymers in 80% DMSO were characterised by both a growing-in and decaying components (see figure 2.1.6 and table 2.1.5). The presence of the growing-in component indicated a diffusion controlled dynamic excimer mechanism¹¹⁰.

Table 2.1.5: Fluorescence decay measurements of pyrene labelled polymers.

Sample	Solvent	Monomer		Excimer	
		Lifetime (ns)	Pre-factor	Lifetime (ns)	Pre-factor
HEC-N+CH ₃ -Py/212	H ₂ O	$\tau_1=105.1\pm 0.2$ $\tau_2=31.9\pm 6.2$ $\langle\tau\rangle 102.8\pm 0.03$	$a_1=0.97\pm 0.01$ $a_2=0.03\pm 0.01$	$\tau_1=361.7\pm 111.1$ $\tau_2=57.3\pm 0.3$ $\langle\tau\rangle 59.8\pm 0.08$	$a_1=0.01\pm 0.0$ $a_2=0.99\pm 0.0$
HEC-N+C ₁₂ -Py/240	H ₂ O	$\tau_1=111.0\pm 1.2$ $\tau_2=38.0\pm 5.3$ $\tau_3=8.9\pm 1.4$ $\langle\tau\rangle 71.5\pm 0.01$	$a_1=0.56\pm 0.02$ $a_2=0.20\pm 0.02$ $a_3=0.24\pm 0.02$	$\tau_1=73.7\pm 3.3$ $\tau_2=43.5\pm 2.0$ $\tau_3=3.9\pm 0.7$ $\langle\tau\rangle 39.4\pm 0.01$	$a_1=0.23\pm 0.05$ $a_2=0.49\pm 0.05$ $a_3=0.28\pm 0.12$
HEC-N+CH ₃ -Py/212	80% DMSO	$\tau_1=103.2\pm 0.5$ $\tau_2=31.3\pm 4.0$ $\langle\tau\rangle 94.9\pm 0.01$	$a_1=0.88\pm 0.01$ $a_2=0.12\pm 0.01$	-	-
HEC-N+C ₁₂ -Py/240	80% DMSO	$\tau_1=98.1\pm 0.4$ $\tau_2=19.9\pm 0.6$ $\langle\tau\rangle 66.6\pm 0.0$	$a_1=0.60\pm 0.01$ $a_2=0.40\pm 0.01$	$\tau_1=56.2\pm 0.0$ $\tau_2=12.2\pm 0.0$ $\tau_3=11.8\pm 0.0$ $\langle\tau\rangle 48.1\pm 0.0$	$a_1=0.98\pm 0.00$ $a_2=0.02\pm 0.00$ $a_3=0.6\pm 0.0$

The fluorescence decay of the monomer and excimer emission for 1.0 g/L solutions of HEC-N+CH₃-Py/212 in water could be fitted to a two component decay, giving average lifetimes of 102.8 ns ($\chi^2 = 1.20$) and 59.8 ns ($\chi^2 = 1.43$), respectively. The fluorescence lifetime of HEC-N+C₁₂-Py/240 (1.0 g/L) was fitted via a three component exponential. The average monomer lifetime was 71.5 ns ($\chi^2 = 1.16$) and the excimer lifetime was 39.4 ns ($\chi^2 = 1.13$). In contrast to the excimer emission decay in 80% DMSO which consisted of a growing-in component in addition to fluorescence decay components, aqueous solutions of the polymers were only characterised by a decay curve profile. It is possible that in aqueous polymer solutions, the pyrene excimer complexes form at a faster rate than could be detected during the time-scale of the measurements⁹⁷.

2.1.2 Solution Properties and Interpolymeric Associations

The aggregation concentration of HEC-N+C₁₂-Py/240 in aqueous solution was determined by monitoring the changes in I_E/I_M over a range of labelled polymer concentrations. As a function of polymer concentration, the aggregation concentration was determined to be 10^{-4} g/L. Using the reported hydrophobic modification of HEC-N+C₁₂ of 2.0×10^{-4} mol C₁₂H₂₅ per gram polymer, the aggregation concentration may be expressed as 10^{-8} mol/L as a function of dodecyl chain concentration. Guillemet and Picullel¹⁰⁴ determined the aggregation concentration of the unlabelled polymer LM200 in aqueous solution to be approximately 0.1% or 1 g/L by fluorescence spectroscopy using the probe pyrene. The lower value obtained in the present study could be attributed to the increased sensitivity of the fluorescence label technique. It may however give an indication that

pyrene labelling increases the hydrophobicity of the polymer and a true comparison with the unlabelled polymer is no longer possible ¹¹¹.

The steady-state fluorescence spectra discussed previously gave considerable evidence of interaction of the hydrophobically-modified HEC-N+C₁₂-Py/240 polymer chains in aqueous solution. It was uncertain however if the large excimer emission resulted from an intramolecular interaction of pyrene moieties within the same polymer chain, or from an intermolecular interaction between chains. To distinguish between these two mechanisms of interaction, fluorescence non-radiative energy transfer experiments were performed between an energy donor naphthalene labelled polymer HEC-N+C₁₂-Np/184 and an energy acceptor pyrene labelled polymer HEC-N+C₁₂-Py/240. Studies were conducted with polymer solutions of concentrations ranging from 0.5 g/L to 5.0x10⁻⁴ g/L in 10⁻³ mol/L sodium chloride aqueous solutions. Very little energy transfer occurred at concentrations below 0.05 g/L, indicating that the chromophores were more than 30 Å apart, the interchromophoric distance required for energy transfer for the Np/Py pair of chromophores ⁵³. When the concentration of the polymer solutions exceeded 0.5 g/L, energy transfer occurred with a ratio of the intensity of pyrene excited by energy transfer to the intensity of naphthalene (I_{Py}/I_{Np}) of 0.47 (see figure 2.1.7). The values of I_{Py}/I_{Np} in the present study were relatively low in comparison with other polymer systems suggesting that the rigid cellulose backbone may hinder the association of polymer chains. The broad excimer band was found to remain relatively large throughout the range of concentrations studied due to the residual emission from directly excited pyrene.

In the case of the control system HEC-N+CH₃-Np/548 and HEC-N+CH₃-Py/212, little or no energy transfer was observed in the concentration range studied. This is attributed to strong electrostatic repulsion of the cationic quaternary ammonium sites between polymer chains. Association of the HEC-N+C₁₂-Np/184 and HEC-N+C₁₂-Py/240 pair is therefore a result of the hydrophobic interaction between the dodecyl groups along the polymer chains.

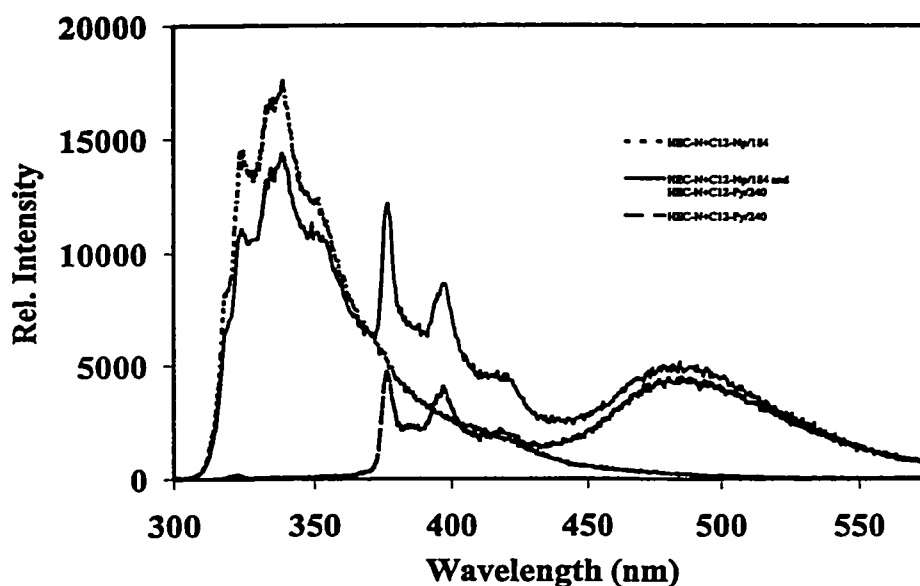


Figure 2.1.7: Steady-state fluorescence spectra of non-radiative energy transfer from HEC-N+C₁₂-Np/184 to HEC-N+C₁₂-Py/240 ($\lambda_{exc} = 290\text{nm}$, ratio of naphthalene to pyrene: 5:1, polymer concentration 0.5 g/L, 25 °C).

2.1.3 Interactions of Labelled Polymers with Surfactants in Aqueous Solution

Steady-state fluorescence spectroscopy was utilised to monitor the interactions of the labelled polymers, HEC-N+CH₃-Py/212 and HEC-N+C₁₂-Py/240, with cationic, anionic and non-ionic surfactants.

Cationic Surfactants

Through phase separation/precipitation experiments, Goddard and Leung reported interactions between cationic surfactants and dodecyl-substituted cationic cellulose ethers¹¹². Association between polymer/surfactant systems of like charge was thought to occur if the polycation is hydrophobically-modified, where hydrophobic associations are the driving force of the interaction. To test this hypothesis, fluorescence experiments using the probe pyrene were conducted¹¹³ [Appendix 1]. The results of this study clearly indicated that, despite unfavourable electrostatic repulsions, an interaction takes place between hydrophobically-modified cationic cellulose ethers and a family of cationic surfactants. The presence of salt on the system did not affect the aggregation concentration.

Steady-state fluorescence studies were conducted next on systems of labelled hydrophobically-modified cationic cellulose ethers and cationic surfactants. Figure 2.1.8 depicts the changes in the ratio of I_E/I_M as a function of dodecyltrimethylammonium chloride (DTAC) concentration (logarithmic scale), for 0.1 g/L solutions of HEC-N+CH₃-Py/212 and HEC-N+C₁₂-Py/240. It clearly illustrates that changes in I_E/I_M only occur in

the case of HEC-N+C₁₂-Py/240. Little or no change was observed for HEC-N+CH₃-Py/212 / DTAC mixed solutions.

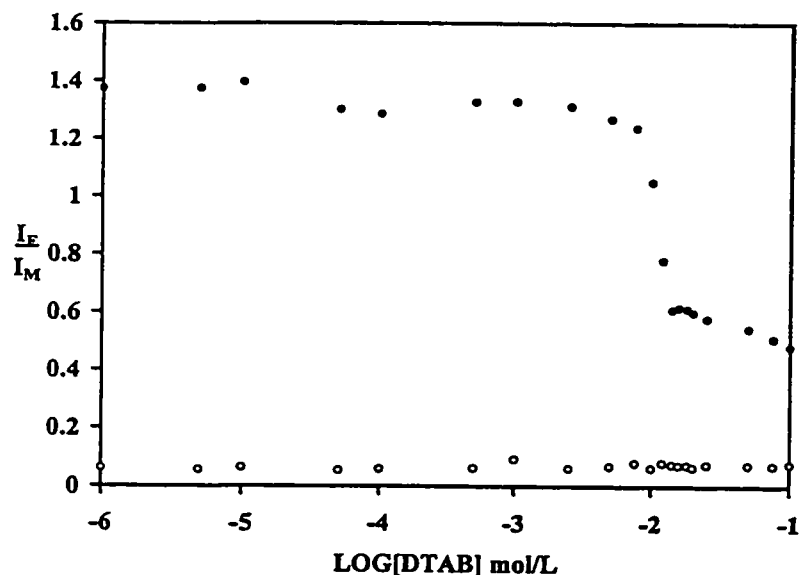


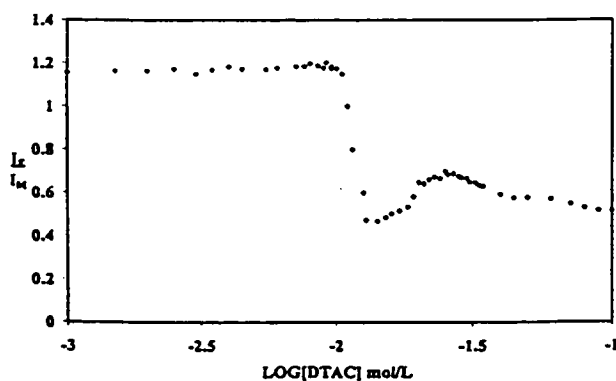
Figure 2.1.8: Plot of I_E/I_M as a function of DTAB concentration (logarithmic scale, 0.1 g/L polymer concentration) for HEC-N+CH₃-Py/212 (open circles) and HEC-N+C₁₂-Py/240 (closed circles).

For mixed DTAC / HEC-N+C₁₂-Py/240 (0.1 g/L) solutions, the onset of aggregation or critical aggregation concentration (CAC), occurred after the addition of 0.013 ± 0.001 mol/L of the surfactant, a value lower than the critical micelle concentration (CMC) of DTAC (0.021 mol/L, ¹¹⁴).

Increasing the concentration of HEC-N+C₁₂-Py/240 to 1.0 g/L led to surprising fluorescence results for this mixed polymer/surfactant system (figure 2.1.9). The CAC value did not change much. The excimer emission decreased sharply at a DTAC concentration of 0.01 ± 0.001 mol/L, a value corresponding to the CAC. However, as the

surfactant concentration increased to 0.018 mol/L, the excimer emission intensity increased to reach a maximum value at 0.028 mol/L, a value slightly higher than the CMC of the surfactant. For increasing surfactant concentration, the excimer emission became negligible. If the cationic surfactant interacts with hydrophobic segments of HEC-N+C₁₂-Py/240, increasing the surfactant concentration is expected to lead to a gradual decrease in the large excimer emission and an increase in the monomer emission of the fluorescence spectrum as a result of the separation of pyrene aggregates and solubilisation with hydrophobic microdomains formed by surfactant and polymeric hydrophobic substituents.

a)



b)

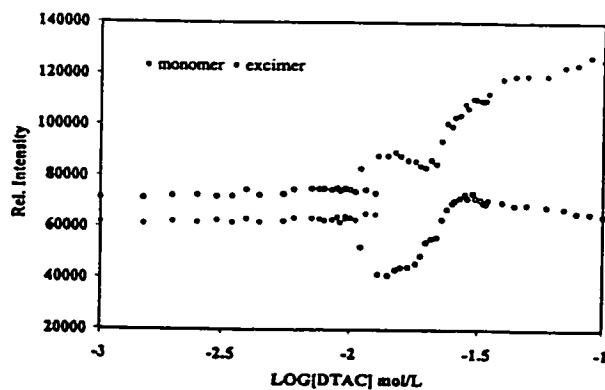


Figure 2.1.9: Plot of a) I_E/I_M and b) I_M and I_E as a function of DTAC concentration (logarithmic scale) for 1.0 g/L HEC-N+C₁₂-Py/240.

The critical aggregation concentration of the mixed system was shown to depend on the alkyl chain length of the surfactant. Aggregation of HEC-N+C₁₂-Py/240 and hexadecyltrimethylammonium chloride (HTAC) mixed solutions occurred for surfactant concentrations of 0.0014 mol/L, which nearly coincides with the CMC of the surfactant (0.0013 mol/L, ^{115, 18}), shown in figure 2.1.10 and 2.1.11.

Mixed polycation/cationic surfactant interactions were further investigated using two surfactants, cetylpyridinium chloride (CPC) and 1-dodecylpyridinium chloride (DPC), which possess headgroups capable of quenching pyrene emission. As a control experiment, interaction of the labelled polymers with 1-ethylpyridinium bromide (EPB) was also studied. This compound is a pyridinium derivative that is readily soluble in water and does not have any amphiphilic characteristics.

Treatment of HEC-N+C₁₂-Py/240 with increasing amounts of CPC resulted in a considerable decrease in the monomer emission intensity and complete quenching of the excimer emission. This can be clearly illustrated using the Stern-Volmer relation plotting the ratio of fluorescence intensity in the absence of quencher to that in the presence of quencher I_0/I as a function of quencher concentration, where the intercept is unity. Figure 2.1.12a illustrates the Stern-Volmer plot for the pyrene monomer emission quenching of HEC-N+C₁₂-Py/240 by CPC. Analysis of the decrease in monomer emission intensity in terms of the Stern-Volmer model, yielded a Stern-Volmer constant (K_{SV}) of 6800 L/mol \pm 110 and rate constant of 94 L/mol·ns \pm 3. Analysis of the decrease in excimer emission intensity upon addition of CPC following the Stern-Volmer model was also performed. In this case, the data were not linear but exhibited an upward curvature. This trend is

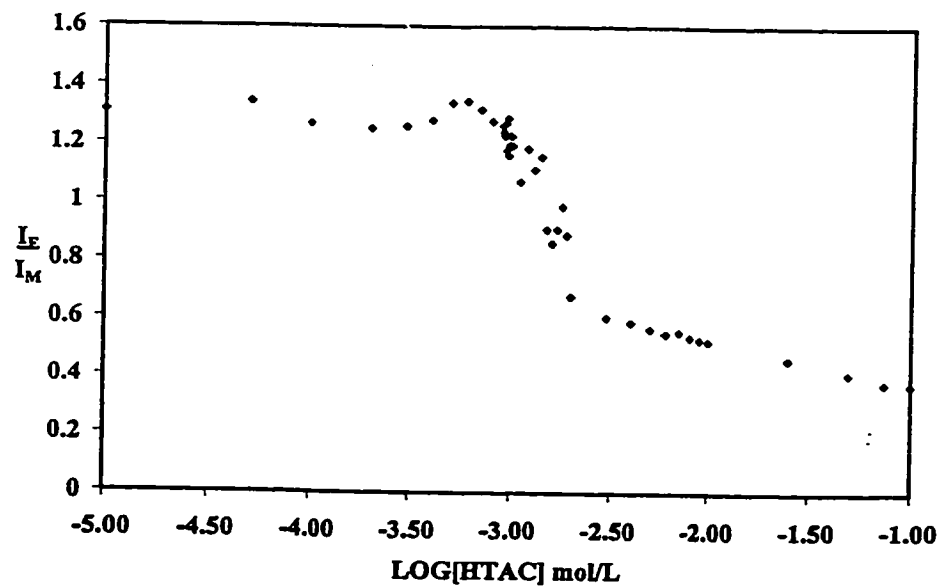


Figure 2.1.10: Plot of I_E/I_M as a function of HTAC concentration (logarithmic scale) for 0.1 g/L HEC-N+C₁₂-Py/240.

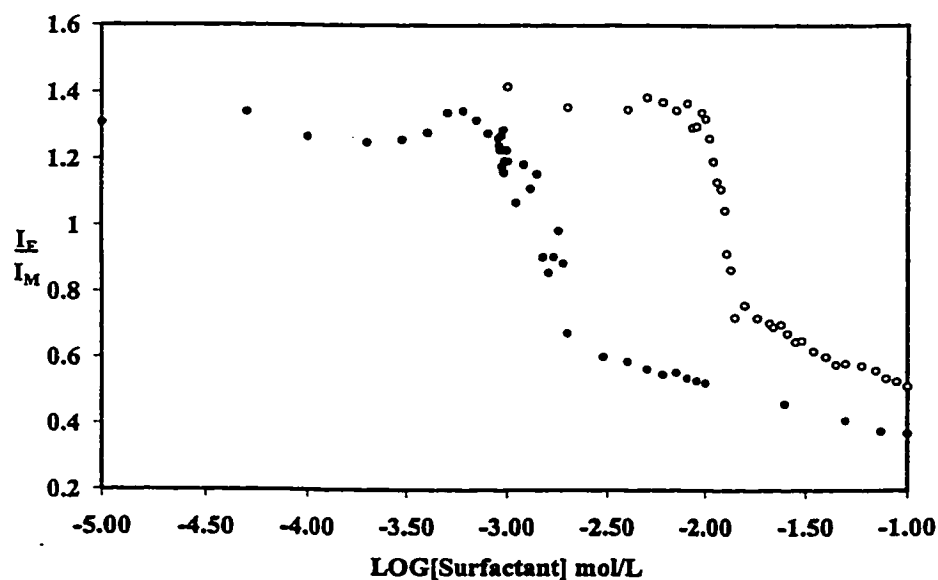
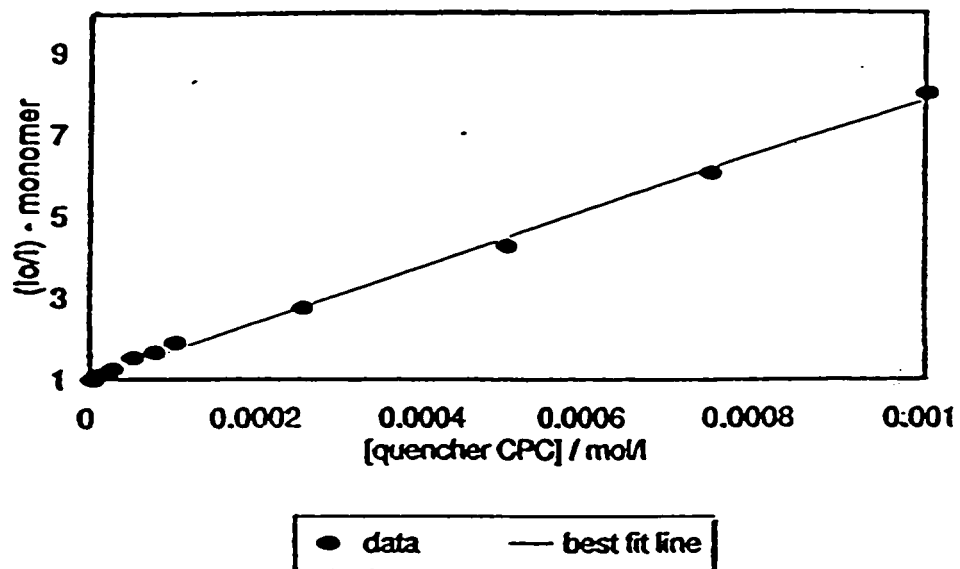


Figure 2.1.11: Plot of I_E/I_M as a function of surfactant concentration (logarithmic scale) for 0.1 g/L HEC-N+C₁₂-Py/240: DTAC (open circles), HTAC (closed circles).

a)



b)

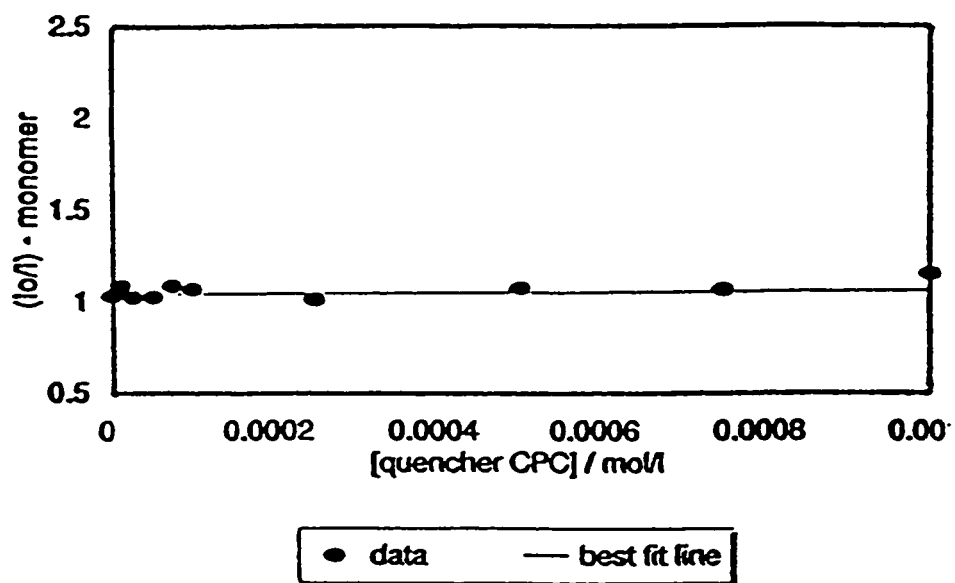


Figure 2.1.12: Stern-Volmer plots of monomer emission quenching by CPC in a) HEC-N+C₁₂-Py/240 and b) HEC-N+CH₃-Py/212 solutions ($\lambda_{exc} = 344\text{nm}$, 25°C).

indicative of static quenching. At DPC concentrations greater than 10^{-4} mol/L, Stern-Volmer plots deviated from linearity for both the monomer and excimer emission.

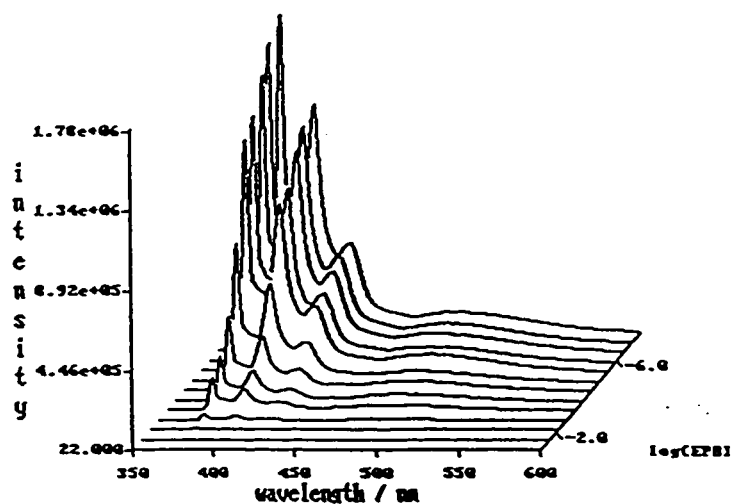
For aqueous solutions of HEC-N+CH₃-Py/212 (1.0 g/L), the intensity of the fluorescence monomer and excimer emissions did not change significantly upon addition of CPC over a concentration range of 10^{-6} to 10^{-3} mol/L. Figure 2.1.12b presents a Stern-Volmer plot corresponding to the monomer emission quenching of this mixed system. The ratio I_0/I remains relatively constant over the quencher concentration range investigated. Strong electrostatic repulsion between the labelled cationic polymer chains and the cationic quenchers take place since this polymer does not contain hydrophobic moieties able to facilitate interaction. In solutions of HEC-N+CH₃-Py/212, fluorescence quenching was not apparent in the presence of DPC until the surfactant concentration of 0.25 mol/L was exceeded.

Table 2.1.6: Stern-Volmer (K_{SV}) and rate constants of quenching of monomer ($k_{q,mon}$) and excimer ($k_{q,exc}$) emission of pyrene labelled polymers with various pyridinium halide derivatives.

Quencher	HEC-N+CH ₃ -Py/212 monomer		HEC-N+C ₁₂ -Py/240 monomer		HEC-N+C ₁₂ -Py/240 excimer	
	K_{SV} (L/mol)	$k_{q,mon}$ (L/mol·ns)	K_{SV} (L/mol)	$k_{q,mon}$ (L/mol·ns)	K_{SV} (L/mol)	$k_{q,exc}$ (L/mol·ns)
EPB	70.4 ± 3.1	0.7 ± 0.03	2.9 ± 0.0	0.04 ± 0.0	2.9 ± 0.0	0.05 ± 0.0
DPC	128.8 ± 4.6	1.3 ± 0.05	348.1 ± 38.1	4.8 ± 0.6	436.9 ± 29.3	7.6 ± 0.5
CPC	82.6 ± 30.7	0.8 ± 0.3	6777.2 ± 113	93.9 ± 2.5	36728.3 ± 2491	637.4 ± 44.3

Spectra of HEC-N+CH₃-Py/212 were monitored in the presence of ethylpyridinium bromide, a simple non-amphiphilic quencher of pyrene fluorescence⁶. Fluorescence spectra recorded from solutions containing increasing amounts of EPB are shown in figure 2.1.13. The fluorescence emission of HEC-N+C₁₂-Py/240 was also

a)



b)

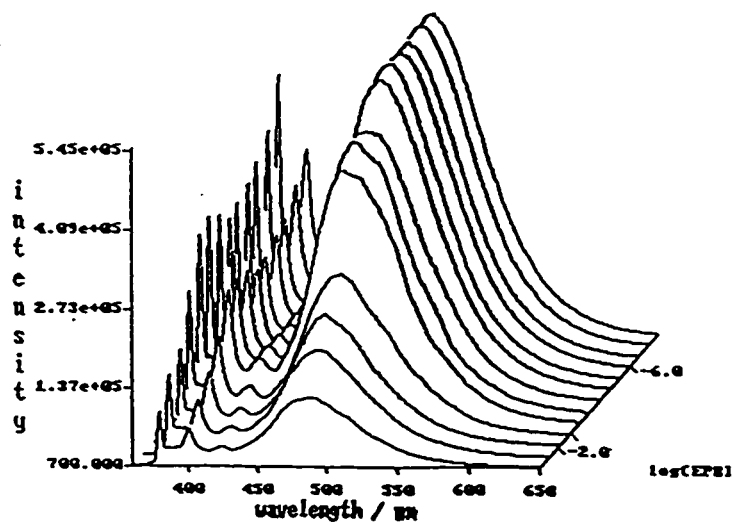


Figure 2.1.13: Fluorescence emission quenching by EPB in a) HEC-N+CH₃-Py/212 and b) HEC-N+C₁₂-Py/240 solutions ($\lambda_{exc} = 344\text{nm}$, 25 °C).

quenched by EPB. At concentrations higher than 10^{-3} M, the Stern-Volmer plots were linear and gave K_{SV} values of 2.9 L/mol for both the monomer and excimer emissions.

Unlike the surfactant quenchers CPC and DPC, the Stern-Volmer constant for both monomer and excimer emission quenching by EPB was an order of magnitude higher for HEC-N+CH₃-Py/212 than for HEC-N+C₁₂-Py/240 (table 2.1.6). It is evident that the quenching of pyrene fluorescence by EPB followed a different mechanism than that of the surfactant quenchers CPC and DPC in the presence of these polymers. Electrostatic forces dominated the interactions. In HEC-N+CH₃-Py/212 solutions, the pyrene labels are attached to sites which are on average not in close proximity to the cationic substituents. Hence, electrostatic repulsions do not hinder the fluorescence quenching by EPB. In the case of HEC-N+C₁₂-Py/240, incomplete pyrene fluorescence quenching was observed. This is in agreement with our postulate of the existence of two sites of attachment of pyrene on the polymer. Quenching of pyrenes in close proximity to the cationic sites is hindered by strong electrostatic repulsions, while quenching of pyrene at sites along the backbone can proceed without interference as in the case of HEC-N+CH₃-Py/212.

Anionic Surfactants

Fluorescence studies were conducted for aqueous solutions of HEC-N+C₁₂-Py/240 and HEC-N+CH₃-Py/212 in the presence of sodium dodecyl sulfate (SDS), sodium decyl sulfate (SDeS) or sodium octyl sulfate (SOS).

Plots of the changes in the ratio of I_E/I_M for HEC-N+C₁₂-Py/240 (0.1 g/L) as a function of added surfactant (SDS, SDeS and SOS) is shown in figure 2.1.14. For all three surfactants, interaction started at 10^{-5} mol/L as indicated by a decrease in I_E/I_M . In the presence of SDS, the midpoint of the transition was 2×10^{-4} mol/L, a surfactant

concentration corresponding to the electrostatic neutralisation point of the charges on the polymer by the surfactant headgroup charges^{104, 109} [Appendix 2]. This concentration was slightly higher for the SOS/polymer system. Turbidity was observed in all systems for surfactant concentrations ranging from 0.005 mol/L to the CMC of the surfactant. Curiously, the ratio I_E/I_M increased for surfactant concentrations corresponding to the respective CMCs (0.008 mol/L for SDS, $3.3 \times 10^{-2} \text{ mol/L}$ for SDeS and $1.3 \times 10^{-1} \text{ mol/L}$ for SOS^{13, 6}). These results are in agreement with our postulate of two sites of pyrene attachment. This seemed to suggest that there were two mechanisms of interaction involved in these studies: firstly interpolymeric until charge neutralization of the polymer was reached and then intrapolymeric. Figure 2.1.15 is a schematic representation of the interactions occurring with increasing anionic surfactant concentration.

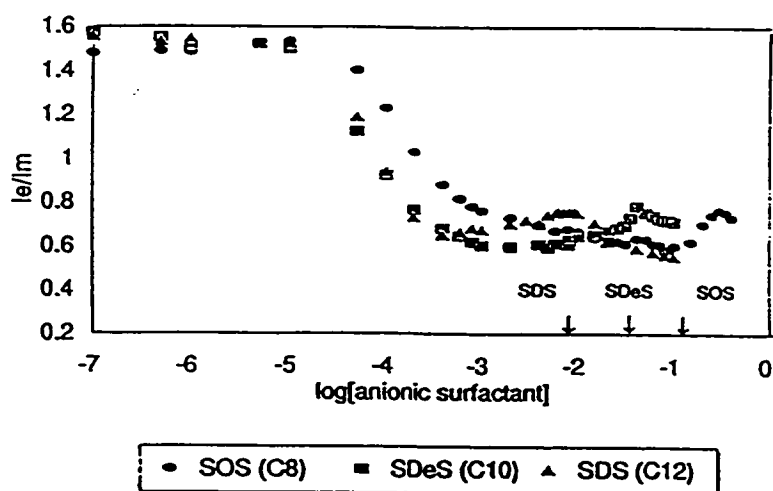


Figure 2.1.14: Plot of I_E/I_M as a function of anionic surfactant concentration (logarithmic scale) for 0.1 g/L HEC-N+C₁₂-Py/240: SDS (triangles), SDeS (squares), and SOS (circles).

In the case of HEC-N+CH₃-Py/212, precipitation also occurred prior to the CMC of the surfactant systems. An unusual behaviour of these mixed systems was observed just prior to the resolubilisation point and was most evident in the presence of SOS, shown in figure 2.1.16. At a SOS concentration of 0.001 mol/L, the monomer emission started to decrease. The excimer emission increased reaching a maximum at 0.05 mol/L. An increase in interpolymeric interaction has been reported to occur leading to a slight increase in viscosity¹¹⁶, explaining the results obtained in this experiment.

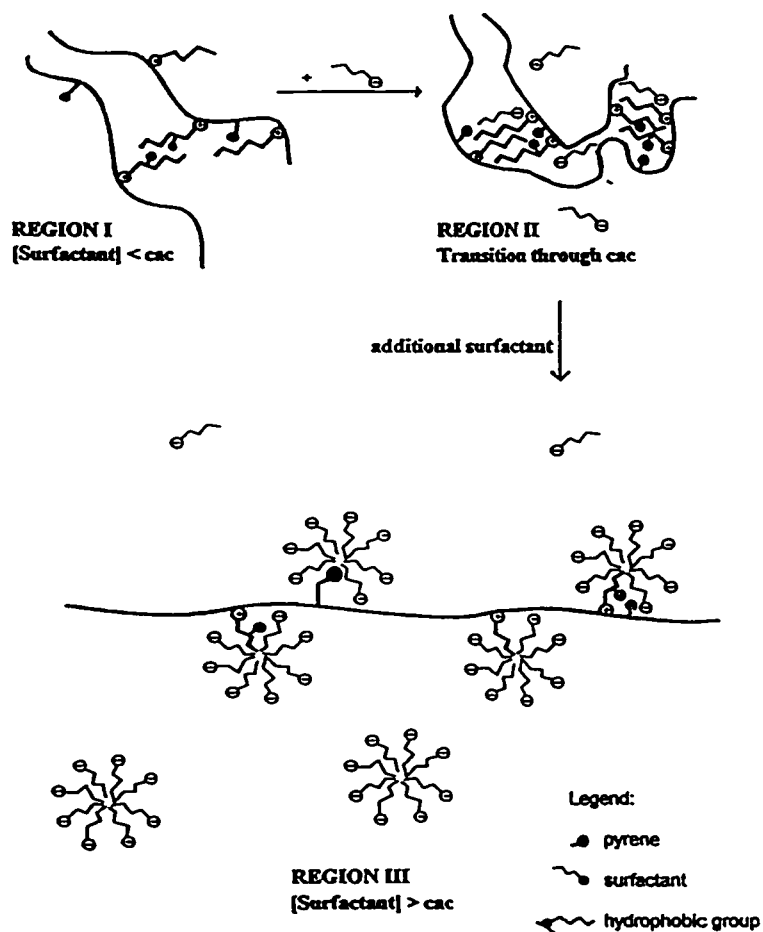
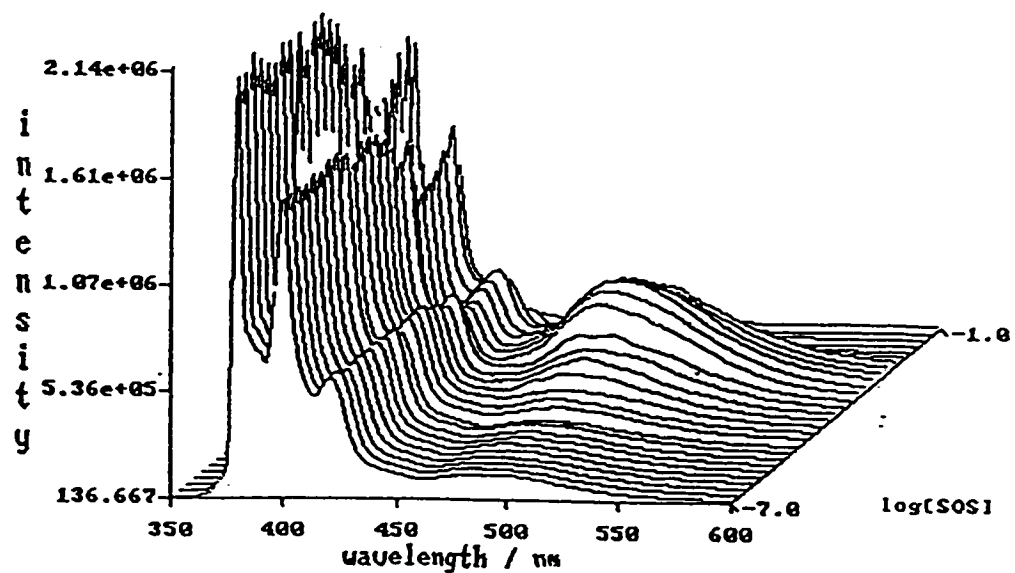


Figure 2.1.15: Schematic diagram of the interactions occurring between HEC-N+C₁₂-Py/240 and anionic surfactants.

a)



b)

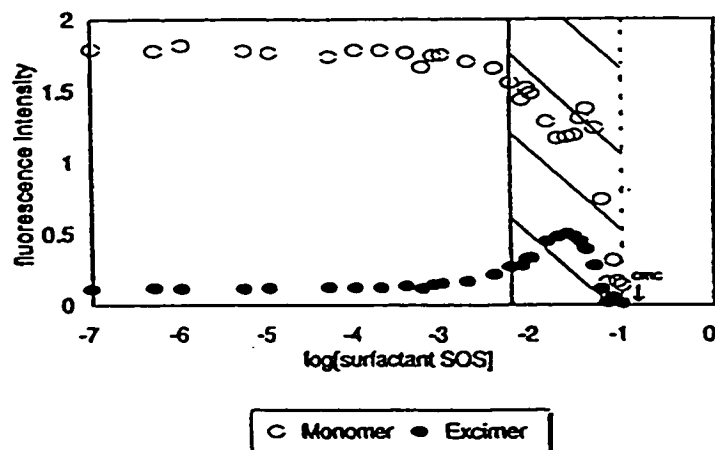


Figure 2.1.16: a) Fluorescence spectra of HEC-N+CH₃-Py/212 and SOS mixed solutions b) plot of I_M and I_E as a function of SOS concentration (logarithmic scale).

Non-ionic Surfactants

Further experiments were carried out to study the effect of non-ionic surfactants on solutions of the cationic cellulose ethers HEC-N+CH₃ and HEC-N+C₁₂. It was found that the addition of either Octyl-β-D-thioglucopyranoside (OTG) or Octa-ethyleneglycol-mono-n-dodecyl ether (C₁₂E₈) to HEC-N+CH₃-Py/212 solutions had no effect on the monomer or excimer emission. Both remained nearly constant over the entire concentration range examined (1×10^{-2} to 1×10^{-5} mol/L). In the solutions studied, no precipitation was observed.

In the case of HEC-N+C₁₂-Py/240 (1.0 g/L) however, upon addition of C₁₂E₈, a significant increase in pyrene monomer intensity took place when the surfactant concentration reached 10^{-4} mol/L, a concentration very close to the CMC of this surfactant (8×10^{-5} mol/L, ⁴¹). The addition of OTG to polymer solutions had the same effect. The onset of the increase in monomer emission occurred at a slightly lower surfactant concentration (2×10^{-3} mol/L) than the CMC of this surfactant (9×10^{-3} mol/L, ¹³).

2.1.4 Section Summary

The aqueous solution properties of HEC-N+CH₃-Py/212 and HEC-N+C₁₂-Py/240 were investigated in this section by various fluorescence techniques. Pyrene and naphthalene moieties were chemically bound to polymers via ether linkages. Fluorescence analysis of the polymers in various solvent systems led to an understanding of the solution properties of the polymers. The aggregation concentration of the HEC-N+C₁₂-Py was determined to be lower than that reported for the unlabelled polymer. A low level of

interpolymeric association was detected in dilute polymer solutions. Studies of several mixed polymer/surfactant systems were carried out. They clearly indicated that despite unfavourable electrostatic repulsive forces, hydrophobic attraction leads to considerable interaction between polymer and surfactant species of like charge. The labelled polymers were also used to investigate the interactions with anionic and non-ionic surfactants in aqueous solution. Taken together, the fluorescence results of mixed polymer/surfactants gave a strong indication that pyrene was attached to two distinct sites along the HEC-N+C₁₂ backbone: a) on the same cellulose substituent in close proximity to the cationic side chain and b) randomly along the cellulose ether backbone. To assess the nature of the interactions occurring at each of these two sites, site specific labelling of the polymer was undertaken, as discussed in the next section.

2.2 Towards Site-Specifically Labelled Cationic Hydrophobically-Modified Hydroxyethyl Cellulose

In the previous section, it was shown that the hydrophobic substituents of HEC-N+C₁₂-Py/240 associate in dilute aqueous solutions, as evidenced by the extremely large excimer emission. It was unclear however, if this excimer emission originated from an interpolymeric or intrapolymeric association. Additionally, fluorescence experiments of HEC-N+C₁₂-Py/240 in the presence of surfactants suggested the presence of two sites of pyrene incorporation, either next to the hydrophobic substituents or along the cellulose backbone. Thus, it became necessary to study two types of labelled polymers. The first type is labelled exclusively along the cellulose backbone and the second type is labelled next to the hydrophobic groups.

This section presents the preparation and characterisation of the first type of site-specifically labelled polymer, as well as the fluorescence investigations directed towards elucidating the solution properties of the new polymers and their interactions with cationic and anionic surfactants. The second type of site-specifically labelled polymer will be investigated in future studies.

2.2.1 Synthesis and Characterisation

2.2.1.1 Synthesis of the Pyrene Labelled Polymers

The polymers were prepared by modification of HEC (series shown in figure 2.2.1) by a two step etherification. First, HEC was labelled with pyrene, than the cationic hydrophobic groups were linked to the pyrene labelled HEC.

Step 1: Pyrene Labelling of Hydroxyethyl Cellulose

Commercial samples of hydroxyethyl cellulose (HEC) of two different molecular weights, HEC QP40 (MW ~ 100,000 Dalton) and HEC QP4400H (MW ~ 400,000 Dalton), were labelled with pyrene via ether linkages. In the following discussion these polymers will be referred to as HEC (LMW) and HEC (HMW), respectively.

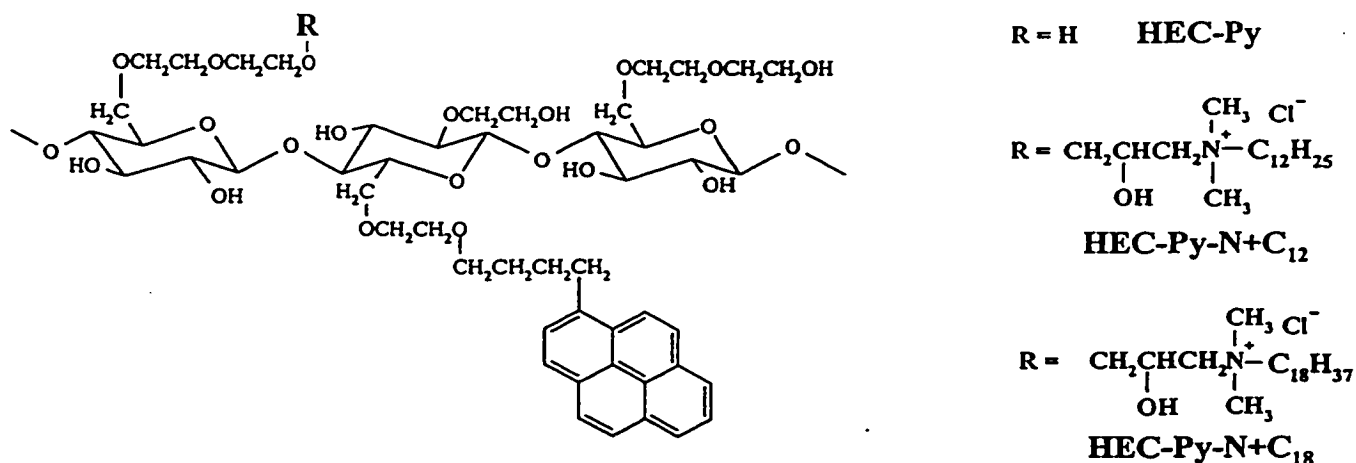


Figure 2.2.1: Idealised structures of the labelled hydroxyethyl cellulose ethers prepared.

Method 1:

The synthetic procedure described by Winnik and co-workers⁹⁷ was used for the random pyrene labelling of HEC. The synthetic scheme is shown in figure 2.2.2. As in the previous cases, ether linkages of the pyrenes to HEC proceeded by reaction of the sodium alkoxide of HEC with 4-(1-pyrenyl)butyl tosylate. Addition of the tosylate to the viscous reaction mixture prior to the addition of base, ensured that the dye was distributed evenly in the solvent medium.

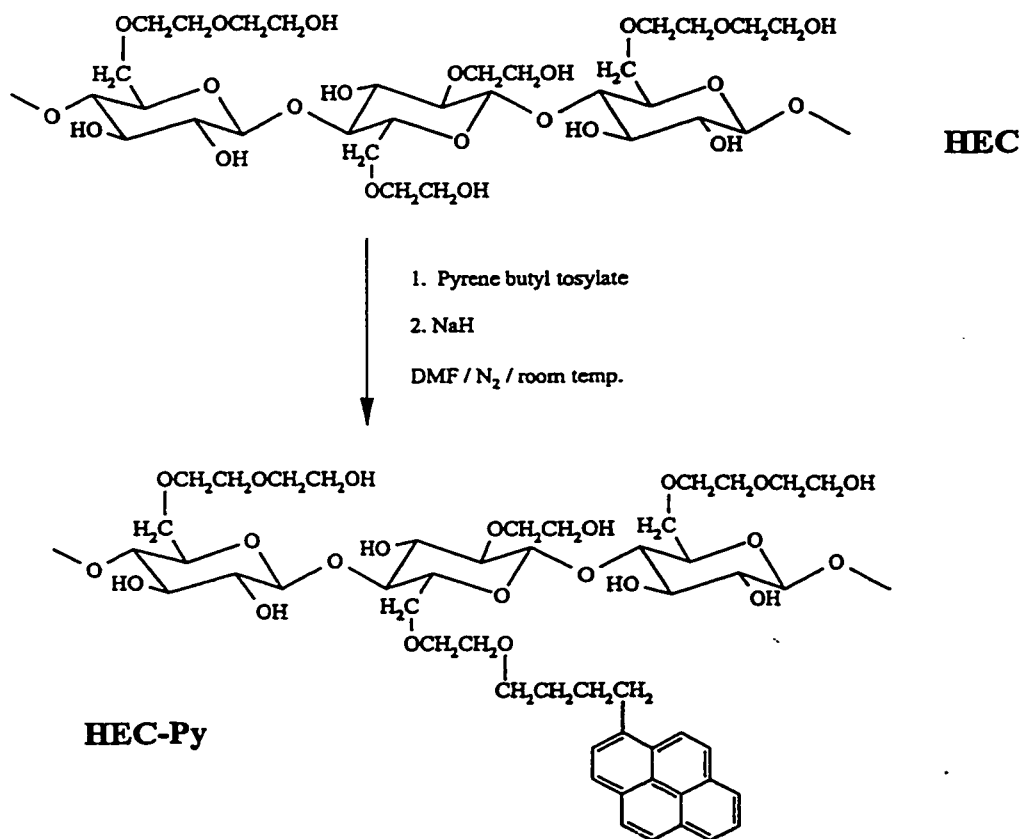


Figure 2.2.2: Synthetic scheme for labelling method 1.

Method 2 :

The second approach (shown in figure 2.2.3) to the pyrene labelling of HEC was as described in section 2.1.1 for the naphthalene labelling of cationic HEC ⁷⁸. The slurry of HEC (LMW) tended to aggregate in the 7:1 tertiary butanol/water solvent system and it was sometimes necessary to break up the gel-like solid into smaller pieces in order to increase the reactive surface area. In contrast to method 1, this ether reaction proceeds with an initial addition of the bulky base benzyltrimethylammonium hydroxide (40 % aqueous solution) to the slurry, leading to the formation of the reactive alkoxide in the

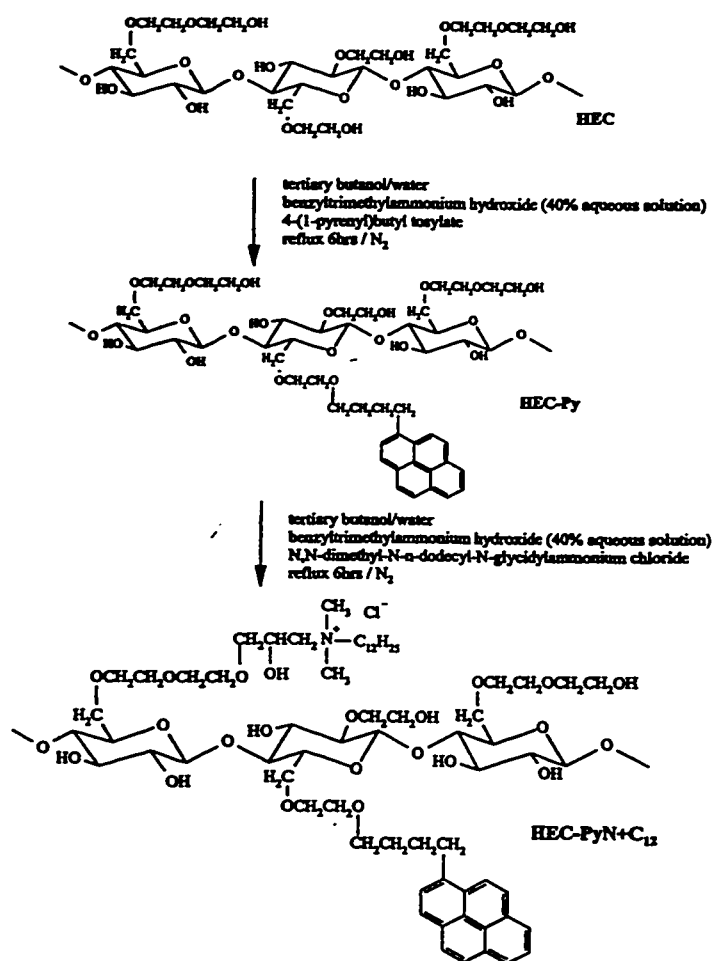


Figure 2.2.3: Synthetic scheme for labelling method 2.

amorphous surface regions of the cellulose ether particles. This bulky counter-ion was selected, since it had been reported to promote higher levels of attachment of hydrophobic moieties, in comparison with smaller counter-ions such as sodium or potassium⁷⁸. The pyrene tosylate in tertiary butanol was added and the etherification reaction was facilitated by refluxing for 6 hours under nitrogen. The pH of the reaction mixture was set between 9 and 10 to achieve the highest level of labelling. Isolation of the product by filtration and rigorous washing first with acetone/water (4:1 v/v) and then acetone, afforded pyrene labelled HEC. The recovery of labelled polymer was very good, typically over 85%. After lyophilisation of their aqueous solutions, some polymers exhibited slight insolubility in cool water, however, solubility was increased by dissolving the polymer solid in water at 60 °C and allowing to cool slowly to room temperature.

Gel permeation chromatography was performed on all pyrene labelled polymers. It was ensured that pyrene was covalently linked to the polymer, and the aqueous solutions contained negligible amounts (< 1%) of low molecular weight impurities. Comparing the chromatograms of labelled and unlabelled polymers confirmed that the modification did not alter the molecular weight or molecular weight distribution of the polymers. Comparison of the chromatograms obtained for the pyrene labelled polymers prepared by the two methods indicated that the second was better at maintaining the molecular weight and distribution of the unlabelled precursor. Chromatograms of solutions of polymer labelled by method 1 presented a higher level of low molecular weight polymers, indicating that some polymer degradation may have occurred. The amount of pyrene incorporated onto the polymer backbone will be discussed in section 2.2.1.2.

Step 2: Attachment of the Cationic Hydrophobic Substituents onto the Pyrene Labelled Hydroxyethyl Cellulose

The second synthetic procedure described in the previous section was used to attach to the pyrene labelled hydroxyethyl cellulose (HEC-Py) either N,N-dimethyl-N-dodecyl-N-glycidyl-ammonium chloride or N,N-dimethyl-N-glycidyl-N-octadecyl-ammonium chloride (synthetic scheme shown in figure 2.2.3). In this reaction, the ether linkages occurred between the reactive alkoxide groups of the swollen HEC-Py and the epoxide groups of these quaternary ammonium derivatives. The syntheses afforded the high and low molecular weight samples of HEC-Py-N+C₁₂ and HEC-Py-N+C₁₈, respectively. Characterisation of these modified pyrene labelled polymers were performed by gel permeation chromatography, UV-vis spectroscopy and ¹H NMR, they will be discussed further in the following section.

2.2.1.2 Characterisation of the Pyrene Labelled Polymers

1. Solubility

Solutions of the pyrene labelled non-ionic and cationic hydrophobically-modified polymers (1.0 g/L) were prepared in deionised water and aqueous solutions of NaCl (0.2 and 10⁻³ mol/L), aqueous methanol (50% and 75% v/v) and aqueous DMSO (80% v/v). Aqueous solutions were prepared by either dissolving the dry polymer in deionised water at room temperature (25 °C) or by adding the solid polymers to deionised water initially at 60 °C and allowing to cool slowly to room temperature. Polymer solutions (1.0 g/L) in

0.2M NaCl were turbid and more viscous than those prepared in 10^{-3} M NaCl of identical concentration. It was found in all cases that a methanol content of 75% led to only partial swelling of the polymer and complete dissolution was not possible. Dissolution of polymer samples in aqueous DMSO (80% v/v) occurred if the polymer was first allowed to swell in DMSO followed by the addition of water.

2. Pyrene Content

Table 2.2.1: Characterisation of pyrene labelled polymers.

Polymer	mols Py per gram polymer ^a	Py per chain ^b	Ratio of Py to Glucose ^c
Py Labelling Method 1			
HEC-Py/145 (LMW)	$3.79 \times 10^{-5} \pm 6.26 \times 10^{-7}$	3.8	1 in 145
HEC-Py/370 (HMW)	$1.50 \times 10^{-5} \pm 4.17 \times 10^{-7}$	6.0	1 in 370
Py Labelling Method 2			
HEC-Py/347 (LMW)	$1.60 \times 10^{-5} \pm 4.27 \times 10^{-7}$	1.6	1 in 347
HEC-Py/97 (HMW)	$5.74 \times 10^{-5} \pm 8.15 \times 10^{-7}$	23.0	1 in 97

^a determined using 0.1 g/L labelled polymer solutions in 80% DMSO using 4-(1-pyrenyl)butanol as a standard compound ($\epsilon = 45435 \pm 397$ in 80% DMSO at 346nm).

^b average number of pyrene moieties per chain of molecular weight 100,000 Dalton (LMW) or 400,000 Dalton (HMW).

^c calculated assuming an average number of glucose units in HEC (HMW) to be 2200 and 550 in HEC (LMW).

The pyrene content of the labelled polymers was determined as described in section 2.1.1. The values are listed in table 2.2.1. The pyrene content of HEC-Py/370 (HMW) prepared using method 1 was approximately 6 pyrene moieties per polymer chain or on average 1 pyrene in 370 glucose units. The pyrene content of HEC-Py/97 (HMW) prepared by labelling method 2 was higher with an average of 97 glucose units per pyrene. In all cases the amount of pyrene incorporation was low, thus the labelling reaction was not expected to substantially increase the hydrophobicity of the polymers.

3. *Cationic Substituent Content*

It turned out to be very difficult to estimate the amount of cationic hydrophobe attached to the modified polymers. An indication of the substituent content could be obtained by analysis of the proton nuclear magnetic resonance spectra of polymer samples in deuterium oxide. The polymer samples formed viscous solutions in this solvent. Samples were insoluble in other common deuterated solvents such as d-DMSO and d-MeOD. The large size of the polymer chains causes the rotational motion to be slow on the time scale of the NMR experiment, leading to the broad peaks observed in the NMR spectra (figure 2.2.4) ¹¹⁷. Proton NMR spectra of HEC and the modified HECs in D₂O present very broad proton resonance signals in the range 3.0 to 3.9 ppm, due to the protons of the glucose rings from the cellulose part of the polymer. The anomeric proton signals of the glucose rings are shifted downfield appearing as a broad singlet at 4.2 ppm. The signals from the alkyl ammonium chains appeared between 0.5 and 3.0 ppm. The terminal methyl group of the alkyl chains appeared as an unresolved multiplet at 0.73 ppm. Comparison of the peak integrations of the terminal methyl group of the alkyl chain of the cationic hydrophobes (0.73 ppm) and the anomeric protons of the glucose rings (4.2 ppm) was used to estimate the extent of hydrophobic modification. The values obtained are reported in table 2.2.2.

Due to the broad NMR peaks obtained, the calculations of the substituent content are not absolute. Performing NMR experiments on samples of the polymers in mixed deuterated DMSO/D₂O (80:20 v/v), may lead to better resolution of the proton NMR spectra. Comparison of these values with other methods such as the elemental analysis of

the nitrogen content, or the chloride counter-ion concentration by standard titration methods may give a better indication of the cationic substituent content on these polymers.

a)



b)

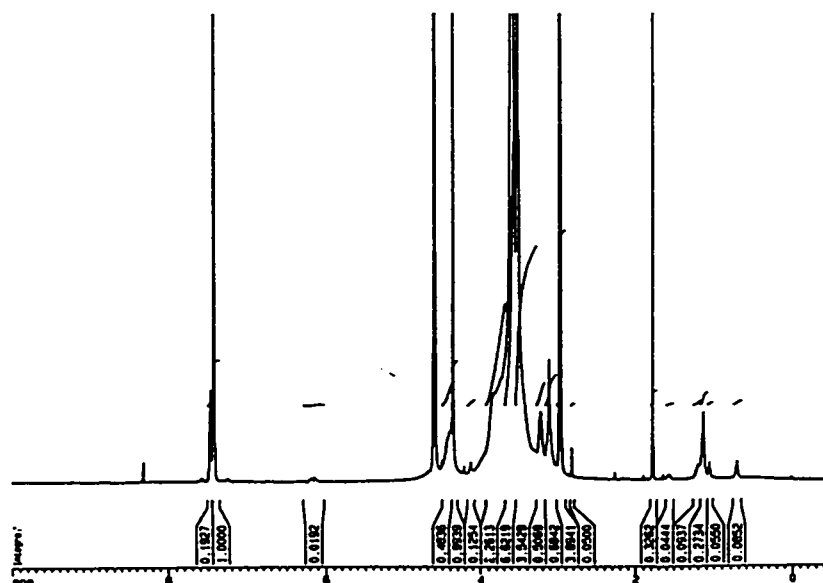


Figure 2.2.4: 500 MHz ¹H NMR spectra of a) HEC (LMW) and b) HEC-Py/145-N+C₁₂ (LMW) in D₂O.

Table 2.2.2: Cationic hydrophobe content on modified pyrene labelled polymers.

Sample	Ratio of Cationic Hydrophobe to Glucose	Cationic Hydrophobe per Glucose Unit ^a	Cationic Hydrophobe per Polymer Chain ^b
HEC-Py/145-N+C ₁₂ (LMW)	1:52	0.019:1	10.7
HEC-Py/347-N+C ₁₂ (LMW)			
HEC-Py/145-N+C ₁₈ (LMW)			
HEC-Py/370-N+C ₁₂ (HMW)	1:286	0.0035:1	7.8
HEC-Py/97-N+C ₁₂ (HMW)			
HEC-Py/370-N+C ₁₈ (HMW)			

^a estimated by comparing the ¹H NMR peak integrations at 0.73 ppm (terminal methyl group) and 4.2 ppm (anomeric proton).

^b calculated assuming an average number of glucose units in HEC (HMW) to be 2200 and 550 in HEC (LMW).

4. *UV-vis Absorbance Spectra – Solvent Effects*

The UV-vis absorbance spectra of solutions of the polymers (1.0 g/L) in: deionised water, aqueous solutions of NaCl (0.2 and 10⁻³ mol/L), aqueous methanol (50% v/v), and aqueous DMSO (80% v/v) were analysed. For polymer solutions in 0.2 mol/L NaCl, a polymer concentration of 0.1 g/L was used since the turbidity of the samples caused considerable scattering. Peak-to-valley ratios were determined by taking the ratio of the absorbance value at the peak (344 nm) to the absorbance value at the valley (336 nm) (table 2.2.3).

Spectra of all aqueous solutions of the labelled polymers exhibited considerable peak broadening. This suggests an aggregation of pyrene moieties on the polymer chains. The broadening was less severe in aqueous solutions of polymers labelled by method 2 suggesting a better distribution of the labels along the polymer. In aqueous solutions of the labelled polymers containing 50% methanol and 80% DMSO, the peak-to-valley ratios of the polymers were greater than in water, indicating that the pyrenes were more isolated in

these solvents. For polymer solutions in the latter solvent system, the peak-to-valley ratios of their respective absorbance spectra start to approach the value obtained for 4(1-pyrenyl)butanol.

Table 2.2.3: UV-vis absorption spectra peak-to-valley ratios for pyrene labelled polymers (1.0 g/L).

Sample	Abs. 344nm/Abs. 336nm					
	Water (cool)	Water (60 °C)	10 ⁻³ M NaCl	0.2M NaCl ^a	50% MeOH	80% DMSO
4(1-pyrenyl)butanol ^b	-	-	-	-	2.74	2.60
HEC-Py/145 (LMW)	1.25	1.78	1.23	1.22	1.41	2.26
HEC-Py/347 (LMW)	1.97	1.94	2.01	1.95	1.64	2.86
HEC-Py/370 (HMW)	1.22	1.23	1.25	1.19	1.65	3.17
HEC-Py/97 (HMW)	1.45	1.37	1.39	1.37	2.48	2.62
HEC-Py/145-N+C ₁₂ (LMW)	1.18	1.17	1.17	1.16	1.30	2.34
HEC-Py/347-N+C ₁₂ (LMW)	2.02	2.03	2.02	2.05	2.37	2.31
HEC-Py/145-N+C ₁₈ (LMW)	1.16	1.17	1.16	1.17	1.43	2.48
HEC-Py/370-N+C ₁₂ (HMW)	1.28	1.29	1.25	1.22	1.46	2.12
HEC-Py/97-N+C ₁₂ (HMW)	1.48	1.44	1.44	1.43	2.29	2.68
HEC-Py/370-N+C ₁₈ (HMW)	1.28	1.30	1.27	1.25	1.60	1.72

^a concentration of polymer solutions was 0.1g/L.

^b concentration of 4(1-pyrenyl)butanol is 0.001 g/L.

5. Emission and Excitation Spectra

Emission spectra of the labelled polymers were measured for polymer solutions in deionised water, 0.2 mol/L aqueous NaCl and 80% aqueous DMSO. Fluorescence spectra of all polymers in aqueous solution were characterised by a strong monomer emission and an excimer band centred at 485 nm. Figure 2.2.5 presents the fluorescence spectra obtained for HEC-Py/370-N+C₁₂ (HMW) labelled using method 1 in aqueous and 80%

aqueous DMSO solutions. In figure 2.2.6, the fluorescence spectra of aqueous and 80% DMSO solutions of HEC-Py/97-N+C₁₂ (HMW) prepared by labelling method 2 are presented. Table 2.2.4 presents the ratios of the intensity of the excimer emission to the intensity of the monomer emission (I_E/I_M) for the labelled polymers. It was observed that the ratio I_E/I_M was higher in the cationic polymers compared to their respective neutral precursors. For example, aqueous solutions of HEC-Py/370 (HMW) exhibited a large excimer emission ($I_E/I_M = 1.0$). After the modification reaction, this value increased to 1.74. The increase in the values of I_E/I_M indicates increased aggregation of the pyrenes in these polymer solutions. Fluorescence spectra of the labelled polymers in the other solvent systems examined, also exhibited an increase in the ratio of I_E/I_M after cationic hydrophobic modification, however the effect was most apparent in aqueous solutions. From UV data, less aggregation of polymer chains was expected to take place in solutions of 80% DMSO, and indeed the excimer emission relative to the monomer emission was weaker in this case.

Comparison of the emission spectra for solutions of pyrene labelled polymers prepared by the two methods leads to several interesting observations. Spectra of polymer solutions labelled using the first method have a larger excimer emission compared to the monomer emission. Spectra of polymer solutions in 80% DMSO labelled with pyrene by method 1 also exhibited a strong excimer emission. In contrast, the emission spectra measured for 80% DMSO solutions of polymers labelled by method 2, exhibited almost no excimer emission resulting in an I_E/I_M ratio of almost zero. This suggests that the pyrene moieties on the polymer chains were too far apart from each other to form

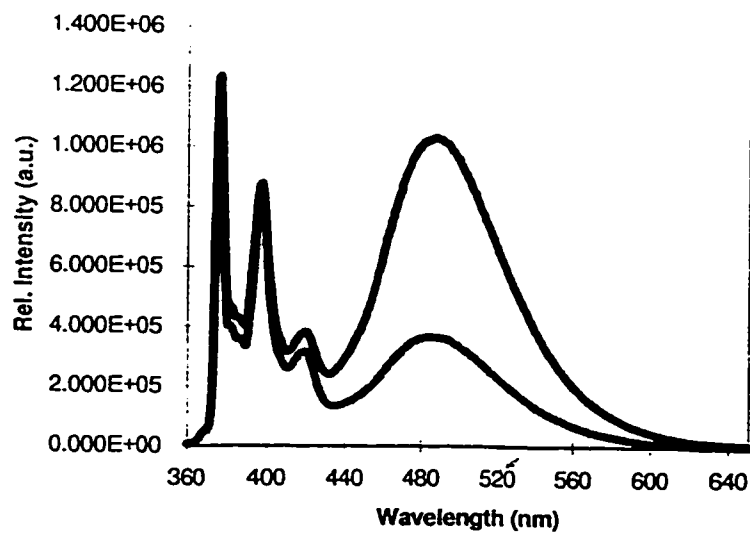


Figure 2.2.5: Fluorescence spectra of 1.0 g/L HEC-Py/370-N+C₁₂ (HMW) in aqueous solution (black line) and aqueous DMSO (80% v/v, grey line).

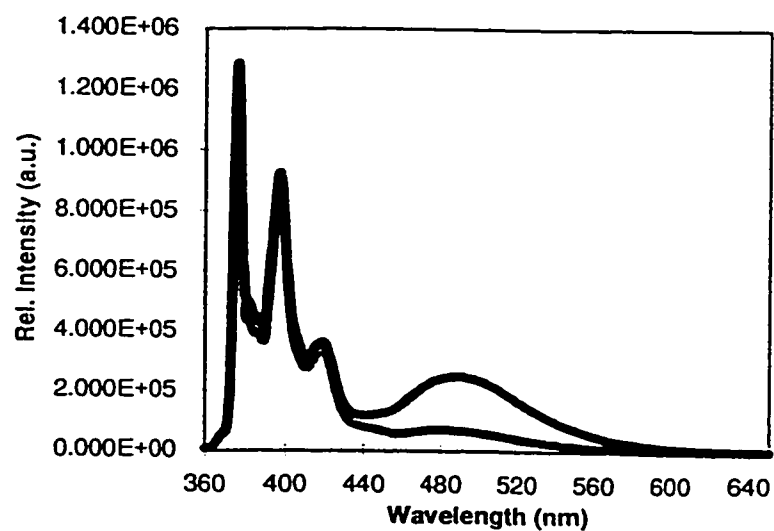


Figure 2.2.6: Fluorescence spectra of 1.0 g/L HEC-Py/97-N+C₁₂ (HMW) in aqueous solution (black line) and in aqueous DMSO (80% v/v, grey line).

intramolecular excited state complexes. This further suggests that by using the first labelling method, the pyrene moieties were distributed in blocks leading to a higher contribution of intramolecular excimer formation within the same chain. The second pyrene labelling method seems to lead to a more random distribution of the pyrene moieties on the polymer chains which predominantly forms intermolecular excimers.

General solvent dependent trends of the excitation spectra provided further evidence that there was a difference in the environment around the pyrenes on the polymers labelled by the two methods. Comparison of the intensity at the peak to the intensity at the valley ratios of excitation spectra for polymer solutions in water and in 80% DMSO showed a general increase in the values monitored at the monomer and excimer wavelengths. This suggested that the pyrene moieties were less aggregated in 80% DMSO. Comparison of the wavelengths of the peak maxima of the two excitation spectra indicated that in 80% DMSO, the mechanism of pyrene excimer emission involved a dynamic interaction. For aqueous polymer solutions, excimer emission arose from preassociated chromophore aggregation as shown by a blue shift in the excitation spectrum monitored at the monomer wavelength relative to the excitation spectrum monitored at the excimer wavelength.

For polymer solutions of high salt concentration, the emission spectra were monitored at 1.0 and 0.1 g/L polymer concentrations. The overall emission intensities of 1.0 g/L polymer solutions were substantially lower than the emission intensities of the corresponding 0.1 g/L polymer solutions recorded under identical conditions and the ratio

Table 2.2.4: Excitation peak-to-valley ratios and values of I_E/I_M for the pyrene labelled polymers.

Sample	Conc. (g/L)	Solvent	I(344)/I(332) monomer	I(344)/I(332) excimer	I_E/I_M
Non-Ionic Polymers					
HEC-Py/145 (LMW)	0.1	H ₂ O	2.32	1.51	0.81
HEC-Py/145 (LMW)	1.0	0.2M NaCl	-	-	1.08
HEC-Py/145 (LMW)	0.1	0.2M NaCl	2.09	1.30	0.59
HEC-Py/145 (LMW)	0.1	80% DMSO	2.38	2.04	0.41
HEC-Py/347 (LMW)	1.0	H ₂ O	1.29	1.38	0.02
HEC-Py/347 (LMW)	1.0	0.2M NaCl	-	-	0.03
HEC-Py/347 (LMW)	0.1	0.2M NaCl	1.71	1.52	0.02
HEC-Py/347 (LMW)	0.1	80% DMSO	1.96	2.03	0.02
HEC-Py/370 (HMW)	1.0	H ₂ O	2.23	1.54	1.03
HEC-Py/370 (HMW)	1.0	0.2M NaCl	-	-	0.61
HEC-Py/370 (HMW)	0.1	0.2M NaCl	2.17	1.53	0.41
HEC-Py/370 (HMW)	0.1	80% DMSO	2.28	2.26	0.25
HEC-Py/97 (HMW)	0.1	H ₂ O	2.07	1.63	0.18
HEC-Py/97 (HMW)	1.0	0.2M NaCl	-	-	0.68
HEC-Py/97 (HMW)	0.1	0.2M NaCl	1.38	1.68	0.24
HEC-Py/97 (HMW)	0.1	80% DMSO	1.78	1.76	0.03
Cationic HM-Polymers					
HEC-Py/145-N+C ₁₂ (LMW)	0.1	H ₂ O	2.40	1.48	0.86
HEC-Py/145-N+C ₁₂ (LMW)	1.0	0.2M NaCl	-	-	1.25
HEC-Py/145-N+C ₁₂ (LMW)	0.1	0.2M NaCl	2.04	1.33	0.74
HEC-Py/145-N+C ₁₂ (LMW)	0.1	80% DMSO	2.43	2.15	0.43
HEC-Py/145-N+C ₁₈ (LMW)	0.1	H ₂ O	2.38	1.47	0.76
HEC-Py/145-N+C ₁₈ (LMW)	1.0	0.2M NaCl	-	-	1.05
HEC-Py/145-N+C ₁₈ (LMW)	0.1	0.2M NaCl	2.02	1.34	0.63
HEC-Py/145-N+C ₁₈ (LMW)	0.1	80% DMSO	2.45	2.14	0.43
HEC-Py/347-N+C ₁₂ (LMW)	1.0	H ₂ O	1.49	1.47	0.04
HEC-Py/347-N+C ₁₂ (LMW)	1.0	0.2M NaCl	-	-	0.08
HEC-Py/347-N+C ₁₂ (LMW)	0.1	0.2M NaCl	1.72	1.52	0.04
HEC-Py/347-N+C ₁₂ (LMW)	0.1	80% DMSO	2.65	2.71	0.02
HEC-Py/370-N+C ₁₂ (HMW)	1.0	H ₂ O	2.54	1.23	1.74
HEC-Py/370-N+C ₁₂ (HMW)	1.0	0.2M NaCl	-	-	1.13
HEC-Py/370-N+C ₁₂ (HMW)	0.1	0.2M NaCl	2.19	1.42	0.98
HEC-Py/370-N+C ₁₂ (HMW)	0.1	80% DMSO	2.59	2.43	0.34
HEC-Py/370-N+C ₁₈ (HMW)	1.0	H ₂ O	2.19	1.42	1.91
HEC-Py/370-N+C ₁₈ (HMW)	1.0	0.2M NaCl	-	-	0.79
HEC-Py/370-N+C ₁₈ (HMW)	0.1	0.2M NaCl	2.18	1.48	0.61
HEC-Py/370-N+C ₁₈ (HMW)	0.1	80% DMSO	2.66	2.45	0.36
HEC-Py/97-N+C ₁₂ (HMW)	0.1	H ₂ O	2.28	1.63	0.18
HEC-Py/97-N+C ₁₂ (HMW)	1.0	0.2M NaCl	-	-	0.47
HEC-Py/97-N+C ₁₂ (HMW)	0.1	0.2M NaCl	1.36	1.02	0.24
HEC-Py/97-N+C ₁₂ (HMW)	0.1	80% DMSO	2.24	2.19	0.06

I_E/I_M was considerably lower for the lower polymer concentration. Excitation spectra were measured for the 0.1 g/L polymer concentrations. The peak-to-valley ratios measured from the various excitation spectra and I_E/I_M for the labelled polymers in 0.2 mol/L NaCl are presented in table 2.2.4.

6. *Fluorescence Lifetimes*

The results of time-resolved measurements of the labelled polymer solutions in water and 80% DMSO are presented in tables 2.2.5 and 2.2.6. The decay curves obtained were fit to a sum of exponentials. Fits consisting of up to four components were used when necessary and an average lifetime is reported in brackets in such cases. In comparing these results, several trends were observed.

The monomer emission decay measured for polymer solutions in 80% DMSO for HEC-Py/370 (HMW) labelled using method 1 consisted of three components resulting in an average lifetime of 58 ns ($\chi^2 = 1.2$). The lifetime measured for a solution of HEC-Py/97 (HMW) in 80% DMSO labelled using method 2 consisted of a two component decay with a higher average lifetime (95 ns, $\chi^2 = 1.4$). Similar results were obtained when comparing the polymers after cationic substituent incorporation (table 2.2.6). The decay measured for a solution of HEC-Py/370-N+C₁₂ (HMW) in 80% DMSO consisted of three components with an average lifetime of 55 ns ($\chi^2 = 1.0$), in comparison to a solution of HEC-Py/97-N+C₁₂ (HMW) which had a two component decay with an average lifetime of 92 ns ($\chi^2 = 1.0$). The excimer emission curves of polymer solutions in 80% DMSO consisted of both a growing-in as well as a decay profile. The excimer measured for polymers labelled using

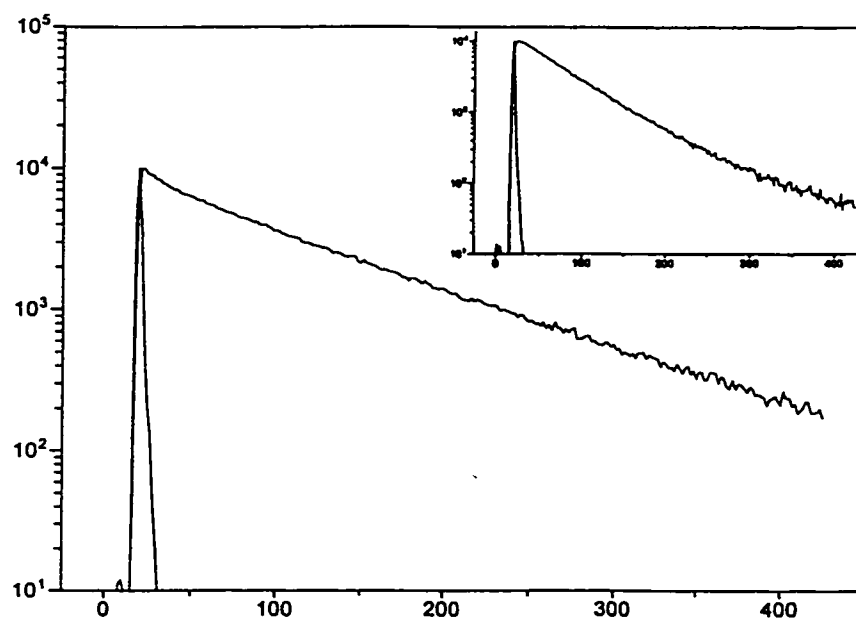
Table 2.2.5: Fluorescence decay measurements of the pyrene labelled polymers in aqueous solution and aqueous DMSO (80% v/v).

Sample	Solvent	Monomer		Excimer	
		Lifetime (ns)	Pre-factor	Lifetime (ns)	Pre-factor
HEC-Py/145 (LMW)	H ₂ O	$\tau_1=108.6\pm 0.49$ $\tau_2=29.3\pm 2.7$ $\langle\tau\rangle 96.9\pm 5.2\times 10^{-3}$	$a_1=0.85\pm 0.01$ $a_2=0.15\pm 0.01$ $\chi^2 = 1.1$	$\tau_1=69.5\pm 0.99$ $\tau_2=38.7\pm 1.5$ $\tau_3=4.29\pm 1.6$ $\langle\tau\rangle 51.0\pm 4.0\times 10^{-3}$	$a_1=0.52\pm 0.03$ $a_2=0.37\pm 0.03$ $a_3=0.11\pm 0.10$ $\chi^2 = 1.1$
HEC-Py/370 (HMW)	H ₂ O	$\tau_1=105\pm 1.2$ $\tau_2=39.5\pm 11$ $\tau_3=9.18\pm 3.0$ $\langle\tau\rangle 82.3\pm 4.1\times 10^{-2}$	$a_1=0.72\pm 0.02$ $a_2=0.13\pm 0.02$ $a_3=0.15\pm 0.03$ $\chi^2 = 1.1$	$\tau_1=62.5\pm 0.27$ $\tau_2=30.9\pm 1.0$ $\langle\tau\rangle 54.0\pm 1.4\times 10^{-3}$	$a_1=0.73\pm 0.01$ $a_2=0.27\pm 0.01$ $\chi^2 = 1.2$
HEC-Py/145 (LMW)	80% DMSO	$\tau_1=100.1\pm 0.3$ $\tau_2=38.0\pm 0.7$ $\tau_3=10.8\pm 0.3$ $\langle\tau\rangle 43.0\pm 0.0$	$a_1=0.43\pm 0.01$ $a_2=0.22\pm 0.01$ $a_3=0.35\pm 0.01$ $\chi^2 = 1.1$	$\tau_1=54.8\pm 0.03$ $\tau_2=54.6\pm 0.03$ $\tau_3=2.67\pm 0.01$ $\tau_4=11.4\pm 0.02$ $\langle\tau\rangle 47.9\pm -1.5\times 10^{-5}$	$a_1=0.54\pm 0.00$ $a_2=0.46\pm 0.00$ $a_3=-0.28\pm 0.00$ $a_4=-0.53\pm 0.00$ $\chi^2 = 1.1$
HEC-Py/347 (LMW)	80% DMSO	$\tau_1=103.2\pm 0.5$	$a_1=1.00\pm 0.01$ $\chi^2 = 0.98$	-	-
HEC-Py/370 (HMW)	80% DMSO	$\tau_1=101.4\pm 1.8$ $\tau_2=11.9\pm 1.5$ $\tau_3=39.3\pm 7.3$ $\langle\tau\rangle 57.6\pm 0.03$	$a_1=0.45\pm 0.02$ $a_2=0.34\pm 0.03$ $a_3=0.21\pm 0.03$ $\chi^2 = 1.2$	$\tau_1=55.1\pm 0.58$ $\tau_2=57.5\pm 0.82$ $\tau_3=8.47\pm 0.03$ $\langle\tau\rangle 49.5\pm 3.0\times 10^{-4}$	$a_1=0.61\pm 0.01$ $a_2=0.39\pm 0.01$ $a_3=-0.78\pm 0.01$ $\chi^2 = 2.9$
HEC-Py/97 (HMW)	80% DMSO	$\tau_1=101.3\pm 0.6$ $\tau_2=35.8\pm 6.1$ $\langle\tau\rangle 95.2\pm 0.02$	$a_1=0.91\pm 0.02$ $a_2=0.09\pm 0.01$ $\chi^2 = 1.2$	$\tau_1=66.8\pm 0.29$ $\tau_2=6.79\pm 0.17$ $\tau_3=15.7\pm 0.55$ $\langle\tau\rangle 57.0\pm -3.3\times 10^{-3}$	$a_1=1.00\pm 0.01$ $a_2=-0.26\pm 0.02$ $a_3=-0.51\pm 0.02$ $\chi^2 = 1.2$

Table 2.2.6: Fluorescence decay measurements of the pyrene labelled cationic hydrophobically-modified polymers in deionised water and aqueous DMSO (80% v/v).

Sample	Solvent	Monomer		Excimer	
		Lifetime (ns)	Pre-factor	Lifetime (ns)	Pre-factor
HEC-Py/145-N+C ₁₂ (LMW)	H ₂ O	$\tau_1=107\pm 0.52$ $\tau_2=30.7\pm 3.3$ $\langle\tau\rangle 97.1\pm 6.5\times 10^{-3}$	$a_1=0.87\pm 0.01$ $a_2=0.13\pm 0.01$ $\chi^2 = 1.1$	$\tau_1=83.0\pm 1.9$ $\tau_2=49.5\pm 1.9$ $\tau_3=50.3\pm 18$ $\langle\tau\rangle 52.6\pm 4.8\times 10^{-3}$	$a_1=0.22\pm 0.03$ $a_2=0.78\pm 0.04$ $a_3=-0.09\pm 0.04$ $\chi^2 = 1.2$
HEC-Py/145-N+C ₁₈ (LMW)	H ₂ O	$\tau_1=111\pm 0.86$ $\tau_2=41.0\pm 6.0$ $\langle\tau\rangle 102\pm 1.8\times 10^{-2}$	$a_1=0.88\pm 0.02$ $a_2=0.12\pm 0.02$ $\chi^2 = 1.1$	-	-
HEC-Py/370-N+C ₁₂ (HMW)	H ₂ O	$\tau_1=104\pm 0.04$ $\tau_2=31.5\pm 0.17$ $\tau_3=5.66\pm 0.06$ $\langle\tau\rangle 74.1\pm 3.4\times 10^{-4}$	$a_1=0.65\pm 0.01$ $a_2=0.16\pm 0.01$ $a_3=0.19\pm 0.01$ $\chi^2 = 1.0$	$\tau_1=66.1\pm 1.4$ $\tau_2=40.4\pm 2.8$ $\langle\tau\rangle 56.8\pm 1.5\times 10^{-2}$	$a_1=0.64\pm 0.07$ $a_2=0.36\pm 0.07$ $\chi^2 = 1.1$
HEC-Py/370-N+C ₁₈ (HMW)	H ₂ O	$\tau_1=103\pm 0.01$ $\tau_2=27.3\pm 0.02$ $\tau_3=5.31\pm 0.01$ $\langle\tau\rangle 74.9\pm 0.0$	$a_1=0.68\pm 0.01$ $a_2=0.15\pm 0.01$ $a_3=0.18\pm 0.01$ $\chi^2 = 1.1$	$\tau_1=64.2\pm 1.1$ $\tau_2=35.7\pm 3.1$ $\langle\tau\rangle 55.9\pm 1.6\times 10^{-2}$	$a_1=0.71\pm 0.05$ $a_2=0.29\pm 0.05$ $\chi^2 = 1.1$
HEC-Py/145-N+C ₁₂ (LMW)	80% DMSO	$\tau_1=102.2\pm 1.7$ $\tau_2=9.4\pm 1.0$ $\tau_3=38.7\pm 4.1$ $\langle\tau\rangle 52.4\pm 0.01$	$a_1=0.38\pm 0.02$ $a_2=0.36\pm 0.02$ $a_3=0.27\pm 0.02$ $\chi^2 = 1.4$	$\tau_1=54.3\pm 0.03$ $\tau_2=50.4\pm 0.03$ $\tau_3=7.55\pm 0.01$ $\langle\tau\rangle 47.1\pm 1.8\times 10^{-6}$	$a_1=0.57\pm 0.00$ $a_2=0.43\pm 0.00$ $a_3=-0.72\pm 0.00$ $\chi^2 = 2.1$
HEC-Py/347-N+C ₁₂ (LMW)	80% DMSO	$\tau_1=102.2\pm 0.2$	$a_1=1.00\pm 0.00$ $\chi^2 = 1.0$	-	-
HEC-Py/145-N+C ₁₈ (LMW)	80% DMSO	$\tau_1=101.7\pm 0.6$ $\tau_2=35.9\pm 1.5$ $\tau_3=9.5\pm 0.7$ $\langle\tau\rangle 54.0\pm 0.01$	$a_1=0.41\pm 0.01$ $a_2=0.27\pm 0.01$ $a_3=0.33\pm 0.02$ $\chi^2 = 1.4$	$\tau_1=52.3\pm 0.01$ $\tau_2=53.7\pm 0.01$ $\tau_3=6.70\pm 0.00$ $\langle\tau\rangle 47.9\pm 0.0$	$a_1=0.61\pm 0.00$ $a_2=0.39\pm 0.00$ $a_3=-0.74\pm 0.00$ $\chi^2 = 2.9$
HEC-Py/370-N+C ₁₂ (HMW)	80% DMSO	$\tau_1=102.4\pm 2.7$ $\tau_2=44.8\pm 5.8$ $\tau_3=11.2\pm 1.2$ $\langle\tau\rangle 55.2\pm 0.02$	$a_1=0.38\pm 0.03$ $a_2=0.28\pm 0.02$ $a_3=0.34\pm 0.02$ $\chi^2 = 1.0$	$\tau_1=57.2\pm 0.03$ $\tau_2=58.9\pm 0.04$ $\tau_3=8.37\pm 0.01$ $\langle\tau\rangle 51.1\pm 1.0\times 10^{-6}$	$a_1=0.59\pm 0.00$ $a_2=0.41\pm 0.00$ $a_3=-0.81\pm 0.00$ $\chi^2 = 3.4$
HEC-Py/97-N+C ₁₂ (HMW)	80% DMSO	$\tau_1=101.9\pm 0.5$ $\tau_2=28.4\pm 3.2$ $\langle\tau\rangle 92.0\pm 0.01$	$a_1=0.86\pm 0.01$ $a_2=0.14\pm 0.01$ $\chi^2 = 1.0$	$\tau_1=65.9\pm 0.50$ $\tau_2=62.6\pm 1.4$ $\tau_3=12.0\pm 0.05$ $\langle\tau\rangle 55.3\pm 5.1\times 10^{-4}$	$a_1=0.72\pm 0.01$ $a_2=0.28\pm 0.01$ $a_3=-0.81\pm 0.01$ $\chi^2 = 2.2$
HEC-Py/370-N+C ₁₈ (HMW)	80% DMSO	$\tau_1=107.2\pm 5.9$ $\tau_2=54.3\pm 9.0$ $\tau_3=13.1\pm 1.2$ $\langle\tau\rangle 56.5\pm 0.04$	$a_1=0.33\pm 0.07$ $a_2=0.30\pm 0.05$ $a_3=0.37\pm 0.02$ $\chi^2 = 1.4$	$\tau_1=56.3\pm 0.01$ $\tau_2=57.8\pm 0.02$ $\tau_3=8.33\pm 0.00$ $\langle\tau\rangle 50.0\pm 0.0$	$a_1=0.71\pm 0.00$ $a_2=0.29\pm 0.00$ $a_3=-0.81\pm 0.00$ $\chi^2 = 3.1$

a)



b)

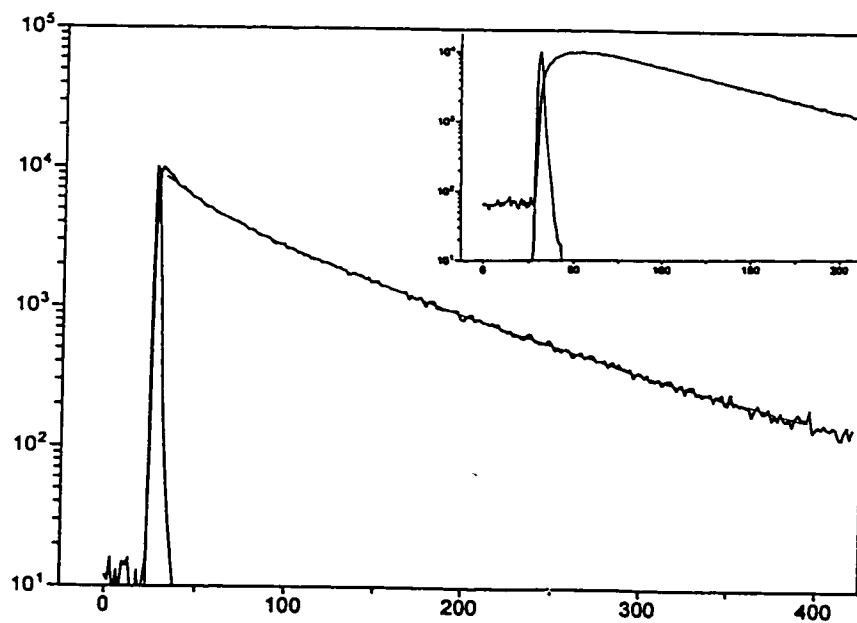


Figure 2.2.7: Fluorescence monomer decay curves and inset excimer decay curves of HEC-Py/370-N+C₁₂ (HMW) in a) water and b) aqueous DMSO (80% v/v).

method 1 had almost the same decay lifetimes as polymers labelled using method 2. The excimer average lifetime for a solution of HEC-Py/370 (HMW) was 50 ns ($\chi^2 = 2.9$) and that of HEC-Py/97 (HMW) was 57 ns ($\chi^2 = 1.2$). The lifetimes of the cationic substituted polymers had similar values. The presence of the growing-in component suggests a diffusion controlled dynamic excimer mechanism for polymer solutions in 80% DMSO ¹¹⁰ as indicated also by the steady-state measurements.

Fluorescence lifetimes were also measured for the labelled polymers in aqueous solution (tables 2.2.5 and 2.2.6). The average lifetimes measured for polymer solutions in water were higher than in 80% DMSO. For example, HEC-Py/370 (HMW) had an average monomer lifetime of 82 ns ($\chi^2 = 1.1$) in aqueous solution and 58 ns ($\chi^2 = 1.2$) in 80% DMSO. After hydrophobic substitution, the average monomer lifetime of HEC-Py/370-N+C₁₂ (HMW) was 74 ns ($\chi^2 = 1.0$). The excimer emission decay curves for aqueous polymer solutions were characterised by a fluorescence decay profile with no growing in component, in contrast to the curves measured for polymer solutions in 80% DMSO. The average excimer lifetimes were also higher in aqueous solution (55 ns) than in 80% DMSO (50 ns). Figure 2.2.7 presents the fluorescence decay curves of the monomer and excimer emissions of HEC-Py/370-N+C₁₂ (HMW) in aqueous and 80% DMSO solutions.

In comparing the average lifetimes obtained for polymer solutions before and after cationic substitution, it was observed that the values recorded were mostly unaffected by the modification in the cationic polymer. For example the monomer lifetime of HEC-Py/370 (HMW) in 80% DMSO decreased by 3 ns after cationic substitution.

2.2.1.3 Synthesis and Characterisation of the Naphthalene Labelled Polymers

Analogous naphthalene labelled cationic hydrophobically-modified polymers (listed in figure 2.2.8) were prepared by a two step synthesis. Method 2 (see above) was used for both etherification steps involved in the preparation of the polymers. High and low molecular weight polymers were labelled with naphthalene by reacting the slurry of hydroxyethyl cellulose with 2-(1-naphthyl)ethyl tosylate using the base benzyltrimethylammonium hydroxide. After purification and characterisation by gel permeation chromatography, UV-vis spectroscopy and proton NMR, a second etherification reaction was performed to attach either N,N-dimethyl-N-dodecyl-N-glycidyl-ammonium chloride or N,N-dimethyl-N-glycidyl-N-octadecyl-ammonium chloride on the naphthalene labelled HECs (synthetic scheme as in figure 2.2.3 for the pyrene labelled analogues). Cationic hydrophobically-modified naphthalene labelled polymers were characterised as described above by gel permeation chromatography, UV-vis spectroscopy, and proton NMR. The naphthalene content in these polymers was determined using 1.0 g/L solutions in 80% DMSO using 2-(1-naphthyl)ethanol as standard ($\epsilon=6600$ L/mol·cm at 286nm, 0.01 g/L in 80% DMSO). The cationic substitution onto the labelled polymers was determined by analysis of the proton NMR spectra as described above for the pyrene labelled cationic hydrophobically-modified polymers. Table 2.2.7 presents the values of pyrene content and cationic substitution obtained for these polymers. Figure 2.2.9 presents the ^1H NMR spectra of HEC-Np/205-N+C₁₂ (LMW).

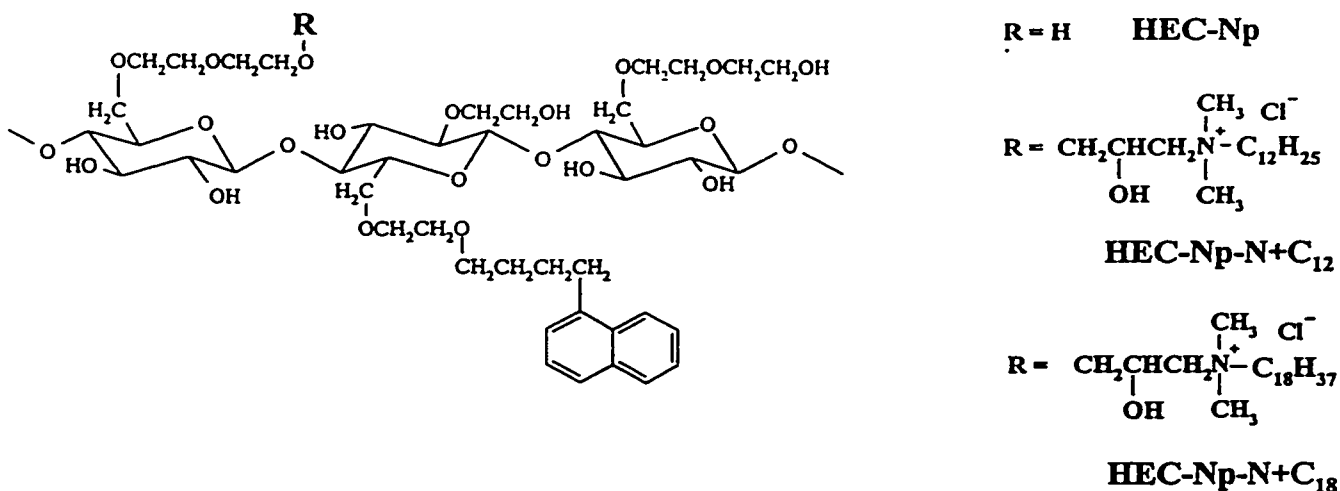


Figure 2.2.8: Structures of the naphthalene labelled polymers prepared.

Table 2.2.7: Characterisation of the naphthalene labelled hydroxyethyl cellulose ethers.

Polymer	Mol Np per Gram Polymer ^a	Np perChain ^b	Ratio of Np to Glucose
HEC-Np/144 (LMW)	$5.06 \times 10^{-5} \pm 6.65 \times 10^{-7}$	5.1	1 in 144
HEC-Np/205 (LMW)	$2.62 \times 10^{-5} \pm 4.14 \times 10^{-7}$	2.6	1 in 205
HEC-Np/950 (HMW)	$5.67 \times 10^{-6} \pm 2.00 \times 10^{-7}$	2.3	1 in 950
HEC-Np/333 (HMW)	$1.82 \times 10^{-5} \pm 3.22 \times 10^{-7}$	7.3	1 in 333
	Cationic Hydrophobe per Glucose Unit ^d	Cationic Hydrophobe per Chain ^c	Ratio of Cationic Hydrophobe to Glucose
HEC-Np/205-N+C ₁₂ (LMW)	0.023	12.7	1 in 44
HEC-Np/333-N+C ₁₂ (HMW)	0.053	29	1 in 19
HEC-Np/144-N+C ₁₈ (LMW)	0.00093	0.52	1 in 1075
HEC-Np/950-N+C ₁₈ (HMW)	0.00437	9.7	1 in 229

^a determined using 1.0 g/L labelled polymer solutions in 80% DMSO using 2-(1-naphthyl)ethanol as a standard compound ($\epsilon = 6638 \pm 63$ at 286nm, 0.01 g/L in 80% DMSO).

^b average number of naphthalene moieties per chain of molecular weight 100,000 Dalton (LMW) or 400,000 Dalton (HMW).

^c calculated assuming an average number of glucose units in HEC (HMW) to be 2200 and 550 in HEC (LMW).

^d estimated by comparing the ¹H NMR peak integrations at 0.73 ppm (terminal methyl group) and 4.2 ppm (anomeric proton).

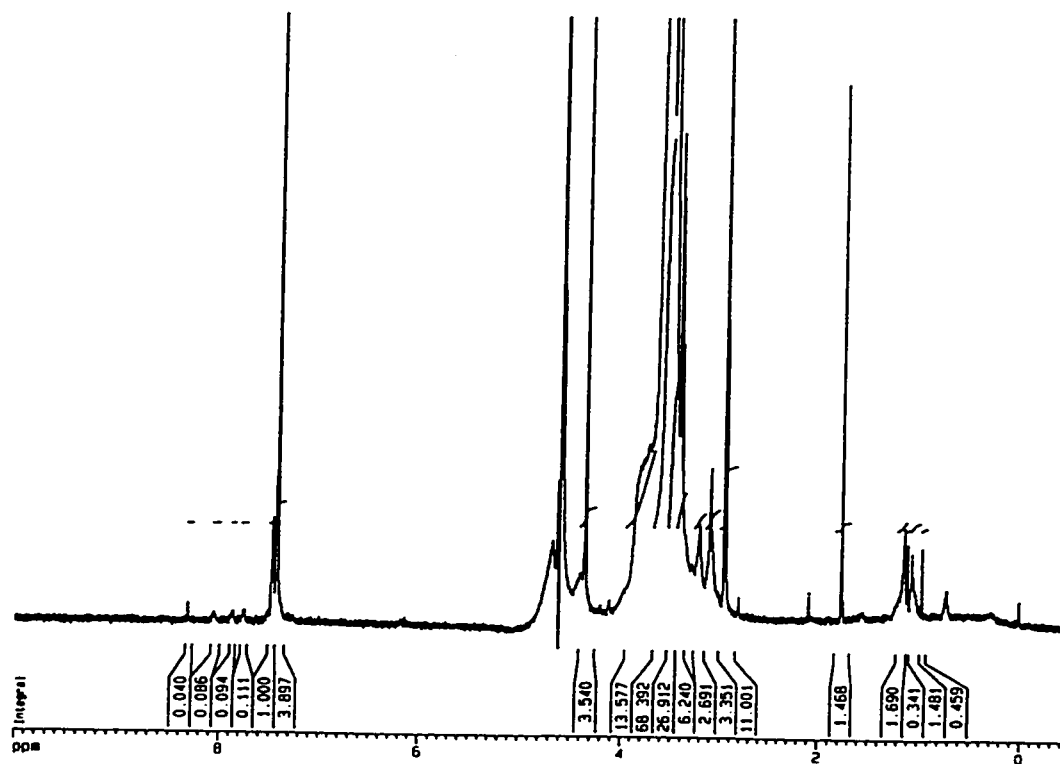


Figure 2.2.9: 500 MHz ^1H NMR spectrum of HEC-Np/205-N+C₁₂ (LMW).

Solubility tests were performed on the neutral and cationic naphthalene labelled polymers in deionised water (dissolved using water at room temperature and preheated to 60 °C), and aqueous solutions of NaCl (10^{-3} mol/L), methanol (50% and 75% v/v), CH₃COOH (0.5 mol/L) and DMSO (80% v/v). Similar solubility trends were found for these polymers as reported for the pyrene labelled polymers.

Figure 2.2.10 presents the steady-state naphthalene fluorescence spectra of 1.0 g/L aqueous solutions of HEC-Np/205 (LMW) and HEC-Np/205-N+C₁₂ (LMW). Both

samples exhibited the characteristic emission spectrum of naphthalene. A small increase in the excimer emission centred at 400 nm was observed in the fluorescence spectrum of HEC-Np/205-N+C₁₂ (LMW) indicating increased aggregation of the naphthalenes on the polymer chains. Spectra of the cationic hydrophobically-modified polymers in aqueous methanol (50% v/v) or aqueous DMSO (80% v/v) did not exhibit this excimer indicating that there was less aggregation of the naphthalene groups.

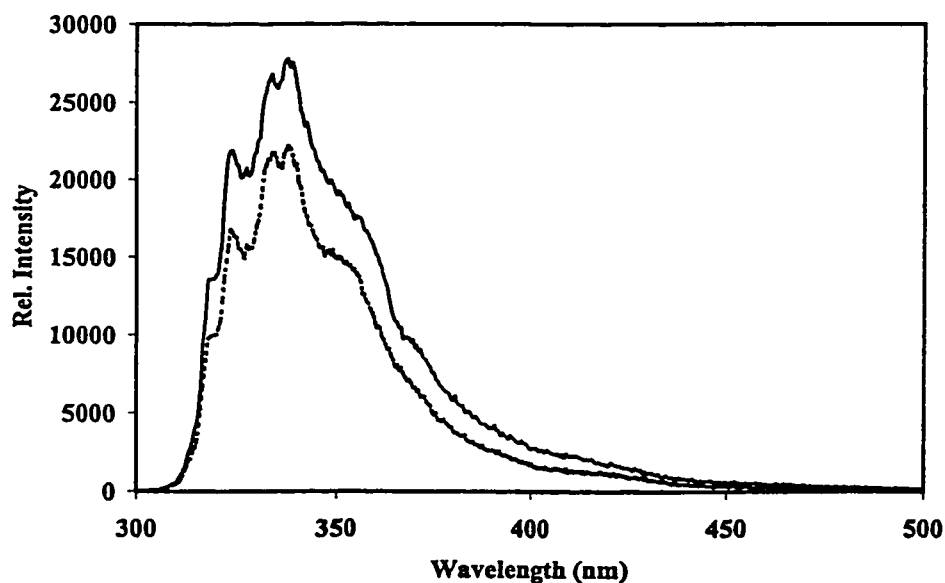


Figure 2.2.10: Fluorescence spectra of 1.0 g/L aqueous solutions of HEC-Np/205 (dashed line) and HEC-Np/205-N+C₁₂ (solid line) ($\lambda_{exc} = 282$ nm, 25 °C).

Fluorescence monomer decay measurements were determined for solutions of all naphthalene labelled neutral and cationic polymers in deionised water and aqueous DMSO (80% v/v). The average lifetime values are listed in table 2.2.8. Naphthalene labelled polymers in aqueous solution had an average lifetime value of 30 ns. For polymer

solutions in aqueous DMSO, the average lifetime increased slightly to 35 ns. It was also observed that aqueous solutions of hydrophobically-modified polymers resulted in decay measurements consisting of three decay components.

Table 2.2.8: Fluorescence decay measurements of 1.0 g/L naphthalene labelled polymers in aqueous and 80% DMSO solutions.

Sample	Water		80% DMSO	
	Lifetime (ns)	Pre-factor	Lifetime (ns)	Pre-factor
Non-Ionic Polymers				
HEC-Np/144 (LMW)	$\tau_1=34.9\pm 0.2$ $\tau_2=10.5\pm 0.9$ $\langle\tau\rangle 30.4\pm 4.1\times 10^{-3}$	$a_1=0.81\pm 0.01$ $a_2=0.19\pm 0.01$ $\chi^2=1.1$	$\tau_1=41.3\pm 0.1$ $\tau_2=7.3\pm 0.8$ $\langle\tau\rangle 36.0\pm 9.8\times 10^{-3}$	$a_1=0.85\pm 0.01$ $a_2=0.15\pm 0.01$ $\chi^2=1.1$
HEC-Np/205 (LMW)	$\tau_1=35.5\pm 0.1$ $\tau_2=8.5\pm 0.8$ $\langle\tau\rangle 31.0\pm 5.9\times 10^{-3}$	$a_1=0.83\pm 0.01$ $a_2=0.17\pm 0.01$ $\chi^2=1.1$	$\tau_1=41.5\pm 0.1$ $\tau_2=5.4\pm 0.5$ $\langle\tau\rangle 34.8\pm 1.2\times 10^{-2}$	$a_1=0.81\pm 0.0$ $a_2=0.19\pm 0.02$ $\chi^2=1.1$
HEC-Np/950 (HMW)	$\tau_1=36.0\pm 0.1$ $\tau_2=8.4\pm 0.7$ $\langle\tau\rangle 31.2\pm 5.0\times 10^{-3}$	$a_1=0.83\pm 0.01$ $a_2=0.17\pm 0.01$ $\chi^2=1.2$	$\tau_1=41.3\pm 0.1$ $\tau_2=5.4\pm 0.6$ $\langle\tau\rangle 34.3\pm 1.5\times 10^{-2}$	$a_1=0.80\pm 0.0$ $a_2=0.20\pm 0.03$ $\chi^2=1.1$
HEC-Np/333 (HMW)	$\tau_1=35.1\pm 0.2$ $\tau_2=6.1\pm 0.6$ $\langle\tau\rangle 29.9\pm 1.1\times 10^{-2}$	$a_1=0.82\pm 0.01$ $a_2=0.18\pm 0.02$ $\chi^2=0.99$	$\tau_1=41.1\pm 0.1$ $\tau_2=7.8\pm 1.0$ $\langle\tau\rangle 36.4\pm 1.2\times 10^{-2}$	$a_1=0.86\pm 0.01$ $a_2=0.14\pm 0.01$ $\chi^2=1.3$
Cationic HM-Polymers				
HEC-Np/205-N+C ₁₂ (LMW)			$\tau_1=41.6\pm 0.1$ $\tau_2=8.0\pm 1.2$ $\langle\tau\rangle 37.2\pm 1.9\times 10^{-2}$	$a_1=0.87\pm 0.01$ $a_2=0.13\pm 0.02$ $\chi^2=1.1$
HEC-Np/333-N+C ₁₂ (HMW)	$\tau_1=38.0\pm 2.2$ $\tau_2=32.1\pm 3.0$ $\tau_3=7.6\pm 1.1$ $\langle\tau\rangle 30.3\pm 0.1$	$a_1=0.44\pm 0.30$ $a_2=0.38\pm 0.30$ $a_3=0.18\pm 0.02$ $\chi^2=1.1$	$\tau_1=41.2\pm 0.1$ $\tau_2=6.2\pm 0.7$ $\langle\tau\rangle 34.7\pm 1.1\times 10^{-2}$	$a_1=0.81\pm 0.00$ $a_2=0.19\pm 0.02$ $\chi^2=1.1$
HEC-Np/144-N+C ₁₈ (LMW)	$\tau_1=36.5\pm 0.9$ $\tau_2=24.2\pm 4.8$ $\tau_3=5.8\pm 1.1$ $\langle\tau\rangle 29.2\pm 0.1$	$a_1=0.67\pm 0.10$ $a_2=0.16\pm 0.10$ $a_3=0.17\pm 0.03$ $\chi^2=1.0$	$\tau_1=41.2\pm 0.1$ $\tau_2=5.9\pm 0.6$ $\langle\tau\rangle 35.0\pm 1.2\times 10^{-2}$	$a_1=0.83\pm 0.00$ $a_2=0.17\pm 0.02$ $\chi^2=1.1$
HEC-Np/950-N+C ₁₈ (HMW)	$\tau_1=21.3\pm 0.8$ $\tau_2=36.2\pm 0.1$ $\tau_3=3.6\pm 0.2$ $\langle\tau\rangle 27.8\pm 1.7\times 10^{-3}$	$a_1=0.11\pm 0.01$ $a_2=0.68\pm 0.00$ $a_3=0.21\pm 0.03$ $\chi^2=0.95$	$\tau_1=41.6\pm 0.1$ $\tau_2=7.6\pm 0.8$ $\langle\tau\rangle 36.4\pm 8.9\times 10^{-3}$	$a_1=0.85\pm 0.00$ $a_2=0.15\pm 0.01$ $\chi^2=1.1$

2.2.2 Interpolymeric Association Studies by Non-Radiative Energy Transfer

Preliminary studies were undertaken to determine the association mechanism of these site-specifically labelled polymers. Non-radiative energy transfer experiments were carried out in mixed polymer solutions consisting of naphthalene and pyrene labelled neutral and cationic hydrophobically-modified polymers. A 5 mol naphthalene to 1 mol pyrene ratio was chosen for these experiments. In solution concentrations where interpolymeric association takes place, excitation of the naphthalene labelled polymers at 290 nm is expected to cause an increase in the fluorescence intensity of the pyrene labelled polymers by non-radiative energy transfer.

At concentrations less than 0.01 g/L, no naphthalene to pyrene energy transfer was detectable for mixed solutions of HEC-Np/333-N+C₁₂ (HMW) and HEC-Py/97-N+C₁₂ (HMW). The spectrum of polymer solutions consisting of 0.5 g/L HEC-Np/333-N+C₁₂ (HMW) and 0.027 g/L HEC-Py/97-N+C₁₂ (HMW), shows a slight increase in the fluorescence emission spectrum of pyrene and a slight decrease in the naphthalene emission spectrum. Figure 2.2.11 illustrates the emission spectra obtained from this experiment. For mixed solutions of the neutral precursors HEC-Np/333 (HMW) and HEC-Np/97 (HMW), the fluorescence spectrum obtained also showed evidence of interpolymeric association under the identical concentration range. This suggests that polymer chains were approaching the intermolecular distance required for energy transfer between the two chromophores. To further investigate the interpolymeric associations of

neutral and cationic hydrophobically-modified cellulose ethers, higher concentration ranges of the mixed polymer solutions should be investigated.

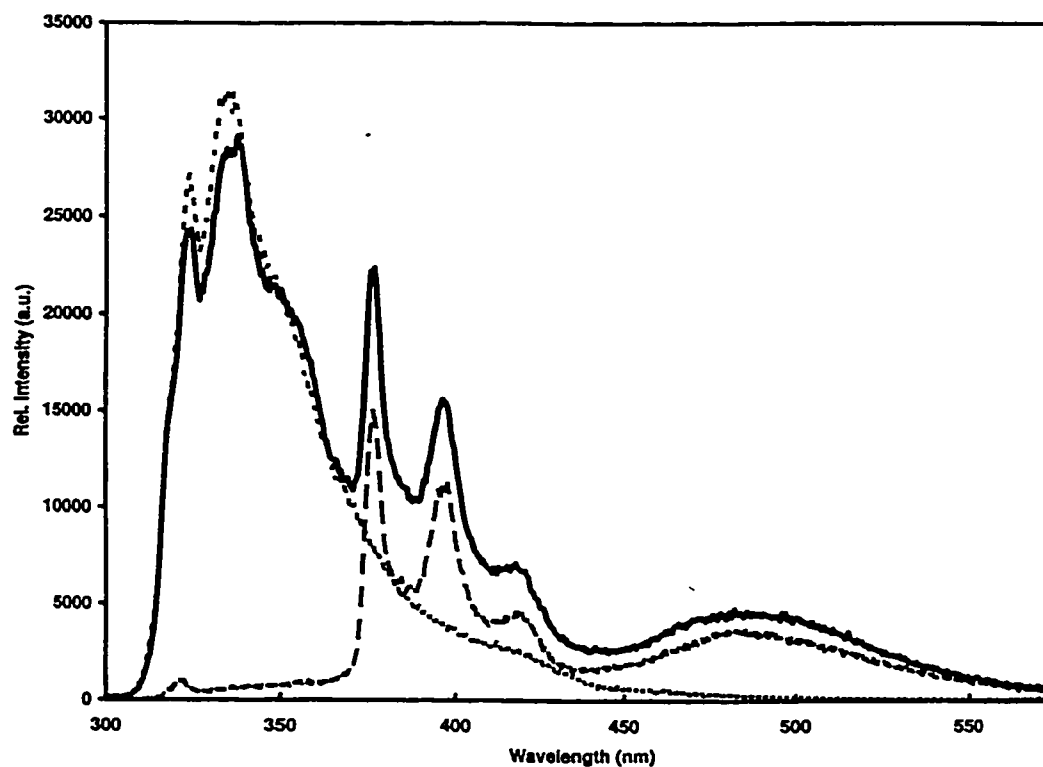


Figure 2.2.11: Fluorescence spectra of HEC-Np/333-N+C₁₂ (HMW, 0.5 g/L, dotted line), and HEC-Py/97-N+C₁₂ (HMW, 0.027 g/L, dashed line) and non-radiative energy transfer from HEC-Np/333-N+C₁₂ (HMW, 0.5 g/L) to HEC-Py/97-N+C₁₂ (HMW, 0.027 g/L), (5 mol Np : 1mol Py; $\lambda_{exc} = 290$ nm, solid line).

2.2.3 Interaction with Surfactants in Aqueous Solution

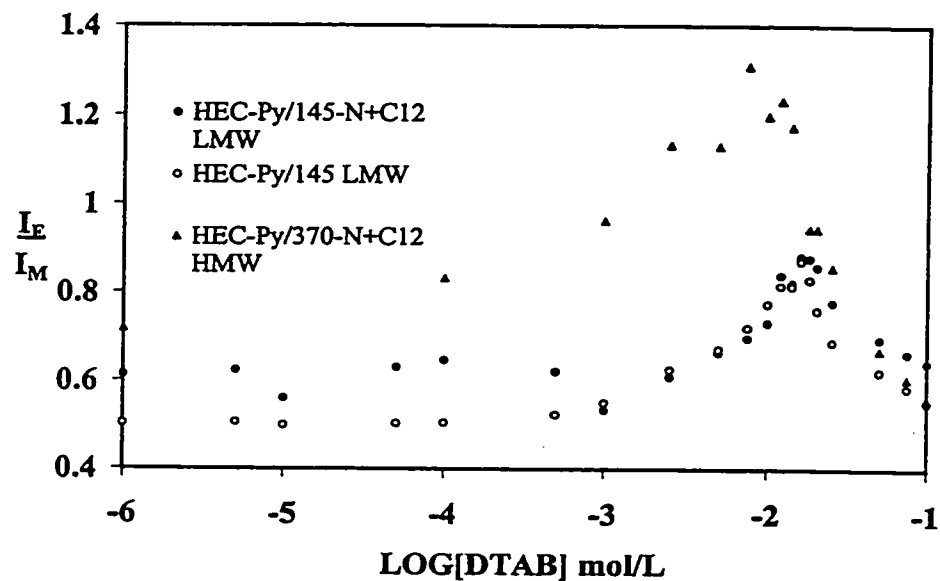
Preliminary fluorescence experiments were conducted to study the interactions of HEC-Py/145 (LMW), HEC-Py/145-N+C₁₂ (LMW) and HEC-Py/370-N+C₁₂ (HMW) with the cationic surfactant (DTAB) and the anionic surfactant (SDS) in aqueous solution.

Cationic Surfactants

In section 2.1.3, fluorescence experiments using the probe pyrene, clearly indicated that despite unfavourable electrostatic repulsions an interaction takes place between hydrophobically-modified cationic cellulose ethers and a family of cationic surfactants, where hydrophobic association is the driving force of the interaction ¹¹³ [Appendix 1].

Fluorescence spectra of mixtures of 0.1 g/L aqueous polymer solutions and DTAB were recorded as a function of surfactant concentration. Figure 2.2.12a presents a plot of I_E/I_M versus the logarithm of DTAB concentration for 0.1 g/L solutions of the neutral polymer HEC-Py/145 (LMW), and the cationic hydrophobically-modified polymers, HEC-Py/145-N+C₁₂ (LMW) and HEC-Py/370-N+C₁₂ (HMW). In all three cases, there is an increase in the value of I_E/I_M centred at a DTAB concentration of 0.016 mol/L (CMC of DTAB = 0.015 mol/L, ¹¹⁸). It is shown that the plot of HEC-Py/145 (LMW) is very similar to the plot of HEC-Py/145-N+C₁₂ (LMW), its' modified analogue. The plot suggests that there is an increasing association of the polymer/surfactant system as shown by the rise in the value of I_E/I_M . Figure 2.2.12b illustrates that at a concentration of 0.016 mol/L DTAB, the monomer emission starts to increase for solutions of HEC-Py/145-N+C₁₂ (LMW). The excimer emission intensity remains stationary possibly due to intramolecular excimer formation. This behaviour suggests that a saturation of the polymer/surfactant matrix is reached, after-which free surfactant micelles start to form in solution.

a)



b)

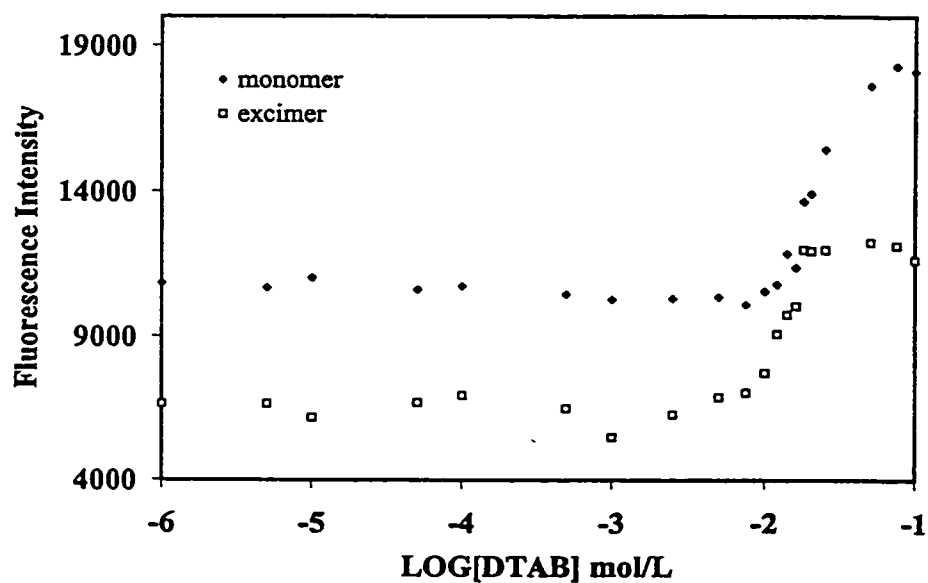
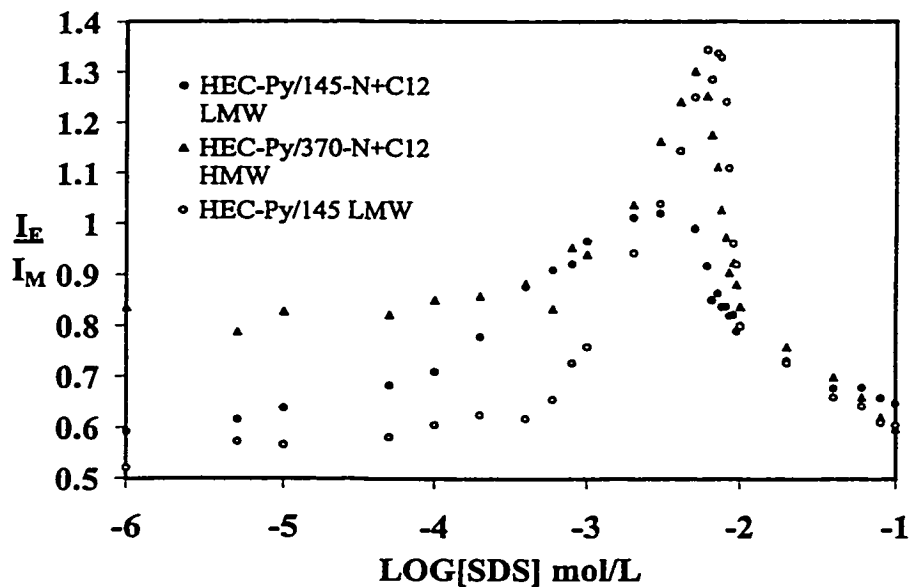


Figure 2.2.12: a) Plot of I_E/I_M versus the logarithm of DTAB concentration (mol/L) for HEC-Py/145-N+C₁₂, HEC-Py/145 (LMW) and HEC-Py/370-N+C₁₂ (HMW) and b) plot of fluorescence intensity of the monomer and excimer emission versus the logarithm of DTAB concentration, for 0.1g/L aqueous solutions of HEC-Py/145-N+C₁₂ (LMW).

Anionic Surfactants

Fluorescence spectra were also measured for aqueous solutions of HEC-Py/145 (LMW), HEC-Py/145-N+C₁₂ (LMW) and HEC-Py/370-N+C₁₂ (HMW) containing increasing SDS concentration. Plots of I_E/I_M as a function of increasing SDS concentration for these three polymers are shown in figure 2.2.13a. In these mixed solutions, there is also an increase in the ratio of I_E/I_M with increasing SDS. For HEC-Py/145 (LMW) / SDS mixed solutions, a maximum is reached at 0.006 mol/L which is slightly below the CMC of the surfactant (0.008 mol/L, ¹³). The plot shows that in mixed solutions of HEC-Py/145-N+C₁₂ (LMW) and SDS this effect is centred at 0.003 mol/L SDS. Solutions of HEC-Py/370-N+C₁₂ (HMW) also behave in a similar manner in the presence of SDS. The effect is more substantial than in the presence of the cationic surfactant DTAB, presumably due to the increased interaction resulting from both electrostatic attraction and hydrophobic interaction. Solutions of HEC-Py/145 (LMW) remained clear at all surfactant concentrations, however, solutions of HEC-Py/145-N+C₁₂ (LMW) became slightly turbid in the region of increased polymer/surfactant interaction as monitored by UV-vis spectroscopy. The turbidity observed indicates that the charges on the polymer chains are saturated by surfactant, reducing the solubility of the polymer in water. The sharp drop in the ratio of I_E/I_M corresponds to the concentration of SDS at which the monomer emission starts to increase while the excimer emission remains constant, as shown in figure 2.2.13b for solutions of HEC-Py/145-N+C₁₂ (LMW).

a)



b)

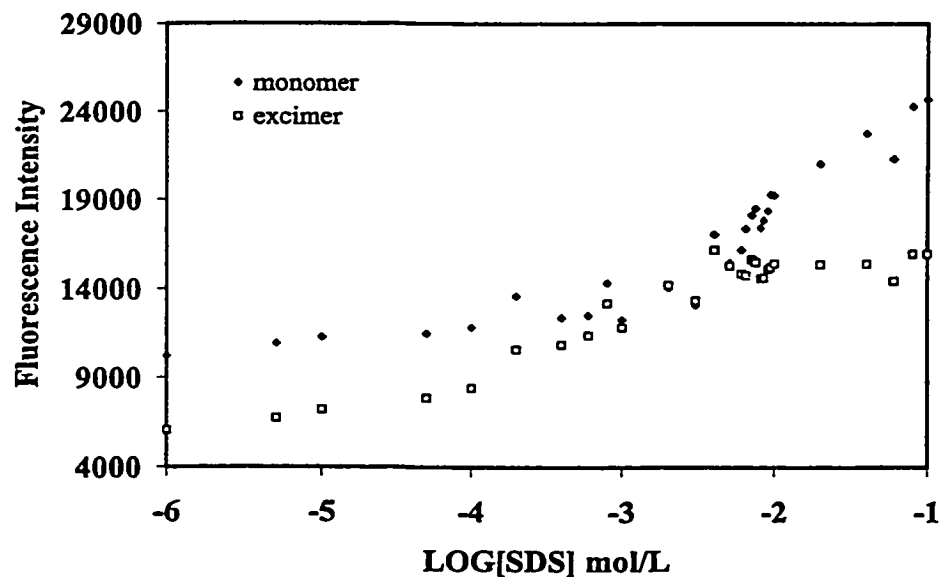


Figure 2.2.13: a) Plot of I_E/I_M versus the logarithm of SDS concentration (mol/L) and b) plot of fluorescence intensity of the monomer and excimer emission versus the logarithm of SDS concentration, for 0.1g/L aqueous solutions of HEC-Py/145-N+C₁₂ (LMW), HEC-Py/370-N+C₁₂ (HMW) and HEC-Py/145 (LMW).

2.2.4 Section Summary

This section has presented the preparation and characterisation of cationic hydrophobically-modified cellulose ethers labelled only along the backbone. Two labelling methods were used to prepare the pyrene labelled polymers. It was concluded through UV-vis and fluorescence studies that the second method led to a more random distribution of the chromophores along the cellulose backbone, while the first method led to a blocky distribution. The second etherification method was used to modify the labelled polymers further, by linking cationic hydrophobic substituents. It was difficult to carry out a quantitative determination of the amount of cationic group incorporation. Repeated etherification reactions should be carried out to increase the amounts of substituents attached to the polymer chains. Analogous naphthalene labelled polymers were also prepared via method 2. They were used to assess the interpolymeric associations between polymers of like charge using non-radiative energy transfer between naphthalene and pyrene labelled cellulose ethers. In the dilute concentration region studied, very little polymer association occurred. Preliminary fluorescence studies of mixed polymer/surfactant solutions indicated that the polymers associated with surfactants. At the CMC of the surfactant, the pyrenes on the polymer chains are saturated by surfactant. With increased surfactant concentration, the polymer/surfactant aggregates are forced apart and free surfactant micelles start to form. The effect was most prevalent in the presence of the anionic surfactant SDS. The similarity of the interactions of the neutral and cationic pyrene labelled polymers with surfactants may be an indication that the level of cationic substituent on the polymers is lower than assessed by ^1H NMR spectroscopy.

Further work is warranted to increase the amount of cationic substituent content on the polymers. The increase in the ratio I_E/I_M around the CMC of the respective surfactants was also observed in mixed polymer/anionic surfactant systems studied in section 2.1 for the randomly labelled cationic cellulose ethers HEC-N+C₁₂-Py/240 (see section 2.1.3). This behaviour is possibly attributed to the hydrophobic interaction of surfactant with pyrene groups along the polymer chain after the charged sites are saturated with surfactant. Fluorescence studies of mixed polymer/surfactant systems with the site-specifically labelled polymer of type 2 may give evidence of the interactions between the cationic hydrophobic substituents and anionic surfactants leading to the predominant change in the ratio I_E/I_M observed for the HEC-N+C₁₂-Py/240 /anionic surfactant systems in section 2.1.3.

2.3 Interfacial Behaviour of Cationic Hydroxyethyl Cellulose Ethers

While most of the work presented here places emphasis on the solution properties of polymers, a few experiments were carried out to correlate the solution properties to the behaviour of the solutions at the air/water interface. The effects of associations were studied by assessment of surface viscoelasticity and by dynamic surface tension experiments.

2.3.1 Dynamic Surface Tension using Axisymmetric Drop Shape Analysis-Profile [Appendix 5] ⁷¹

A preliminary investigation of the dynamic surface behaviour of HEC-N+CH₃ is presented in Appendix 5. Dilute solutions of the polymer (concentration < 0.05 wt%) exhibited an elevation of the surface tension of water from 71.9 to 72.7 mJ/m² (23 °C) under both static and dynamic conditions. At a solution concentration of 0.01 wt% HEC-N+CH₃ an interesting inversed surface tension profile was obtained, consisting of a decrease in surface tension during the drop expansion phase and an increase in surface tension during the compression phase. This phenomenon was reproducible but concentration dependent. The inversed surface tension profile has been attributed to the presence of polyelectrolyte cations at the air/water interface. The more conventional behaviour of water surface tension depression and decreases in the surface tension during the contraction cycle was observed for solutions of concentrations higher than 0.05 wt%.

2.3.1.1 Dynamic Surface Tension of Mixed HEC-N+CH₃/SDS

The values of surface tension obtained for the various mixed HEC-N+CH₃ / SDS solution concentrations are given in table 2.3.1. It was observed that the surface tension increased as the solution went from a fluid to viscoelastic sample. Also, the surface tension of the 0.01% JR400 / 0.01% SDS solution was much lower than that of the surface tension of the polymer or surfactant alone at this concentration.

Table 2.3.1: Dynamic surface tension values of mixed HEC-N+CH₃/SDS solutions at 23 °C, mJ/m².

Sample	Surface Flow Behaviour ^a	Surface Tension mJ/m ²
0.005 wt% HEC-N+CH ₃ / 0.0015 wt% SDS	VE	55.0
0.01 wt% HEC-N+CH ₃ / 0.01 wt% SDS	VE	49.5
0.25 wt% HEC-N+CH ₃ / 0.025 wt% SDS	VE	47.5
0.05 wt% HEC-N+CH ₃ / 0.15 wt% SDS	V	40.0
0.1 wt% HEC-N+CH ₃ / 0.5 wt% SDS	F	36.5
0.01 wt% HEC-N+CH ₃	F	71.8
0.01 wt% SDS	F	66.5

^a determined by the talc test for viscoelasticity [Appendix 3].

2.3.2 Surface Viscoelasticity [Appendices 3 and 4]

A simple technique to determine the interfacial association structures present in aqueous polymer and mixed polymer/surfactant systems was devised. This technique referred to as the talc method ⁷³ [Appendices 3 and 4], relies on the effect of the interfacial composition on the surface rheology of mixed solutions. The polymer investigated was the cationic cellulose ether HEC-N+CH₃. In the absence of surfactant,

this polymer was found to exhibit fluid flow behaviour in the concentration range studied [Appendix 3]. It was expected that the polymer by itself was feebly surface active. Foams and lamellar films formed from aqueous solutions of this polymer were very unstable [Appendix 4].

2.3.2.1 Effect of Hydrophobic Modification [Appendix 3]

The effect of hydrophobic modification on the interfacial behaviour of cationic cellulose ethers was also studied by surface viscoelasticity experiments. Polymer solutions of HEC-N+C₁₂ were studied in the same concentration range as discussed for HEC-N+CH₃ [Appendix 3]. In brief, this represents a situation where the polymer is by itself surface active. For dilute polymer concentrations, the hydrophobic portions of the polymer chains can be envisaged as adsorbing at the air/water interface creating a viscous fluid surface flow behaviour. The interaction is however too weak to lead to a viscoelastic surface.

2.3.2.2 Mixed Cationic Polymer/Anionic Surfactant Complexation [Appendices 3 and 4]

The interfacial association behaviour of HEC-N+CH₃ and the anionic surfactant, sodium dodecyl sulfate (SDS), was investigated by studying the effect of this mixed complex on the foam and film stability of aqueous solutions [Appendices 3 and 4]. In brief, it was reported that in a critical concentration range of mixed HEC-N+CH₃ / SDS solutions, the surface flow behaviour exhibits both viscous and elastic properties.

However, independently, solutions of either surfactant or polymer alone exhibits fluid flow behaviour. Additionally, the presence of this rigid mixed system at the air/water interface substantially improved the foam and film stability in comparison to solutions of surfactant or polymer alone. The effect of surfactant chain length on the foaming of mixed polymer/surfactant solutions was also investigated. Foam enhancement by the polymer was also observed with sodium decyl sulfate (SDeS) and sodium octyl sulfate (SOS), but the largest effect and best foaming results were found with the shorter chain length surfactant SOS/HEC-N+CH₃ systems.

2.3.3 Section Summary

The results reported in this section confirmed that a strong interfacial interaction occurs between cationic cellulose ethers and surfactants of opposite charge at the air/water interface. The rigid interfacial structure leads to improved film and foam stabilisation. It was also reported that the surfactants SOS and SDeS containing alkyl chains of 8 and 10 methylene units were also effective at stabilising the aqueous foams and films of HEC-N+CH₃. Hydrophobic modification of the polymers increased the surface viscoelasticity of mixed surfactant/polymer solutions. The preliminary dynamic surface tension studies showed a decrease in the surface tension of water with increased polymer concentration, with an elevation of the surface tension of water occurring at dilute polymer concentrations. Also, mixed solutions of polymer and surfactant were found to have a lower surface tension than solutions of the polymer and surfactant alone at the same concentrations.

CHAPTER 3

CHAPTER 3: CONCLUSIONS AND RECOMMENDATIONS FOR FUTURE WORK

3.1 Conclusions

Experiments aimed at elucidating various aspects of the molecular associations exhibited by hydrophobically-modified cationic cellulose ethers were presented in this thesis as a means of interpreting their behaviour on a macroscopic level. The association of polyelectrolyte cellulose ethers in dilute aqueous solutions was investigated by using fluorescent dye labelled derivatives.

Section 2.1 presented the preparation, characterisation and solution properties of randomly labelled HEC-N+CH₃ and HEC-N+C₁₂. The aggregation concentration of the HEC-N+C₁₂-Py/240 was determined to be lower than that reported for the unlabelled polymer, perhaps due to the additional hydrophobicity introduced by the incorporation of dye. Low levels of interpolymeric association between polymers of like charge were detected in dilute polymer solutions. Studies of mixed polymer/surfactant systems clearly indicated that despite unfavourable electrostatic repulsive forces, hydrophobic attraction leads to considerable interaction between polymer and surfactant species of like charge. Fluorescence results of mixed polymer/surfactants gave a strong indication that pyrene was attached to two distinct sites along the HEC-N+C₁₂ backbone: a) on the same cellulose substituent in close proximity to the cationic side chain and b) randomly along the cellulose ether backbone.

To assess the nature of the interactions occurring at each of these two sites, site-specific labelling of the polymer was undertaken. Section 2.2 presented the results towards the preparation and characterisation of cationic hydrophobically-modified cellulose ethers labelled specifically along the backbone. UV-vis and fluorescence studies indicated that the second labelling method led to a more random distribution of the chromophores along the cellulose backbone, while the first method led to a blocky distribution. The cationic hydrophobic groups were substituted onto the polymers using the second method. The level of cationic substituent incorporation could not be determined accurately suggesting a lower level than the expected yield of the reaction. Repeated etherification reactions may lead to a higher level of modification of the polymers. In the dilute concentration region studied, very little polymer association occurred between polymers of like charge. This is attributed either to the low concentration region studied or to the low levels of hydrophobic modification. Preliminary fluorescence studies of mixed polymer/surfactant solutions indicated that for surfactant concentrations in the vicinity of the CMC, the polymers associated with surfactants creating an enhanced network structure. The effect, most prevalent in the case of the anionic surfactant SDS, was observed in both mixed neutral and cationic hydrophobically-modified polymers. These results also suggest that the level of cationic substitution on the polymers may be very low. The effect was also observed for the mixed solutions of the randomly labelled cationic polymers and anionic surfactants studied in section 2.1.3. This suggests that the polymer/surfactant interactions occurring here are hydrophobic interactions of the surfactant with the pyrene groups on the polymer backbone. Further studies may give conclusive evidence that these two effects

are arising from the same interaction.

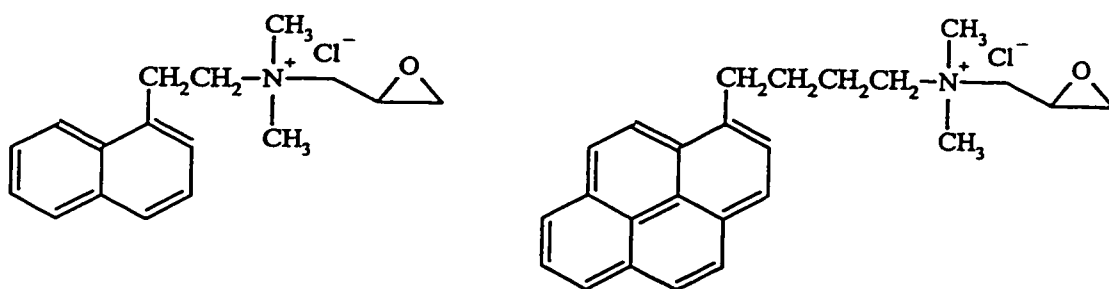
The results of section 2.3 indicated that a strong interfacial interaction occurs between cationic cellulose ethers and surfactants of opposite charge at the air/water interface. The rigid interfacial structure leads to improved film and foam stabilisation. Complexation of HEC-N+CH₃ with the surfactants SOS and SDeS formed stable aqueous foams and films. Hydrophobic modification of the polymer increased the surface viscoelasticity of mixed solutions. Preliminary dynamic surface tension studies were found to show a decrease in the surface tension of water with increased polymer/surfactant concentration. Mixed solutions of polymer and surfactant were found to have a lower surface tension than solutions of the polymer and surfactant alone at the same concentration.

3.2 Recommendations for Future Work

There are several recommendations for further studies. It is desirable to increase the amount of cationic hydrophobic groups on the polymers and to be able to characterise this more accurately. This may be accomplished by repeated etherification reactions. By increasing the cationic substituents, preferably to the amounts attached to the commercially prepared cationic cellulose ethers, HEC-N+CH₃ and HEC-N+C₁₂, a better comparison of the two polymers systems may be made. Further studies of the site-specifically labelled polymers are required to understand the aqueous solution properties of these polymers and their interactions with surfactants. Comparison of the solution properties of these site-specifically labelled polymers with the randomly labelled cationic

cellulose ethers may give further evidence of two sites of pyrene incorporation in the latter.

a)



b)

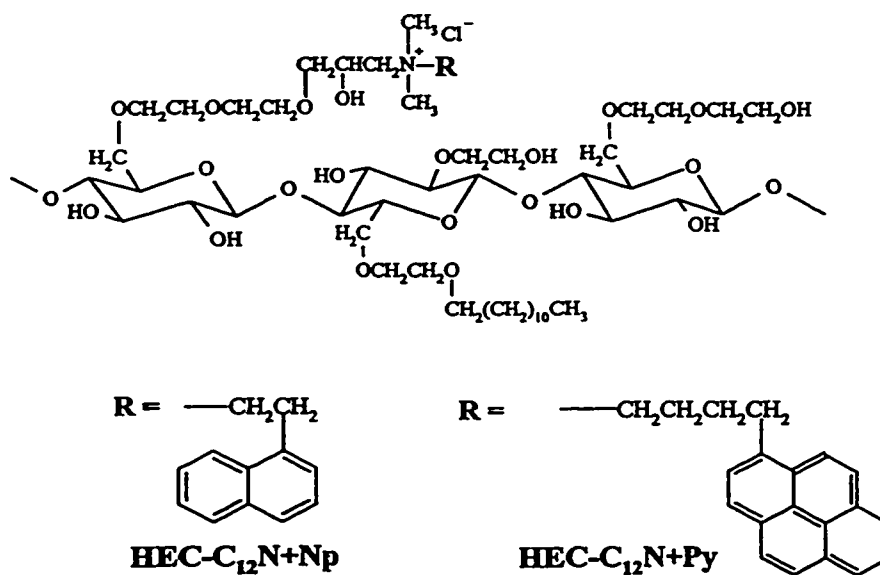


Figure 3.2.1: Idealised chemical structures of a) the cationic pyrene and naphthalene derivatives and b) the site-specifically labelled polymers.

Studying the solution properties of cellulose ethers labelled with cationic pyrene derivatives of the types shown in figure 3.2.1, will be able to give an indication of the microenvironment exhibited around the charged sites. By studying the interactions of these polymers with surfactants, evidence of the second labelling site on the randomly labelled cationic cellulose ethers may be established.

CHAPTER 4

CHAPTER 4: EXPERIMENTAL

4.1 Materials

Polymers:

Two samples of hydroxyethyl cellulose (HEC) were obtained from Amerchol Inc., New Jersey USA, HEC QP40 (lot no. W8169G), having an approximate molecular weight of 100,000 Dalton and HEC QP4400H (lot no. W6758L), with a molecular weight of about 400,000 Dalton. The molecular weights were confirmed by gel permeation chromatography (GPC) using pullulan or polymaltotriose polysaccharide standards (SHODEX standards P-82, MW range 5,900 to 788,000 Dalton, Showa Denko K.K.). The cationic derivative of hydroxyethyl cellulose, UCARE Polymer JR400, and its hydrophobically-modified derivative Quatrisoft® LM200, are commercial binders prepared by Amerchol Inc., New Jersey, USA. They were obtained as gifts and used without further purification. Polymer JR400 (lot no. L9661C, MW 400,000 Dalton), contains approximately 5.4mol% of the chloride salt of N,N,N-trimethylammonium groups attached randomly along the hydroxyethyl cellulose backbone via ether linkages⁸⁰. In the case of Quatrisoft® LM200 (lot no. H8021745, MW 100,000 Dalton), hydroxyethyl cellulose is randomly modified with 5.4mol% of the chloride salt of N,N-dimethyl-N-n-dodecylammonium groups. Both polymers have an average ethylene oxide molecular substitution (MS_{EO}) of 2.5.

Surfactants and Quenchers:

The surfactants used in this study were of the anionic series: sodium dodecyl sulfate (SDS) obtained from Sigma (>99%), sodium decyl sulfate (SDeS) obtained from Caledon Chemicals (>99%), and sodium octyl sulfate (SOS) purchased from Acros Organics (>94%). The cationic surfactants used were dodecyltrimethylammonium chloride (DTAC) obtained from TCI America, tetradecyltrimethylammonium bromide (TTAB, Sigma), dodecyltrimethylammonium bromide (DTAB) and hexadecyltrimethylammonium chloride (HTAC) were obtained from Kodak Chemicals. The non-ionic surfactants used were octyl- β -D-thioglucopyranoside (OTG) purchased from Sigma and octa-ethyleneglycol-mono-n-dodecyl ether ($C_{12}E_8$) supplied by Nikko Chemicals Co. The quenchers used in this investigation were 1-hexadecylpyridinium chloride or cetylpyridinium chloride (CPC) obtained from Aldrich (>95%), 1-dodecylpyridinium chloride (DPC) obtained from TCI America (>95%) and 1-ethylpyridinium bromide (EPB) from Acros Organics (>98%). All surfactants and quenchers were used without further purification.

Chemicals:

1-Pyrenebutanol, 1-naphthaleneethanol, p-toluenesulfonyl chloride, N,N-dimethyl-N-dodecylamine, epichlorohydrin, and benzyltrimethylammonium hydroxide(40% in water) were obtained from Aldrich. N,N-dimethyl-N-octadecylamine was obtained from TCI America. 4-(1-pyrenyl)butyl tosylate was prepared as described previously⁹⁷. N,N-dimethylformamide (DMF) was distilled over calcium hydride. All other chemicals and

solvents were of reagent grade. Water was deionised with a Barnstead NANOpure water purification system.

4.2 Instrumentation and Methods

Steady state fluorescence spectra were recorded on a SPEX Fluorolog 212 spectrometer using a NESLAB thermostated water bath set at 25 °C and equipped with Datamax 3.2 data analysis system. Fluorescence pyrene probe studies of the unlabelled polymers were performed in pyrene saturated water (pyrene concentration, 10^{-7} M), excitation wavelength set at 334 nm and scanning the emission from 360 to 550 nm. Variation in solution micropolarity was observed by monitoring changes in the ratio of I_1/I_3 , the intensity of the first vibronic band (377 nm) to the third vibronic band (398 nm). Pyrene emission spectra of labelled polymers were run in sample mode using excitation wavelengths of 344 nm or 346 nm, scanning from 365 to 600 nm. Slit widths were set at 2.0 mm (excitation) and 0.5 mm (emission). In pyrene label studies, changes in the I_E/I_M intensity ratio of pyrene emission spectra was monitored. It was taken as the ratio of the excimer intensity (485 nm) to the monomer intensity calculated as the half sum of the emission intensities at 377 nm and 398 nm. Excitation spectra were run in the ratio mode, scanning from 250 to 360 nm, monitoring at 377 nm (monomer) and 485 nm (excimer). Slits were set at 1.0 mm for both excitation and emission monochromators. Naphthalene emission spectra were run in sample mode using an excitation wavelength of 282 nm, scanning from 300 to 600 nm. Slit widths were set at 2.0 mm (excitation) and 1.0 mm (emission). Fluorescence non-radiative energy transfer experiments were performed in

sample mode using an excitation wavelength of 290 nm and monitoring the emission from 300 to 550 nm. Slit widths were set at 1.5 nm for both excitation and emission monochromators. Spectra were not corrected unless otherwise stated. Fluorescence decay measurements were run on Photon Technology International Inc. SPC-Fluorescence Lifetime Spectrometer LS-100 using Fluorescence Lifetime Analysis V.2.03 software for data analysis. UV-Vis spectra were recorded on a Hewlett-Packard 8452 photodiode array spectrometer equipped with a Hewlett-Packard 89090A temperature controller and operated under the HP ChemStation software version HP8452 Win system revA.01.06. Gel permeation chromatography (GPC) of the labelled polymers was performed using a Waters 510 HPLC pump. The instrument was equipped with both a Waters 486 Tunable UV-Visible detector (set at 282 nm (naphthalene) or 344 nm (pyrene)), and a Waters 410 differential refractometer (internal temperature 35 °C). Two Waters Ultrahydrogel columns (120 (6 μm) and LINEAR (6-13 μm)) connected in series were thermostated at 30 °C and eluted with 0.5 M aqueous acetic acid (CH₃COOH) at a flow rate of 0.7 ml/min. The system was operated using Waters Millennium 2010 software version 2.1. The columns were calibrated using pullulan polysaccharide standards with a molecular weight range from 5,900 to 788,000 Dalton (SHODEX Standard P-82, Showa Denko K.K.). The attachment of chromophores to the polymers was confirmed using gel permeation chromatography by monitoring both the absorbance at 344 nm (pyrene) or 282 nm (naphthalene) and the refractive index of 1.0 g/L samples in 0.5 M CH₃COOH. Proton and Carbon-13 NMR spectra of all organic compounds and the labelled polymers were run on 200 MHz or 500 MHz Bruker nuclear magnetic resonance spectrometers respectively.

Fourier transform infra-red spectroscopy was performed on a Bio-Rad FTS-40 spectrometer equipped with Bio-Rad WinIR tm Version 4.14 Level II software. Specific densities were determined using a Calculating Digital Density Meter, AP PAAR DMA45 at either 23 °C or 30 °C. Surface tension of the aqueous polymer solutions was determined using an Axisymmetric Drop Shape Analysis-Profile instrumental setup as described previously by Neumann ⁶⁴. Experiments were run at 23 °C unless otherwise stated, using G13 TEFLON tubing having an internal diameter of 1.9mm. Two analysis methods were used to run the experiments. The first consisted of a 6 minute pumping cycle in which a pendant drop was continuously compressed and expanded in a sawtooth-shaped variation in surface area, and imaged twice each second for the first 2 minutes and then imaged every second for the next 4 minutes, after which the stationary drop was imaged every 5 seconds for a total run time of 15 minutes. Three runs on different drops were performed to obtain statistical information. The second method sequence consisted of two separate experiments. The first had an initial sequence as in method one, but was followed by a further 15 minute stationary phase where the pendant drop was imaged every 2 minutes, after which a 2 minute pumping cycle was applied followed by a final 2 minute stationary phase. In the second experiment, 16 images were taken of a new drop over a 30 minute period, after which the pumping cycle as described in method one was initiated.

4.3 Labelled Polymer Characterisation Methods

The solubility of the labelled polymers were tested in several solvents by preparing

1.0 g/L solutions in 25 °C and 60 °C water, 10⁻³ M aqueous sodium chloride, 50% v/v aqueous methanol, 75% v/v aqueous methanol, 100% methanol, 80% v/v aqueous dimethyl sulfoxide (DMSO) and 0.5 M CH₃COOH. The pyrene content in 0.1 g/L polymer samples in 80% DMSO was calculated by UV-vis spectroscopic analysis using 4-(1-pyrenyl)butanol as a standard ($\epsilon = 45435 \pm 397$ L/mol·cm at 346nm, 0.001 g/L in 80% DMSO). Naphthalene content of 1.0g/L polymer samples in 80% DMSO was calculated by UV-vis spectroscopic analysis using 2-(1-naphthyl)ethanol as a standard ($\epsilon = 6638 \pm 63$ L/mol·cm at 286nm, 0.01g/L in 80% DMSO). The extinction coefficient (ϵ) of a 0.001 g/L solution 4-(1-pyrenyl)butanol in 80% DMSO was calculated using the Beer-Lambert law relating the absorbance to the product of the extinction coefficient, cell path length and chromophore concentration ($A = \epsilon bc$). The calculated extinction coefficients were taken as the average ϵ value from at least five measurements. The ϵ value of 2-(1-naphthyl)ethanol was determined in a similar manner using a solution of 0.1 g/L in 80% DMSO. When determining the chromophore content of the labelled polymers, each solution was analysed at least three times to propagate error in measurement. Fluorescence quantum yield measurements were determined for 0.1 g/L polymer solutions in water and 50% aqueous methanol. The absorbance and fluorescence spectra were determined for each polymer solution and compared to the standard quinine sulfate in 1.0 N H₂SO₄ ($\Phi_{\text{std}} = 0.546$) using the equation:

$$\Phi_F = \Phi_{\text{std}} \frac{(A_{\text{unk}} \cdot F_{\text{unk}} \cdot n^2)}{(A_{\text{std}} \cdot F_{\text{std}} \cdot n_0^2)} \quad (4.3.1)$$

where A is the absorbance intensity at the maximum absorbance wavelength, F is the

fluorescence peak area observed, and n and n_0 were the refractive indices of the solvents used (1.33 (water) and 1.338 (1.0 N H₂SO₄) respectively). To determine the fluorescence peak area, all fluorescence spectra were corrected, the excimer subtracted from the entire spectrum, and the wavelength was converted to wavenumbers before integration. Nanosecond fluorescence decay measurements of the labelled polymers were determined for polymer solutions in water and 80% DMSO. Solutions were degassed using argon. Pyrene labelled polymer solutions, were prepared such that the absorption at the excitation wavelength was between 0.2 and 0.3 absorbance units, concentrations ranged from 0.1-0.3 g/L. The samples were excited at 344 nm (water) or 346 nm (80% DMSO) and the fluorescence emission decay was monitored at 377 nm (monomer) and 485 nm (excimer). Naphthalene labelled polymers (1.0 g/L) were excited at 282 nm (water) or 286 nm (80% DMSO) and the fluorescence emission decay was monitored at 340 nm. Lifetimes were determined by analysis of the decay profiles which were fit to a sum of exponentials using: $I(t) = \sum a_i \exp(-t/\tau_i)$. When required, lifetimes consisting of up to three components were chosen to ensure the best fit of the data. In cases where the decay deviated from a one component lifetime, an average lifetime was calculated using the equation: $\tau_{avg} = \sum a_i \tau_i$. Proton nuclear magnetic resonance spectra (¹H NMR) of the labelled polymers were performed on a 500 MHz NMR spectrometer using 5 mg polymer samples in D₂O. NMR spectra indicated the presence of pyrene or naphthalene groups on the polymers observed as a sharp peak at 8.3 ppm. Spectra were also used to estimate the extent of cationic hydrophobic modification by comparing the peak intensities of the terminal methyl group of the alkyl chain (0.73 ppm) to the anomeric protons taken at 4.2 ppm

4.4 Synthetic Preparations

4.4.1 Preparation of Randomly Labelled Cationic Hydrophobically-modified Hydroxyethyl Cellulose Ethers

Synthesis of 2-(1-naphthyl)ethyl tosylate

The synthesis of 2-(1-naphthyl)ethyl tosylate ^{119, 97} was carried out using 3.02g (0.0175 mol) 2-(1-naphthyl)ethanol in 30ml of chloroform flushed over alumina. To this, 2.8ml of pyridine was added followed by 5.22g p-toluenesulfonyl chloride. The reaction mixture was allowed to stir under nitrogen until the reaction was complete as monitored by TLC. Diethyl ether was added, and the mixture was filtered into a separatory funnel removing the pyridinium salt solid. The mixture was extracted thrice with each of 10% HCl, distilled water and saturated NaCl solution. The organic layer was allowed to dry over magnesium sulfate and was evaporated under *vacuo* to yield a yellow oil. The crude 2-(1-naphthyl)ethyl tosylate was column chromatographed with Silica Gel 100-200 Mesh (Fisher Scientific) using 2% ether/petroleum ether. Mass of oil obtained was 5.52g (96% yield). ¹H NMR (CDCl₃, 200 MHz, ppm): 2.34(s, 3H, Ph-CH₃), 3.40(t, 2H, CH₂), 4.32(t, 2H, CH₂), 7.11-7.15(d, 2H, Ph), 7.56-7.60(d, 2H, Ph), 7.30 -7.91(m, 7H, Np); ¹³C NMR (CDCl₃, 200 MHz, ppm): 128.9, 127.3, 127.2, 126.0, 125.7, 125.5, 123.6, 63.0, 36.2; FT-IR (KBr salt, cm⁻¹): 3056 (aromatic C-H stretching), 2961, 1924, 1349, 1188 (aryl-O), 1098 (CH-O-), 772 (aromatic C-H bending), 657, 577.

Synthesis of Randomly Pyrene Labelled Cationic Cellulose Ethers HEC-N+CH₃-Py and HEC-N+C₁₂-Py

The preparation of the pyrene labelled analogues of HEC-N+CH₃ and HEC-N+C₁₂ (HEC-N+CH₃-Py and HEC-N+C₁₂-Py, respectively) was accomplished via a Williamson ether synthesis as outlined by Winnik et.al.⁹⁷. The reaction was carried out by dissolving 4.0g (10⁻⁵ mols) HEC-N+CH₃ in dry DMF. To this viscous mixture, 0.16g (3.73x10⁻⁴ mols) 4-(1-pyrenyl)butyl tosylate^{119, 97} in dry DMF was added slowly via syringe. After allowing the mixture to stir for 2h under nitrogen, 0.2g sodium hydride in dry DMF was added carefully via syringe. Vigorous bubbling occurred upon addition indicating the evolution of H₂ gas. The mixture was allowed to stir under nitrogen at room temperature in the dark until the mixture formed a gel. The labelled polymer was worked up by neutralisation using 3:1 glacial acetic acid to water, removal of solvent by vacuum distillation, and repeated precipitation into hexane from 2:1 CH₂Cl₂/MeOH. The residue was dried under *vacuo* at 60 °C overnight, and lyophilised to yield a dry mass of 2.77g HEC-N+CH₃-Py/212. The attachment of pyrene to the polymer was confirmed using gel permeation chromatography. The pyrene content of a 0.1g/L sample in 80% dimethyl sulfoxide, was calculated to be $2.6 \times 10^{-5} \pm 5.2 \times 10^{-7}$ mols pyrene per gram of polymer or 1 pyrene per 212 glucose units by UV analysis using 4-(1-pyrenyl)butanol ($\epsilon = 45435$ at 346nm, 80% dimethyl sulfoxide) as a standard. This corresponds to on average, 10.5 pyrene moieties per chain for a polymer of molecular weight 400,000 Dalton.

Pyrene labelled HEC-N+C₁₂, HEC-N+C₁₂-Py/240 was prepared and characterised using the method described above using 4.0g HEC-N+C₁₂, 0.16g 4-(1-pyrenyl)butyl

tosylate and 0.2g NaH. A final mass of 2.74g was obtained after lyophilisation. The pyrene content in the case of HEC-N+C₁₂-Py/240, which has a reported mass of 100,000 Dalton, was calculated to be $2.3 \times 10^{-5} \pm 4.9 \times 10^{-7}$ mols pyrene per gram polymer. This corresponds to 1 pyrene per 240 glucose units or approximately 2.3 chromophores per chain.

Synthesis of Randomly Naphthalene Labelled Cationic Cellulose Ethers: HEC-N+CH₃-Np and HEC-N+C₁₂-Np

Method 1: The method described above was also used to prepare a sample of HEC-N+C₁₂-Np using 4.05g HEC-N+C₁₂, 1.0ml of the 2-(1-naphthyl)ethyl tosylate oil in 15 ml DMF and 0.375g NaH. The reaction was allowed to proceed in the dark under nitrogen for 3 days, until a gel-like solid formed. Workup and purification was as described above. An off-white solid of mass 3.70g was obtained after freeze drying and labelled HEC-N+C₁₂-Np/1117. Attachment of naphthalene was ensured by gel permeation chromatography. The naphthalene content was calculated to be $4.98 \times 10^{-6} \pm 1.78 \times 10^{-7}$ mols naphthalene per gram of polymer or 1 pyrene per 1117 glucose units by UV analysis using 2-(1-naphthyl)ethanol ($\epsilon = 6638$ at 286nm, 0.01 g/L in 80% DMSO) as a standard. This corresponds to $8.9 \times 10^{-4} \pm 3.2 \times 10^{-5}$ naphthalene moieties per glucose unit or 0.5 naphthalenes per chain, for a polymer of molecular weight 100,000 Dalton.

Method 2: The attachment of 2-(1-naphthyl)ethyl tosylate to HEC-N+C₁₂ was also attempted by a heterogeneous slurry reaction⁷⁸. 5.075g HEC-N+C₁₂ was placed in a 3-necked 250ml round bottomed flask equipped with a reflux condenser. Addition of 35ml

tertiary butanol and 7ml distilled deionised water to the polymer solid formed a slurry after allowing to stir under nitrogen for 1hr. To this mixture, 7ml 40% aqueous benzyltrimethylammonium hydroxide was added drop-wise and allowed to stir for 1hr. 1.25g 2-(1-naphthyl)ethyl tosylate oil in tertiary butanol was added dropwise and the reaction mixture was refluxed under nitrogen for 6 hours. After cooling to room temperature, 1.5ml glacial acetic acid was added to neutralise the reaction mixture. The product was collected by vacuum filtration and washed with 100ml of 4:1 acetone/water. The gelatinous solid was transferred to an Erlenmeyer flask and was washed with vigorous stirring four times with 250ml of 4:1 acetone/water and finally with 250ml of acetone. The solid was dried in an oven at 50°C to yield a mass of 5.58g. This residue was dissolved in distilled deionised water, freeze dried to yield an off-white solid of mass 3.86g and labelled HEC-N+C₁₂-Np/184. Characterisation was as described previously. The naphthalene content was calculated to be $3.1 \times 10^{-5} \pm 4.4 \times 10^{-7}$ mols naphthalene per gram of polymer or 1 naphthalene per 184 glucose units by UV analysis using 2-(1-naphthyl)ethanol as a standard ($\epsilon = 6638$ at 286nm, 80% dimethyl sulfoxide). This corresponds to 3.0 naphthalene moieties per polymer chain.

Method 2 was used to prepare a sample of naphthalene labelled HEC-N+CH₃, HEC-N+CH₃-Np using 5.07g HEC-N+CH₃ and 2.22g 2-(1-naphthyl)ethyl tosylate. Mass of recovered polymer HEC-N+CH₃-Np/549 was 4.52g. The naphthalene content on HEC-N+CH₃-Np was calculated to be $1.0 \times 10^{-5} \pm 2.6 \times 10^{-7}$ mols naphthalene per gram of polymer or 1 pyrene per 549 glucose units by UV analysis using 2-(1-naphthyl)ethanol ($\epsilon = 6638$ at 286nm, 80% DMSO) as a standard. This corresponds to 4.1 naphthalene

moieties per chain for a polymer of molecular weight 400,000 Dalton.

4.4.2 Preparation of Site-Specifically Labelled Cationic Hydrophobically-modified Hydroxyethyl Cellulose Ethers

Synthesis of N,N-dimethyl-N-n-dodecyl-N-glycidylammonium Chloride

To a 100ml round bottomed flask equipped with a reflux condenser, 10.1g of N,N-dimethyl-N-n-dodecylamine in 50ml of absolute ethanol was introduced and stirred under nitrogen for 1hr. Epichlorohydrin (3.7ml) in 10ml absolute ethanol was added drop-wise via syringe over 5min. The reaction was allowed to proceed under reflux for 1.5hrs¹²⁰. The mixture was allowed to cool to room temperature and the solvent was evaporated under *vacuo* to yield a yellow oil. Crystallisation from diethyl ether yielded 13.3g (92% yield) of white crystalline product. ¹H NMR (CDCl₃, 200 MHz, ppm): 0.84 (t, 3H, CH₃), 1.21 (s, 18H, 9CH₂), 1.63 (br s, 2H, CH₂), 3.35 (m, 1H, -CH-O) 3.45 (s, 6H, N(CH₃)₂), 3.61 (m, 2H, NCH₂-alkyl), 4.25(s, 2H, NCH₂-epoxy), 6.45 (m, 2H, CH₂-O); FT-IR (neat, cm⁻¹): 3396, 2920 (aliphatic C-H stretching), 2852, 1637, 1469 (-CH₂- bending), 1101 (-CH-O-), 722.

Synthesis of N,N-dimethyl-N-glycidyl-N-n-octadecylammonium Chloride

The method described above was followed to prepare the octadecyl analogue using 10.06g (0.0338mol) of N,N-dimethyl-N-n-octadecylamine, and epichlorohydrin (3.25g, 0.0351mol) in absolute ethanol. Crystallization of the pale yellow oil yielded 12.24g of

product (93% yield). ^1H NMR (CDCl_3 , 200MHz, ppm): 0.76 (t, 3H, CH_3), 1.17 (s, 30H, 15CH_2), 1.60 (br s, 2H, CH_2), 3.34 (m, 1H, CH-O) 3.39 (s, 6H, $\text{N}(\text{CH}_3)_2$), 3.60 (m, 2H, NCH_2), 4.20(s, 2H, $\text{NCH}_2\text{-epoxy}$), 6.35 (m, 2H, $\text{CH}_2\text{-O}$); FT-IR (neat, cm^{-1}): 3396, 2920 (aliphatic C-H stretching), 2852, 1637, 1469 ($-\text{CH}_2\text{-}$ bending), 1101 ($-\text{CH-O-}$), 722.

Synthesis of Pyrene Labelled Hydroxyethylcellulose

Method 1 : HEC QP4400H (high molecular weight) (2.0g) was transferred to a 250ml round bottomed flask containing 75 ml of dry DMF. The mixture was allowed to stir overnight under nitrogen to yield a viscous mixture, to which was added 1.19g (2.78×10^{-3} mols) 4-(1-pyrenyl)butyl tosylate in 15 ml dry DMF. After allowing the mixture to stir for 2 hours, 2.20g NaH was carefully dissolved in DMF and added slowly to the reaction mixture. The reaction was allowed to proceed in the dark under nitrogen overnight, until a gel-like solid formed. The mixture was neutralised and an additional 2.58g NaH was added in an attempt to allow the reaction to proceed to completion. The reaction however, was not complete as determined by TLC and the reaction mixture was worked up. A 1:3 acetic acid/water solution was used to neutralise the mixture and the DMF was distilled off under vacuum in two batches. The resulting mixtures were dissolved in a dichloromethane/methanol mixture (2 :1) and precipitated into hexane. After repeating twice more, half of the resulting residue was dried under vacuum at 60°C and finally freeze dried to obtain an off-white solid of mass 1.53g and labelled HEC-Py/370 (HMW). The polymer was characterised by gel permeation chromatography to confirm the attachment of the chromophore onto the polymer, 500MHz ^1H NMR and UV-

vis spectroscopy to determine the pyrene content on the polymer. The pyrene content of a 0.1g/L sample in 80% dimethyl sulfoxide, was calculated to be $1.5 \times 10^{-5} \pm 4.2 \times 10^{-7}$ mols pyrene per gram of polymer or 1 pyrene per 370 glucose units by UV analysis using 4-(1-pyrenyl)butanol ($\epsilon = 45435$ at 346nm, 80% aqueous dimethyl sulfoxide) as a standard. This corresponds to 6 pyrene moieties per chain for a polymer of molecular weight 400,000 Dalton.

The synthesis of pyrene labelled low molecular weight hydroxyethylcellulose was carried out as above using 4.0g HEC QP40, 1.5g (3.50×10^{-3} mols) 4-(1-pyrenyl)butyl tosylate and 1.0g NaH. A solid of mass 3.78g was obtained and labelled HEC-Py/145 (LMW). Characterisation of the polymer was carried out as stated above for HEC-Py/370 (HMW). The pyrene content of a 0.1g/L sample in 80% dimethyl sulfoxide, was determined to be $4.5 \times 10^{-5} \pm 7.0 \times 10^{-7}$ mols pyrene per gram of polymer or 1 pyrene per 122 glucose units by UV analysis using 4-(1-pyrenyl)butanol ($\epsilon = 45435$ at 346nm, 80% aqueous dimethyl sulfoxide) as a standard. This corresponds to 4.5 pyrene moieties per chain for a polymer of molecular weight 100,000 Dalton.

Method 2: The slurry reaction using benzyltrimethylammonium hydroxide was followed to prepare the randomly pyrene labelled HEC samples. HEC QP4400H (HMW) (5.0g) was placed in a 2-necked 100ml round bottomed flask equipped with a reflux condenser, oil-bath and magnetic stirrer. A slurry was prepared by adding 35ml tertiary butanol and 7ml distilled deionised water. After stirring under nitrogen for 2 hours, 7ml 40% aqueous benzyltrimethylammonium hydroxide was added drop-wise and allowed to stir for a further hour. To this mixture, 1.73g (4.04×10^{-3} mols) 4-(1-pyrenyl)butyl tosylate

in methanol was added and the reaction mixture was refluxed under nitrogen for 6 hours. After cooling to room temperature, 1.5ml glacial acetic acid was added to neutralise the mixture. The product was collected by vacuum filtration and washed with 100ml of 4:1 acetone/water. The gelatinous solid was transferred to a beaker and was washed with vigorous stirring four times with 250ml of 4:1 acetone/water and finally with 250ml of acetone. The solid was dried to yield a mass of 6.46g. From this residue, 0.84g was dissolved in distilled deionised water, lyophilised to yield an off-white solid of mass 0.64g and labelled HEC-Py/97(HMW). The polymer was characterised as stated above for HEC-Py/370 (HMW). Pyrene content of a 0.1g/L sample in 80% dimethyl sulfoxide, was determined to be $1.2 \times 10^{-4} \pm 1.5 \times 10^{-6}$ mols pyrene per gram of polymer or 1 pyrene per 45 glucose units, corresponding to 48 pyrene moieties per chain. The remaining mass was used in the next step to attach the cationic hydrophobe which proceeded in a similar manner by preparing a slurry of 5.56g HEC-Py/97 (HMW) in tertiary butanol/water to which was reacted 1.72g N,N-dimethyl-N-n-dodecyl-N-glycidylammonium chloride. After workup and purification, 3.72g of product was obtained and labelled HEC-Py/97-N+C₁₂.

Synthesis of Pyrene Labelled Cationic Hydrophobically-modified Hydroxyethyl Cellulose Ethers

Method 2, described above was also used to prepare samples of randomly pyrene labelled hydroxyethyl cellulose ethers which were subsequently reacted with either N,N-dimethyl-N-n-dodecyl-N-glycidyl-ammonium chloride or N,N-dimethyl-N-n-octadecyl-N-

glycidyl-ammonium chloride to obtain the cationic hydrophobically-modified analogues as outlined in the following table.

Table 4.4.1: Synthetic preparation of pyrene labelled cationic hydrophobically-modified hydroxyethyl cellulose ethers.

Sample Name ^a	Mass Polymer Used (grams)	4(1-pyrenyl) butyl tosylate (mols)	N,N-dimethyl-N-dodecyl-N-glycidyl-ammonium chloride (mols)	N,N-dimethyl-N-octadecyl-N-glycidyl-ammonium chloride (mols)	Mass Recovered Polymer (grams)
HEC-Py/145(d)-N+C ₁₂ (LMW)	1.09	-	7.58x10 ⁻³	-	1.01
HEC-Py/370(d)-N+C ₁₂ (HMW)	1.06	-	6.24x10 ⁻³	-	0.67
HEC-Py/347(p)-N+C ₁₂ (LMW)	5.04	1.51x10 ⁻³	5.56x10 ⁻³	-	4.27
HEC-Py/97(p)-N+C ₁₂ (HMW)	5.56	-	5.63x10 ⁻³	-	3.72
HEC-Py/145(d)-N+C ₁₈ (LMW)	1.02	-	-	1.32x10 ⁻³	0.95
HEC-Py/370(d)-N+C ₁₈ (HMW)	0.26	-	-	6.21x10 ⁻⁴	0.20

^a number indicates the number of glucose units per pyrene moiety

Synthesis of Naphthalene Labelled Cationic Hydrophobically-modified Polymers

Method 2 as described above was used to prepare all naphthalene labelled samples as outlined in the following table.

Table 4.4.2: Synthetic preparation of naphthalene labelled cationic hydrophobically-modified hydroxyethyl cellulose ethers.

Sample Name ^a	Mass Polymer Used (grams)	2(1-naphthyl) ethyl tosylate (mols)	N,N-dimethyl-N-dodecyl-N-glycidyl-ammonium chloride (mols)	N,N-dimethyl-N-octadecyl-N-glycidyl-ammonium chloride (mols)	Mass Recovered Polymer (grams)
HEC-Np/144 (LMW)	5.12	1.01×10^{-3}	-	-	4.65
HEC-Np/950 (HMW)	5.13	8.92×10^{-4}	-	-	4.04
HEC-Np/205-N+C ₁₂ (LMW)	5.08	6.41×10^{-4}	1.33×10^{-3}	-	4.06
HEC-Np/333-N+C ₁₂ (HMW)	5.03	6.32×10^{-4}	1.29×10^{-3}	-	3.33
HEC-Np144-N+C ₁₈ (LMW)	2.00	-	-	2.76×10^{-3}	2.12
HEC-Np/950-N+C ₁₈ (HMW)	2.00	-	-	2.62×10^{-3}	1.97

^a number indicates the number of glucose units per naphthalene moiety

4.5 Solution Preparation

Pyrene labelled polymer solutions were prepared by dissolving the polymer into water (1.0g/L) and dilution of this stock solution after allowing to equilibrate for 24h at room temperature in the dark. SDS solutions of various concentrations were prepared by dilution of a 1.0mol/L stock solution. Stock solutions of the other surfactants and quenchers were prepared in a similar manner. Solutions for spectroscopic analysis were prepared by mixing aliquots of surfactant solutions (0.3mL) with aliquots of polymer (2.7mL) and allowing them to equilibrate overnight in the dark.

Polymer solutions for non-radiative energy transfer experiments were prepared by first dissolving the polymer into water (1.0g/L) and after determining the respective chromophore content, a 5 mol naphthalene to 1 mol pyrene ratio was adopted. The 1.0g/L pyrene labelled polymer solution was diluted accordingly. Solutions were prepared by

diluting 1.5ml of the polymer stock solution into a total volume of 3.0ml. In mixed solutions 1.5ml of each polymer solution was used.

Solutions for the dynamic surface tension experiments were prepared as follows. Stock solutions (0.5wt%) of Polymer JR400 and HEC QP4400H prepared in deionised water and subsequently ultrafiltrated using Diaflo YM30 43mm membranes having a 30,000 molecular weight cutoff to remove any low molecular weight moieties. After freeze drying the concentrated polymeric solution, the following dilutions were prepared using NANOpure deionised water: 0.5, 0.1, 0.05, 0.001, 0.005, 0.001wt%. A 0.01wt% solution of HEC was prepared in a similar manner. Mixed Polymer JR400/SDS solution concentrations displaying either fluid(F), viscous(V) or viscoelastic(VE) surface flow behaviour by the talc test were also chosen for investigation. These were 0.005%JR400/0.0015%SDS, VE; 0.01%JR400/0.01%SDS, VE; 0.025%JR400/0.025% SDS, VE; 0.05%JR400/0.015%SDS, V; 0.1%JR400/0.5%SDS, F. As a control, 0.01%SDS and 0.01%JR400 were also prepared.

CHAPTER 5

CHAPTER 5: REFERENCES

1. Israelachvili, J., In *Proceedings of the International School of Physics "Enrico Fermi" : Physics of Amphiphiles: Micelles, Vesicles and Microemulsions*; Degiorgio, V., Corti, M., Eds.; North-Holland Physics Publishing: Amsterdam, 1985; pp 24-58.
2. Williams, D., *Polymer Science and Engineering*; Prentice Hall Inc.: Englewood Cliffs, NJ, 1971;
3. Bello, M.; de Besi, P.; Rezzonico, R.; Righetti, P.; Gasiraghi, E., *Electrophoresis* 1994, 15, 623-626.
4. Goddard, E.D.; Ananthapadmanabhan, K.P., In *Polymer-Surfactant Systems*; Kwak, J.C.T., Ed.; Marcel Dekker Inc.: New York, 1998; pp 21-64.
5. Kabalnov, A.; Lindman, B.; Olsson, U.; Piculell, L.; Thuresson, K.; Wennerström, H., *Colloid Polym.Sci.* 1996, 274, 297-308.
6. Kalyanasundaram, K., *Photochemistry in Microheterogeneous Systems*; Academic Press Inc. (Harcourt Brace Jovanovich, Publishers): Orlando, 1987;
7. Gilbert, A.; Baggott, J., *Essentials of Molecular Photochemistry*; CRC Press: Boca Raton, 1991;
8. Winnik, F.M., *Chem.Rev.* 1993, 93, 587-614.
9. Just, E. K. and Majewicz, T. G., Cellulose Ethers. (3), 226-269. 1984. New York, John Wiley & Sons. Encyclopedia of Polymer Science and Engineering.
10. Maitland, G.C.; Rigby, M.; Smith, E.B.; Wakeham, W.A., *Intermolecular Forces: Their Origin and Determination*; Clarendon Press: Oxford, 1981;
11. *Fundamentals of Interface and Colloid Science*; ed. Lyklema, J., Academic Press: London, 1991;
12. Tanford, C., *The Hydrophobic Effect: Formation of Micelles and Biological Membranes*; John Wiley & Sons: New York, 1973; pp 1-200.
13. van Os, N.M.; Haak, J.R.; Rupert, L.A.M., *Physico-Chemical Properties of Selected Anionic, Cationic and Nonionic Surfactants*; Elsevier Science Publishers: Amsterdam, 1993;

14. Kahlweit, M.; Busse, G.; Jen, J., *J.Phys.Chem.* **1991**, *95*, 5580-5586.
15. Shaw, D.J., *Introduction to Colloid and Surface Chemistry*; Butterworth & Co. Ltd.: London, 1980;
16. Thuresson, K., *Solution Properties of a Hydrophobically Modified Polymer.* 1996. University of Lund, Sweden.
17. Berr, S.S.; Caponetti, E.; Johnson, J.S.; Jones, R.R.M.; Magid, L.J., *J.Phys.Chem.* **1986**, *90*, 5766-5770.
18. Roelants, E.; De Schryver, F.C., *Langmuir* **1987**, *3*, 209-214.
19. Evans, D.F.; Wennerström, H., *The Colloidal Domain: where Physics, Chemistry, Biology and Technology Meet*; VCH Publishers: New York, 1994;
20. Israelachvili, J., *Intermolecular & Surface Forces*; Academic Press: New York, 1991;
21. Tartar, H.V., *J.Phys.Chem.* **1955**, *59*, 1195-1199.
22. Lindman, B. and Wennerström, H., *Micelles: amphiphile aggregation in aqueous solution*, *Top.Curr.Chem.* **87**, 1-83. 1980.
23. Mukerjee, P.; Mysels, K.J., *CMC of Aqueous Surfactant Systems*; U.S. National Bureau of Standards: 1971;
24. Cowie, J.M.G., *Polymers: Chemistry & Physics of Modern Materials*; Blackie Academic & Professional, an imprint of Chapman & Hall: London, 1991;
25. *Interactions of Surfactants with Polymers and Proteins*; eds. Goddard, E.D., Ananthapadmanabhan, K.P., CRC Press: Boca Raton, FL, 1993;
26. Cockbain, E.G., *Trans.Faraday Soc.* **1953**, *49*, 104-111.
27. Jones, M.N., *J.Colloid and Interface Sci.* **1967**, *23*, 36-42.
28. Morishima, Y., *Progr.Polym.Sci.* **1990**, *15*, 949-997.
29. Purcell, I.P.; Thomas, R.K.; Penfold, J.; Howe, A.M., *Colloids and Surfaces* **1995**, *94*, 125-130.
30. Penfold, J.; Staples, E.J.; Tucker, I.; Creeth, A.M.; Hines, J.; Thompson, L.; Cummins, P.G.; Thomas, R.K.; Warren, N., *Colloids and Surfaces A: Physicochemical and Engineering Aspects* **1997**, *128*, 107-117.

31. Kästner, U.; Hoffmann, H.; Doenges, R.; Ehrler, R., *Progr. Colloid Polym. Sci.* **1995**, *98*, 57-62.
32. Chari, K.; Hossain, T.Z., *J. Phys. Chem.* **1991**, *95*, 3302-3305.
33. Lindman, B.; Piculell, L.; Karlström, G.; Thuresson, K.; Zhang, K. In Ordax, F.A., Arrizabalaga, A., Barrio, R., Eds.; R.S.E.Q.: Vitoria-Gasteiz, Spain, 1995; pp 147-160.
34. Piculell, L.; Guillemet, F.; Thuresson, K.; Shubin, V.; Ericsson, O., *Adv. Coll. and Interface Sci.* **1996**, *63*, 1-21.
35. Wallen, T.; Linse, P., *Langmuir* **1998**, *14*, 2940-2949.
36. *Polymer-Surfactant Systems*; ed. Kwak, J.C.T., Marcel Dekker Inc.: New York, 1998;
37. Linse, P.; Piculell, L.; Hansson, P., In *Polymer-Surfactant Systems*; Kwak, J.C.T., Ed.; Marcel Dekker Inc: New York, 1998; pp 193-238.
38. Norwood, D.P.; Minatti, E.; Reed, W.F., *Macromolecules* **1998**, *31*, 2957-2965.
39. Minatti, E.; Norwood, D.P.; Reed, W.F., *Macromolecules* **1998**, *31*, 2966-2971.
40. Persson, K.; Wang, G.; Olofsson, G., *J. Chem. Soc. Faraday Trans.* **1994**, *90*, 3555-3562.
41. Sivadasan, K.; Somasundaran, P., *Colloids and Surfaces* **1990**, *49*, 229-239.
42. Herkstroeter, W.G.; Martic, P.A.; Hartman, S.E.; Williams, J.L.R.; Farid, S., *Journal of Polymer Science: Polymer Chemistry Edition* **1983**, *21*, 2473-2490.
43. Winnik, F.M., In *Interaction of Surfactants with Polymers and Proteins*; Goddard, E.D., Ed.; CRC Press Inc: Boca Raton, 1993; pp 367-394.
44. Winnik, F.M.; Regismond, S.T.A., *Colloids and Surfaces A: Physicochemical and Engineering Aspects* **1996**, *118*, 1-39.
45. Winnik, F.M.; Regismond, S.T.A., In *Polymer-Surfactant Systems*; Kwak, J.C.T., Ed.; Marcel Dekker Inc: New York, 1998; pp 267-316.
46. Berlman, I.B., *Handbook of Fluorescence Spectra of Aromatic Molecules*; Academic Press Inc.: New York, 1971;

47. Birks, J.B., *Photophysics of Aromatic Molecules*; Wiley-Interscience, a division of John Wiley & Sons Ltd: London, 1970;
48. Dong, D.C.; Winnik, M.A., *Can.J.Chem.* 1985, 62, 2560-2565.
49. Förster, Th.; Kasper, K., *Z.Phys.Chem.N.F.* 1954, 1, 275-277.
50. Birks, J.B., *Rep.Prog.Phys.* 1975, 38, 903-974.
51. O'Connor, D.V.; Phillips, D., *Time-correlated Single Photon Counting*; Academic Press Inc. (Harcourt Brace Jovanovich, Publishers): London, 1984;
52. Sienicki, K.; Winnik, M.A., *Chem.Phys.* 1988, 121, 163-174.
53. Winnik, F.M., *Polymer* 1990, 31, 2125-2134.
54. Creeth, A.M.; Cummins, P.G.; Staples, E.J.; Thompson, L.; Tucker, I.; Penfold, J.; Thomas, R.K.; Warren, N., *Faraday Discuss.* 1996, 104, 245-260.
55. Cohen Stuart, M.A.; Fokkink, R.G.; van der Horst, P.M.; Lichtenbelt, J.W.Th., *Colloid Polym.Sci.* 1998, 276, 335-341.
56. Prigogine, I.; Marechal, J., *J.Colloid Science* 1951, 7, 122-127.
57. Gaines Jr, G.L., *J.Phys.Chem.* 1969, 73, 3143-3150.
58. Siow, K.S.; Patterson, D., *J.Phys.Chem.* 1973, 77, 356-365.
59. Chang, S.A.; Gray, D.G., *J.Colloid and Interface Sci.* 1978, 67, 255-265.
60. Fleer, G.J.; Cohen Stuart, M.A.; Scheutjens, J.M.H.M.; Cosgrove, T.; Vincent, B., *Polymers at Interfaces*; Chapman & Hall: London, 1993;
61. Lovell, E.L.; Hibbert, H., *J.Am.Chem.Soc.* 1940, 62, 2144-2148.
62. Al-Madfi, S.; Frisch, H.L., *J.Am.Chem.Soc.* 1958, 80, 5613-5614.
63. Frisch, H.L.; Al-Madfi, S., *J.Am.Chem.Soc.* 1958, 80, 3561-3565.
64. Chen, P.; Policova, Z.; Susnar, S.S.; Pace-Asciak, C.R.; Demin, P.M.; Neumann, A.W., *Colloids and Surfaces A: Physicochemical and Engineering Aspects* 1996, 114, 99-111.
65. Voigt, A.; Thiel, O.; Williams, D.; Policova, Z.; Zingg, W.; Neumann, A.W., *Colloids and Surfaces* 1991, 58, 315-326.

66. Zhang, J.; Pelton, R., *Langmuir* 1999, in press.
67. Zhang, J.; Pelton, R., *Colloids and Surfaces A: Physicochemical and Engineering Aspects* 1999, in press.
68. Um, S.-U.; Poptoshev, E.; Pugh, R.J., *J. Colloid and Interface Sci.* 1997, 193, 41-49.
69. Svensson, E.; Gudmundsson, M.; Eliasson, A.-C., *Colloids and Surfaces B: Biointerfaces* 1996, 6, 227-233.
70. Girault, H.H.J.; Schiffrin, D.J.; Smith, B.D.V., *J. Colloid and Interface Sci.* 1984, 101, 257
71. Lahooti, S.; Del Rio, O.I.; Neumann, A.W.; Cheng, P., In *Applied Surface Thermodynamics*; Neumann, A.W., Spelt, J.K., Eds.; Marcel Dekker Inc.: New York, 1996; pp 491-507.
72. Cheng, P.; Li, D.; Boruvka, Y.; Rotenberg, Y.; Neumann, A.W., *Colloids and Surfaces* 1990, 43, 151-167.
73. Davies, J.T.; Rideal, E.K., *Interfacial Phenomena*; Academic Press: New York, 1961; pp 257-258.
74. Regismond, S.T.A.; Winnik, F.M.; Goddard, E.D., *Colloids and Surfaces A: Physicochemical and Engineering Aspects* 1996, 119, 221-228.
75. Klitzing, R.v.; Espert, A.; Asnacios, A.; Hellweg, T.; Colin, A.; Langevin, D., *Colloids and Surfaces A: Physicochemical and Engineering Aspects* 1999, 149, 131-140.
76. *Cellulosics: Chemical, Biochemical and Material Aspects*; eds. Kennedy, J.F., Phillips, G.O., Williams, P.A., Ellis Horwood: New York, 1993;
77. *Cellulose and Cellulose Derivatives: Physico-chemical aspects and industrial applications*; eds. Kennedy, J.F., Phillips, G.O., Williams, P.A., Piculell, L., Woodhead Publishing Ltd.: Cambridge, 1995;
78. Glass, J.E.; Buettner, A.M.; Lowther, R.G.; Young, C.S.; Cosby, L.A., *Carbohydrate Research* 1980, 84, 245-263.
79. Glass, J.E.; Shah, S.; Lu, D.-L.; Seneker, S.D., In *Polymer Adsorption and Dispersion Stability*; Goddard, E.D., Vincent, B., Eds.; ACS: 1984;
80. Stone, F. W. and Rutherford, J. M. Union Carbide Corp. (Patent 3,472,840). 10-14-1969.

81. Goddard, E.D.; Leung, P.S., *Colloids and Surfaces* 1992, 65, 211-219.
82. Carlsson, A.; Karlström, G.; Lindman, B., *Colloids and Surfaces* 1990, 47, 147-165.
83. Evertsson, H.; Nilsson, S., *Macromolecules* 1997, 30, 2377-2385.
84. Goldszal, A.; Costeux, S.; Djabourov, M., *Colloids and Surfaces A: Physicochemical and Engineering Aspects* 1996, 112, 141-154.
85. Holmberg, C.; Sundelöf, L.-O., *Langmuir* 1996, 12, 883-889.
86. Kamenka, N.; Burgaud, I.; Zana, R.; Lindman, B., *J.Phys.Chem.* 1994, 98, 6785-6789.
87. Medeiros, G.M.M.; Costa, S.M.B., *Colloids and Surfaces A: Physicochemical and Engineering Aspects* 1996, 119, 141-148.
88. Nyström, B.; Lindman, B., *Macromolecules* 1995, 28, 967-974.
89. Thuresson, K.; Joabsson, F., *Colloids and Surfaces A: Physicochemical and Engineering Aspects* 1999, 151, 513-523.
90. Walderhaug, H.; Nyström, B., *Colloids and Surfaces A: Physicochemical and Engineering Aspects* 1999, 149, 379-387.
91. Kjønixsen, A.-L.; Nyström, B.; Lindman, B., *Colloids and Surfaces A: Physicochemical and Engineering Aspects* 1999, 149, 347-354.
92. Thuresson, K.; Nilsson, S.; Lindman, B., In *Cellulose and cellulose derivatives: Physico-chemical aspects and industrial applications*; Kennedy, J.F., Phillips, G.O., Williams, P.A., Piculell, L., Eds.; Woodhead Publishing Ltd.: Cambridge, U.K., 1995; pp 323-329.
93. Gerharz, B.; Horst, R., *Colloid Polym.Sci.* 1996, 274, 439-445.
94. Hwang, F.S.; Hogen-Esch, T.E., *Macromolecules* 1998, 26, 3156-3160.
95. Kumar, V.; Steiner, C.A., *Colloids and Surfaces A: Physicochemical and Engineering Aspects* 1999, 147, 27-38.
96. Kiratzis, N.; Faers, M.; Luckham, P.F., *Colloids and Surfaces A: Physicochemical and Engineering Aspects* 1999, 151, 461-471.
97. Winnik, F.M.; Winnik, M.A.; Tazuke, S.; Ober, C.K., *Macromolecules* 1987, 20, 38-44.

98. Winnik, F.M., *Macromolecules* **1987**, *20*, 2745-2750.
99. Winnik, F.M.; Winnik, M.A., *Polymer Journal* **1990**, *22*, 482-488.
100. Winnik, M.A.; Winnik, F.M., In *Structure-Property Relations in Polymers*; Urban, M.W., Craver, C.D., Eds.; American Chemical Society: Washington, DC, 1993; pp 485-505.
101. Ananthapadmanabhan, K.P.; Leung, P.S.; Goddard, E.D., *Colloids and Surfaces* **1985**, *13*, 63-72.
102. Kästner, U.; Hoffmann, H.; Dönges, R.; Ehrler, R., *Colloids and Surfaces A: Physicochemical and Engineering Aspects* **1994**, *82*, 279-297.
103. Kästner, U.; Hoffmann, H.; Dönges, R.; Ehrler, R., *Colloids and Surfaces A: Physicochemical and Engineering Aspects* **1996**, *112*, 209-225.
104. Guillemet, F.; Piculell, L., *J.Phys.Chem.* **1995**, *99*, 9201-9209.
105. Thuresson, K.; Nilsson, S.; Lindman, B., *Langmuir* **1996**, *12*, 530-537.
106. Argillier, J.-F.; Ramachandran, R.; Harris, W.C.; Tirrell, M., *J.Colloid and Interface Sci.* **1991**, *146*, 242-250.
107. Shubin, V.; Petrov, P.; Lindman, B., *Colloid Polym.Sci.* **1994**, *272*, 1590-1601.
108. Suzuki, Y.; Tazuke, S., *Macromolecules* **1981**, *14*, 1742-1747.
109. Winnik, F. M., Regismond, S. T. A., Goddard, E. D., *Langmuir* **1997**, *13*, 111-115.
110. Sienicki, K.; Winnik, M.A., *J.Chem.Phys.* **1987**, *87*, 2766-2772.
111. Morawetz, H., *Macromolecules* **1996**, *29*, 2689-2690.
112. Goddard, E.D.; Leung, P.S., *Langmuir* **1992**, *8*, 1499-1500.
113. Winnik, F.M.; Regismond, S.T.A.; Goddard, E.D., *Colloids and Surfaces A: Physicochemical and Engineering Aspects* **1996**, *106*, 243-247.
114. Magny, B.; Iliopoulos, I.; Zana, R.; Audebert, R., *Langmuir* **1994**, *10*, 3180-3187.
115. Roelants, E.; Geladé, E.; Smid, J.; De Schryver, F.C., *J.Colloid and Interface Sci.* **1985**, *107*, 337-344.

116. Goldraich, M.; Schwartz, J.R.; Burns, J.L.; Talmon, Y., *Colloids and Surfaces A: Physicochemical and Engineering Aspects* **1997**, *125*, 231
117. Stilbs, P. In *Polymer-Surfactant Systems*; Kwak, J.C.T., Ed.; Marcel Dekker Inc.: New York, NY, 1998; pp 239-266.
118. Chu, D.-Y.; Thomas, J.K., *J. Am. Chem. Soc.* **1986**, *108*, 6270-6276.
119. Kabalka, G.W.; Varma, M.; Varma, R.S.; Srivastava, P.C.; Knapp Jr, F.F., *J. Org. Chem.* **1986**, *51*, 2386-2388.
120. Doughty, J. B. and Klem, R. E. Process for Making Quaternary Amines of Epichlorohydrin. Westvaco Corp. 445067(Patent 4,066,673). 3-1-1978. NY, New York, USA.

APPENDICES

Colloids and Surfaces A: Physicochemical and Engineering Aspects, 1996, 106, 243-247.

Brief Note

Interactions of cationic surfactants with a hydrophobically-modified cationic cellulose polymer: a study by fluorescence spectroscopy

F. M. Winnik^{1*}, S. T. A. Regismond¹, E. D. Goddard²

¹Department of Chemistry, McMaster University, 1280 Main Street W., Hamilton, Ont. L8S 4M1, Canada

²349, Pleasant Lane, Haworth, NJ 07941, USA

Received 25 May 1995; accepted 31 July 1995
© 1996 Elsevier Science B.V. All rights reserved.

Keywords: Cationic surfactants, Fluorescence, Quatrisoft® LM200, Pyrene.

1. Introduction

The interactions taking place in aqueous solutions of surfactants and hydrophobically-modified polyelectrolytes are the subject of intense current investigation, as they play a key role in controlling the rheology of many industrially important fluids [1]. The interactions result from one or both of two main driving forces : (1) electrostatic attraction, usually reinforced by hydrophobic forces similar to those involved in the self-association of the bound surfactants, and (2) association of the hydrophobic groups on the polymers and those of the surfactant molecules. The process of complex formation between polyelectrolytes and oppositely-charged surfactants proceeds cooperatively at a critical surfactant concentration, the critical aggregation concentration (CAC). This concentration is usually considerably lower than the critical micelle concentration (CMC) of the corresponding surfactants in the absence of polymer [2].

Recently, Bakeev et al. reported the formation of complexes between cationic surfactants and amphiphilic polycations [3]. The polymers examined were copolymers of N-ethyl-4-vinylpyridinium bromide and (low levels) of either N-dodecyl-4-vinylpyridinium bromide or N-cetyl-4-vinylpyridinium bromide. An important feature of this work is that it is one of the first reported accounts of the unambiguous detection of complexes between polycations and surfactants of like charge. This phenomenon, while rather unusual, is not unique. It was also observed in mixtures of an anionic surfactant, sodium dodecylsulfate, and certain hydrophobically-modified polyanions [4,5]. In the case of cationic surfactants and positively-charged polyelectrolytes, it was detected for the first time in the course of phase separation/precipitation experiments for combinations of cationic surfactants and a dodecyl-substituted cationic cellulose polymer [6,7].

This note reports further evidence originating from fluorescence experiments of the interactions between the cationic cellulosic polymer investigated by Goddard and Leung [6,7] and a homologous series of alkyltrimethylammonium halides. The polymer, Quatrisoft® LM200, is the chloride salt of a N,N-dimethyl-N-dodecyl derivative of hydroxyethyl cellulose [8,9] (Fig. 1). We have examined the interaction of Quatrisoft® LM200 in dilute aqueous solution with dodecyl-, tetradecyl-, and hexadecyl-trimethylammonium halides, where the halide is either the bromide or the chloride ion. The data were compared with those gathered from control experiments (1) with the surfactants in the absence of polymer but in dilute NaCl solution of ionic strength comparable in magnitude to that of the polymer solution, and (2) in the presence of a

« conventional » cationic cellulose ether, Polymer JR400 (Fig. 1), that does not carry hydrophobic groups along its backbone.

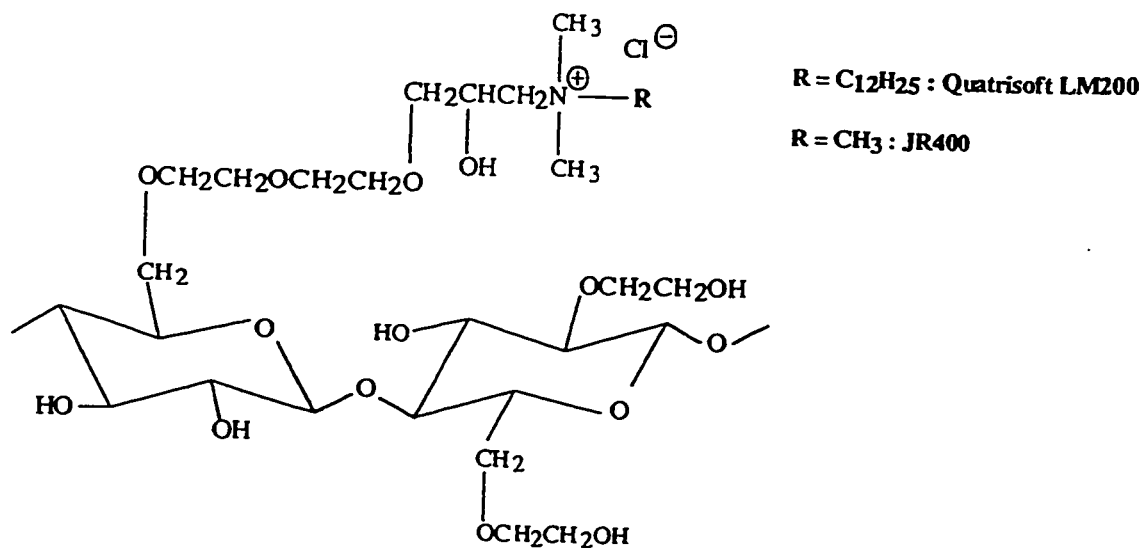


Figure 1: Idealized chemical structure of the polymers used in this study.

2. Experimental

2.1. Materials

The polymers Quatrisoft® LM200 and Polymer JR400 were obtained from Amerchol Inc. and used without further purification. Tetradecyl- and dodecyl-trimethylammonium bromide (TTAB and DTAB, respectively) were obtained from Sigma. Hexadecyl- and dodecyltrimethylammonium chloride (HTAC and DTAC, respectively) were purchased from TCI America. Pyrene (99%, Aldrich) was purified by

repeated recrystallization from absolute ethanol and subsequent sublimation. Water was deionized using a NANOpure water purification system.

2.2. Instrumentation and methods

UV absorption spectra were recorded with a Hewlett-Packard diode array spectrometer. Steady state fluorescence spectra were run on a SPEX Fluorolog 212 spectrometer equipped with a DM3000F data system. Emission spectra were not corrected. Spectra for the measurement of I_1/I_3 were obtained with the excitation wavelength set at 334nm. The slit widths were set at 2.5nm (excitation) and at 0.5nm (emission).

2.3. Samples for spectroscopic analysis

Solutions of LM200 or JR400 were prepared by dissolving the polymer in pyrene-saturated water, previously filtered to remove pyrene microcrystals. They were allowed to equilibrate for 24 h. Surfactant solutions of varying concentrations were obtained by dilutions of a stock solution in water (1.0 mol/L). Aliquots of these solutions (0.3 ml) were added to aliquots (2.7 ml) of a polymer solution (usually 1.0 g/L) in pyrene-saturated water. Solutions for analysis were prepared 2 h before spectroscopic measurements.

3. Results and discussion

The emission of pyrene exhibits a marked medium sensitivity in its vibrational fine structure, and the important tool is the ratio I_1/I_3 of the relative intensities of the (0,0) and (0,3) bands, respectively, in the emission of pyrene added to the system as an extrinsic probe. The ratio I_1/I_3 increases with increasing polarity [10]. For example, in hydrocarbon

solvents it has a value of about 0.70, while in water its value is approximately 1.80. This feature was first exploited by Kalyanasundaram and Thomas in a study of surfactant micelles [11], and it is often employed to detect and characterize complexes between polymers and surfactants [1]. In these experiments, the value I_1/I_3 is monitored as a function of surfactant concentration. A typical curve of I_1/I_3 vs. surfactant concentration can be characterised by three distinct concentration regions : (a) below the CMC, as pyrene resides predominantly in water, the ratio will be constant and adopt a value close to that in water ; (b) as the CMC is reached, pyrene becomes solubilized by surfactant micelles, and the ratio thus undergoes a sharp decrease; (c) at concentrations higher than the CMC, pyrene is solubilized in the micelles and a further increase in surfactant concentration has little effect. It is important to remember that I_1/I_3 is a measure of the polarity averaged over all solubilization sites.

In aqueous solutions of Quatrisoft® LM200, the ratio I_1/I_3 of the emission of pyrene (concentrations $\approx 5 \times 10^{-7}$ mol/L) is slightly lower than in pure water. It exhibits a mild dependence on polymer concentration, ranging from 1.74 in a 0.5 g/L solution to 1.61 in a 1.5 g/L solution. This observation suggests that hydrophobic microdomains are formed in aqueous solutions of the polymer. These provide preferential solubilization sites for the pyrene probe. The variations of I_1/I_3 were measured in aqueous solutions containing fixed amounts of Quatrisoft LM200 (1.0 g/L) and increasing amounts of DTAB. It was observed (Fig. 2) that for DTAB concentrations lower than 10^{-3} mol/L, the ratio is not affected. With a further increase in DTAB concentration, the ratio decreased until a saturation value was reached for $[DTAB] = 0.02$ mol/L, a concentration

approximately equal to the CMC of DTAB (15×10^{-3} mol/L) [12]. Note that the concentration domain from the onset of the decrease in I_1/I_3 to the CMC covers nearly two decades of surfactant concentration, in contrast to the curve obtained in solutions of the surfactant alone which exhibits a very sharp transition with a midpoint corresponding to the CMC. This observation implies that the association between DTAB and Quatrisoft LM200 takes place via a mechanism of relatively low cooperation, as also reported in fluorescence studies of the interactions of neutral amphiphilic polymers and either anionic or cationic surfactants [13].

The addition of DTAB to a pyrene-containing solution of the cationic cellulose derivative Polymer JR400 (1.0 g/L) was monitored under the same conditions. In this case, the plot of I_1/I_3 as a function of [DTAB] exhibited a sharp transition centered at 1.51×10^{-2} mol/L, a concentration nearly equal to the CMC of DTAB (Fig. 2). This pattern is diagnostic of a cooperative mechanism associated with the formation of surfactant micelles. Since the midpoint of the transition coincides with the CMC of the surfactant alone, the data indicate that the surfactant does not interact with the positively-charged cellulosic polymer JR400, but rather forms micelles which are free to diffuse in solution. This behaviour differs from that commonly observed when monitoring complex formation between interacting surfactants and polyelectrolytes of opposite charges [1] or between charged surfactants and neutral polymers such as poly(ethylene oxide) [14] or hydroxypropylcellulose [15]. In such situations, the midpoint of the transition is lower than the CMC of the surfactant.

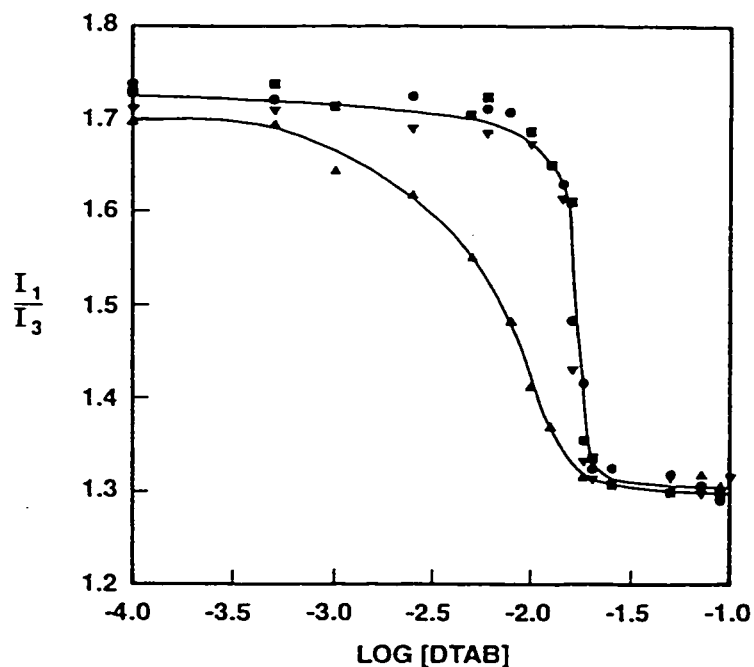


Figure 2: Plots of I_1/I_3 for the emission of pyrene in aqueous solutions of Quatrisoft® LM200 (1.0 g/L) (-), Polymer JR400 (1.0 g/L) (o), water (?) and aqueous NaCl (6×10^{-4} mol/L) (∇) as a function of DTAB concentration (logarithmic scale).

The experiments were repeated with DTAC ($CMC = 21.0 \times 10^{-3}$ mol/L [16]) to assess the effect of the counterion, and with cationic surfactants of longer chain length, namely TTAB ($CMC = 3.6 \times 10^{-3}$ mol/L [17]) and HTAC ($CMC = 1.3 \times 10^{-3}$ mol/L [15]). In all cases, association of the surfactant molecules with the hydrophobically-modified polymer was demonstrated by plots of the changes in I_1/I_3 with surfactant concentration (Fig. 3).

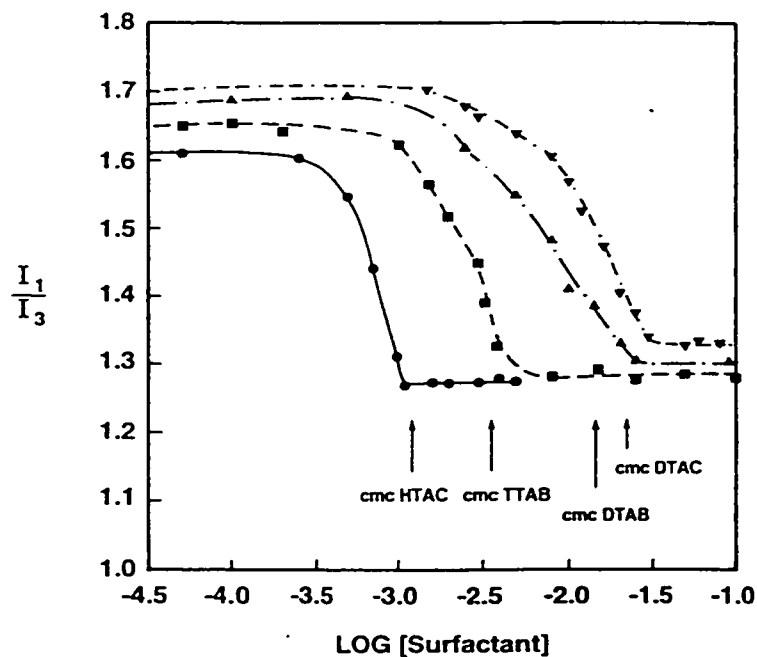


Figure 3: Plot of I_1/I_3 for the emission of pyrene in aqueous solution of Quatrisoft® LM200 (1.0 g/L) as a function of surfactant concentration: DTAB (-), DTAC (o), TTAB (i) and HTAC (?) (logarithmic scale). The arrows indicate the CMC of the surfactants in water.

4. Conclusions

From our fluorescence measurements it is clearly shown that, despite the unfavorable electrostatic repulsions, alkyltrimethylammonium surfactants associate with cationic cellulosic polyelectrolytes when these polymers contain hydrophobic groups. Hydrophobic interactions are the driving force in this type of association. Their effects seem to mirror those produced by the same hydrophobic substituents when attached to anionic polyelectrolytes or neutral water-soluble polymers. The results confirm the conclusion reached previously on the basis of precipitation and redissolution effects near

the CMC of the surfactant [6,7]. Earlier observations [18] of precipitation in mixtures of like-charged polyelectrolytes and surfactants should be acknowledged, although these involved non-surface active polymers and very high concentrations of surfactant to achieve precipitation and resolubilization of the polymer. It should be pointed out that, when the polyelectrolyte is hydrophobically-modified, binding of an oppositely charged surfactant has been observed at minute concentrations ($< 1\mu\text{m}$) of added surfactant, as exemplified by fluorescence measurements on the Quatrisoft/SDS system [19].

Acknowledgments

F.M.W. and S.T.A.R. thank the Natural Science and Engineering Research Council of Canada for financial support.

References

- [1] E.D. Goddard and K.P. Ananthapadmanabhan (Eds.), *Interactions of Surfactants with Polymers and Proteins*, CRC Press, Boca Raton, FL, 1993.
- [2] E.D. Goddard, *Colloids Surfaces*, 1986, 19, 301.
- [3] K.N. Bakeev, E.A. Ponomarenko, T.V. Shishkanova, D.A. Tirrell, A.B. Zezin, V.A. Kabanov, *Macromolecules*, 1995, 28, 2886.
- [4] M.J. McGlade, F.J. Randall, N. Tcheurekdjian, *Macromolecules*, 1987, 20, 1782.
M.J. McGlade, J.L. Olufs, *Macromolecules*, 1988, 21, 2346.
- [5] I. Iliopoulos, T.K. Wang, R. Audebert, *Langmuir*, 1991, 7, 617.

- [6] E.D. Goddard, P.S. Leung, *Langmuir*, **1992**, *8*, 1499.
- [7] E.D. Goddard, P.S. Leung, *Colloids Surfaces*, **1992**, *65*, 211.
- [8] G.L. Brode, E.D. Goddard, W.C. Harris, G.A. Salensky, *Polym. Sci. Eng. Proc., Am. Chem. Soc.* **1990**, *63*, 696.
- [9] V. Shubin, *Langmuir*, **1994**, *10*, 1093.
- [10] D.C. Dong, M.A. Winnik, *Can. J. Chem.*, **1985**, *62*, 2560.
- [11] K. Kalyanasundaram, J.K. Thomas, *J. Am. Chem. Soc.*, **1977**, *99*, 2039.
- [12] D.-Y. Chu, J.K. Thomas, *J. Am. Chem. Soc.*, **1986**, *108*, 6270.
- [13] F.M. Winnik, H. Ringsdorf, J. Venzmer, *Langmuir*, **1991**, *7*, 905.
- [14] N.J. Turro, B.H. Baretz, P.-L. Kuo, *Macromolecules*, **1984**, *17*, 1321.
- [15] F.M. Winnik, M.A. Winnik, S. Tazuke, *J. Phys. Chem.*, **1987**, *91*, 594.
- [16] B. Magny, I. Iliopoulos, R. Zana, R. Audebert, *Langmuir*, **1994**, *10*, 3180.
- [17] P. Lianos, R. Zana, *J. Colloid Interface Sci.*, **1985**, *107*, 2.
- [18] B. Lindman, K. Thalberg, in Ref. [1], p. 1257.
- [19] K.P. Anathapadmanabhan, P.S. Leung and E.D. Goddard, Polymer Association Structures, Symposium Series, No. 384, Am. Chem. Soc., Washington, DC, **1989**.

Langmuir, 1997, 13, 111-114.

Interactions of an anionic surfactant with a fluorescent-dye-labelled hydrophobically-modified cationic cellulose ether

Françoise M. Winnik^{1*}, Sudarshi T.A. Regismond¹, and E. Desmond Goddard²

¹Department of Chemistry, McMaster University, 1280 Main Street West, Hamilton, Ontario

L8S 4M1, Canada

²349 Pleasant Lane, Haworth, New Jersey 07641

Received July 19, 1996. In final form October 4, 1996

© 1997 American Chemical Society

1. Introduction

Hydrophobically-modified polymers form a unique class of water soluble polymers which have attracted considerable attention, owing to their outstanding solution properties and numerous practical applications [1]. These polymers exhibit a strong tendency to self-associate via inter- or intrapolymeric interactions of the hydrophobic side chains. The commercial polymer Quatrisoft LM200 is a (hydroxyethyl)cellulose ether substituted at a low level with cationic hydrophobic side chains. The polymer in water forms cationic hydrophobic microdomains via intra- and interpolymer association of the side chains. Upon addition of anionic surfactants to aqueous solutions of Quatrisoft LM200, mixed micelles form readily, since both electrostatic and hydrophobic forces promote the interactions. Near charge neutralization, associative phase separation takes place, as typically observed in strongly interacting polyelectrolyte/oppositely-charged surfactant systems [2]. When excess surfactant is added, redissolution occurs. At high polymer concentrations (1-20 g/L), the Quatrisoft LM200/SDS system forms gels in the

resolubilization zone, as well as in the preprecipitation zone, as reported by Goddard and Leung [3]. In the dilute regime (0.2-1 g/L) formation of gels is not observed ; nonetheless, interaction takes place, as reported by Guillemet and Piculell in a recent study of the system by fluorescence probe spectroscopy and viscosity determination [4]. Their data give clear evidence of binding of SDS to the polymer at surfactant concentrations as low as 10^{-5} mol/L, confirming observations reported earlier [5]. The binding continues for concentrations much higher than the SDS concentration at the redissolution point. Corroborative rheological studies of Quatrisoft LM200 solutions of varying ionic strength [3] suggested that two factors essentially control the phase behaviour of the mixture : (1) the stoichiometry of the mixed micelles and (2) the amount of external electrolyte, surfactant, or inorganic salt.

We report here the results of experiments carried out on the same system, Quatrisoft LM200/SDS, but the polymer (LM200-Py) was modified by covalent linkage of a small amount of fluorescent dye. The pyrene label was attached by ether formation between 4-(1-pyrenyl)butyltosylate and hydroxyl groups present along the LM200 chain. Pyrene groups have been attached by this method to various cellulose ethers, such as (hydroxypropyl)cellulose [6], tylose, and methylcellulose [7]. In all cases, spectroscopic measurements have shown that in aqueous solutions, the fluorescently-labelled cellulose ethers form interpolymeric aggregates via clusters of hydrophobic chromophores. The fluorescence spectra of these polymers exhibit two emissions : a well-resolved emission with the (0,0) band at 377 nm due to locally excited pyrenes (intensity I_M , monomer emission) and a broad emission centered at 485 nm (intensity I_E , excimer emission),

which originates primarily from pyrene aggregates. The addition of anionic surfactants to aqueous solutions of pyrene-labelled cellulose ethers causes a disruption of these aggregates, resulting in an increase in pyrene monomer emission at the expense of pyrene excimer emission [8]. In this study we report the response of the polymer LM200-Py to the addition of SDS and to changes in ionic strength. The experimental tool is the ratio I_E/I_M of the pyrene monomer emission intensity to the pyrene excimer emission intensity and its change as a function of surfactant or salt concentration. We chose experimental conditions similar to those reported by Guillemet and Piculell, to allow a comparison with the results of their experiments.

2. Experimental Section

2.1. Materials

Sodium dodecyl sulfate (SDS) was obtained from Sigma (purity > 99%). Water was deionized using a NANOpure water purification system. The polymer Quatrisoft LM200 was a gift from Amerchol Inc., and it was used without further purification. It is the chloride salt of an N,N-dimethyl-N-dodecyl derivative of (hydroxyethyl)cellulose with a molar mass of approximately 100,000 Da [3]. The degree of substitution was reported to be 2.0×10^{-4} mol of $C_{12}H_{25}$ per gram of polymer or on average 1 dodecyl group per 19 glucose units. Pyrene-labelled Quatrisoft LM200 (LM200-Py, Figure 2) was prepared by reaction of Quatrisoft LM200 with 4-(1-pyrenyl)butyl tosylate in N,N-dimethylformamide in the presence of sodium hydride [9,10]. The amount of pyrene (Py) incorporated,

determined by UV spectroscopy, was 2.9×10^{-5} mol of Py g^{-1} of polymer or on average 1 Py per 190 glucose units.

2.2. Fluorescence Measurements

The fluorescence spectra were recorded at room temperature on a SPEX Fluorolog 212 spectrometer equipped with a DM3000F data system. Emission spectra were not corrected. The excimer to monomer intensity ratio (I_E/I_M) was calculated by taking the ratio of the emission intensity at 485 nm to the half-sum of the emission intensities at 377 and 398 nm. Polymer solutions were prepared by dissolving the polymer into water (1 or 0.1 g/L). They were allowed to equilibrate at room temperature for 24 h. SDS solutions of various concentrations were obtained by dilution of a stock solution (288.4 g/L, 1.0 mol/L). Solutions for analysis were obtained by mixing aliquots of SDS solutions (0.3 ml) and aliquots (2.7 ml) of the polymer solution. Solutions in sodium chloride were obtained in a similar manner using dilutions of a NaCl stock solution (292 g/L, 5.0 mol/L). Solutions for analysis were allowed to equilibrate overnight prior to fluorescence measurements.

3. Results and Discussion

Fluorescence spectra of LM200-Py are shown in Figure 1 for a solution in water (1 g/L) and in polymer solutions containing incremental amounts of SDS. In pure water, the emission is characterized by a broad excimer emission (intensity I_E) centered at 485 nm and a well-resolved pyrene monomer emission (intensity I_M) with the (0,0) band at 377 nm. Evidence from excitation spectra, UV absorbance, and quantum yield determinations

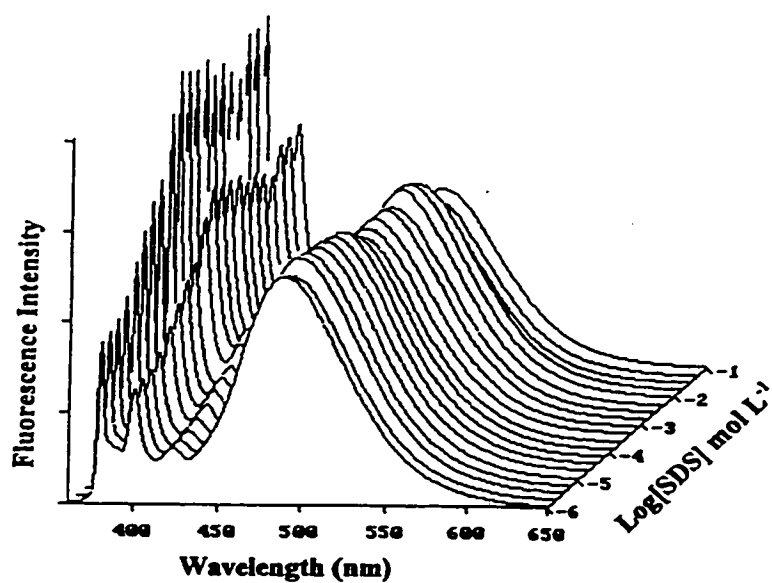


Figure 1: Fluorescence spectra of LM200-Py (1 g/L) measured at several sodium dodecyl sulfate (SDS) concentrations. $\bar{\epsilon}_{\text{exc}} = 346 \text{ nm}$.

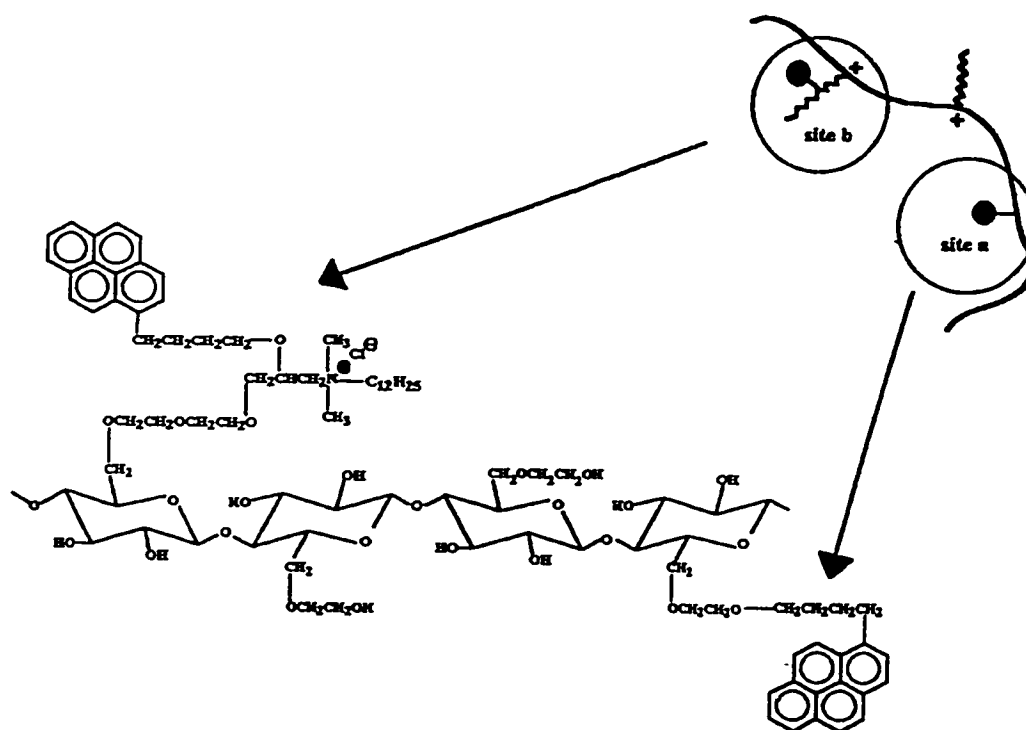


Figure 2: Chemical structure of LM200-Py indicating the two sites of pyrene incorporation.

indicate that a significant fraction of the pyrene excimer emission from LM200-Py in water originates from preformed pyrene dimers or higher aggregates stabilized by hydrophobic bonding, as observed for aqueous solutions of related cellulose ethers [10]. It is important to note, however, that the polymer LM200 offers two different sites for pyrene incorporation, namely, primary hydroxyl groups of the hydroxyethyl substituents on the glucopyranose ring (site a, Figure 2) and hydroxyl groups of the hydrophobic substituents (site b, Figure 2). Pyrene groups linked to sites a and sites b are expected to experience a different environment; hence, they may exhibit different photophysical properties. The observed pyrene aggregates may occur between pyrenes attached on the glucose rings and on the hydrophobic substituents within a single polymer chain. Interpolymer interactions via pyrene-pyrene association may take place as well and contribute to the self-association via hydrophobic interactions and contribute to the interpolymeric association known to occur even in dilute solutions of the unlabelled polymer.

Addition of SDS to LM200-Py aqueous solutions has no effect on the emission spectrum until the surfactant reaches a concentration of 1.0×10^{-5} mol/L. Then, one observes a gradual increase in the intensity of the monomer emission, which reaches a plateau for surfactant concentrations exceeding 2×10^{-4} mol/L (Figure 3). This concentration coincides with the neutralization value, that is the point where all the charges of the polymer are compensated by the surfactant sulfate groups, a value estimated from the reported concentration of dodecyl side chains on Quatrisoft LM200 [4]. It corresponds also to the macroscopic phase separation of the polymer/surfactant complexes

[11]. Further increases in SDS concentration result only in minor changes in the polymer emission. An unusual spectroscopic feature occurs near the redissolution point, $[\text{SDS}] \sim 8 \times 10^{-3} \text{ mol/L}$, a concentration which is also the surfactant critical micelle concentration in water [12]. In a very narrow concentration range around this value, the monomer emission intensity exhibits a minimum and the excimer emission intensity displays a weak maximum. This feature is noticeable in plots of the changes of I_M and I_E as a function of surfactant concentration (Figure 3). It may signal the existence of a narrow surfactant concentration range where SDS/LM200-Py mixed micelles entrap at least two pyrene groups capable of forming excimers. Upon further increase of the SDS concentration, the pyrene groups are solubilized as separated entities within larger, or more numerous, mixed micelles. Both the SDS concentration for onset of interaction and the saturation value depend on polymer concentration, as shown in Figure 4, where we plot the changes in I_E/I_M as a function of $[\text{SDS}]$ in the cases of solutions of LM200-Py of 1.0 and 0.1 g/L. For the lower concentration polymer solution the I_E/I_M saturation takes place at $[\text{SDS}] \sim 2.0 \times 10^{-5} \text{ mol/L}$, the neutralization point in this case.

In previous studies of the interactions of pyrene-labelled cellulose ethers with surfactants, similar trends in I_E/I_M were observed. However, in all cases the increase in Py monomer emission intensity occurred at the expense of the excimer emission, which became extremely weak at high surfactant concentrations [8]. In the case of LM200-Py, in contrast, plots of I_E and I_M as a function of SDS concentration show that the excimer emission intensity is not affected significantly by the addition of surfactant : it remains nearly constant over the entire range of surfactant concentration. Thus, the marked

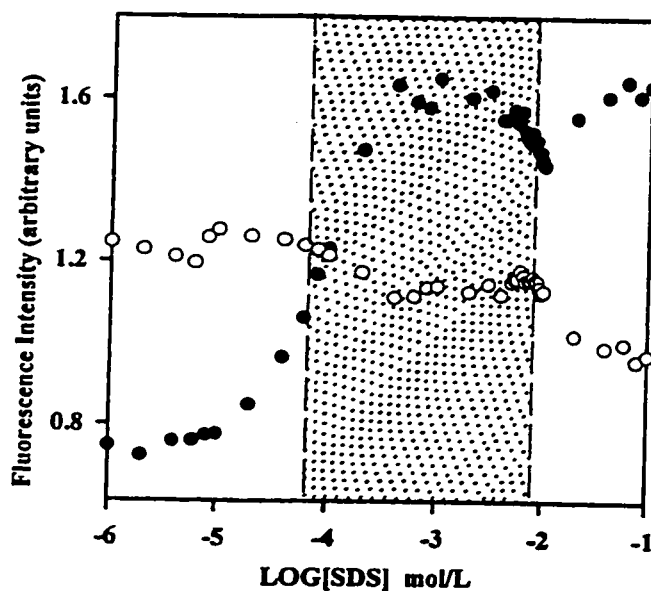


Figure 3: Plots of the monomer (I_M , full circles) and excimer (I_E , open circles) emission intensities of aqueous LM200-Py solutions as a function of sodium dodecyl sulfate concentration (polymer concentration: 1.0 g/L). The shaded area indicates the precipitation zone.

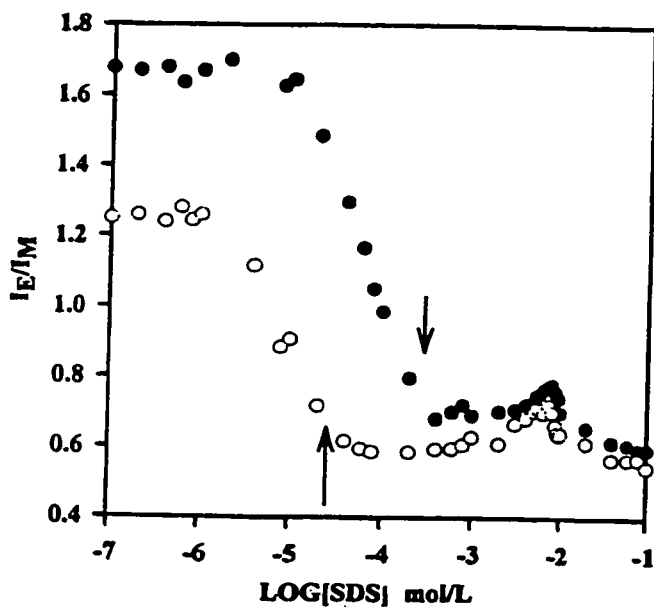


Figure 4: Plots of the excimer to monomer emission intensity ratio (I_E/I_M) of aqueous solutions of LM200-Py as a function of sodium dodecyl sulfate (SDS) concentration: (open circles) 0.1 g/L LM200-Py; (full circles) 1 g/L LM200-Py; the arrows indicate the SDS concentration corresponding to charge neutralization.

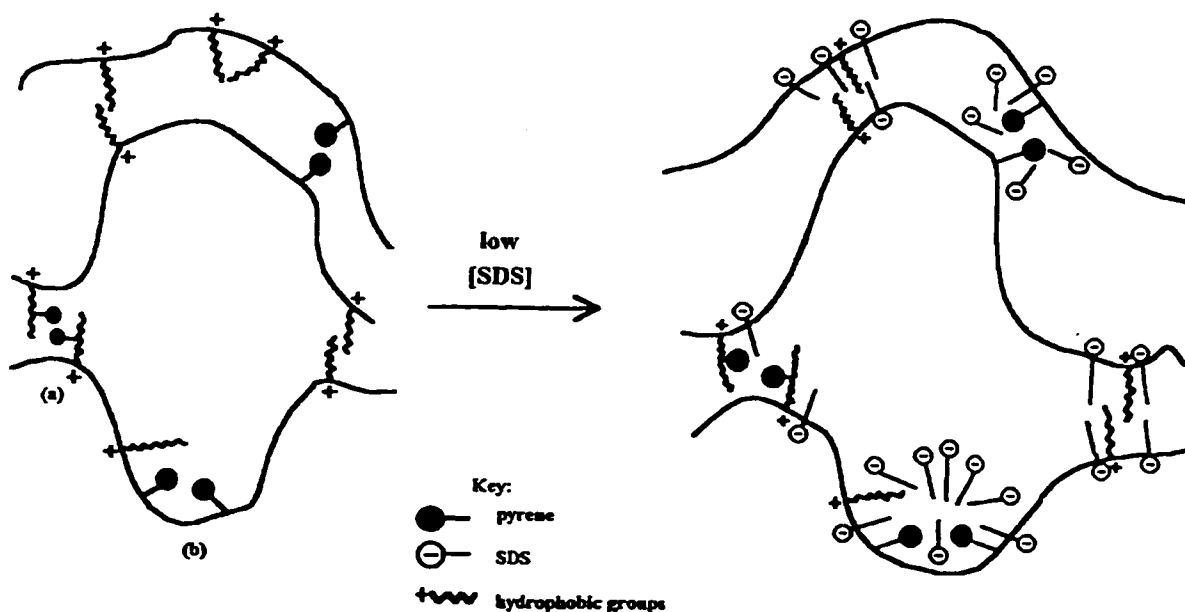


Figure 5: Interactions between LM200-Py and sodium dodecyl sulfate: a schematic representation. The two pyrene sites correspond to those shown in Figure 2.

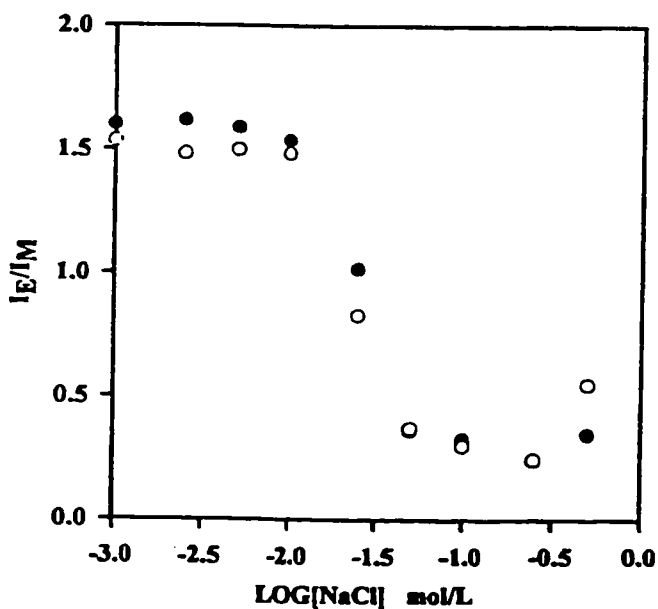


Figure 6: Plots of the excimer to monomer emission intensity ratio (I_E/I_M) of aqueous solutions of LM200-Py as a function of sodium chloride concentration: (open circles) 0.5 g/L LM200-Py; (full circles) 1 g/L LM200-Py.

increase in monomer emission originates primarily from a relief of pyrene self-quenching, presumably due to nonemissive aggregates in aqueous LM200-Py solutions. These aggregates are disrupted, and pyrene groups are incorporated within the SDS/polymer side chain mixed micelles that grow on the polymer chain (Figure 5). Further studies on LM200 samples labelled specifically, either along the main chain or on the hydrophobic substituents, are needed for a complete interpretation of the unusual trends observed with the randomly labelled sample LM200-Py examined here.

The LM200 coil dimensions are determined by an interplay between two opposite forces : electrostatic repulsions between the charges on the hydrophobic substituents and attractive forces between the alkyl groups. At low ionic strength the electrostatic repulsions prevail. At a certain salt concentration, however, the electrostatic repulsions are reduced and the polymer coil contracts as a result of increased intrachain hydrophobic aggregation [13]. Salt-induced transitions in the conformation of LM200-Py are detected by changes in the pyrene photophysical properties. A plot of the ratio I_E/I_M as a function of $[NaCl]$ for polymer solutions of concentrations 0.5 and 1.0 g/L is shown in Figure 6. The ratio remains constant until a critical NaCl concentration, where it decreases sharply. The salt concentration corresponding to the midpoint of the transition in the curve, $[NaCl] = 0.02$ mol/L, does not appear to depend on polymer concentration. This salt concentration corresponds to the onset of macroscopic phase separation, as reported by Guillemet and Piculell [4]. Thus LM200-Py precipitation is revealed by an increase in pyrene monomer emission. This may reflect the solubilization of isolated pyrene groups

within the hydrophobic microdomains created in the collapsed coils (Figure 7). This phenomenon bears similarities to the heat-induced phase separation of aqueous solutions of neutral polymers, such as (hydroxypropyl)cellulose. Solutions of pyrene-labelled cellulose ethers exhibit also a sharp increase in pyrene monomer emission as they undergo phase separation [14].

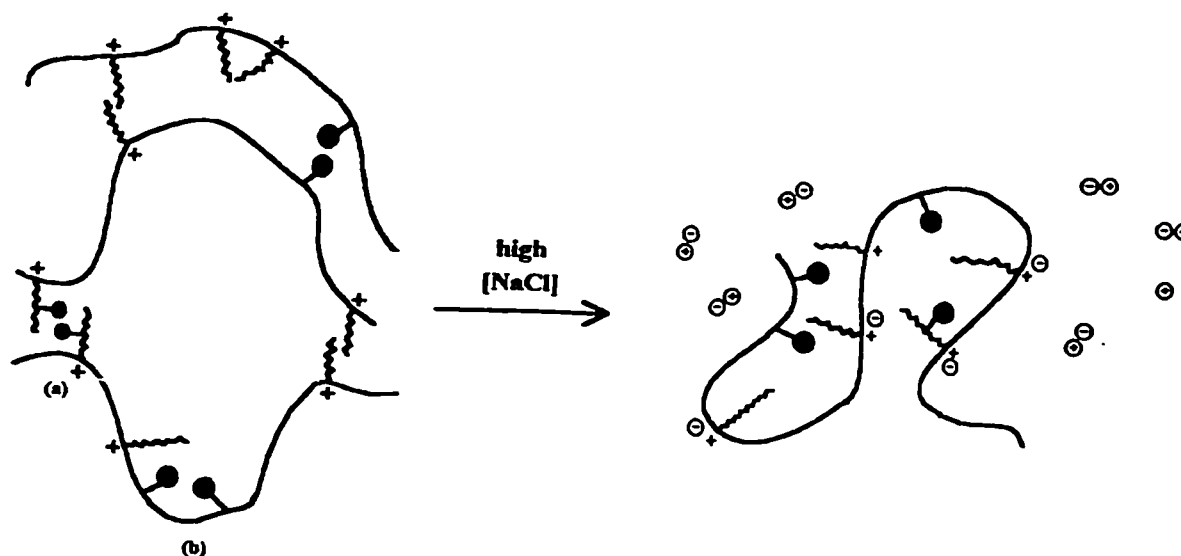


Figure 7: Schematic representation of the polymer conformation in solutions of high salt content (right) and in water (left).

4. Conclusions

The fluorescence label experiments presented here confirm that mixed micelles form between SDS and the alkyl side chains of LM200-Py. Our data are best explained by

involving two different sites of attachment of the pyrene moieties to the polymer. Work in progress is aimed at the study of Quatrisoft LM200 labelled specifically, either on the hydrophobic side chain or along the polymer backbone.

Acknowledgment

F.M.W. and S.T.A.R. thank the Natural Science and Engineering Research Council of Canada for financial support.

References

- [1] J.E. Glass, Ed., *Polymers in Aqueous Media: Performance through Association*, Advances in Chemistry Series 213, American Chemical Society, Washington DC, 1989.; S.W. Shalaby, C.L. McCormick, G.B. Butler, Eds., ACS Symposium Series 467, American Chemical Society, Washington, DC, 1991.
- [2] E.D. Goddard, in *Interactions of Surfactants with Polymers and Proteins*, E.D. Goddard, and K.P. Ananthapadmanabhan, Eds., CRC Press, Boca Raton, FL, 1993, pp 171-202.
- [3] E.D. Goddard, P.S. Leung, *Colloids Surfaces*, 1992, 65, 211.
- [4] F. Guillemet, L. Piculell, *J. Phys. Chem.*, 1995, 99, 9201.
- [5] K.P. Ananthapadmanabhan, P.S. Leung, and E.D. Goddard, in *Polymer Association Structures*, M.A. El-Nokaly, Ed., ACS Symposium Series 384, American Chemical Society, Washington, DC, 1989, p 297.

- [6] F.M. Winnik, M.A. Winnik, S. Tazuke, C.K. Ober, *Macromolecules*, **1987**, *20*, 38.
- [7] F.M. Winnik, in *Hydrophobic Polymers: Performance with Environmental Acceptability*, J.E. Glass, Ed., *Advances in Chemistry Series 248*, American Chemical Society, Washington, DC, **1996**, p 409.
- [8] F.M. Winnik, M.A. Winnik, S. Tazuke, *J. Phys. Chem.*, **1987**, *91*, 594.
- [9] The general procedure was described in refs 6 and 7 and references therein. Full synthetic details will be reported elsewhere.
- [10] F.M. Winnik, *Chem. Rev.*, **1993**, *93*, 587.
- [11] Note that, at the low concentration of polymer used here, the phase separation was barely detectable visually. We ascertained that the small increase in sample turbidity did not interfere significantly with the fluorescence measurements.
- [12] N.M. Van Os, J.R. Haack, L.A.M. Ruppert, *Physico-chemical Properties of Selected Anionic, Cationic, and Non-Ionic Surfactants*, Elsevier, Amsterdam, **1993**.
- [13] M. Magny, I. Iliopoulos, R. Audebert, in *Macromolecular Complexes in Chemistry and Biology*, Dubin, Bock, Davis, Schulz, Thies, Eds., Springer-Verlag, Berlin, **1994**, Chapter 4.
- [14] F.M. Winnik, *Macromolecules*, **1987**, *20*, 2745.

Colloids and Surfaces A : Physicochemical and Engineering Aspects, 1996, 119, 221-228

Surface viscoelasticity in mixed polycation anionic surfactant systems studied by a simple test

S.T.A. Regismond^a, F.M. Winnik^a, E.D. Goddard^b

^aDepartment of Chemistry, McMaster University, 1280 Main St. W. Hamilton, Ontario
Canada L8S 4M1,

^b349 Pleasant Lane, Haworth, New Jersey, USA, 07941

Received 6 May 1996; accepted 23 July 1996

© 1996 Elsevier Science B.V. All rights reserved.

Abstract

The talc particle test, performed on mixed solutions of polyelectrolyte and oppositely charged surfactant, was used to examine the changes in rheology of the air/water interace of these solutions over a large range of compositions. The systems scrutinized consisted of sodium dodecyl sulfate (SDS, concentrations ranging from 0.005 to 0.5 g/L) and either the cationic cellulosic polymer, Polymer JR400, or the corresponding hydrophobically-modified polymer, Quatrisoft LM200, of concentration ranging from 0.001 to 1 g/L. Clear indications of viscoelasticity at the air/water interface were obtained over a wide composition domain in both instances. Viscoelasticity provides evidence of a synergistic adsorption of the two components at the air/water interface. When the SDS was increased sufficiently with respect to the polyelectrolyte concentration, the viscoelasticity vanished, and the interface became fluid ; the fluidity recovery is an indication that the interface is denuded of polyelectrolytes by growing competition from micellar interfaces in solution.

Keywords : Surface viscoelasticity ; Polyelectrolyte ; Surfactant ; Cellulosic polymers ; Polymer JR400

1. Introduction

The interactions between polymers and surfactants of opposite charge have been characterised in great detail over the last few decades [1,2]. The physicochemical changes occurring in bulk water upon addition of an oppositely charged surfactant to a polyelectrolyte solution are interpreted in terms of the formation of polymer/surfactant complexes and of the distribution of the surfactant between the free amphiphile state and the micellar or aggregated state. In contrast, there have been relatively few attempts to examine and interpret the changes in the adsorption of the surfactant or the polymer at the air/water interface under the same conditions. The interfacial behaviour of polymer/surfactant systems is a controlling factor in many of their practical applications, such as wetting and flotation agents of minerals, deposition aids, and surface conditioners. The present contribution presents results of a simple technique to assess the characteristics of the air/water interface of a range of mixed surfactant/polymer solutions.

Boundary tension methods, such as surface tension or interfacial tension, when applied to mixtures of polymer and surfactant, have in fact been used traditionally to interpret and assess possible interactions of these species in solution [1,3-5]. One of us (E.D.G.), however, presented an interpretation of the surface tension of mixed solutions of a non-surface active cationic polymer and sodium dodecyl sulfate (SDS), in terms of the formation of highly surface-active « complexes » of these species, at least in the lower

surfactant concentration ranges [6,7]. A similar interpretation can be inferred from surface tension measurements on dilute solutions of SDS and poly-L-lysine by Buckingham et al. [8]. At higher concentrations of SDS, the micellar interface competes progressively successfully with the air/water interface for the polymer which then becomes largely, if not exclusively, associated with bulk micelles. Thermodynamic interpretation of the surface tension behaviour of polymer/surfactant mixtures can be carried out, but such analysis yields limited information about the physical state of the molecules at the interface, although insightful predictions in this respect have been offered recently [9,10].

Current applications of newer investigative techniques to the study of interfaces is reviving interest in the detailed composition and state of interfaces in which the contacting liquid is an aqueous solution of polymer and added surfactant. For example, by use of specular neutron reflection, Purcell et al. [11] showed that, at low SDS concentrations, the presence of poly(vinylpyrrolidone) markedly increases the surface concentration of SDS at the air/water interface. Radiotracer studies on the same system reported by Chari and Hossain [12], also provided evidence for a polymer-induced change of the surfactant concentration at the air/water interface. Thin film drainage studies, coupled with X-ray reflectivity, on the SDS/poly(ethylene oxide) (PEO) system have been interpreted as indicating the presence of a thin layer of PEO underlying the adsorbed monolayer [13]. Using the sum frequency infrared method, Duffy et al. [14] showed that the presence of polyanions markedly reduced the concentration of tetradecyltrimethylammonium ions required to achieve a certain level of orientation of these ions at a hydrophobic solid/aqueous solution interface. Another relevant result is that of Kilau and Voltz [15]

who demonstrated synergistic wetting of a hydrophobic coal surface when polyethylene oxide was used in conjunction with a sulfonate surfactant. A similar synergistic effect was observed by Somasundaran and Lee in a study of the flotation of quartz in a mixed solution of a cationic polyacrylamide and sodium dodecane sulfonate [16]. Taken together all these observations suggest mixed surfactant/polymer film formation at the interface.

It seems desirable to have a simple means to determine if interfacial association structures are present in mixed polymer/surfactant systems. A potential method for detecting the occurrence of polymer/surfactant complexes at the air/water interface is the simple «talc test» described below [17]. This test relies on the effect of the interface composition on the surface rheology of the solution. In particular, the presence of a high-molecular-weight polymer at an interface is expected to affect the 2-dimensional flow properties. Compelling indications, in this respect, of surface-structure development have already come from insoluble-monolayer studies of sodium docosyl sulfate and from the observation of marked surface-viscoelasticity when a small amount of cationic polymer (10 ppm) was introduced into the subsolution [7]. In the work to be described the polymer/surfactant pair was chosen to ensure strong interaction between charged polymer and oppositely charged surfactant. The polymer selected is the cationic cellulosic polymer, Polymer JR400 (Fig. 1), and the anionic surfactant is SDS. For comparison, experiments were also carried out on mixed solutions of SDS and a hydrophobically-modified analogue, Quatrisoft[®]LM200 (Fig.1), containing pendant dodecyl groups, for which phase studies have already been reported [18].

2.2. Solution Preparation

Stock solutions of Polymer JR400 or Quatrisoft® LM200 (2 g /L) were prepared by dissolving the polymer in water. They were allowed to equilibrate for 24 h. Surfactant solutions of varying concentrations, ranging from 0.01 to 10 g/L, were obtained by dilutions of a stock solution in water. Mixed surfactant/polymer solutions, subsequently prepared, spanned surfactant concentrations from 0.005 to 5.0 g/L. The solutions were mixed and allowed to stand in Petri dishes for at least 30 min. The known solubility diagrams of the Polymer JR400/SDS and Quatrisoft® LM200 systems [6,7,18] were used to guide the choice of absolute and relative concentrations of the two components. Emphasis was placed on fairly dilute solutions of polymer (≤ 1 g/L) in order to lessen possible contributions of bulk phase effects to the observed surface behaviour.

2.3. The Talc Method

A small quantity of calcined talc powder was sprinkled on the aqueous surface of a solution contained in a Petri dish 10 cm in diameter. A gentle current of air was directed tangentially at the talc particles for a second or two and then removed. The observed movement of the particles along the surface was recorded. The following qualitative characterisations of the interface were made, where F denotes fluid ; V, viscous ; VE, viscoelastic ; G, gel ; and S, solid). While in category G no net-flow results, in category VE, both a net movement of the particles is observed, together with some recovery upon removing the air current. This procedure has long been used as a sensitive, qualitative measure of the fluid/mechanical conditions of spread or adsorbed monolayers [17].

3. Results and discussion

Clear indications of viscoelasticity at the air/water interface were obtained over substantial concentration regions of the SDS/Polymer JR400 system. A phase map representing dilute aqueous mixtures of these two species is shown in Fig. 2a, together with the corresponding bulk-phase diagram recorded from the same solutions. The latter is identical to the diagram reported by Goddard and Hannan in their original publications on the system [7,19]. In the surface-rheology maps the areas of viscoelasticity correspond, in general, to systems shown previously to exhibit synergistic lowering of the aqueous surface tension [6,7].

Referring to Fig. 2a one notices that the surface VE systems occur on the left-hand side of the two-component matrix, i.e. in the regions of relatively low SDS concentration in the mixtures. Another observation is that many of the systems which show bulk-phase incompatibility, i.e. turbidity or in some cases solid-phase precipitation, display pronounced surface viscoelasticity. This means that interaction in the bulk phase is mirrored in interaction at the surface. Yet another observation is that the VE effect is detectable at polymer concentrations as low as 10 ppm (0.001%), the lowest level tested. It should be emphasized that the polymer by itself is very feebly surface-active and certainly exhibits no surface viscoelasticity. This is a particularly strong indicator of the synergistic interaction of the two components at the interface.

The SDS/Quatrisoft® LM200 system was analysed by the same technique (Fig. 3). In many respects, this case is different from the SDS/Polymer JR400 system in that, by

dint of the presence of hydrophobic groups, the polymer molecule itself is surface-active. It thus presents the case where the polymer will adsorb at the water/air interface in its own right. However, solutions of the polymer alone were found to show no or negligible

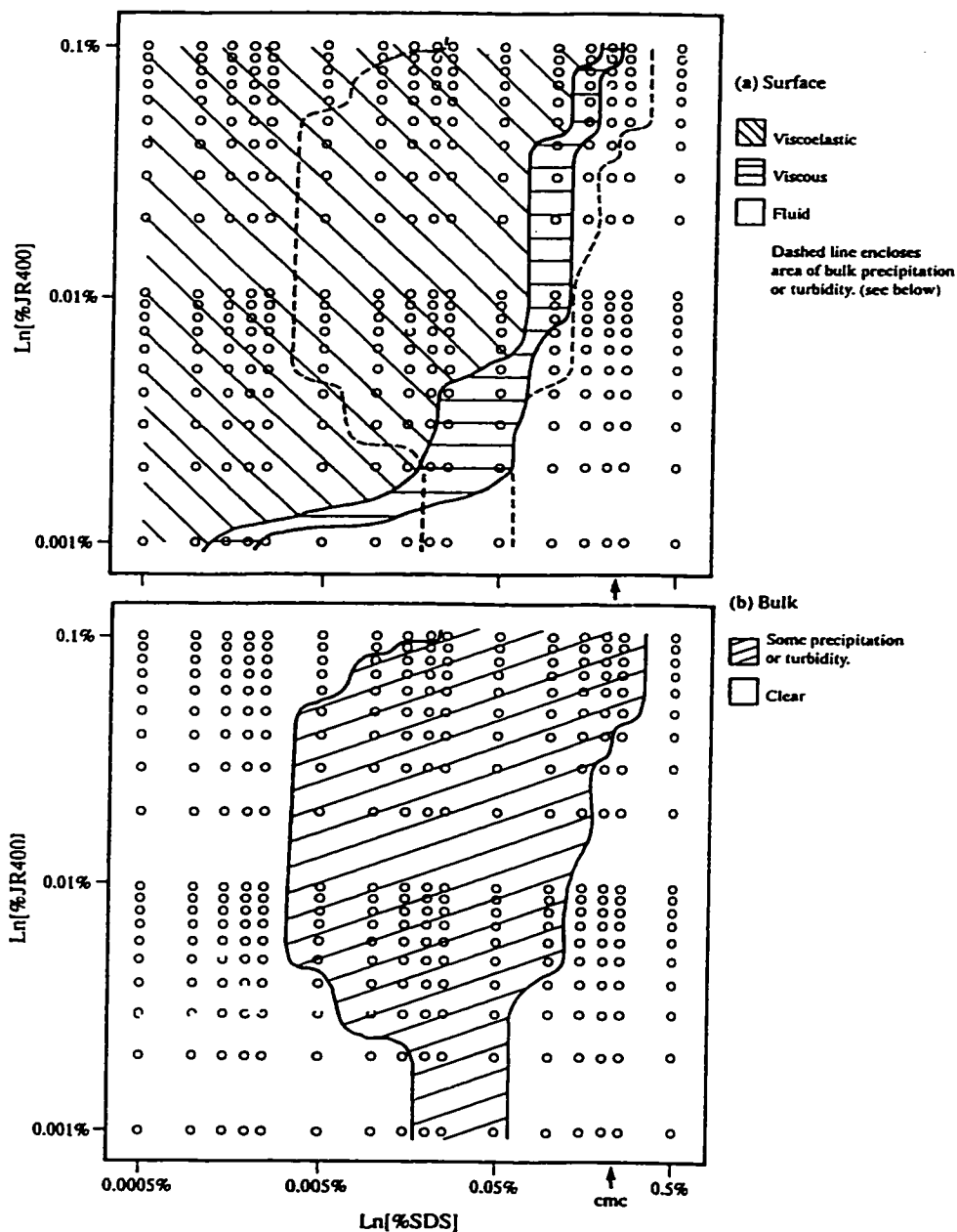


Figure 2: Surface-phase map (a) and solubility diagram (b) of the SDS/Polymer JR400 system; the open circles represent the observation points.

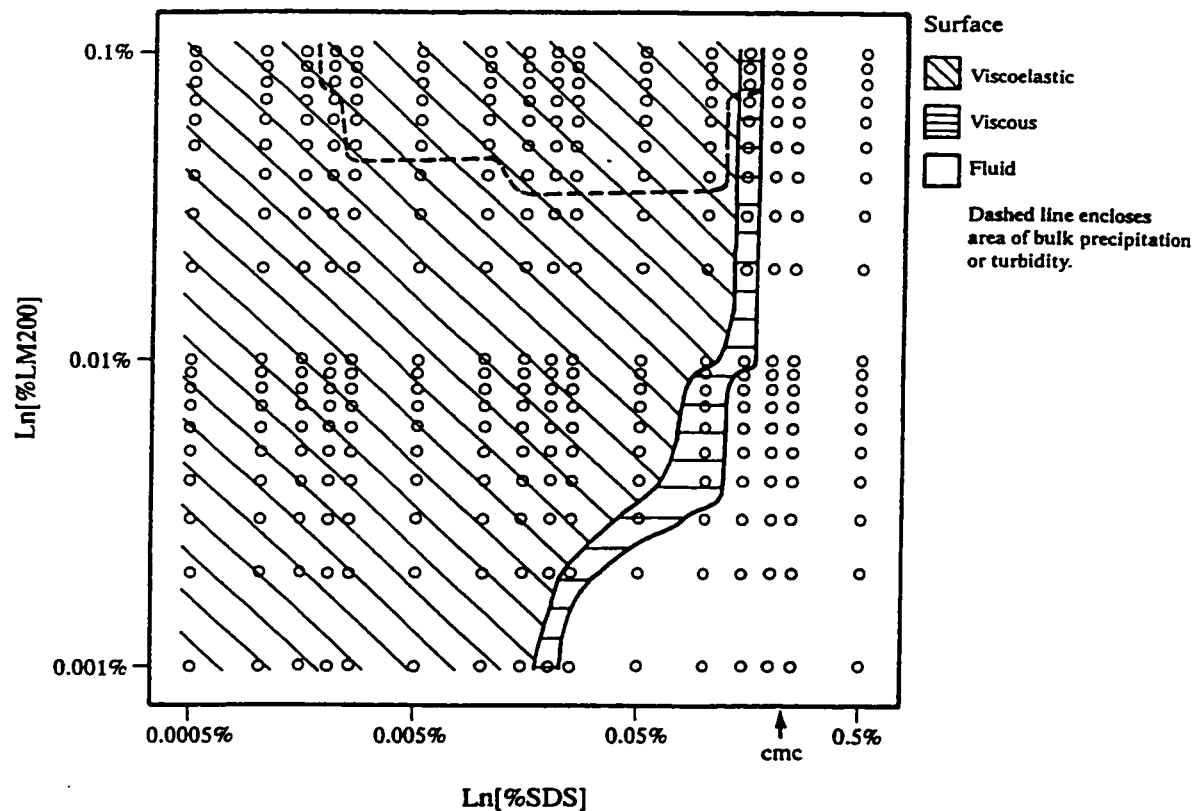


Figure 3: Surface-phase map and solubility diagram of the SDS/Quatrisoft LM200 system; the open circles represent the observation points.

surface viscoelasticity. In contrast, as in the case of the SDS/Polymer JR400 system, the addition of traces of SDS transforms the surface region to one exhibiting VE behaviour.

As before, when the SDS concentration is increased sufficiently, the growing micellar interface denudes the air/water interface of polymer and surface viscoelasticity is eliminated.

It is appropriate here to reexamine the model developed [4,16-18] to account for the solubility, bulk-phase viscosity, dye solubilization, and the surface-tension behaviour of the Polymer JR400/SDS systems [6,7,20-22]. It presupposed strong binding of the surfactant by the polymer mainly as a result of electrostatic forces, reinforced by hydrophobic interaction forces.

3.1. The bulk

Early studies revealed that the addition of surfactant to solutions of the polymer confers dye-solubilization power to the latter [20]. Solubilization of the oil-soluble dye Orange OT was observed at very low concentrations of added SDS, a phenomenon interpreted as an indication of clustering of surfactant molecules through hydrophobic interactions involving individual polymer molecules. Further addition of SDS, prior to reaching the precipitation range, can lead to substantial increases in solution viscosity, suggesting that bound surfactant-molecules are involved, again through hydrophobic interactions, in crosslinking of the polymer chains. The process culminates in precipitation, the maximum occurring near the charge-charge stoichiometric ratio of the two species. Beyond these regions, resolubilization takes place but without the high viscosity registered below the stoichiometric range. This resolubilization corresponds to a region of high solubilization of the oil-soluble dye. The phenomenon has been loosely attributed to the « formation of an adsorbed double-layer of surfactant on the polymer », resulting in a highly negatively charged complex. An explanation, more in keeping with current views of polyelectrolytes, including proteins, interacting with surfactants, invokes

the formation of an array of surfactant micelles with polymer wrapped around them, i.e. the beads and necklace model [23-25].

3.2. The surface

At a freshly formed surface of a mixed solution we may suppose that diffusion of faster moving surfactants results at first in the formation of an adsorbed layer of surfactant. This array of negatively charged groups at the air/water interface would constitute a potent attractive force upon the polycation molecules. Thus, we envisage the formation of an adsorbed layer of polymer which is responsible for the marked synergism in surface-tension lowering [6] and for the registering of surface viscoelasticity (Fig. 4). As noted above, even though further addition of SDS can lead to progressive precipitation, the synergistic lowering of surface tension persists throughout the precipitation composition range, again providing strong presumptive evidence for the formation of polymer/surfactant « complexes » in the surface. At higher concentrations of SDS, the system is dominated progressively by bulk-phase surfactant micelles which eventually denude the air/water interface of the polymer, so all traces of viscoelasticity and synergistic lowering of surface tension are lost. We reiterate that under conditions of maximum precipitation, when the least amount of polymer is in solution, the presence of surface-adsorbed polymer, by VE criteria, is clearly indicated, except for the most dilute polymer series (10 ppm).

The development of surface viscoelasticity in the case of Quatrisoft® LM200 lends support to the above interpretation, since here the formation of a mixed film with SDS can safely be assumed in view of the intrinsic surface-activity of this polymer. In some

respects there is, thus, a similarity of this system to protein/surfactant mixtures, another group of mixed polymer/surfactant systems whose surface behaviour has been widely studied [26,27]. Similarities include a tendency for the macromolecule to be stripped from the surface at high relative concentrations of surfactant. A difference from the present system is that adsorbed films of protein can be quite viscous in their own right.

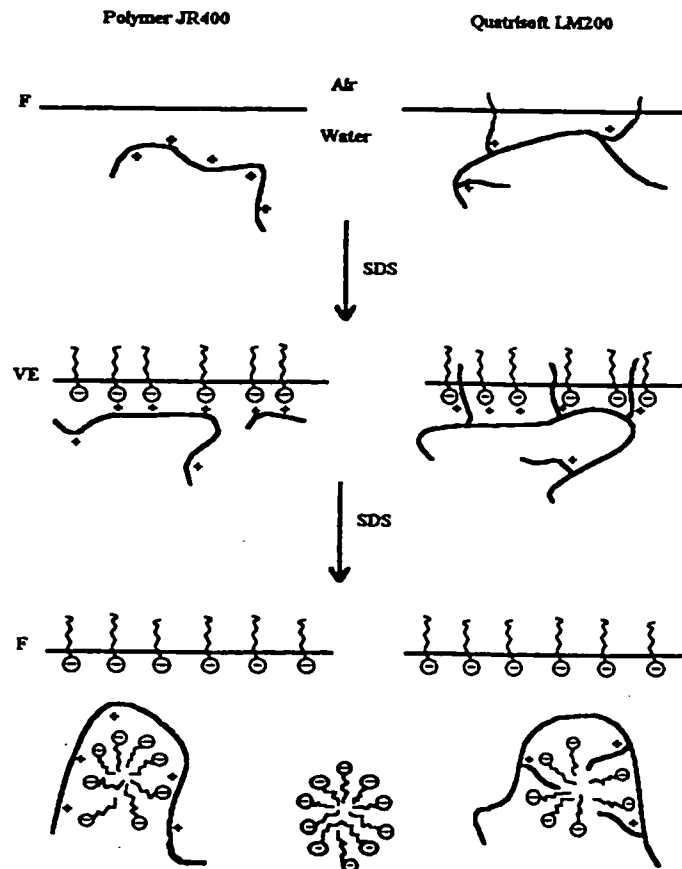


Figure 4: Schematic representation of the polycation/anionic surfactant interactions as a function of surfactant concentration in the bulk and at the air/water interface, in the cases where the polycation is Polymer JR400 (left) and Quatrisoft[®] LM200 (right), F, fluid; VE, viscoelastic.

Confirmation of the early finding [7] of synergistic lowering of the surface tension of polyelectrolyte/oppositely charged surfactant pairs is provided in a recent publication [28]. Based on observations of thin film/disjoining pressure-curves the latter work presents evidence of polymer-surfactant network formation in the body of the thin film itself. This is consistent with previous work on the high stability of foams generated from similar polymer/surfactant systems [7], and also with evidence of «bridging» of thin films of polyelectrolyte/surfactant pairs in solution constrained between mica plates [29].

4. Conclusions

While the «talc test» lacks the rigour of state-of-the-art techniques of interface characterisation, such as specular neutron reflection or sum frequency IR, we have demonstrated that it can provide a simple, yet sensitive method to detect polymer/surfactant interactions on the surface, even in the absence of any macroscopic indications. It is not, by any means, limited to the systems presented here. In fact it is currently being applied to the study of various polycation/anionic surfactant and polyanion/cationic surfactant systems.

Acknowledgments

F.M.W. and S.T.A.R. thank the Natural Sciences and Engineering Research Council of Canada for financial support.

References

- [1] E.D. Goddard and K.P. Ananthapadmanabhan (Eds.), *Interactions of Surfactants with Polymers and Proteins*, CRC Press, Boca Raton, FL, 1993.
- [2] Y.-C. Wei, S.M. Hudson, *J. Macromol. Sci.-Rev. Macromol. Chem. Phys.*, **1995**, C35, 15.
- [3] E.G. Cockbain, *Trans. Faraday Soc.*, **1953**, 49, 104.
- [4] M.N. Jones, *J. Colloid Interface Sci.*, **1967**, 23, 36.
- [5] H. Lange, *Kolloid Z. Z. Polym.*, **1971**, 243, 101.
- [6] E.D. Goddard, T.S. Phillips, R.B. Hannan, *J. Soc. Cosmet. Chem.*, **1975**, 26, 461.
- [7] E.D. Goddard, R.B. Hannan, *J. Colloid Interface Sci.*, **1976**, 55, 73.
- [8] J.H. Buckingham, J. Lucassen, F. Hollway, *J. Colloid Interface Sci.*, **1978**, 67, 423.
- [9] M. Barck, P. Stenius, *Colloids Surfaces A : Physicochem. Eng. Aspects*, **1994**, 89, 59.
- [10] P.G. De Gennes, *J. Phys. Chem.*, **1990**, 94, 8407.
- [11] I.P. Purcell, R.K. Thomas, J. Penfold, A.M. Howe, *Colloids Surfaces*, **1995**, 94, 125.
- [12] K. Chari, T.Z. Hossain, *J. Phys. Chem.*, **1991**, 95, 3302.
- [13] S. Cohen-Addad, J. M. Di Meglio, *Langmuir*, **1994**, 10, 773 ; *C.R. Acad. Sci. Paris II*, **1992**, 315, 39.
- [14] D.C. Duffy, P.B. Davies, A.M. Creeth, *Langmuir*, **1995**, 11, 2931.

- [15] H.W. Kilau, J.I. Voltz, *Colloids Surfaces*, **1991**, *57*, 17.
- [16] P. Somasundaran, L.T.Lee, *Sep. Sci. Technol.*, **1981**, *16*, 1475.
- [17] J.T. Davies and E.K. Rideal, *Interfacial Phenomena*, Academic Press, New York, **1961**, pp. 257-258.
- [18] E.D. Goddard, P.S. Leung, *Colloids Surfaces*, **1992**, *65*, 211.
- [19] E.D. Goddard, R.B. Hannan, *J. Am. Oil Chem. Soc.*, **1977**, *54*, 561.
- [20] E.D. Goddard, R.B. Hannan, G.H. Matteson, *J. Colloid Interface Sci.*, **1977**, *60*, 214.
- [21] P.S. Leung, E.D. Goddard, C. Han, C.J. Glinka, *Colloids Surfaces*, **1985**, *13*, 47.
- [22] E.D. Goddard, *Colloids Surfaces*, **1986**, *19*, 301.
- [23] K. Shirahama, K. Tsuji, T. Takagi, *J. Biochem. (Tokyo)*, **1974**, *75*, 309.
- [24] K. Ohbu, O. Hiraishi, I. Kashira, *J. Am. Oil Chem. Soc.*, **1982**, *59*, 108.
- [25] N.J. Turro, X.G. Lei, K.P. Ananthapadmanabhan, M. Aronson, *Langmuir*, **1995**, *11*, 2525.
- [26] E. Dickinson, in E.D. Goddard and K.P. Ananthapadmanabhan (Eds.), *Interactions of Surfactants with Polymers and Surfactants*, CRC Press, Boca Raton, FL, **1993**, p.295.
- [27] S.W.H. Eijt, M.M. Wittebrood, M.A.C. Devillers, Th. Rasing, *Langmuir*, **1994**, *10*, 4498.
- [28] V. Bergeron, D. Langevin, A. Asnacios, *Langmuir*, **1996**, *12*, 1550.
- [29] K.P. Ananthapadmanabhan, G.-Z. Mao, E.D. Goddard, M. Tirrell, *Colloids Surfaces*, **1991**, *61*, 167.

Colloids and Surfaces A : Physicochemical and Engineering Aspects, 1998, 141, 165-171

Stabilization of aqueous foams by polymer/surfactant systems: effect of surfactant chain length

S.T.A. Regismond^a, F.M. Winnik^a, E.D. Goddard^b

^aDepartment of Chemistry, McMaster University, 1280 Main St. W. Hamilton, Ontario
Canada L8S 4M1,

^b349 Pleasant Lane, Haworth, New Jersey, USA, 07941

Received 26 August 1997; received in revised form 2 December 1997; accepted 10
December 1997

© 1998 Elsevier Science B.V. All rights reserved.

Abstract

The foaming of mixed polymer/surfactant solutions was investigated as a function of surfactant chain length for the system consisting of the cationic cellulose ether Polymer JR400 and a series of sodium alkyl sulfates ($C_nH_{2n+1}SO_4Na$, $n=8, 10$ and 12) and sodium decane sulfonate. Foam enhancement by the polymer was observed with all of these surfactants, but the largest effect and best foaming results were found with the shorter chain length surfactants/Polymer JR400 systems, especially the sodium octyl sulfate/Polymer JR400 system. The foaming results correlated with surface viscoelasticity measurements and also with film drainage observations on selected systems.

Keywords: Film drainage ; Foaming ; Polymer JR400 ; Surface viscoelasticity ; Surfactant

1. Introduction

Although the use of surface tension methods to study interactions between polymers and surfactants is quite old, they have been employed mainly as an indicator of interactions occurring in the bulk phase [1]. The method in effect utilizes the fact that the surfactant is generally much more surface active than the polymer and, hence, the surface tension is taken as an indicator of “free” surfactant in solution in equilibrium with the air/water interface. Some years ago, Goddard and co-workers showed highly synergistic surface tension lowering in systems in which the polymer was a polyelectrolyte and the surfactant bore a charge opposite in sign [2, 3]. Such reduction in surface tension took place even when the polyelectrolyte by itself was only feebly surface active. This led these authors to postulate the existence of highly surface-active complexes of polymer and surfactant. This picture has, in general, been confirmed by later workers and by follow-up studies involving qualitative assessment of the surface rheology of such systems using the “talc particle” test: substantial areas of the two-dimensional phase map revealed pronounced surface viscosity or, indeed, surface viscoelasticity [4].

Aqueous foams are used in many industrial processes and products in a wide application spectrum, including foodstuffs, detergents, cosmetics formulations and fire-fighting fluid [5]. It is well-known from extensive previous work that viscous “rigid” surfaces in soap films can promote slowness in draining and hence longevity and stability of generated films and foams [6]. Such effects could be achieved when a suitable foaming additive was incorporated with the main surfactant, the best known being dodecanol added to sodium dodecyl sulfate (SDS) [7]. Similar effects were observed in preliminary tests of

the foaming [3], and subsequently surface rheology [4], of combinations of SDS and a cationic cellulose ether (Polymer JR400, see Scheme 1). Qualitative indications of foam stability in mixtures of this polymer with shorter chain length surfactants had been obtained during phase diagram studies [8], but were not reported [9]. It was the purpose of the present work to examine the effect of the reduction of surfactant chain length of homologous surfactants on the foaming, film drainage and surface rheology of such combinations of surfactant and polymer. In order to initiate a study of the generality of the observed phenomena, one of the shorter chain surfactants was an alkyl sulfate, while the other was an alkane sulfonate.

2. Experimental

2.1. Materials

Polymer JR400 (Scheme 1), the chloride salt of a trimethylammonium derivative of hydroxyethyl cellulose of molecular weight about 400,000 daltons, was a gift from Amerchol Corp. It was used without further purification. Sodium dodecyl sulfate (>99% pure) was obtained from Sigma Chemicals. Sodium octyl sulfate, sodium decyl sulfate and sodium decane sulfonate were obtained from Aldrich Chemicals. Water was deionized using a NANOpure water purification system. The talc powder was calcined at 350 °C to remove possible surface-active contaminants.

2.2. Solution preparation

A stock solution of Polymer JR400 (1% w/w) was prepared by dissolving the polymer in water and allowing it to equilibrate for 24 h. Surfactant solutions of varying

concentrations, ranging from 0.005 to 0.5% w/w, were obtained by dilution of stock solutions in water. Mixed surfactant/polymer solutions, subsequently prepared, spanned surfactant concentrations from 0.001 to 0.25% w/w.

2.3. The talc method

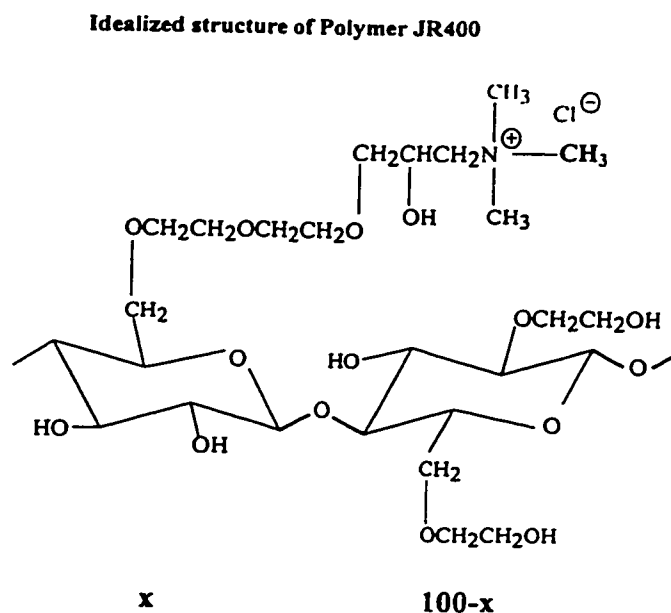
A small quantity of calcined talc powder was sprinkled on the surface of a solution contained in a Petri dish 10 cm in diameter, after the solutions had been allowed to stand for 30 min. A gentle current of air was directed tangentially at the talc particles for a second or two and then removed. The observed movement of the particles along the surface was recorded. Qualitative characterisations of the surface were done, where F denotes fluid, V viscous, VE viscoelastic and G gel. In category VE, a net movement of the particles is observed, together with some recovery upon removing the air current. In category V, a net (slow) movement of the particles is observed, with no recovery upon removing the air current. In category G, no net flow of the particles can be detected.

2.4. Foaming

The conventional cylinder shake test was used to evaluate the foaming performance of surfactant/polymer mixtures. It combines good reproducibility with ease of execution [3]. Briefly, a foaming solution (30 ml) was placed in a 100 ml graduated cylinder. The stoppered cylinder was then shaken manually in standard fashion, twelve times through an arc of approximately 50 cm. The mixtures were allowed to stand for 30 min, then the foam height was recorded with a reproducibility of 5%. To test foam stability, selected mixtures were subjected to the standardized shake test and the foam height was recorded as a function of time over 24 h.

2.5. Draining lamella test

The drainage of films was monitored by the procedure pioneered by Mysels, where a single lamella of solution is formed in a glass frame [7]. A specially designed cell [10, 11] was used to study the drainage characteristics of the films. In this procedure a single lamella of solution is formed in the glass frame by tilting the cell from a vertical to a horizontal position and gently erecting it. The draining characteristics of the film so formed within the frame were noted by examining the film illuminated with a fluorescent light for observing light interference patterns. A fast draining film shows a series of widely spaced parallel bands moving downwards with their spacing steadily widening. A slow draining film typically shows a pattern of more closely spaced, “wavy” interference bands moving downwards much more slowly as the film drains.



Scheme 1: Idealized chemical structure of Polymer JR400.

3. Results and discussion

Considerable areas of foam enhancement of the sodium octyl sulfate, sodium decyl sulfate and sodium decane sulfonate were occasioned by the presence of the cationic polymer are evident from Figs. 1-3. These areas correspond broadly to systems showing surface viscoelasticity (VE) or surface viscosity (V) by the talc powder test as illustrated in corresponding two-component phase maps shown in Figs. 4-5. Previously determined foaming (Fig. 6) and surface viscoelasticity data (Fig. 7) for the corresponding SDS/Polymer JR400 system had already suggested this correlation. Comparison of Figs. 1 and 2 with the data reported previously [4] for the sodium dodecyl sulfate/Polymer JR400 system indicates that foaming of the sodium octyl sulfate and sodium decyl sulfonate/Polymer JR400 systems is actually superior to that of the dodecyl sulfate/polymer system, in the sense of covering a broader range of compositions where no precipitation takes place. For a given surfactant/polymer pair, the stability of the foams with time depends on the exact composition of the mixture. In Fig. 8 we present the volume decays of the foams obtained with several SOS/Polymer JR400 mixtures. For a given polymer concentration, initial foam height and stability increased with surfactant concentration. At constant surfactant concentration, initial foam volume increased with increasing polymer concentration, but the foam stability was more variable with this parameter. Collapse time of the foams in many cases exceeded 24 h. It is interesting to note that even small amounts of polymer improve the foaming of this surfactant.

Film drainage analysis on a selected series of compositions gave further evidence of the favorable effect of short chain surfactant/polymer mixtures in stabilizing aqueous

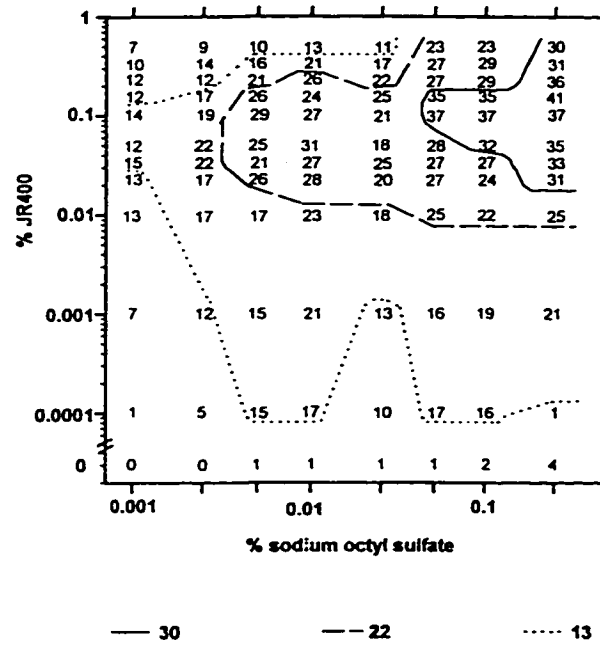


Figure 1: Contour maps of the foam volumes obtained for mixtures of sodium octyl sulfate and Polymer JR400. The values in the diagram indicate the measured foam volume (ml). The contours delineate the compositions yielding foam heights of 30 ml (full line), 22 ml (dashed line), and 13 ml (dotted line).

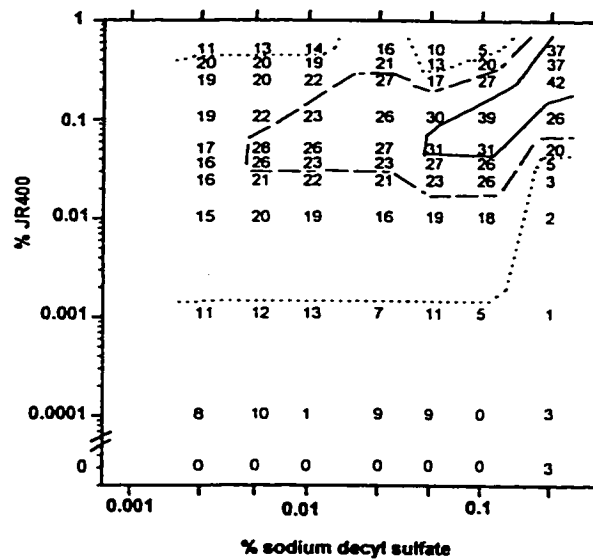


Figure 2: Contour maps of the foam volume obtained for mixtures of sodium decyl sulfate and Polymer JR400 (see legend to Figure 1).

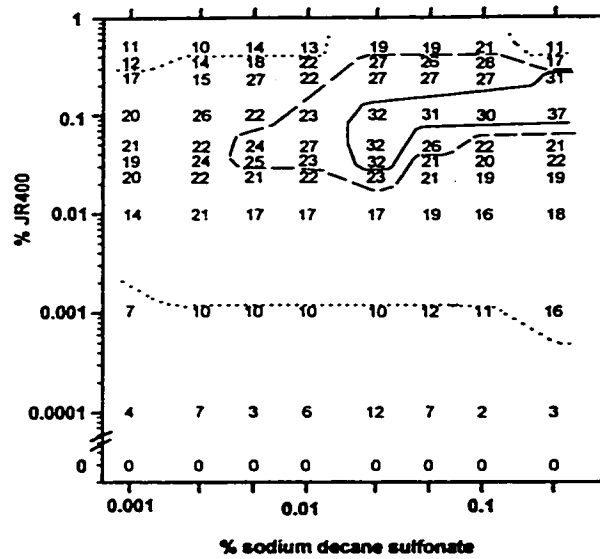


Figure 3: Contour maps of the foam volumes obtained for mixtures of sodium decane sulfonate and Polymer JR400 (see legend to Figure 1).

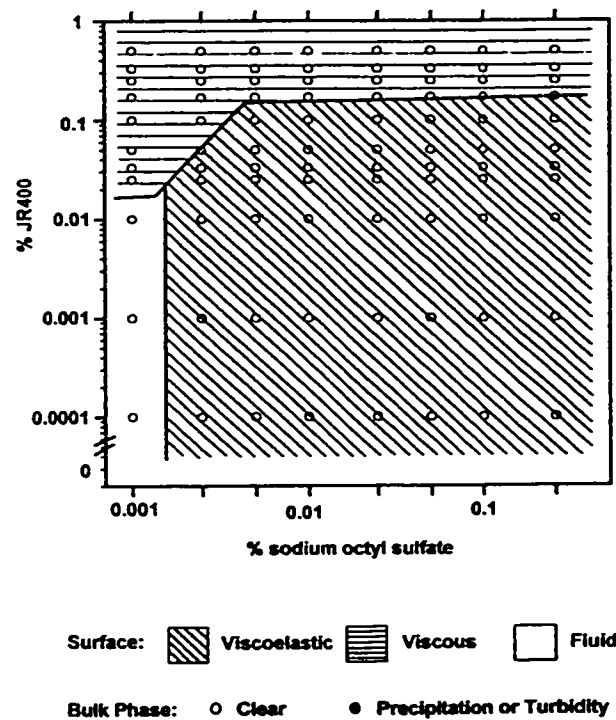


Figure 4: Surface-phase map of the sodium octyl sulfate/Polymer JR400 system. The circles represent the observations points.

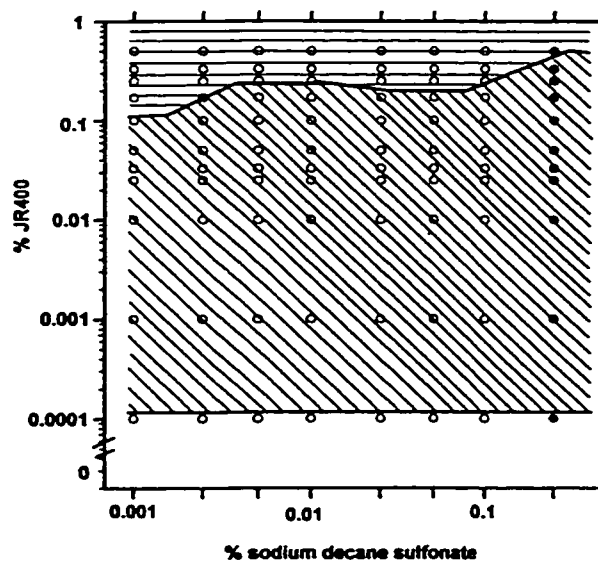


Figure 5: Surface-phase map of the sodium decane sulfonate/Polymer JR400 system. The circles represent the observation points. Full circles correspond to mixtures showing turbidity or precipitation (see legend to Figure 4).

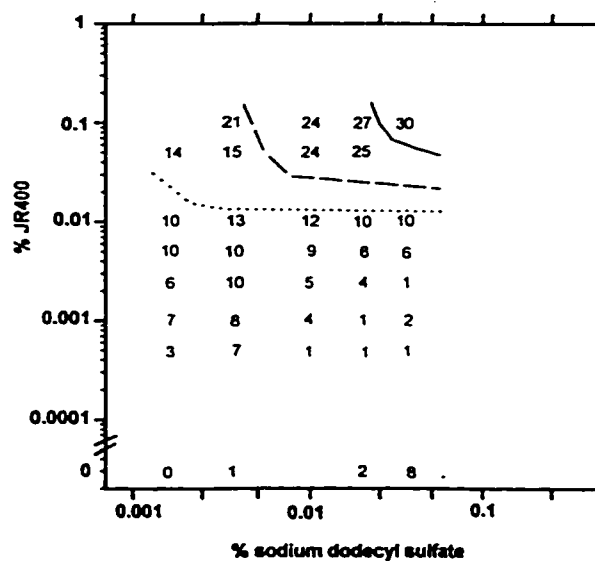


Figure 6: Contour maps of the foam volumes obtained for mixtures of sodium dodecyl sulfate and Polymer JR400 (see legend to Figure 1).

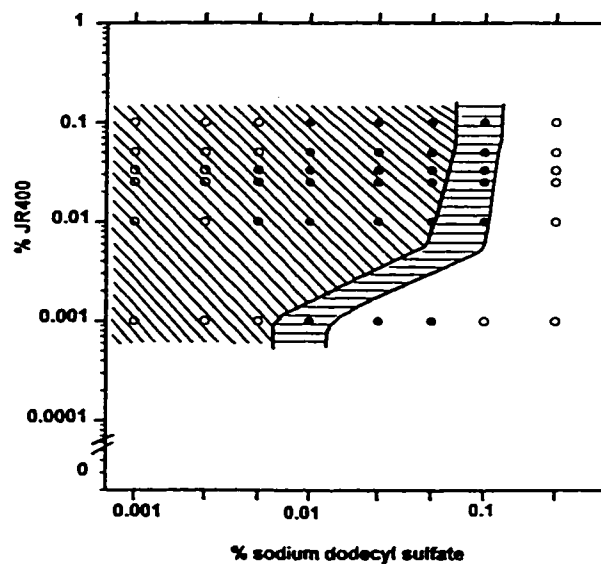


Figure 7: Surface-phase map of the sodium dodecyl sulfate/Polymer JR400 system. The circles represent the observation points. Full circles correspond to mixtures showing turbidity or precipitation (see legend to Figure 4).

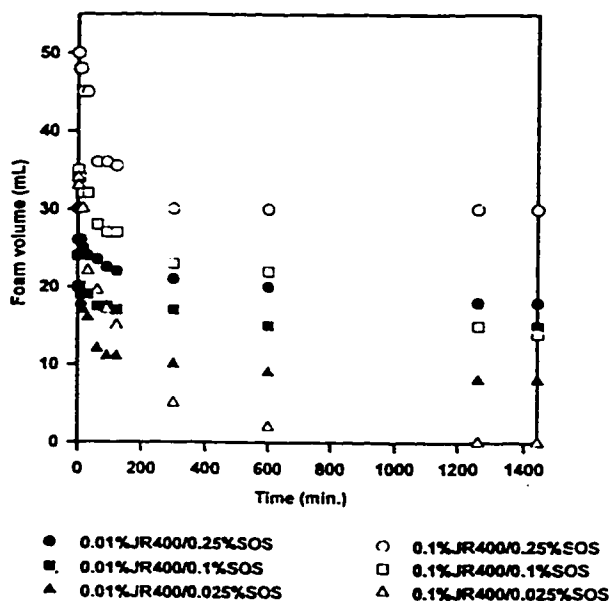


Figure 8: Plots of the changes in foam volumes as a function of time for foams formed in the presence of sodium octyl sulfate/Polymer JR400 of various compositions.

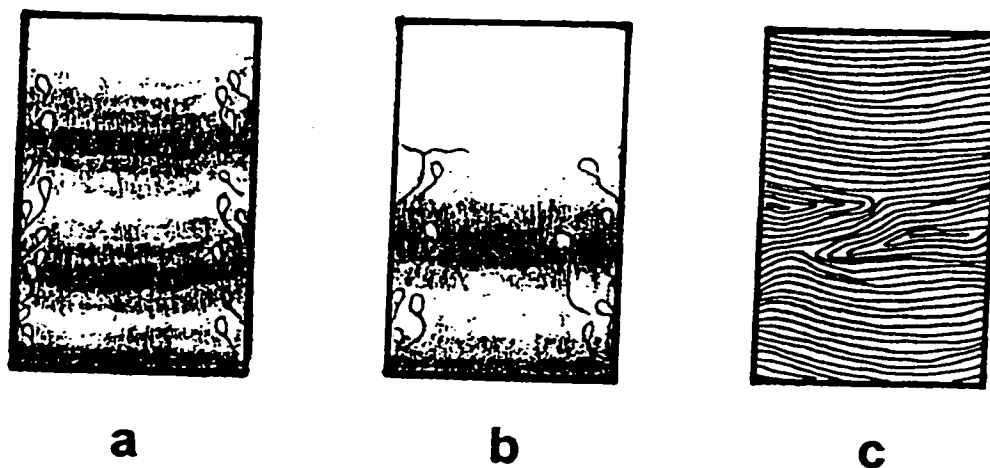


Figure 9: Pictorial representation of film drainage for a solution of sodium dodecyl sulfate (1% w/w) observed after 5 s (a) and after 30 s (b) and for a solution of sodium dodecyl sulfate (0.01% w/w)/Polymer JR400 (0.01% w/w) after 30 s (c).

foams. For example, the single lamellae formed from 0.01% w/w solution of Polymer JR400 containing sodium octyl sulfate or sodium decane sulfonate showed remarkable stability. They appeared static, giving little indication of any drainage. By contrast single lamellae formed from solutions of Polymer JR400 alone showed incessant activity and seldom lasted more than 5 to 15 s. Solutions of surfactant alone formed extremely fast draining films. As expected, the surfactant yielding the highest stability alone was sodium dodecyl sulfate. A pictorial representation of the patterns observed with films of this surfactant alone (1% w/w) after 5 s and after 30 s is given in Figs. 9(a) and (b). Interference bands moved rapidly until the films drained completely. Along the edge of the glass frame slight fluid motion upwards was also observed. Overall, film drainage to

the stage showing no interference occurred in approximately 2.5 min. In contrast, film obtained from 0.01% w/w SDS/0.01% w/w Polymer JR400 were much more static (Fig. 9(c)). At first the film appeared motionless, then after 15 s very closely-spaced interference bands formed. Thereafter, the film disruption time appeared to be variable but of the order of minutes. We note that it is difficult to form films from solutions of 0.01% w/w SDS: lifetimes were short and variable and the films were very fast draining.

The above information on foaming is interesting in light of the well-known fact that interfacial activity, in practical foaming and detergency, is generally found to peak at dodecyl to tetradecyl chain lengths within a homologous surfactant series. Further increase in activity is limited by solubility and maximum attainable surfactant monomer concentration. A deductive interpretation is that the active species in the present mixed systems is not the free surfactant, but the polymer/surfactant complex with its high intrinsic surface activity and surface bonding, as revealed by surface viscoelasticity measurements. Such complexation of charged surfactants with oppositely charged polyelectrolytes thus constitutes a novel way of shifting the peak of interfacial performance in a family of ionic surfactants to lower chain lengths and of markedly improving foaming behaviour. Solubility limitations of the complexes are also reduced in this way [8].

We should point out that reports of stabilization of SDS films by uncharged water-soluble polymers, namely polyethylene oxide [12] and poly(N-vinylpyrrolidone) [13, 14], involve systems with much weaker interaction forces and much weaker effects on foaming. Stronger effects recently reported in dodecyltrimethylammonium

bromide/AMPS systems [15, 16] are more comparable to our observations. In our tests sodium decyl sulfate and sodium decane sulfonate exhibited very similar behaviour.

Acknowledgment

F.M.W. and S.T.A.R thank the Natural Sciences and Engineering Research Council of Canada for financial support.

References

- [1] See, E.D. Goddard, K.P. Ananthapadmanabhan (Eds.), *Interactions of Surfactants with Polymers and Proteins*, CRC Press, Boca Raton, FL, 1993.
- [2] E.D. Goddard, T.S. Phillips, R.B. Hannan, *J. Soc. Cosmet. Chem.* 1975, 26, 461.
- [3] E.D. Goddard, R.B. Hannan, *J. Colloid Interface Sci.*, 1976, 55, 73.
- [4] S.T.A. Regismond, F.M. Winnik, E.D. Goddard, *Colloids Surf. A: Physicochem. Eng. Aspects*, 1996, 119, 221.
- [5] R.J. Ackers, in: *Foams*, Academic Press, London, 1976.
- [6] K.J. Mysels, *J. Phys. Chem.*, 1964, 68, 3441.
- [7] K.J. Mysels, K. Shinoda, S. Frankel, in: *Soap Films*, Pergamon Press, New York, 1959.
- [8] E.D. Goddard, R.B. Hannan, *J. Am. Oil Chem. Soc.*, 1977, 54, 561.
- [9] E.D. Goddard, R.B. Hannan, unpublished results.

- [10] K.P. Ananthapadmanabhan, P.S. Leung, E.D. Goddard, in: M. El Nokali (Ed.), *Polymer Association Structures*, American Chemical Society Symposium Series 384, American Chemical Society, Washington, DC, 1989, ch. 18.
- [11] E.D. Goddard, D.B. Braun, *Cosmetics and Toiletries*, 1985, 100, 41.
- [12] S.L. Addad, J.-M. di Meglio, *Langmuir*, 1992, 8, 324.
- [13] O. Krichevsky, J. Stavans, *Phys. Rev. Lett.*, 1994, 73, 696.
- [14] K. Chari, T.Z. Hossain, *J. Phys. Chem.*, 1991, 95, 3302.
- [15] V. Bergeron, D. Langevin, A. Asnacios, *Langmuir*, 1996, 12, 4498.
- [16] A. Asnacios, D. Langevin, J.-F. Argillier, *Macromolecules*, 1996, 29, 7412.

Colloids and Surfaces A : Physicochemical and Engineering Aspects, 1999, 156, 157-162.

Static and dynamic surface tension of dilute polyelectrolyte solutions

S.T.A. Regismond^a, Z. Policova^b, A.W. Neumann^b, E.D. Goddard^c and F.M. Winnik^{a*}

^aDepartment of Chemistry, McMaster University, 1280 Main St. W. Hamilton, Ontario
Canada L8S 4M1,

^bDepartment of Mechanical Engineering, University of Toronto, 5 King's College Road,
Toronto, Ontario Canada M5S 1A4

^c849 Buccaneer Lane, Manahawkin, New Jersey, USA, 08050

Abstract

The surface tension of aqueous solutions of Polymer JR400, the chloride salt of a trimethylammonium derivative of hydroxyethyl cellulose, has been measured as a function of polymer concentration. Axisymmetric Drop Shape Analysis-Profile has been employed to record the dynamic surface tension response of the solutions to a sawtooth-shaped variation in the surface area. Dilute solutions of the polymer (concentration < 0.05 weight %) exhibited an elevation of the surface tension of water, from 71.9 mJ/m² to 72.7 mJ/m² (23 °C) under both static and dynamic conditions. Under the latter, elevations of as much as 3 mJ/m² were observed during the surface contraction cycle. Solutions of concentrations higher than 0.05 weight% recovered the more conventional behaviour of water surface tension depression and, in the dynamic measurement mode, decreases in the surface tension during the contraction cycle.

Keywords: Dynamic surface tension; Axisymmetric drop shape analysis; Polyelectrolyte; Cellulose ether

1. Introduction

A fact, currently of largely historical interest, is that water-soluble electrolytes, such as sodium chloride, raise the surface tension of water [1]. The effect is generally small, amounting to a few mJ/m^2 , and occurs at high concentration of electrolyte (>1 mol/L). It has been ascribed to negative adsorption, or surface depletion, of the electrolyte ions. Water interacts strongly with ions, thus considerable energy is required to move a highly hydrated ion from the bulk to the water/air interface. It has been argued that the interface layer of the solution will be essentially pure water, the ions being effectively excluded from this region. The surface tension, however, is not that of pure water. It is increased slightly due to the surface deficiency of solute. The effect is not limited to electrolytes, other highly solvated solutes, such as sucrose, also show the effect [2]. Aqueous solutions of polymers constitute a case of special interest. One could anticipate that if an increase in surface tension were found, it would become manifest at much lower concentration (w/w) and, furthermore, in view of the large size of such molecules, that significant time effects in the adsorption and desorption processes could be encountered.

We report here preliminary data on the surface tension of solutions of a cationic polyelectrolyte, Polymer JR400 (Structure 1a), whose foaming characteristics [3] and surface rheology [4] in mixtures with anionic surfactants have been reported recently. This polymer is obtained by chemical modification of the neutral cellulose ether, hydroxyethyl cellulose (HEC, Structure 1b). Axisymmetric Drop Shape Analysis-Profile [ADSA-P] was employed, allowing us to measure the dynamic surface tension response to surface variations under controlled conditions of surface perturbation [5].

2. Experimental

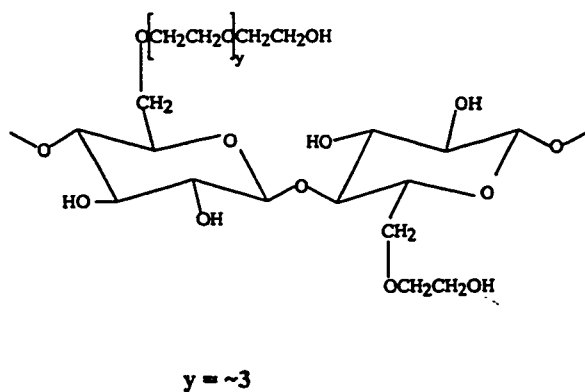
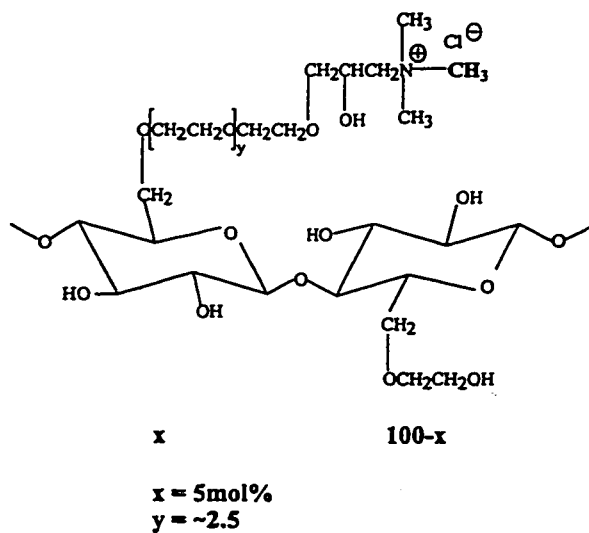
2.1. Materials

Water was deionized using a NANOpure water filtration system. Hydroxyethyl cellulose (Cellosize HEC QP4400H, MW 400,000, DS_{EO} : ~ 3) and Polymer JR400 (chloride salt of a trimethylammonium derivative of hydroxyethyl cellulose, MW 400,000, approximate level of cationic substitution: 5 mol%, DS_{EO} : ~ 2.5) were gifts from Amerchol Corporation (Edison NJ). The polymers were purified by ultrafiltration, using a Diaflo YM30 (Amicon) fitted with 43 mm membranes of 30,000 MW cut-off. The polymers were recovered by freeze-drying.

2.2. Methods

Specific densities were measured at 23 °C or 30 °C, using a Calculating Digital Density Meter, AP PAAR DMA45. Surface tensions were determined using the Axisymmetric Drop Shape Analysis-Profile (ADSA-P) instrumental setup described elsewhere [6]. Experiments were run at 23 °C unless otherwise stated, using G13 TEFLON tubing (internal diameter: 1.9 mm). Two time sequences were used to run the experiments. The first consisted of a 6 minute pumping cycle in which a pendant drop was continuously compressed and expanded in a sawtooth-shaped variation in surface area, and imaged twice each second for the first 2 minutes and then imaged every second for the next 4 minutes. This was followed by imaging the drop every 5 seconds for a total run time of 15 minutes. Three runs on different drops were performed to obtain statistical information. The second method sequence consisted of two separate experiments. The initial sequence was identical to that described in the method above. It was followed by a

further 15 minutes stationary phase where the pendant drop was imaged every 2 minutes. Then, a two minutes pumping cycle was applied followed by a final two minute stationary phase. The second experiment consisted of a 30 minute stationary phase where the pendant drop was imaged every two minutes, followed by a 6 minute pumping cycle and a 9 minute stationary phase, as described above.



Structures: Idealized chemical structures of Polymer JR400 (a) and HEC (b).

3. Results

At first, we measured the surface tensions of a series of solutions of the polyelectrolyte Polymer JR400, of increasing concentrations, ranging from 0.001 to 0.5 weight %. As expected, a gradual lowering of the surface tension was observed, however solutions of low polyelectrolyte concentration (0.01 wt%) seemed to show a surprising *elevation* of surface tension (Table 1). In order to investigate this surprising effect in more detail, we performed a series of dynamic surface tension measurements for polyelectrolyte solutions of concentrations ranging from 0.01 to 0.05 weight%.

Table 1: Concentration dependence of the surface tension of aqueous solutions of Polymer JR400 measured at 23 °C.

Solution concentration (wt%)	Initial surface tension (mJ/m ²)	Surface tension after 15 min (mJ/m ²)
Water	72.4 ± 0.2	72.4 ± 0.2
0.001	72.5 ± 0.3	72.6 ± 0.1
0.005	72.2 ± 0.1	71.9 ± 0.3
0.010	72.8 ± 0.3	72.7 ± 0.2
0.050	72.5 ± 0.2	71.1 ± 0.3
0.100	71.8 ± 0.1	69.7 ± 0.2
0.500	67.7 ± 0.3	65.0 ± 0.1

A typical time profile recorded in an oscillating drop measurement of the surface tension of a Polymer JR400 solution (0.05 weight%) is shown in Figure 1. The top portion of the figure represents the changes in surface tension in response to contractions and expansion of the drop. It is observed that as the surface area is reduced, the surface tension decreases, while upon increase of the drop area, the surface tension increases. This is the usual behaviour of amphiphile solutions. It can be explained in the following manner. As the surface area is reduced, the concentration of the solute per unit area in the interface

increases more rapidly than the amphiphiles can desorb, thus the surface tension decreases. Similarly as the surface is expanded, the concentration of solute per unit area decreases faster than adsorption can occur, and consequently, the surface tension increases.

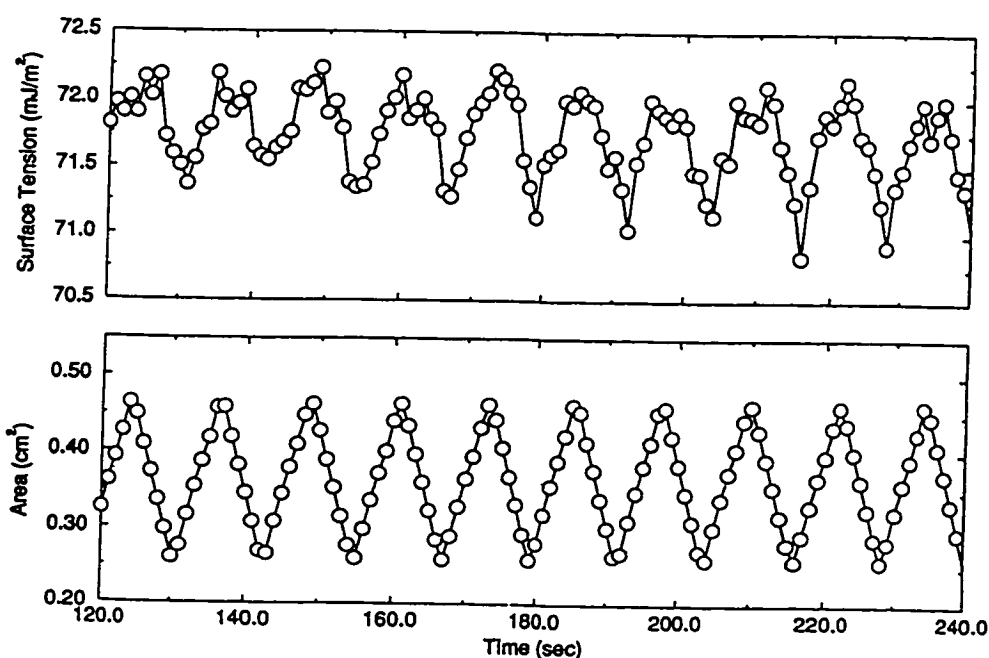


Figure 1: Dynamic surface tension response to the sawtooth change in the surface area of a Polymer JR400 aqueous solution at a concentration of 0.05 weight%.

An extremely interesting effect was observed on cycling a more dilute solution of the polyelectrolyte (0.01 weight%): as the area of the drop was compressed, the surface tension *increased*, and when the drop was expanded, the surface tension *decreased* to a value somewhat higher than that of water ($72.4 \pm 0.2 \text{ mJ/m}^2$) (Figure 2). This behaviour was reproducible, as demonstrated by performing many consecutive runs with the same

solution, but different drops and with newly prepared solutions. A solution of a lower polyelectrolyte concentration (0.005 weight%) was analysed as well. It exhibited the 'mirror image' phenomenon characteristic of the 0.01 weight% solution in one experiment, but not in a repeat experiment, suggesting sensitivity to contamination of these extremely low concentration systems.

A second series of experiments was conducted with Polymer JR400 solutions that were allowed to equilibrate for 45 min. The same trends were observed, even though the surface tensions recorded were slightly lower than those reported in Table 1 (e.g. 0.001 weight%: 71.2 mJ/m^2). Indeed, the 0.01 weight% solution still displayed the 'mirror effect' in its surface tension profile.

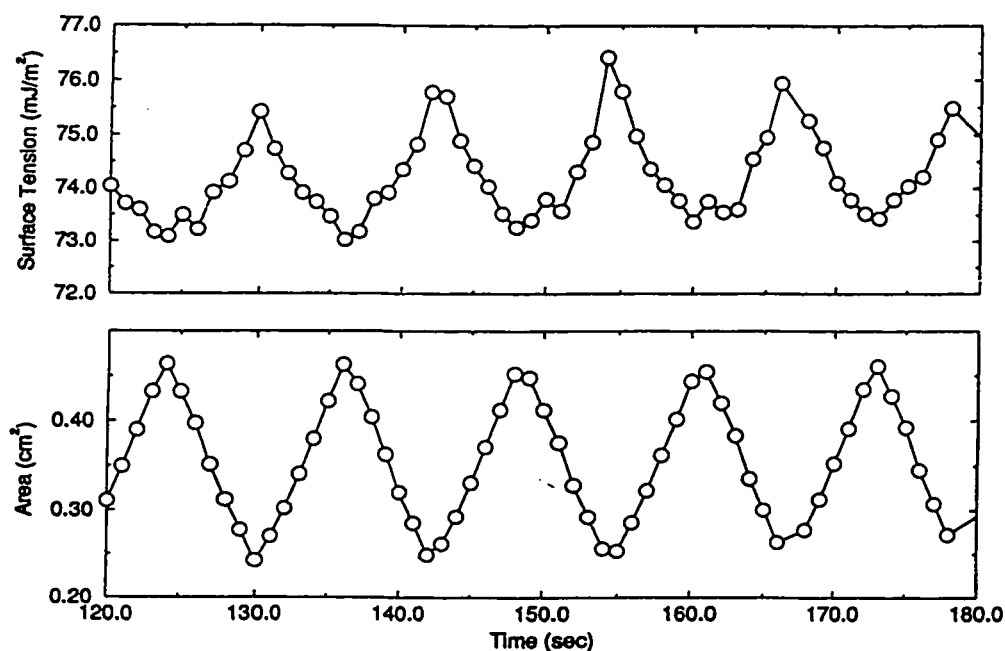


Figure 2: Dynamic surface tension response to the sawtooth change in the surface area of a Polymer JR400 aqueous solution at a concentration of 0.01 weight%.

Very preliminary experiments were carried out with solutions of the 'parent' polymer of the cationic polyelectrolyte, the uncharged cellulose ether, hydroxyethyl cellulose (HEC, structure 1b). In a solution of 0.01 weight% concentration, this polymer, which lacks the solubilizing ionic groups of Polymer JR400, has a slight but definite surface activity, in agreement with previous reports [7]. It lowers the surface tension of water by approximately 5mJ/m^2 , as expected for aqueous solutions of moderately surface active polymers [8]. Despite this, the solution displayed the 'mirror effect' in the cycling experiment: a surface tension increase was registered when the surface area was decreased, and vice-versa (Figure 3, bottom). An interesting feature is that, when the temperature was increased from 23 to 30 °C, the effect disappeared and the solution returned to the conventional behaviour (Figure 3, top).

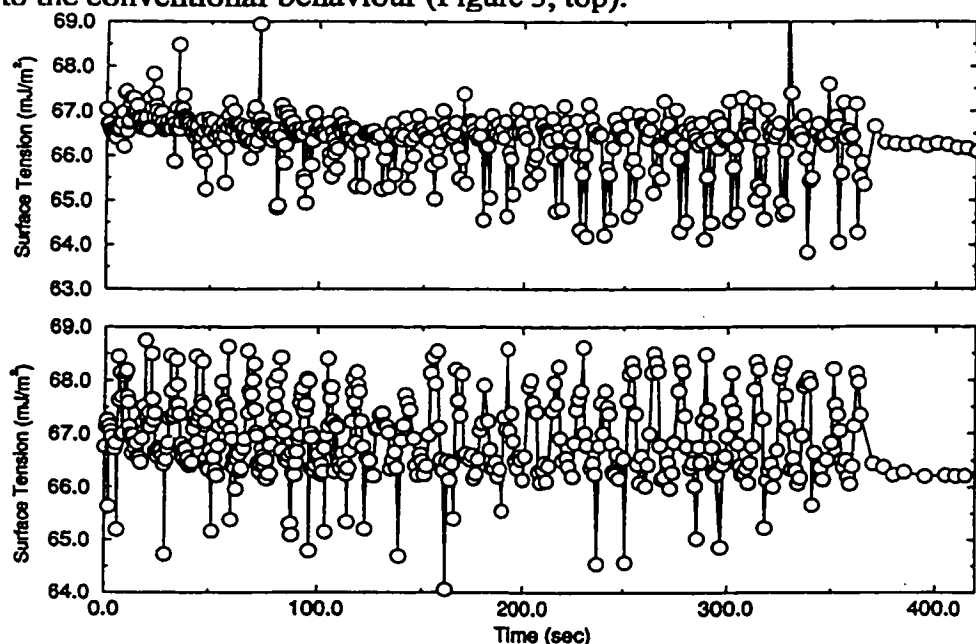


Figure 3: Dynamic surface tension responses to the area change in the surface of a HEC aqueous solution (0.01 weight%) measured at two different temperatures: top: 30 °C; bottom: 23 °C.

4. Discussion

We ascribe the elevation of static surface tension of the 0.01 weight% polymer solution to the classical 'electrolyte' effect of negative adsorption. Two possible interpretations of the increase in surface tension on compression can be envisaged. In one interpretation, we consider that, although this increase signifies a negative surface excess, it does not mean that the surface concentration of polymer is zero; indeed, it will be finite. Upon compression, the surface concentration and surface potential will increase. If the relaxation time for the desorption process exceeds the cycling time, a further barrier to polymer adsorption occurs, resulting in the further increase of surface tension observed. A similar explanation was put forward before, to account for the boundary tension increases exhibited by bovine serum albumin solutions of low concentration [9, 10].

A second explanation can be made in terms of a sublayer of polymer formed by desorption to achieve a negative surface excess. If the sublayer is also compressed and expanded in the cycling process, during the former it could also constitute a barrier to adsorption and, again, be registered as an increase in surface tension during compression. This sublayer would have some similarity to, but important differences as well, from that suggested by Ward and Tordai for the adsorption of surfactants [11]. Experiments in which the frequency of cycling is varied will help in illuminating the mechanism.

The next question to answer concerns the unusual effect of polyelectrolyte concentration. Two tentative explanations are offered. One is that there may be a concentration-dependant configurational change of the polymer, with the form favored at

higher concentration being more surface active, leading to the more conventional adsorption behaviour observed with solutions of higher polyelectrolyte concentrations. The second interpretation is that the polymer itself, in common with many synthetic polymers, is not homogeneous, and that at sufficiently high solution concentration conventional surface tension lowering could be attained due to the presence of more surface active components. More refined purification methods may be needed, in order to verify the unusual effect of polymer concentration.

Our interpretation of the phenomena recorded with the solutions of the uncharged cellulose ether HEC is that there exists an entropic repulsion between the polymer molecules in the air/water interface and those in the bulk. The effects are expected to increase as the surface is compressed. The detectable influence of the solution temperature brings further support to this explanation. Polyethoxylated materials are known to have inverse solubility properties [12]. A slight configurational change of the polymer, resulting from temperature-induced changes in its level of hydration, can be responsible for the observed change in its surface activity.

5. Conclusions

The foregoing is a preliminary report of the elevation of the surface tension of water by a dissolved polyelectrolyte and a further elevation of surface tension upon periodic compression of the surface. Explanations of the phenomena are proposed. Further studies are needed, in order to fully understand the surface activity of this polyelectrolyte.

Acknowledgments

The work was supported by grants to FMW and AWN of the Natural Sciences and Engineering Research Council of Canada.

References

- [1] N.K. Adam, *The Physics and Chemistry of Surfaces*, 3rd Ed. Oxford University Press, London, UK, 1941; chapter 3.
- [2] P.C. Hiemenz, R. Rajagopalan, *Principles of Colloid and Surface Chemistry*, 3rd Ed. Marcel Dekker Inc., New York, NY, 1997; p 328.
- [3] S.T.A. Regismond, F.M. Winnik, E.D. Goddard, *Colloids and Surfaces A: Physicochem. Eng. Aspects*, 1998, 141, 165.
- [4] F.M. Winnik, S.T.A. Regismond, E.D. Goddard, *Colloids and Surfaces A: Physicochem. Eng. Aspects*, 1996, 106, 243.
- [5] S. Lahooti, O.I. Del Rio, A.W. Neumann, and P. Cheng, in *Applied Surface Thermodynamics*, A.W. Neumann and J.K. Spelt, Eds. Marcel Dekker, New York, NY, 1996, pp 491-507.
- [6] S.S. Susnar, P. Chen, O.I. Del Rio, A.W. Neumann, *Colloids and Surfaces A: Physicochem. Eng. Aspects*, 1996, 116, 181.
- [7] U. Kastner, H. Hoffmann, R. Donges, R. Ehrler, *Progr. Colloid Polym. Sci.*, 1995, 98, 57; B. Persson, S. Nilsson, L.O. Sundelof, *Carbohydrate Polym.*, 1996, 29, 119.

- [8] S.A. Chang, D.G. Gray, *J. Colloids Interface Sci.*, **1978**, *67*, 255 and references therein.
- [9] P. Chen, Z. Policova, S.S. Susnar, C.R. Pace-Asciak, P.M. Demin, A.W. Neumann, *Colloids and Surfaces A: Physicochem. Eng. Aspects*, **1996**, *114*, 99.
- [10] P. Chen, S. Lahooti, Z. Policova, M.A. Cabrezio-Vilmchez, A.W. Neumann, *Colloids and Surfaces B: Biointerfaces*, **1996**, *6*, 279.
- [11] A.F.H. Ward, L. Tordai, *J. Chem. Phys.*, **1946**, *14*, 453.
- [12] See for example: Handbook of Water-Soluble Gums and Resins, R.L. Davidson, Ed.; McGraw Hill, New York, NY, **1980**; Chapter 13; Water-Soluble Polymers, J.E. Glass, Ed. ACS Symp. Ser. 213, American Chemical Society, Washington DC **1986**.